Evaluating the role of CD200 signalling in renal cell carcinoma immune evasion

Elise Rees

Thesis submitted for the award of PhD

31st March 2020

Ysgoloriaethau Sgiliau Economi Gwybodaeth
Knowledge Economy Skills Scholarships

UNDEB EWROPEAIDD
EUROPEAN UNION

Llywodraeth Cymru
Welsh Government

Cronfa Gymdeithasol Ewrop
European Social Fund

Abstract

CD200 is a transmembrane protein with known immunosuppressive properties. This ligand functions by engaging its receptor, CD200R, found on many immune cell populations. Overexpression of CD200 has been linked to a number of cancer types as a mechanism of immune evasion. An in-human study has demonstrated a clinical benefit of targeting this ligand, which has led to the interest in identifying other cancer types that may also benefit from CD200 checkpoint inhibition.

The main aim of this project was to determine whether CD200 expression was a relevant therapeutic target in renal cell carcinoma (RCC). We demonstrated that CD200 is expressed at protein level across RCC subtypes, which we suggest originates from the cell of origin for this cancer type, the renal tubules. We characterised the impact of CD200 expression level on the immune infiltrate and demonstrated a significant reduction in the presence of helper T cells, whilst NK cell presence remained relatively unaffected and suggestive of NK cell dysfunction. Using cell culture assays, we demonstrate that tumour CD200 expression inhibited CD200R+ NK cell function, both the cytotoxic and effector activity, which led to a diminished ability to kill CD200 expressing target cells. Blocking the CD200 signal was sufficient to restore NK cell activity *in vitro* and restore tumour cell killing. In addition to providing an inhibitory signal to interacting NK cells, the engagement of CD200R by its ligand induced the up-regulation of the Fas death receptor pathway, which resulted in apoptosis of the NK cell via induction of the caspase 8-dependent extrinsic pathway. These findings reveal a novel immunosuppressive mechanism by which both NK cell activity and presence at the tumour bed is inhibited. This study provides evidence that suggests that some RCC patients may benefit from CD200 immune checkpoint inhibition.

Acknowledgements

Firstly, I would express my heartfelt thanks to my supervisor, Dr Girish Patel, for giving me this opportunity and for his continual help, encouragement and guidance throughout my PhD. Secondly, many thanks go to my second supervisor, Dr Richard Clarkson, for his support and advice. I am very grateful to all the members of the GKP lab group, both past and present, for their help and advice as well as their friendship and support. I am also thankful the support I received from members of The European Cancer Stem Cell Research Institute. I would also like to thank KESSII and the European Social Fund, who made this project possible as well as member of the local health board that gave me an insight into the clinical side of cancer. Finally, I would like to thank my family and friends for their ongoing support throughout my time at university.

List of Abbreviations

AD - Alzheimer's disease

ADAMs - Membrane-anchored proteins disintegrin and metalloprotease domains

AJCC - American joint committee on cancer

AML - Acute myeloid leukaemia

AP-3 - Adaptor protein 3

APC - Antigen presenting cells

BAP1 - BRCA1 associated protein-1

BCC - Basal cell carcinoma

ccRCC - Clear cell renal cell carcinoma

CD200 - Cluster of differentiation 200

CD200R - CD200 receptor

CD200tg - CD200 transgene

cFLIP - caspase 8-like inhibitory protein

chRCC - Chromophobe renal cell carcinoma

CIA - Collagen-induced arthritis

CLL - Chronic lymphocytic leukaemia

CLP - Common lymphoid progenitor

CNS - Central nervous system

CRs - Completed responses

CSCC - Cutaneous squamous cell carcinoma

CSCs - Cancer stem cells

cSMAC - Central supramolecular activation complex

CTL - Cytotoxic T cell

CTLA-4 - Cytotoxic T lymphocyte-associated Antigen 4

DCs - Dendritic cells

DD - Death domain

DP - Double positive thymocytes

DR - Death receptor

dSMAC - Distal supramolecular activation complex

ERKs - Extracellular signal-regulated kinases

F-actin - Filamentous actin

FADD - FAS-associated death domain

FasL - Fas ligand

FHL3 - Familial haemophagocytic lymphohistiocytosis subset 3

FoxP3 - Forkhead box P3

GATA3 - GATA-binding protein

HCC - Hepatocellular carcinoma

HIF1-α - Hypoxia-inducible factor 1 alpha

HIF2-α - Hypoxia-inducible factor 2 alpha

HNSCC - Head and neck squamous cell carcinoma

HPS2 - Hermansky-Pudlak syndrome subset 2

HSCs - Hematopoietic stem cells

IFNγ - Interferon gamma

Ig - Immunoglobulin

IgSF - Ig superfamily

IL- - Interleukin

iNK - Immature NK cell

IPEX - Immune Dysregulation Polyendocrinopathy, Enteropathy, X-linked disease

IS - Immunological synapse

ITAM - Immunoreceptor tyrosine-based activation motif

ITIM - Immunoreceptor tyrosine-based inhibition motif

iTregs - Induced Tregs

KIRs - Killer immunoglobulin-like receptors

LAG-3 - Lymphocyte activation gene-3

MAPKs - Mitogen-activated protein kinases

MDP - Macrophage-dendritic cell progenitor

MHC - Major histocompatibility complex

MPPs - Multipotent progenitors

mRCC - Metastatic renal cell carcinoma

MTOC - Microtubule organisation centre

mTOR - Mammalian target of rapamycin

mTORC - Mammalian target of rapamycin complex

MZ - Marginal zone B cell

NCR - Natural cytotoxicity receptor

NK - Natural killer cells

NKG2D - Natural-killer group 2, member D

NSCLC - Non-small-cell lung cancer

nTreg - Natural Tregs

ORR - Overall response rate

OS - Overall survival

PBRM1 - Polybromo 1

PD-1 - Programmed cell death protein 1

PDGFB - Platelet-derived growth factor beta

PFS - Progression free survival

PI3K - Phosphatidylinositol-3-kinase

PMBCL - Primary mediastinal B-cell lymphoma

pRCC - Papillary renal cell carcinoma

pSMAC - Peripheral supramolecular activation complex

PTB - Phosphotyriosine-binding

RCC - Renal cell carcinoma

sCD200 - soluble form CD200

sFasL - Soluble fas ligand

SHIP 1 - Lipid phosphatase SH2 domain-containing inositol-5-phosphatase

SHP-1 - SRC homology-containing tyrosine phosphatase 1

SMAC - Supramolecular activation cluster

SNAREs - Soluble N-ethylmaleimide-sensitive factor attachment protein receptors

SP - Single positive thymocytes

TCR - T cell receptor

TGF - Transforming growth factor

TIL – Tumour infiltrating lymphocyte

TIM-3 - T cell immunoglobulin and mucin domain 3

TKI - Tyrosine kinase inhibitor

TME - Tumour microenvironment

TNF - Tumour necrosis factor

TNFR - TNF-receptor

TNM - Tumour-node-metastasis

TRADD - TNFR-associated death domain

TRAIL - TNF-related apoptosis-inducing ligand

TRAIL-R - TNF-related apoptosis-inducing ligand receptor

Tregs - Regulatory T cells

VEGF - Vascular endothelial growth factor

VEGFR - Vascular endothelial growth factor receptor

VHL - Von Hippel-Lindau

VISTA - V-domain immunoglobulin-containing suppressor of T-cell activation

WAS - Wiskott-Aldrich syndrome

WASp - Wiskott-Aldrich syndrome protein

WT - Wild-type

Table of Contents

List of Figures

Chapter 1: Introduction

Chapter 3: Characterising CD200 expression in renal cell carcinoma

Chapter 4: Defining the inflammatory response in renal cell carcinoma

List of Tables

Chapter 4: Defining the inflammatory response in renal cell carcinoma

Chapter 1: Introduction

Chapter 1: Introduction

1.1 Hallmarks of cancer

Our knowledge of cancer has rapidly evolved over the past century. Tumorigenesis is now considered a multistep process, in which normal cells become progressively transformed to malignancy through the acquisition of damage to the genome. This process requires the cell to acquire the hallmarks of cancer, first described in the seminal peer-reviewed article published in 2000 by Douglas Hanahan and Robert Weinberg (Hanahan and Weinberg, 2000). This paper identified six hallmarks that describe distinctive and complimentary capabilities that enable tumour growth and metastases. These hallmarks include (1) sustaining proliferative signalling, (2) evading growth suppressors, (3) resisting cell death, (4) enabling replicative immortality, (5) inducing angiogenesis, and (6) activating invasion and metastasis. These provided a solid foundation for understanding the biology of cancer and led to the development of the mechanisms underpinning tumour development. This led to the identification and addition of an additional two hallmarks - reprogramming of energy metabolism and evading immune destruction (Hanahan and Weinberg, 2011). These additions highlighted the notion that the biology of tumours cannot be understood completely by analysing the cancer cell alone, but instead that tumour development involves the complex interplay between cancer cells and their microenvironment, the tumour microenvironment (TME), and immune cells therein.

1.1.1 The tumour microenvironment

Cancers are more than just the malignant cells that make up the tumour mass. Interactions between the tumour cells and the surrounding tissue are now known to play a crucial role in enabling tumour growth. In addition to the malignant cells, the TME contains the extracellular matrix, tumour vasculature and lymphatics, fibroblasts, pericytes and sometimes adipocytes, and cells of the immune system (Balkwill *et al.,* 2012). Cancer research focus has now shifted from only the malignant cells themselves to the tumour microenvironment and the complex interactions. Much of this research had led to the development of novel therapeutics that target these interactions. One of the most promising targets is the interaction between malignant and immune cells.

1.2 Cells of the immune system

All the cellular elements of blood, including the red blood cells (erythrocytes) that transport oxygen, the platelets that trigger blood clotting in damaged tissues, and the white blood cells of the immune system, derive ultimately from the same progenitor or precursor cells—the hematopoietic stem cells (HSCs) in the bone marrow (Asada *et al.,* 2017). These stem cells are known as pluripotent hematopoietic stem cells as they are able to give rise to all of the different types of blood cells. These cells have all the key characteristics of a classical stem cell, with the ability to self-replicate and differentiate into progeny of multiple lineages.

Haematopoiesis describes the process of differentiating from HSCs to mature, functional cell types of the blood (Figure 1.1). The classical model of the haemopoietic lineage is organised with HSCs sitting at the top of the hierarchy, which give rise to committed progenitor cells that give rise to mature, differentiated cells (Seita J and Weissman IL, 2010). Initially, HSCs give rise to two types of stem cells with more limited potential. The two major differences between HSCs and these committed progenitors is that HSCs are multipotent, and they have the ability to self-renew indefinitely. The multipotent progenitors (MPPs) still have the potential to differentiate into any cell type but cannot divide continuously so must be renewed by the differentiation of HSCs. MPPs further give rise to oligopotent progenitors which are common lymphoid and myeloid progenitors (Kondo, 2010). These oligopotent progenitors differentiate into their restricted linage commitment. More recently, this developmental scheme has been challenged with evidence of heterogeneity within HSC and progenitor populations (Cheng *et al.,* 2020). Next-generation techniques have identified new haemopoietic cell populations and it is now thought that haemopoiesis is better represented as a continuum which ultimately executes myeloid and lymphoid differentiation, generating the two classical branches of the immune system (Carrelha *et al.,* 2018; Karamitros *et al.,* 2018).

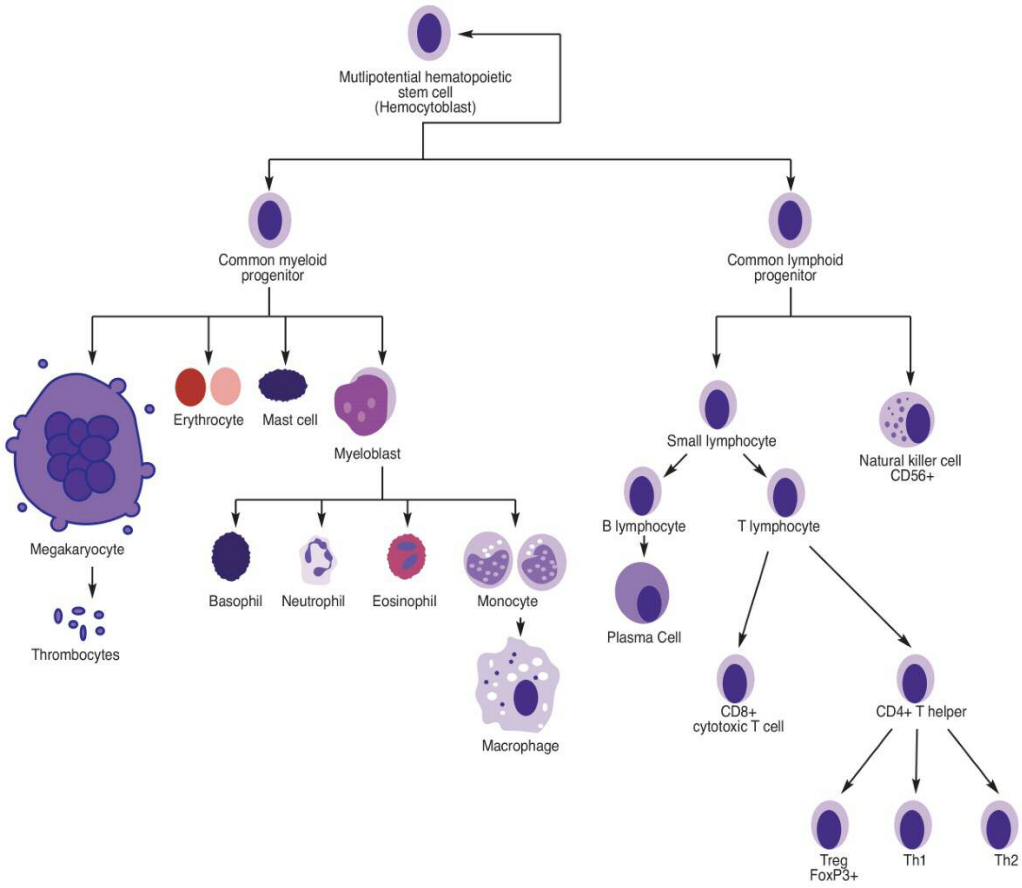

Figure 1.1: The classical adult haematopoietic differentiation hierarchy. Schematic diagram of haematopoiesis, highlighting the major cellular blood components. Long-term self-renewing HSCs are at the apex of a hierarchy of multiple progenitor cell stages giving rise to all blood cell lineages. Adapted from (Ebdon *et al.,* 2013).

1.2.1 Myeloid Lineage

The myeloid lineage includes granulocytes, macrophages, dendritic cells, and mast cells of the immune system.

1.2.1.1 Granulocytes

Granulocytes are named after their dense granule content in their cytoplasm. There are four main types of granulocytes, all of which are relatively short lived and are produced in increased numbers during immune responses (Hong, 2017). Granulocytes from part of the first line of defence against pathogens (Lin and Loré, 2017). As part of an immune response, they leave the blood and migrate to sites of infection and inflammation and release a number of different effector molecules including histamine, cytokines, chemokines, enzymes and growth factors. There are four main types of granulocytes: neutrophils, eosinophils, basophils and mast cells.

1.2.1.1.1 Neutrophils

These are the most abundant leukocytes found in human blood (Rosales, 2018). They are a type of phagocyte, capable of ingesting microorganisms or particles. They are also capable of degranulation, releasing an assortment of proteins that help combat an infection. They are often one of the first responders of inflammatory cells to migrate towards the site of inflammation.

1.2.1.1.2 Basophils

The least common type of granulocyte, basophils, make up only 0.5% of the circulating blood leukocytes (Min and Paul, 2008). They are involved in a number of functions such as antigen presentation, stimulation and differentiation of CD4+ T cells. When activated, basophils degranulate to release histamine, proteoglycans (e.g. heparin and chondroitin), and proteolytic enzymes (e.g. elastase and lysophospholipase) (Borriello *et al.,* 2017). They also secrete lipid mediators and several cytokines.

1.2.1.1.3 Eosinophils

Eosinophils make up approximately 1% of circulating leukocytes (Stone *et al.,* 2010). Eosinophils play an important and varied role in the immune responses and in the pathogenesis of allergic or autoimmune disease. Eosinophils express a range of receptors, which allows them to respond to a multitude of cytokines, chemokines and lipid mediators. Following activation, eosinophils degranulate to release an array of cytotoxic granule cationic proteins that are capable of inducing tissue damage and dysfunction as well as inflammatory mediators.

1.2.1.1.4 Mast Cells

Mast cells are a type of granulocyte whose granules are rich in heparin and histamine. These long-lived tissue-resident cells play an important role in inflammatory settings (Theoharides *et al.,* 2012). They are located at the boundaries between tissues and the external environment, such as at the mucosal surface of the gut and lungs. When activated, a mast cell can either selectively release (piecemeal degranulation) or rapidly release (anaphylactic degranulation) "mediators", or compounds that induce inflammation, from storage granules into the local microenvironment.

1.2.1.2 Macrophages

Another mature cell of the myeloid lineage is the macrophage. Macrophages are specialised cells involved in the detection, phagocytosis and destruction of bacteria and other harmful organisms (Mosser and Edwards, 2008). They also present antigens to T cells and initiate inflammation by releasing cytokines that activate other immune cells. Macrophages originate from blood monocytes that leave the circulation to differentiate in different tissues. The heterogeneity seen in macrophage populations is thought to reflect the specialisation required for the environment they reside. This heterogeneity is reflected by the type of pathogens they recognise as well as the levels of inflammatory cytokines they produce.

1.2.1.3 Dendritic Cells

Myeloid dendritic cells (DCs) are responsible for the initiation of adaptive immune responses as the most potent type of antigen-presenting cells (Rossi and Young, 2005). DCs and macrophages share the common myeloid progenitor called macrophage-dendritic cell progenitor (MDP). Immature DCs migrate to peripheral tissues where they patrol the area by taking up pathogens by phagocytosis and extracellular fluid by micropinocytosis. Upon recognition of a danger signal, the DC matures and upregulates chemokine receptors for migration to the lymph nodes, increasing expression of major histocompatibility complex (MHC) molecules and up-regulating co-stimulatory B7 molecules. Once in the lymph node, they produce the CCL18 chemokine to attract native T cells and prime the antigen specific T cell differentiation.

DCs are specialised to capture and process antigens, converting proteins to peptides that are presented on MHC molecules recognised by T cells. All DCs are capable of antigen uptake, processing and presentation to naive T cells, however, similar to macrophages, DCs are heterogenous (Collin and Bigley, 2018). Different subtypes have distinct markers and differ in locations, migratory pathways, detailed immunological function and dependence on infections or inflammatory stimuli for their generation. During the development of an adaptive immune response, the phenotype and function of DCs play an extremely important role in initiating tolerance, memory, and polarised T-helper 1 (Th1), Th2 and Th17 differentiation.

1.2.2 Lymphoid Lineage

The lymphoid lineage gives rise to the lymphocytes, which include B cells, T cells and natural killer (NK) cells, depending on different stimuli.

1.2.2.1 B Lymphocytes

B cell development continues in the bone marrow. The first cell committed to B-lymphoid differentiation is the pro-B cell. B cell differentiation from CLP is regulated by several factors that are a result of interaction of interleukin 7 (IL-7) and their receptor CD127 (IL-7Rα) existent in the B lymphocyte (Dias *et al.,* 2005). B cells remain in the bone marrow, where pro-B cells develop into immature B cells by completing initial immunoglobulin gene rearrangement to form and express complete IgM molecules, before migrating to peripheral lymphoid organs where they mature into naive B cells that express both IgD and IgM (Yam-Puc *et al.,* 2018). Mature B cells are usually divided into three subgroups: follicular B cells, marginal zone (MZ) B-cell and B1 cells. B cell activation begins by the recognition and binding of an antigen by the B cell receptor, either in a T cell dependent or T cell independent manner. Once bound, receptor mediated endocytosis takes place engulfing the antigen into the B cell, where the antigen is then degraded. These degraded antigen fragments are then presented on the surface of the B cell in complex with MHC class II molecules to T cells. Upon activation, B cells form germinal centres where they differentiate into memory B cells or plasma cells. Following differentiation into plasma cells, additional signals initiate and regulate antibody secretion. The primary function of plasma cells is the secretion of B cell clone-specific antibodies. Each plasma cell secretes antibodies containing a clonally unique antigen-binding region joined to a constant immunoglobulin (Ig) isotype-defining region. These antibodies bind antigens, identifying a target for attack by other immune cells or neutralising the target directly.

1.2.2.2 T Lymphocytes

Lymphoid progenitors in the bone marrow migrate to the thymus to complete their antigen-independent maturation into functional T cells (Germain, 2002). The developing progenitors within the thymus, also known as thymocytes, undergo a series of maturation steps that can be identified based on the expression of different cell surface markers. T cell development occurs in the thymus where the microenvironment directs differentiation, where T cells develop their specific T cell markers, including TCR, CD3, CD4 or CD8, and CD2 (Gameiro *et al.,* 2010). In the thymus they are also subject to thymic education through positive and negative selection.

The earliest developing thymocytes begin to express CD2 but have not yet rearranged their TCR genes (CD2+ CD3-) and lack the expression of the co-receptors CD4 and CD8 and are termed double negative. These cells then express the adhesion molecule CD44, then the α-chain of the IL-2 receptor (CD25). These cells then undergo T cell receptor (TCR) rearrangement to generate CD4+ CD8+ double positive (DP) thymocytes. These DP cells undergo selection and give rise to CD4+ or CD8+ single positive (SP) thymocytes that emerge into the periphery as naïve T cells. These cells are distinguished by expression of CCR7, a chemokine receptor which recruits cells to the lymph nodes, in combination with the naïve cell marker CD45RA.

1.2.2.2.1 CD4+ T cells

CD4 T cells are also known as T helper cells. Their principal function is to activate and promote the responses of other immune cells (Zhu and Paul, 2008). The initial step of differentiation of naïve T cells is the antigenic stimulation of TCR and CD4 (as a co-receptor) interaction with antigen MHC II complex, presented by antigen presenting cells (APCs). TCR and CD3 activation induces downstream signalling pathways that lead to naïve cell proliferation and differentiation into specific effector cells. CD4 T cell responses support the immune response by generating cytokines and chemokines that either activate neighbouring cells to perform specific functions (cytokines) or recruit new immune cell subsets (chemokines). CD4 T cells can be subdivided, with differentiation of lineages depending on a network of specific cytokine signalling and transcription factors (Zhu *et al.,* 2010).

1.2.2.2.1a Th1 Differentiation

The classical T-helper 1 cells develop in response to the Interleukin 12 (IL-12) and interferon γ (IFNγ) cytokine signalling (Heufler *et al.,* 1996). Large amounts of IL-12 is secreted by APCs after their activation through pattern recognition receptors. The master regulator for Th1 differentiation is the T-box transcription factor (T-bet), which significantly enhances the production of IFNγ, and suppresses the development of opposing cell lineages, such as Th2. Chemokine receptors CXCR3 and CCR5 are characteristic of Th1 cells (Kim *et al.,* 2001). Th1 cells can also be distinguished from Th2 cells by specific cytokines that they secrete in response to antigenic stimulation as well as the type of immune response they produce (Kaiko *et al.,* 2008). Th1 cells primarily produce interferon IFNγ and IL-2, which in turn stimulates production of additional Th1 cells. This simultaneously inhibits Th2 development. Th1 cells tend to generate responses against intracellular parasites such as bacteria and viruses.

1.2.2.2.1b Th2 Differentiation

The classical T-helper 2 cells develop in response to the IL-2 and IL-4 (Zhu, 2015). The major transcription factor involved in Th2 lineage differentiation includes the IL-4-induced STAT6, which upregulates the expression of the master regulator GATA3 (GATA-binding protein) (Zhu, 2010). GATA3 has been found to suppress Th1 differentiation, with GATA3 deficient mice differentiation of naïve cells was diverted towards the Th1 lineage. The chemokine receptors CXCR4, CCR3, CCR4, CCR7 and CCR8 are associated with Th2 cells (Kim *et al.,* 2001). Th2 cells produce IL-4, IL-5, IL-6, IL-10, and IL-13. These cells produce immune responses against helminths and other extracellular parasites (Nutman, 2015).

1.2.2.2.1c Regulatory T cells

Regulatory T cells (Tregs) are the third main subset of CD4 T cells. In humans, Tregs can either arise in the thymus (natural Tregs / nTreg) or can be induced from peripheral naïve CD4 T cells in response to transforming growth factor (TGF-β) (induced Tregs / iTreg) (Workman *et al.,* 2009). nTregs are selected for in the thymus by their recognition of self-antigen, but instead of being deleted are directed toward a separate differentiation pathway. Tregs are classically defined as CD4+CD25+CD127+FoxP3+

cells. FoxP3 (Forkhead box P3) is the defining property which determines Treg development and function, both in the thymus and in those developing in the periphery. However, FoxP3 can also be found on activated CD4 and CD8 cells so it cannot be assumed that every FoxP3+ T cell is a Treg.

The primary function of Tregs was originally defined as prevention of autoimmune disease by maintaining self-tolerance (Sakaguchi *et al.,* 1995). The FoxP3 transcriptional regulator is crucial for maintaining suppression of the immune system as evidenced by IPEX syndrome (Immune Dysregulation, Polyendocrinopathy, Enteropathy, X-Linked), a severe autoimmune disease caused by mutations that cause loss of function of FoxP3 that results in self-reactive lymphocytes (Mercer F and Unutmaz D, 2009). Subsequent studies have since revealed several other functions of these cells. As with effector T cells, Tregs must be activated through their TCR (Corthay, 2009). Tregs suppress activation, proliferation and cytokine production of both CD4 and CD8 T cells, as well as suppressing B cells and dendritic cells. The mechanisms by which Tregs supress different immune cells can either be considered direct, whereby Tregs themselves elicit a direct response on a target cell, or indirect, in which a third-party cell or molecule is affected and in turn suppresses the target cell (Romano *et al.,* 2019). The presence of these inhibitory cells has been associated with various autoimmune diseases and cancers.

1.2.2.2.2 CD8+ T cells

CD8+ T cells, like CD4+ Helper T cells, are generated in the thymus and express the T cell receptor (Zhang and Bevan, 2011). CD8 T cells recognise peptides presented by MHC class I molecules, found on all nucleated cells. The CD8 heterodimer binds to a conserved region of the MHC class I and functions as a co-receptor. CD8 T cells are often called cytotoxic T lymphocytes because the main function of CD8 T cells is thought to be the elimination of aberrant cells by cytotoxic means. These cells are very important in the defence against intracellular pathogens, including viruses and bacteria, and for tumour surveillance. When CD8 T cells become activated, they have three major mechanisms to kill target cells: (i) secretion of cytokines, primarily TNF-α and IFN-γ, (ii) the production and release of cytotoxic granules, and (iii) via Fas/FasL interactions. These processes are discussed below (see 1.2.3.1-.4).

1.2.2.2.3 Memory T cells

Naïve T cells are those that have not previously responded to a pathogen. When they recognise a pathogen they rapidly divide and express molecules such as cytokine proteins that help to fight infection. These responding cells are called effector T cells and they can migrate into inflamed tissues and kill infected cells. Once the pathogen has been eliminated, most effector cells die, but a small pool of long-lived memory cells remain. These cells are poised to respond rapidly if reinfection occurs. Which cells give rise to memory T cells has been extensively studied and has resulted in two proposed general possibilities (Farber *et al.,* 2014). The cells either arise from a subset of effector cells that escape death, or instead descend directly from naïve T cells, which could, as early as their first cell division, give rise to cells with effector-T-cell or memory-T-cell potential. Some of these memory cells circulate through the body, whilst others reside in tissues and provide the first line of defence against infection at sites where pathogens will often first enter the body.

1.2.2.3 T cell Activation

T cell activation is an antigen-dependent process (Smith-Garvin *et al.,* 2009). Antigen recognition by T cells triggers a cascade of events that produces expanded clones of differentiated effector cells. Each T cell is programmed to be specific for one particular antigen, which is recognised by their unique T cell receptor (TCR). Early activation, also referred to as T cell priming, is generated by the recognition of their specific antigen on the surface of antigen presenting cells (APCs) as they circulate through the body. APCs digest pathogens and display their fragment to the major histocompatibility complex (MHC) molecules. This initial recognition of their antigen begins the T cell activation and can lead to T cell activation, proliferation, differentiation, apoptosis, or cytokine release (Figure 1.2). This initial T cell activation normally takes place in the lymph nodes.

T cell activation requires two simultaneous signals: a primary and a coactivating signal. This leads to intracellular signal transduction cascades and new gene expression. The first signal is the binding of the TCR to an MHC molecule carrying a peptide antigen (Smith-Garvin *et al.,* 2009). T cell activation is initiated by interaction of the TCR-CD3 complex with a processed antigenic peptide bound to either a class I (CD8+) or class II

(CD4+) MHC molecules. The co-receptor CD4 or CD8 proteins on the T-cell surface form a complex with the CD3 protein, which can then recognise the MHC. These co-receptors act as cellular adhesion molecules that bind their respective MHC molecules and stabilise the interaction of T cells and APCs. This process guarantees antigen specificity of the T cell activation.

MHC binding alone is not sufficient to produce a T cell response. Those cells that lack the secondary costimulatory signal sends the cell into anergy. The second signal is provided by the binding of costimulatory molecules on the T cell binding to costimulatory proteins on the APC. One such interaction is B7 ligand binding by T cell costimulatory proteins, such as CD28. The lack of binding to a second signal result in the apoptosis of the cells. Because most native cells do not possess B7, this system prevents T cells from reacting to the host's own proteins.

Once the T cell has received a specific antigen signal and an appropriate secondary signal has been generated, it may receive additional signals that will ultimately determine what type of effector T cells it will become. These additional signals come in the form of cytokines. For example, CD4+ cells may differentiate into either Th1 or Th2 type cells depending on exposure to either IL-12 or IL-4, respectively. The resulting cell populations will then migrate to the site of inflammation where they will carry out their respective roles to eliminate the threat.

Upon entering the site of inflammation, each T cell population will again encounter their target antigen which will induce their effector response. CD8+ T cells recognise and bind antigen via MHC class I, which is present on all nucleated cells, therefore can become activated either by APCs present or antigen present on the target cell, such as tumour cells. Activation of cytotoxic (CD8) T cells can therefore results in the direct lysis of target cells through the production and release of cytotoxic granules directed through the immune synapse. Target cell death may also be induced by the ligation of death ligands on the T cell surface with their cognate death receptors on tumour cells. CD8+ T cells may also kill malignant cells via the secretion of cytokines, such as TNF-α and IFN-γ. A more detailed summary of lymphocyte cytotoxic effector function is discussed below

(see 1.2.3.1-.4). CD4+ T cell antigen recognition is mediated via MCH class II expression, which is restricted to antigen presenting cells, therefore activation of helper (CD4) T cells is normally mediated by these antigen presenting cells. This interaction induces multiple downstream effects including synthesis of important pro-inflammatory molecules (cytokines) such as tumour-necrosis factor; enhancement of antibody secretion by B cells, and enhanced killing by cytotoxic CD8 cells.

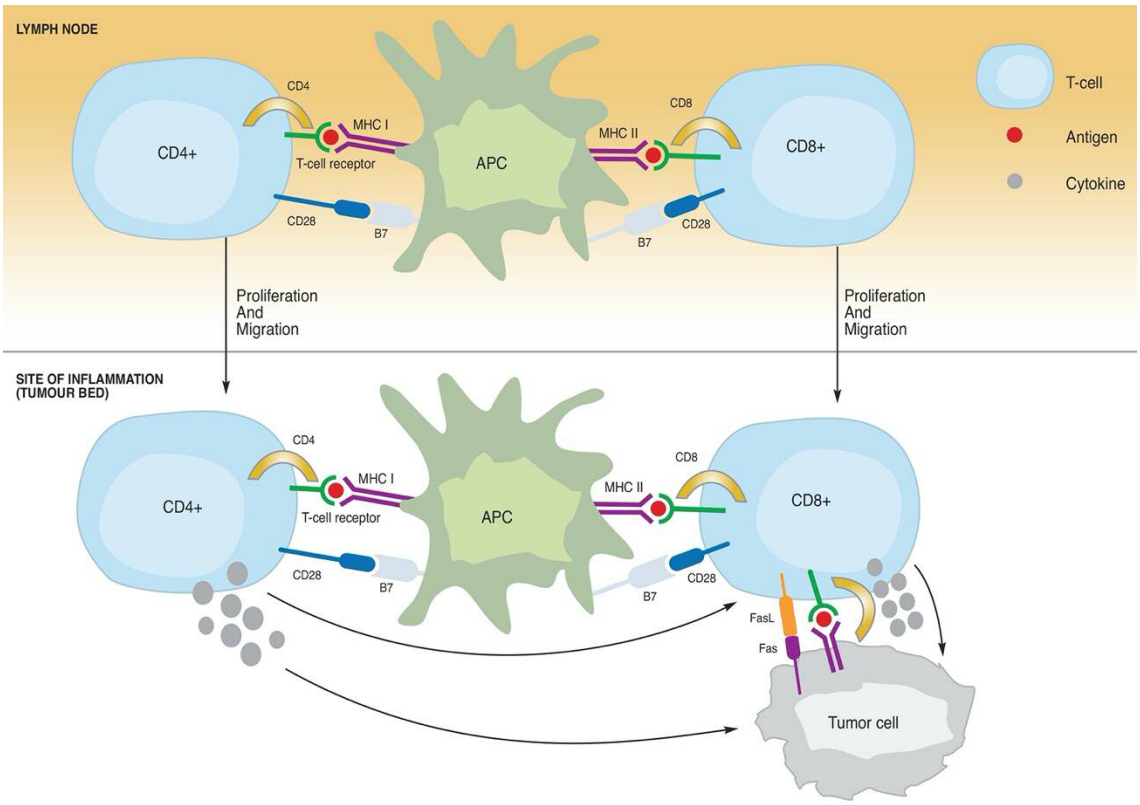

Figure 1.2: T cell activation. A T cell response is initiated with the recognition of antigen presented by APCs to the naïve T cell in the lymph node. CD8+ and CD4+ recognition of antigen is mediated via MHC I and MHC II, respectively. The antigen-MHC complex binds to the TCR, where CD4 or CD8 molecules stabilising the interaction. A second co-stimulatory signal is required to activate the T cell, such as B7 ligand binding by T cell costimulatory proteins, such as CD28. Once activated, these T cells begin proliferation and migration towards the site of inflammation. Here, the T cells bind their respective antigens and may begin an effector response.

T cell activation is a tightly regulated process that enables efficient and specific immune response. This response is regulated by a balance of receptors found on T cells.

1.2.2.3.1 T cell receptor

The T cell receptor (TCR) enables the T cell to recognise and respond to foreign or "non-self" material. The TCR is a disulphide-linked membrane heterodimeric protein, normally consisting of highly variable α and β chains expressed as part of a complex with the invariant CD3 chain molecules (Smith-Garvin *et al.,* 2009). T cells expressing these two chains are referred to as α:β (or αβ) T cells, though a minority of T cells express an alternate receptor, formed by variable γ and σ chains, referred as γσ T cells (Dudley *et al.,* 1995). TCR development occurs through a lymphocyte specific process of gene recombination, which results in the assembly of a final sequence. This determines the antigen to which the TCR will bind. This process generates a diverse recognition capacity.

1.2.2.3.1a Stimulatory Receptors

As discussed above, ligation of the TCR alone is not sufficient to elicit activation. For activation to occur, there must be ligation and induction of a second stimulatory event. Co-stimulatory receptors were originally described to share a common sequence motif called immunoreceptor tyrosine-based activation motif (ITAM) consisting of two YxxL amino acid sequences (where x corresponds to a variable region), separated by 7–12 amino acids (Isakov, 1997). This motif binds and interacts with protein tyrosine kinases via their src homology 2 domain (SH2), a prototypical signalling molecule, and leads to T cell activation (Chen and Flies, 2013). One of the best characterized co-stimulatory molecules expressed by T cells is CD28, which interacts with CD80 (B7.1) and CD86 (B7.2) on the membrane of APC. Besides the prototype co-stimulatory receptor CD28, T cells also express a variety of other co-stimulatory receptors.

1.2.2.3.1b Inhibitory Receptors

To prevent unwanted or prolonged T cell activation, activating receptors are balanced and inhibited by another set of receptors (Figure 1.3). Inhibitory receptors are co-inhibitory molecules that negatively interfere with T cell activation and function (Odorizzi and Wherry, 2012). These inhibitory receptors contain an inhibitory motif

(immunoreceptor tyrosine-based inhibitory motif, ITIM), which, like the ITAM motif, interacts with SH2 domains. Inhibitory receptors can interfere with T cell function at several levels: (i) through competition with co-stimulatory receptors for binding to shared ligands or interference in the formation of micro-clusters and lipid rafts, (ii) by interfering with downstream signals from co-activating and TCRs, and (iii) by upregulating genes that are involved in T cell dysfunction. The repertoire of co-signalling receptors expressed in T cells is highly versatile and responsive to changes in the tissue environment.

Two of the most well studied inhibitory receptors are programmed cell death 1 (PDCD1, also called PD1) and cytotoxic T lymphocyte-associated antigen 4 (CTLA-4), which are described in more detail below. These molecules are normally only expressed on T cells that have already been activated. Defects in these co-inhibitory receptors lead to aberrant immune responses, such as lymphoproliferation and autoimmunity (Zhang and Vignali, 2016).

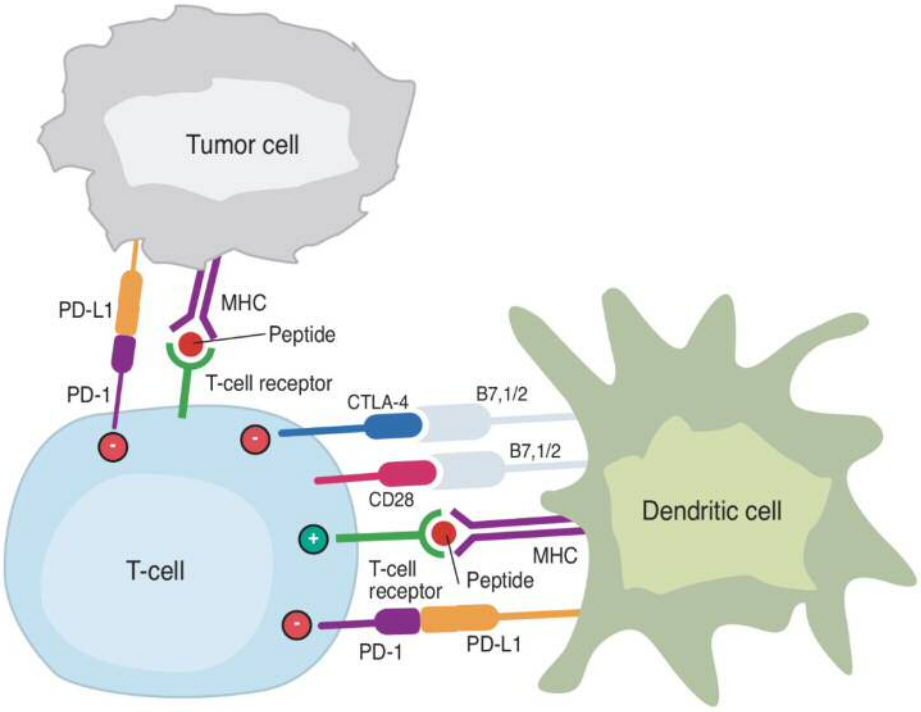

Figure 1.3: Co-inhibitory receptors inhibiting the activation of T cells. T cell activation requires two signals. The first signal is the binding of the TCR to an antigen presented by an MHC molecule, the second signal is provided by the binding of costimulatory molecules. This immune cell function is tightly controlled by a combination of co-stimulatory and co-inhibitory molecules

1.2.2.4 Natural Killer Cells

NK cells represent the third part of the lymphocyte family, constituting around 5-15% of circulating lymphocytes in healthy adults (Paul and Lal, 2017). There are many functional similarities between NK cells and T cells, particularly CD8+ T cells. However, the ways in which these two cell types develop in the body, detect defected cells and become activated are distinct.

1.2.2.4.1 NK cell development and maturation

NK cells were initially thought to develop in the bone marrow; however, it is now well accepted that they can also develop and mature in secondary lymphoid tissues, including tonsils, spleen and lymph nodes (Freud *et al.,* 2014). A subset of this early progenitor defined as pre-NK cell precursors (pre-NKPs) expresses the IL-2 receptor β chain (CD122) to become NKPs (Rosmaraki *et al.,* 2001; Abel *et al.,* 2018). HSC commitment to NK cell differentiation is governed by the integrated effects of various transcription factors and external signalling pathways, such as regulatory cytokines (Brillantes and Beaulieu, 2019).

Expression of CD122 (IL-2Rβ) marks the irreversible fate decision of CLPs into NK lineage (Abel *et al.,* 2018). Expression of CD56 (neural cell adhesion molecule) indicates a final transition of immature NK cell (iNK) into mature NK cells. Most of the iNK cells transition into a minor CD56bright population (~5%) that convert into major CD56dim (>90%) population. It is also suggested that iNK cells can directly give rise to CD56dim population. NK cells are distinguished by their unique functions and expression of surface antigens. These cells lack the clonotypic TCR of T and NKT cells and its associated signal-transducing adaptor, CD3.

1.2.2.4.2 NK cell subsets

Phenotypically, NK cells are defined by the expression of CD56 and the lack of CD3-TCR complex, identified as CD45+CD3-CD56+ (Sánchez *et al.,* 1993). They are further classified based on expression of CD16 and their relative expression of CD56, with five distinct sub-populations having been identified: (1) $CD56^{bright}$ CD16- (normally ~ 15% of NK cells), (2) $CD56^{bright}$ CD16+ (rare), (3) $CD56^{dim}$ CD16- (rare), (4) $CD56^{dim}$ CD16+ (~80%) and (5) CD56-CD16+ (rare) (Poli *et al.,* 2009). In healthy individuals, The $CD56^{dim}$ CD16+ population is predominant in peripheral blood, whereas NK cells from secondary lymphoid tissue and from other tissues are primarily $CD56^{bright}$, and populations (3) and (5) are in the minority. The cytotoxic activity of $CD56^{dim}$ NK cells is thought to be significantly higher than that of $CD56^{bright}$ NK cells, containing much more perforin, granzymes and cytolytic granules (Cooper *et al.,* 2001). Conversely, the $CD56^{bright}$ NK cells are the most efficient cytokine producers (Poli *et al.,* 2009).

1.2.2.4.3 Regulation of NK cell activation

Similar to T cells, NK cell stimulation and effector function is dependent upon the integration of signals derived from two distinct types of receptors - activating and inhibitory receptors (Paul and Lal, 2017). NK cells do not act on healthy, MHC class I-expressing cells. The MHC class I molecules act as ligands for inhibitory receptors. Downregulation of surface expression of MHC class I molecules leads to a lower inhibitory signal in NK cell, and is a mechanism by which NK cells are able to detect aberrant cells. The cellular stress associated with damaged cells, such as in viral infection or DNA damage in tumour cells, may also lead to the upregulation of ligands for activating receptors. As a result, the signal shifts from inhibitory to activating and consequently the elimination of the target cell (Figure 1.3).

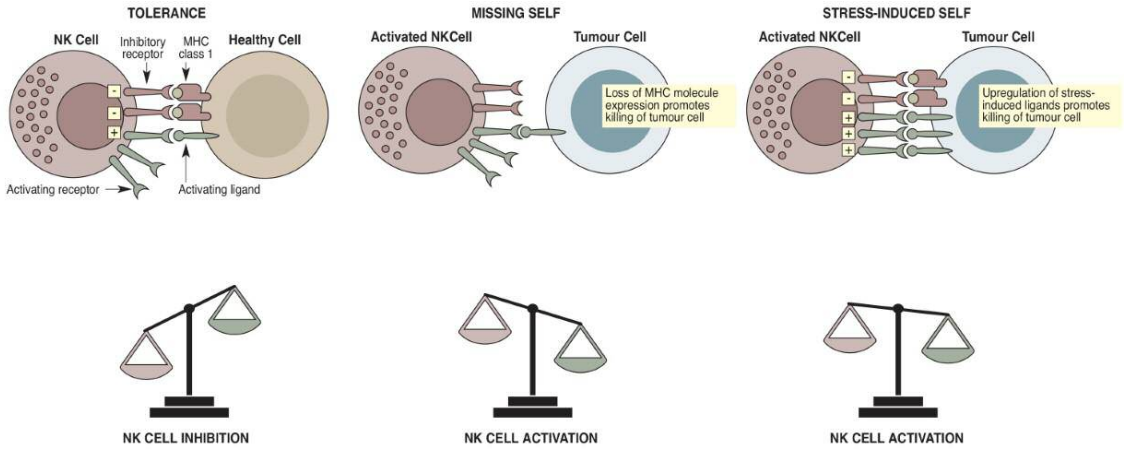

Figure 1.4: NK cell recognition of target tumour cell. Recognition of MHC class I molecules by inhibitory receptors induces an inhibitory signal and results in tolerance. Downregulation or loss of MHC expression on tumour cells reduces the inhibitory signal, activating the NK cell. NK cells may also become activated by cells that express MHC class I molecules but also express multiple activation ligands that overcomes the inhibitory signalling from the inhibitory receptors. Adapted from (Vivier *et al.,* 2012).

1.2.2.4.3a Inhibitory Receptors on NK cells

Similar to T cells, NK cell inhibitory receptors signal through ITIMs present in their cytoplasmic tail. These ITIMs undergo phosphorylation upon ligand binding, which in turn leads to the recruitment of phosphatases such as Src homology-containing tyrosine phosphatase 1 (SHP-1), SHP-2, and lipid phosphatase SH2 domain-containing inositol-5-phosphatase (SHIP). This leads to an inhibitory signal (Lanier, 2008). During NK cell inhibitory signalling, the phosphatases SHP-1 and SHP-2 dephosphorylate the ITAM-bearing Vav-1 molecules and prevent the downstream signalling.

NK cells sense MHC class I in two ways: by direct recognition of individual MHC class Ia alleles or by indirect recognition of an MHC class Ib allele complexed with peptides derived from class Ia molecules (Sternberg-Simon *et al.,* 2013). Inhibitory recognition of MHC class Ib molecules is performed by the NKG2A receptor in mice and humans, whilst direct recognition of MHC class Ia is recognised by killer immunoglobulin-like receptors

(KIRs). NKG2A (CD94-natural-killer group 2, member A) is expressed as a heterodimer and contains ITIM. This receptor family receptor specifically recognizes non-classical MHC molecules on target cells and protect host cells against inappropriate NK cell activation. Expression of this inhibitory protein has been shown to be modulated by various cytokines present in the tissue microenvironment, consequently affecting NK cell function. KIRs are a family of type I transmembrane proteins containing two or three IgG-like domains and a short or long cytoplasmic tail. These receptors bind to the peptide-binding region of the HLA-A, -B, and -C molecules. Inhibitory KIRs include KIR2DL1–3, KIR2DL5, and KIR3DL1–3, with heterogeneity seen among different individuals. A table of the main inhibitory receptors can be seen below (Table 1.1).

1.2.2.4.3b Activating Receptors on NK cells

Lack of MHC class I on the target cell is not sufficient to trigger NK cell activation (Paul and Lal, 2017). Full NK cell activation also requires recognition of stress-induced molecules by NK cell activating receptors. Unlike the inhibitory receptors, these activating receptors contain and signal though ITAMs. Upon ligand engagement, the ITAM is phosphorylated by Src family of tyrosine kinases and the subsequent recruitment and activation of the tyrosine kinase Syk and Zap70. This in turn leads to signalling though various pathways, such as activation of mitogen-activated protein kinases (MAPKs) and extracellular signal-regulated kinases (ERKs). The outcome of these signals result in the release of cytolytic granules and transcription of cytokine and chemokine genes (Paul and Lal, 2017).

The activating receptor natural-killer group 2, member D (NKG2D) and its ligands are the most extensively studied of the NK cell activating receptors. The receptor is also expressed by γδ T cells, NKT cells, and CD8+ T cells and under certain conditions, can be induced on some CD4+ T cells and some myeloid cells (Stojanovic *et al.,* 2018). Both humans and mice possess several genes that encode NKGD2 ligands and the regulation of expression of these proteins is complex, involving both transcriptional and posttranscriptional mechanisms in different cell types. NKG2D ligands are expressed at low levels in healthy adult cells in both mice and human, however, these ligands are upregulated and widely expressed in tumours of diverse tissue origin.

Natural cytotoxicity receptors (NCRs) are an immunoglobulin superfamily of activating receptors (Moretta *et al.,* 2000). Human NK cells express three distinct types of NCRs such as NKp46 (NCR1 or CD335), NKp44 (NCR2 or CD336), and NKp30 (NCR3 or CD337) while mouse NK cells express only NKp46. NKp46 and NKp30 are expressed on both resting and activated NK cells, whereas NKp44 expression is restricted to activated NK cells. NCRs have been proposed to bind many cellular ligands (Barrow *et al.,* 2019). The importance of these receptors in tumour immune surveillance has been demonstrated in several studies. In the absence of NKp46, the *in vivo* growth of lymphoma tumours was enhanced (Halfteck *at al.,* 2009). A table of the main activating receptors can be seen below (Table 1.1).

Table 1.1: NK cell receptors and their ligands.

Activating	Ligand	Inhibitory	Ligand
NKG2D	MIC-A/-B, ULBP1-4	KIR2DL1	HLA-C2
NKG2C	HLA-E	KIR2DL2	HLA-C1
KIR2DL4	HLA-G	KIR2DL3	HLA-C1
KIR2DS1	HLA-C2	KIR3DL1	HLA-Bw4
KIR2DS2	HLA-C1	KIR3DL2	HLA-A3, A-11
KIR2DS3	Unknown	KIR3DL3	Unknown
KIR2DS4	HLA-A11	KIR2DL5A	Unknown
KIR2DS5	Unknown	KIR2DL5B	Unknown
KIR3DS1	HLA-Bw4	NKR-P1A	LLTI
NKp30	B7H6, BAT3, BAG6	NKG2A	HLA-E
NKp44	PCNA, viral HA	ILT2 (CD85j)	HLA-1, -B, -C, -G1
NKp46	Heparin, viral HA	CD244 (2B4)	CD48
DNAM-1	CD112, -155	TIGIT	CD112, -113, -155

1.2.3 NK cell activity

Unlike T cells, which develop in the thymus and require prior sensitisation, NK cells are characterised by their inherent capacity to recognise and kill foreign, infected or malignant cells in the absence of MHC class I expression (Freud *et al.,* 2017). NK cells exert their immune function either though cytotoxic and/or effector means.

1.2.3.1 Cytotoxic Immune Response of NK cells

The process by which NK cells recognise target cells has been described above. Once recognised, the NK cells interact directly with the target cell. The interface between the NK cell and its target is termed the lytic immunological synapse and is formed by the close apposition of the surface membranes of the two cells. Upon receiving cues from activating receptors and the initiation of signalling cascades, the process of lytic granule exocytosis is initiated. This process is coordinated by a rearrangement of proteins to allow for lytic granules to fuse with the cell surface at the synapse. This process leads to the release of cytotoxic molecules such as perforin and granzyme, termed degranulation. This process is tightly regulated and highly ordered, where cell death is specific and unidirectional and ultimately ensuring that NK cells do not kill indiscriminately.

The NK cell cytotoxic response can be divided into four major steps (Topham and Hewitt, 2009):

I. Formation of immunological synapse (IS) between target and NK cell and the reorganisation of the actin skeleton
II. Polarisation of microtubule organisation centre (MTOC) and secretory lysosome toward lytic synapse
III. Docking of secretory lysosome with the plasma membrane of NK cells
IV. Fusion of secretory lysosome with the plasma membrane of target cells

V. Formation of immunological synapse between target and NK cell and the reorganisation of the actin skeleton

Upon recognition of a target cell, a lytic synapse (also known as an immunological synapse) develops at the point of contact between the target and NK cell (Orange *et al.,* 2003; Orange, 2007). This synapse is also known as the supramolecular activation cluster (SMAC), which is composed of concentric rings. In the centre is the central supramolecular activation complex (cSMAC), which contains receptors like the TCR, CD28, CD4, CD8 and CD2. The ring surrounding the cSMAC is called the peripheral supramolecular activation complex (pSMAC) and is mainly populated by adhesion molecules such as lymphocyte function-associated antigen (LFA-1). Outside of the pSMAC is the distal supramolecular activation complex (dSMAC). Upon recognition and contact with the target cell, adhesion molecules such as LFA-1 (CD11a/CD18) and Mac-1 (CD11b/CD18), segregate into an outer region of the synapse where they mediate the formation of a tight conjugate between the cells (Vyas *et al.,* 2001). These molecules also play an important role in the generation of initial activation cues. For example, LFA-1 signalling is required for the phosphorylation of several signalling molecules such as Src, LAT, PKCs, ERK1/2, and JNK (Perez *et al.,* 2004; Chen *et al.,* 2006). The cSMAC is thought to be the focal point for exocytosis of secretory lysosomes, similar to that observed in cytotoxic T lymphocytes (CTLs) (Stinchcombe and Griffiths, 2007).

VI. Polarisation of microtubule organisation centre and secretory lysosome toward lytic synapse

In this next stage, the microtubule-organising centre and secretory lysosomes become polarised towards the lytic synapse (Topham and Hewitt, 2009). Movement of the MTOC to the lytic synapse is thought to be a requisite for the polarisation of secretory lysosomes. It is thought that the secretory lysosomes move along microtubules in the dynein-dynactin complex-dependent manner to the lytic synapse as seen in CTLs. In this mechanism, secretory lysosomes are transported into close proximity with the plasma membrane as the MTOC moves towards the synapse and in CTLs, contacts the plasma membrane.

VII. Docking of secretory lysosome with the plasma membrane of NK cells

In this third stage, secretory lysosomes move into close proximity and docking to the plasma membrane. In CTLs, this docking requires the small GTPase Rab27a (Stinchcombe *et al.,* 2001). In CTLs that lack functional Rab27a, secretory lysosomes cluster around the MTOC but are unable to fuse with the plasma membrane. Although initial reports demonstrated that Rab27a is required for NK cell cytotoxicity, this GTPase is dispensable under certain circumstances for secretory lysosome exocytosis in NK cells. This suggests that there are both Rab27a-dependent and -independent pathways for exocytosis in NK cells. Myosin IIa is also required for the docking of secretory lysosomes with the plasma membrane. This protein is recruited to the lytic synapse on NK cell activation (Krzewski *et al.,* 2006).

VIII. Fusion of secretory lysosome with the plasma membrane of target cells

The final step of lytic granulation is the fusion of the secretory lysosomes with the plasma membrane at the lytic synapse. In this final stage of the process, the secretory lysosome mobilised to the lytic synapse fuse with the plasma membrane, which in turn enables the release of their cytotoxic content. Fusion between two cellular membranes in the exocytic and endocytic pathways is catalysed by soluble N-ethylmaleimide-sensitive factor attachment protein receptors (SNAREs) (Jahn and Scheller, 2006). SNAREs mediate membrane fusion by forming a highly stable SNARE complex comprising four conserved SNARE motifs across two membranes. These proteins are essential for degranulation of NK cells and mutations in several of these proteins has been linked to defective NK cell lytic granule exocytosis. NK cells do not release all of the polarised lytic granules at once and this is thought to be due to the fact that they are able to kill several target cells. This process leads to the fusion of secretory lysosomes with the plasma membrane where they release their cytotoxic contents in secretory lysosomes towards the target cell plasma membrane.

1.2.2.5.2 Lytic Granules

Lytic granules are often referred to as "secretory lysosomes" because of their similarities with lysosomes (Burkhardt *et al.,* 1990). Lysosomes are defined as membrane bound organelles that contain digestive enzymes. Their content is separated from the cytoplasm by a bi-layer membrane. They are composed of a variety of enzymes that are typical to lysosomes and well as containing proteins that are unique to lytic granules. Lytic granules include granzymes, perforin, Fas ligand (FasL; CD178), TNF-related apoptosis-inducing ligand (TRAIL; CD253), granulysin, and small anti-microbial peptides (Krzewski and Coligan, 2012).

1.2.2.5.2a Perforin/Granzyme Apoptosis Pathway

The perforin/granzyme apoptosis pathway is the primary mechanism used by cytotoxic lymphocytes to eliminate target cells. Granzymes are a family of structurally related serine proteases. There are five granzyme (Gr- A, B, H K and M) genes that have been identified in humans, with all being constitutively transcribed in NK cells (Ewen *et al.,* 2012; Salcedo *et al.,* 1993). Granzymes are synthesised as pro-enzymes and reach the lytic granules mainly through the mannose-6-phosphate receptor (MPR) pathway. Once in the granules, the granzymes are processed to an active form by cathepsin C and are packed tightly through complexing with serglycin. The mechanisms by which granzymes induce apoptosis is still an active area of research, with different granzymes known to cause target cell death by a variety of mechanisms. Perforin is essential in the lytic activity of cytotoxic lymphocytes (Voskoboinik *et al.,* 2010). This cytolytic protein functions by binding to the plasma membrane of the target cell and oligomerises in a Ca2+ dependent manner to form pores. These pores allow for the passive diffusion of a family of pro-apoptotic proteases (granzymes) into the target cell. Perforin is constitutively transcribed in NK cells, with higher levels found in the more mature $CD56^{dim}$ NK cells (Salcedo *et al.,* 1993).

1.2.2.5.2b Other contents of lytic granules

In addition to the secretion of components of the perforin/granzyme apoptosis pathway, other cell death inducing molecules have been found in the lytic granules of NK cells. FasL and TRAIL are pro-apoptotic molecules that have been found to localize to the lytic granules of NK cells (Bossi and Griffiths, 1999; Krzewski and Coligan, 2012). The mechanisms by which these molecules signal apoptosis to the target cell are discussed below.

1.2.2.5.3 Death receptor-mediated apoptosis pathways

Another process by which NK cells can induce apoptosis of target cells is through the activation of death receptors present on the surface of the target cell. Death receptors are members of the tumour necrosis receptor superfamily. The tumour necrosis factor (TNF) superfamily comprises of several plasma membrane receptors that share homology in their extracellular domains, which is characterised by the presence of up to six cysteine-rich domains (Guicciardi and Gores, 2009). Within this superfamily, death receptors, are characterised by a ~80 amino acid cytoplasmic sequence termed the death domain (DD), which enables them to initiate cytotoxic signals when engaged by cognate ligands.

The most extensively studied death receptors are Fas (CD95/APO-1), TNF-receptor 1 (TNF-R1/p55/CD120a), TNF-related apoptosis-inducing ligand receptor 1 (TRAIL-R1/Death Receptor 4 (DR4)), and receptor 2 (TRAIL-R2/DR5/APO-2/KILLER). Much less is known about two other DD-containing receptors, namely Death Receptors 3 (DR3/APO-3/TRAMP/WSL-1/LARD) and 6 (DR6), which are not potent inducers of apoptosis. Activation of Fas, TRAIL-R1, and TRAIL-R2 is often associated with cell death. Death receptors are activated by their cognate ligands, often referred to as death ligands. These are complementary cytokines that belong to the TNF protein family and are mainly expressed as type II transmembrane proteins. These proteins can often be released as soluble cytokines by proteolytic cleavage. The apoptosis-inducing capacity of these soluble forms is generally lower than compared to their corresponding membrane bound forms.

1.2.2.5.4 Death receptor signalling process

Death receptors share a signalling process (Guicciardi and Gores, 2009). Signal transduction is initiated by the binding of the cognate ligand to its receptor. This binding causes a conformational change in the preassembled receptor that leads to the recruitment of different adaptor proteins. Death receptors contain death domains within their cytoplasmic tail that, upon receptor activation, recruit intracellular death domain containing adaptors such as FAS-associated death domain (FADD) and TNFR-associated death domain (TRADD) (Hehlgans and Pfeffer, 2005). These adaptor proteins contain protein-binding motifs, which facilitate the generation of protein complexes and are essential in signal transduction pathways. In death receptor signalling, these proteins couple receptor ligation to the activation of cell death effectors, namely the initiator caspases (caspase-8 and caspase-10) and the long form of the cellular FLICE/caspase 8-like inhibitory protein (cFLIP). Binding of the ligand to its corresponding death receptor results in the formation of the death-inducing signalling complex, through the recruitment of adapter protein and initiator procaspase-8-10. Activation of caspase 8 and 10 initiate a proteolytic cascade and activation of the extrinsic apoptosis pathway (Figure 1.5).

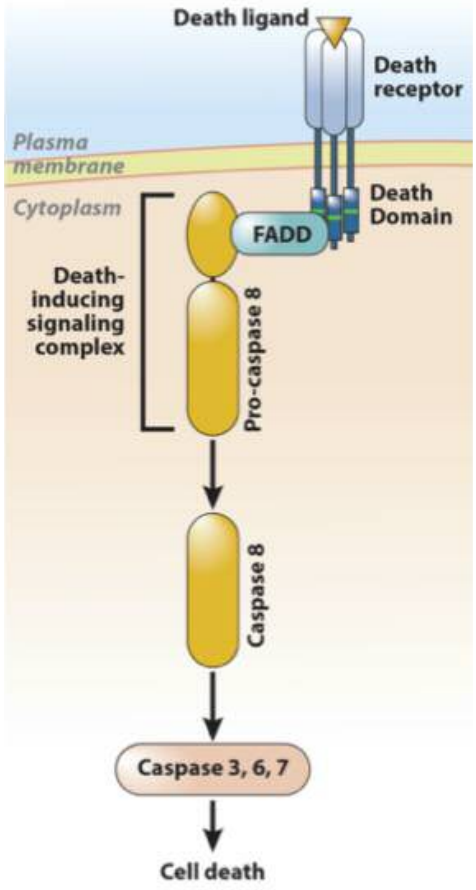

Figure 1.5: Cell death mediated death receptor signalling. Ligation of a death ligand results in the recruitment of adaptor proteins such as FADD to the intracellular death domain of the receptor. Adaptor protein associates with pro-caspase 8 to form a signalling platform termed the death-inducing signalling complex (DISC). Pro-caspase 8 then undergoes proteolytic cleavage autoactivation which in turn results in the activation of executioner caspases (3, 6, 7) and the inductions of apoptotic cell death.

Expression of death receptors and their ligands has been extensively documented on cells of the immune system. NK cells express TNF receptor ligands FasL, TNF and TRAIL. These ligands bind to their corresponding receptors on target cells, which inducing the apoptotic signal.

1.2.2.5.4a TRAIL

TRAIL is a type II transmembrane protein initially identified and cloned based on the sequence homology of its extracellular domain with FasL (Wang and El-Deiry, 2003). TRAIL is constitutively present in many tissues at the level of mRNA, but it is mainly expressed mainly by cells of the immune system. This ligand is especially expressed on NK cells, NKT cells, and macrophages (Falschlehner *et al.,* 2009). TRAIL induces apoptosis through interacting with its receptors. TRAIL interacts with five distinct receptors that are encoded by separate genes. There are four plasma membrane expressed TRAIL receptors, including DR4, KILLER/DR5, TRID/DcR1/TRAIL-R3, and TRAIL-R4/DcR2 as well as one soluble TRAIL receptor, (Osteoprotegerin) (Walczak, 2013). Both DR4 and DR5 contain the death domain and are capable of inducing apoptosis. Down regulation of these receptors on the cell surface of tumours has been characterised as a mechanism of tumour immune evasion and resistance to TRAIL-induced apoptosis.

1.2.2.5.4b Fas

Fas (also called CD95 or APO-1 or TNFRSF6) is a type I transmembrane protein that contains a death domain in its cytoplasmic region. The receptor is ubiquitously expressed but is particularly expressed in liver, heart, kidney, pancreas, brain, thymus, lymphoid tissues and activated mature T lymphocytes (Guicciardi and Gores, 2009). Whilst largely found as a plasma membrane-bound protein, soluble forms of the receptor lacking the transmembrane domain have been identified as a result of alternative splicing. This soluble form appears to have a negatively regulatory effect on the membrane-bound Fas, likely due to competitively binding to Fas ligand (FasL) (Hohlbaum *et al.,* 2000).

The Fas signalling pathway is activated upon ligation to its cognate ligands, FasL This protein was originally defined as a 40-kDa type II transmembrane protein belonging to the TNF family. The membrane bound form of FasL can be cleaved from the cell surface by metalloproteinases to produce a truncated soluble product (sFasL) of 26kDa, derived from the extracellular domain (Tanaka *et al.,* 1995). The activation of the Fas receptor leads to the stimulation of several signalling cascades: activation of caspase cascade,

activation of intrinsic apoptotic pathway mediated by mitochondria, and activation of JNK-cascade.

CTL and NK cells are known to express FasL during activation and exert granule-independent cytotoxicity via Fas/FasL interaction (Lynch *et al.,* 1995). This mechanism has been reported to play an important role in NK-tumour cell interaction (Zhu *et al.,* 2016).

1.2.2.5.4c TNF-R1 and TNF -α

The TNF/TNF-receptor signalling system consists of two distinct receptors, TNF-R1 and TNF-R2, and three ligands, the membrane-bound TNF-α (mTNF-α), the soluble TNF-α (sTNF-α), and the soluble lymphocyte-derived cytokine (LTα/TNF-β) (Wallach *et al.,* 1999; Guicciardi and Gores, 2009). Only TNF-R1 is considered a canonical death receptor, as TNR-R2 does not possess an intracellular death domain. Both TNF-R1 and TNF-R2 interact with the two TNF-α isoforms as well as with TNF-β, TNF-R1 is thought to be largely responsible for TNF signalling in most cells. TNF-α activation of TNFR2 enhances NK cell cytotoxicity and has also been activate the production of cytokines, such as seen in the increase of IFNγ production from IL-2-/IL-12-treated NK cells *in vitro* (Almishri *et al.,* 2016).

1.2.2.6 Effector immune response of NK cells

Activated NK cells secrete a wide variety of cytokines such as IFN-γ, TNF-α and IL-15, as well as chemokines such as CCL2, CCL3, CCL4, CCL5 and IL-8 (Fauriat *et al.,* 2010). NK cells are a major producer of IFN-γ, whose secretion plays a crucial role in antiviral, antibacterial, and antitumor activity. Production and secretion of this cytokine by NK cells has been linked to signalling through activating receptor NKG2D and the presence of IL-12 produced by other immune cells (Paul *et al.,* 2016). The role of IL-12 in activation of NK cells was illustrated by inhibition of tumour metastasis in a NKG2D and perforin-dependent manner with IL-12 treatment (Smyth *et al.,* 2004). In contrast, TGF-β inhibits the production of IFN-γ and TNF-α in NK cells (Bellone *et al.,* 1995). IL-15 is known to activate NK cell function and suppress tumour growth, which demonstrates that cytokine secretion by NK cells provide an additional activating signal (Carson *et al.,*

1994). Similarly, the cytokines secreted by other immune cells or stromal cells in the tumour microenvironment can positively or negatively influence the antitumor function of NK cells (Paul and Lal, 2017). NK cells also play a role in influencing the immune infiltrate by the secretion of chemokines that have been shown to induce the migration of both naïve and activated T cells (Roda *et al.,* 2006). These chemokines are important regulators of immune surveillance (Vilgelm and Richmond, 2019).

1.3 The immune response

An intact immune response includes contributions from many types of leukocytes. The immune response is divided into the innate and adaptive response (Chaplin, 2010). The first line of defence is the innate immune response, whose main purpose is to prevent the spread and movement of foreign pathogens throughout the body. These pathogens are recognised and processed by a number of immune cells that patrol the body, and include various phagocytes, such as macrophages and dendritic cells, that process the foreign antigen and initiate a further immune response. NK cells also play a role in the innate immune response, destroying infected host cells in order to stop the spread of an infection. A significant function of the innate immune response is to activate the second branch of the response, the adaptive immune response. The adaptive response is antigen specific, resulting in a directed response. The adaptive immune system consists of B and T cells. When a naïve lymphocyte recognises its antigen and receives appropriate stimulatory signals, it proliferates to create a clonal population. Once the danger has been resolved, a small proportion of the clonal cells, so-called 'memory' lymphocytes are maintained in case of re-infection. The purpose of an immune response is to detect an eliminate pathogens and cells that risk danger to the host. This includes eliminating aberrant tumour cells.

1.3.1 Immune surveillance of tumours

The concept that the immune system can recognise and eliminate emerging tumours has existed for over 100 years, with Paul Ehrlich one of the first to propose the idea that the immune system plays a role in suppressing emerging tumours (Ehrlich, 1909). This idea was later developed by Thomas and Burnet into the hypothesis of cancer immunosurveillance (Burnet, 1957). Evidence supporting the existence of cancer immunosurveillance in humans comes from the analysis of individuals with congenital or acquired immunodeficiencies or patients undergoing immunosuppressive therapy (Penn, 1988). There it documented an elevated incidence of virally induced malignancies such as Kaposi's sarcoma, non-Hodgkin's lymphoma, cutaneous squamous cell carcinoma and cancers of the anal and urogenital tracts when compared to immunocompetent individuals. Despite the evidence above supporting the existence of

a functional cancer immunosurveillance process, immunocompetent individuals still develop cancer.

1.3.2 The cancer-immunity cycle

An anti-cancer immune response is triggered by a series of events, which has been referred to as the cancer-immunity cycle (Chen and Mellman, 2013). The cycle begins with the neoantigens created by oncogenesis and the generation of mutated proteins that elicit an immune response by cells of the innate immune system. These tumour antigens are released and captured by antigen presenting cells (APCs), such as DCs. Uptake of the tumour antigen must be accompanied by signals that support the initiation of an immune response, such as the presence of proinflammatory cytokines. These APCs then migrate to the lymph nodes, activating the adaptive arm of the immune response. The APCs then present the captured antigens on MHC I and MHC II molecules to T cells and an effector T cell response against the tumour. These T cells then traffic and infiltrate the tumour bed where they specifically recognise and bind to tumour cells through interaction with the TCR. The cycle ends with the killing of the tumour cell. Killing of the tumour cells results in additional release of tumour antigens, which initiates the cycle again, increase the breadth and depth of the response in subsequent revolutions.

This cancer-immunity cycle does not perform optimally in cancer patients. The cycle can be hindered at various stages. Tumour antigens may not be detected, antigens detected may be treated as “self” and induce a Treg response, those T cells that do become activated may be inhibited from infiltrating the tumour bed and/or could be directly suppressed by factors in the tumour microenvironment. Interactions between the tumour and their environment ultimately determine whether the primary tumour is eradicated, metastasises or remains dormant. The threshold that must be overcome to generate effective cancer immunity has been termed the cancer-immune set point (Chen and Mellman, 2017). This set point is determined by the contribution of stimulatory factors and the inhibitory factors.

1.3.4 Cancer immunoediting

Cancer immunoediting is the process by which the immune system can both constrain and promote tumour development (Dunn *et al.,* 2002). The tumour immunoediting concept is divided into 3 phases: elimination, equilibrium, and escape (Dunn *et al.,* 2004). Throughout these phases, tumour immunogenicity is edited and immunosuppressive mechanisms that enable disease progression are acquired.

1.3.4.1 Elimination

The elimination phase represents the original concept of cancer immunosurveillance. In this phase, the innate and adaptive immunity work together to destroy developing tumours that have escaped intrinsic tumour suppression, eliminating them before they become clinically apparent. The anti-tumour immune response is initiated when cells of the innate system become alerted to the presence of an emerging tumour. Once recruited to the tumour, cells such as macrophages and NK cells may recognise molecules, such as ligand for the NKG2D, that have that have been induced on tumour cells either by the incipient inflammation or the cellular transformation process itself. Recognition of the tumour results in the progression and amplification of the immune response, through the production of cytokines and chemokines that recruit more cells of the innate system to the tumour. This response is maintained by a positive feedback loop of cytokine production between different immune cells. The process results in the killing of a proportion of the tumour and a source of tumour antigens from dead tumour cells becomes available and the adaptive immune system is recruited into the process. Activated, antigen-bearing mature DCs then migrate to the draining lymph node, where they induce the activation of naïve tumour-specific Th1 CD4+ T cells. Th1 cells facilitate the development of tumour-specific CD8+ CTL induced via cross-presentation of antigenic tumour peptides on DC MHC class I molecules. Tumour-specific CD4+ and CD8+ T cells home to the tumour site, where they participate in the killing of antigen-positive tumour cells. The development of a tumour-specific adaptive immunity provides the host with the capacity to eliminate the tumour. If tumour cell destruction occurs, elimination constitutes the totality of the immunoediting process.

1.3.4.2 Equilibrium

In the equilibrium phase, tumour cell variants that were not destroyed in the elimination phase, enter a dynamic equilibrium. Here, the tumour mass is contained as the outgrowth is prevented by immunologic mechanisms, but the cells have not been fully extinguished. The tumour may contain genetically unstable and mutating tumours. The selective pressure from the adaptive immune system coupled with this genetic instability can select for tumour subclones with reduced immunogenicity that can evade immune recognition and destruction. The equilibrium phase may occur over a period of many years.

1.3.4.3 Escape

The immune-edited tumours with reduced immunogenicity can then enter into the escape phase. These selected tumour cell variants can now grow in an immunologically intact environment, where their growth is unrestrained. These tumours are likely to be capable of evading both the innate and adaptive immune system. Tumours may employ multiple immunosuppressive strategies. Tumour have been shown to indirectly impede the development of antitumor immune responses either through the elaboration of immunosuppressive cytokines (such as TGF-β and IL-10) or via mechanisms involving T cells with immunosuppressive activities (i.e., Tregs) (Rabinovich *et al.,* 2007). They have also been shown to escape through changes that occur directly at the level of the tumour, such as alterations that affect tumour recognition by immune effector cells, such as such as loss of antigen expression, development of IFN-γ and expression of immune inhibitory ligands, immune checkpoints. The growth of a tumour mass during this phase results in the disease becoming clinically apparent.

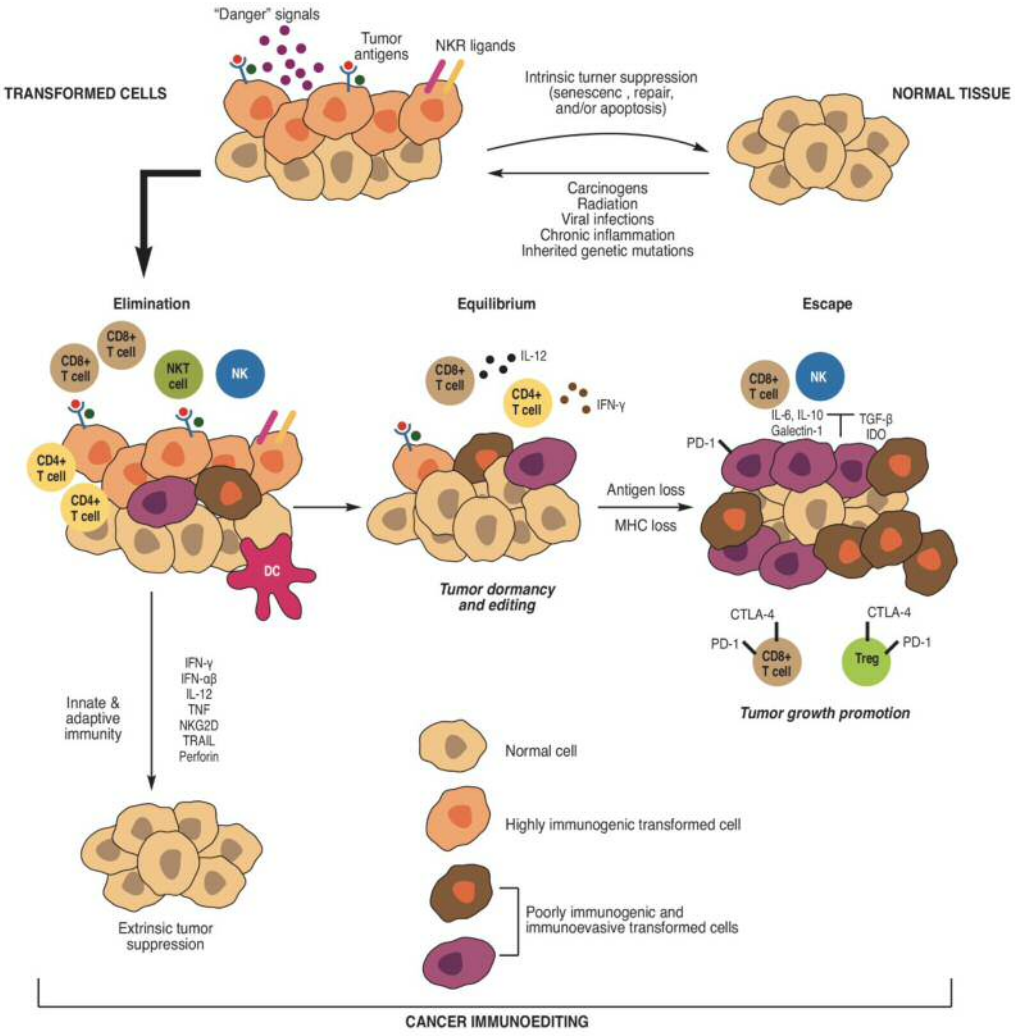

Figure 1.6: The concept of immunoediting and its three phases - elimination, equilibrium, and escape. Adapted from (Vesely *et al.,* 2011)

1.3.5 Immunosuppressive strategies employed by cancer cells

Cancer cells display multiple immunosuppressive mechanisms to evade an immune response, either by avoiding immune recognition or by disabling effector cell function. These include alterations of components of the antigen presentation machinery, defects in proximal TCR signalling, secretion of immunosuppressive and proapoptotic factors, activation of negative regulatory pathways and specific recruitment of regulatory cell populations (Rabinovich *et al.,* 2007).

1.3.5.1 Antigen presentation

Impaired antigen presentation is one of the best studied mechanisms used by tumours to evade recognition and ultimately, destruction. The generation and selection of tumour cells with reduced immunogenicity has been described above. Downregulation of the antigen processing machinery has been documented in a variety of tumours and has been considered as the most common strategy exploited by tumours cells to escape T-cell control (Drake *et al.*, 2006). Downregulation or the complete absence of MHC molecules caused my mutations or alterations prevents recognition by CTLs. Additional loss of HLA alleles has also been reported, facilitating evasion of T cell responses (Rodríguez, 2017). Whilst downregulation of MHC molecules may in turn sensitise NK cells to attack, tumour cells have been reported to display additional or alternative mechanisms to evade NK cell mediated recognition.

1.3.5.2 TCR mediated signalling

Defects in T cell signalling has been detected in different types of tumours. Mutations and/or the reduction in TCR elements have been shown to impair TCR signalling, inhibiting lytic function. Circulating T cells in patients with cancer are often found with low or absent expression of the TCR-associated ζ chain (Whiteside, 2004). The tumour microenvironment is thought to affect TCR signalling in infiltrating T cells. For example, it is hypothesised that the high TGF-β levels in the environment induce the downregulation of TCR components and signalling molecules such as ZAP70, and CD3-ζ chains, which results in an insufficient T cell signal transduction (di Bari *et al.,* 2009). Defects in this signalling has been observed clinically in CTLs and NK cells from patients

with melanoma, colon, breast and prostate carcinoma (Whiteside, 1999; Whiteside, 2006).

1.3.5.3 Secretion of immunoregulatory cytokines

A number of biologically active agents secreted by both the tumour and the surrounding stroma have been shown to exert a suppressive effect on the immune system. TGF-β is a pleiotropic cytokine that has been shown to have immunosuppressive effects on T cells, inhibiting their activation, proliferation and differentiation. TGF-β acts on CTLs to specifically repress the expression of different cytolytic gene products; namely perforin, granzyme A, granzyme B, FasL and IFN-γ, which are collectively responsible for CTL-mediated tumour cytotoxicity (Thomas and Massagué, 2005). Antibody mediated neutralisation of TGF-β has been shown to restore genes in tumour-specific CTLs, leading to tumour clearance *in vivo.* Elevated levels of serum TGF-β have been associated with poor prognosis in a number of malignancies. In addition to TGF-β, a number of other cytokines in the TME have been shown to impair the anti-tumour immune response. Several inflammatory mediators, such as TNF-α, IL-6, and IL-10, have been shown to participate in both the initiation and progression of cancer.

1.3.5.4 Negative costimulatory pathways

As earlier described, immune cell activation is regulated by a balance between co-stimulatory and co-inhibitory signals. In order for the immune cell to become activated, the balance of these signals must favour the stimulatory signal. In cancer, however, the signal is often tilted towards an inhibitory signal and thus downregulating and/or inhibiting the required anti-tumour immune response. Investigation into manipulating these signals has gained much interest.

1.4 Immune checkpoints

Maintaining immune homeostasis is critical for host survival. As discussed above, the activation of an immune response is regulated by a balance between co-stimulatory and inhibitory signals. These signals are collectively referred to as immune checkpoints, with several of these having been identified. As the primary mediators of immune effector functions, T cells express multiple co-inhibitory receptors. The two most well studied are the programmed cell death protein 1 (PD-1) and cytotoxic T-lymphocyte-associated protein 4 (CTLA-4). These immune checkpoints have been shown to module T cell responses. Targeting these pathways to encourage or restore the anti-tumour response has proved a successful approach to cancer therapy. A full list of the current approved immune checkpoint inhibitors for the treatment can be seen below (Table 1.2).

Table 1.2: Approved CTLA-4 and PD-1/PD-L1 inhibitor drugs for the treatment of cancer. Adapted from (Rotte, 2019)

Drug	Use
CTLA-4 inhibtors	
Ipilimumab	As monotherapy for metastatic melanoma and surgically resectable 'high-risk' melanoma (adjuvant setting)
PD-1 inhibitors	
Nivolumab	Metastatic melanoma, metastatic non-small-cell lung cancer (NSCLC), renal cell carcinoma (RCC), classical Hodgkin's lymphoma, head and neck squamous cell carcinoma (HNSCC), metastatic urothelial carcinoma, hepatocellular carcinoma (HCC), colorectal cancer
Pembrolizumab	Metastatic melanoma, surgically resectable 'high-risk' melanoma (adjuvant setting), metastatic NSCLC, classical Hodgkin's lymphoma, primary mediastinal B-cell lymphoma (PMBCL), HNSCC, gastric cancer, solid tumours with MSI-H and MMR aberrations, metastatic urothelial carcinoma, Merkel cell carcinoma, RCC, cervical cancer, hepatocellular carcinoma, high-risk bladder cancer, head and neck cancer, metastatic small cell lung cancer, advanced oesophageal squamous cell cancer, advanced endometrial carcinoma
Cemiplimab	Metastatic cutaneous squamous cell carcinoma (CSCC) or locally advanced CSCC who are not candidates for curative surgery or curative radiation
PD-L1 inhibitors	
Atezolizumab	Metastatic urothelial carcinoma, metastatic NSCLC (monotherapy and in combination with chemotherapy), metastatic SCLC (in combination with chemotherapy) and metastatic triple negative breast cancer (in combination with paclitaxel)
Avelumab	Merkel cell carcinoma, metastatic urothelial carcinoma, advanced RCC
Durvalumab	Metastatic urothelial carcinoma, unresectable stage III NSCLC
Combination of CTLA-4 and PD-1 inhibitors	
Ipilimumab plus nivolumab	Metastatic melanoma, metastatic RCC, colorectal cancer

1.4.1 CTLA-4 (cluster of differentiation 152, CD152)

The mechanism by which CTLA-4 inhibits T cell activity has been extensively characterised. CTLA-4 is not detectable in naïve T cells but is rapidly induced upon T cell activation. In resting naïve T cells, CTLA-4 is an intracellular protein, which upon engagement of the TCR and the co-stimulatory signal through CD28, translocates to the cell surface (Linsley *et al.,* 1996). At the surface, CTLA-4 binds to ligands CD80 and CD86 on antigen presenting cells, competing with the CD28 receptor. CTLA-4 receptors bind to B7 ligands with higher affinity and at a lower surface density and thereby outcompete CD28 receptors for binding with B7 ligands. The relative amount of CD28:B7 binding versus CTLA-4:B7 binding determines whether a T cell will undergo activation or anergy. This results in the lack of secondary activation signal required for the activation of T cells and leads to anergy of that T cell. Unlike in the case of conventional T cells, Treg cells express CTLA-4 constitutively on the cell surface. This is thought to be important for their suppressive functions (Takahashi *et al.,* 2000). CTLA4 engagement has been reported to inhibit IL-2 production, block T cell proliferation and induce cell cycle arrest (Gatta *et al.,* 2002). The aim of this co-inhibitor is thought to be the minimisation of damage to normal tissue from unwanted immunity. Engagement of this receptor has also been shown to lead to TGF-β production in CD4+ T cells (Chen *et al.,* 1998).

The exact mechanism by which anti-CTLA4 antibodies induce an anti-tumour immune response is unclear. It is thought that blocking CTLA-4 affects the immune priming phase, supporting the activation and proliferation of effector T cells and simultaneously reducing Treg-mediated suppression of T-cell responses. Anti-CTLA-4 blockade with ipilimumab was the first FDA approved treatment to prolong overall survival in patients with advanced melanoma in 2011 (Hodi *et al.,* 2010; Lipson and Drake, 2011). This inhibitor has since been approved for the treatment of other cancer types (Table 1.2).

1.4.2 PD-1/PD-L1 axis

PD-1 (PDCD1 or CD279) is a cell surface receptor commonly seen on T cells, B cells and NK cells. The engagement of PD-1 by its ligands results in the recruitment of Src homology 2 (SH2) domain containing phosphatases 1/2 (SHP1/2) and then inhibits T cell proliferation and cytokine secretion mediated by TCR (Sharpe and Pauken, 2018). PD-L1 (B7-H1 or CD274) and PD-L2 (B7-DC or CD273) are the two ligands for PD-1. They are members of the B7 family of type I transmembrane protein receptors. PD-L1 is broadly expressed by many somatic cells whilst PD-L2 has a more restricted expression in APCs. The intracellular domain of PD-L1 is short comprising of 30 amino acids, and there is no known function for this domain. Inflammation-induced PD-L1 expression in the tumour microenvironment results in PD-1–mediated T cell exhaustion, inhibiting the antitumor cytotoxic T cell response (Alsaab *et al.,* 2017). In addition to inhibiting the activation of T cells, PD-1 can promote T lymphocytes apoptosis, as observed in various cancer types (Shi *et al.,* 2011; Chiu *et al.,* 2018). Reactive PD-L1 expression is stimulated by proinflammatory cytokines, including IFN-γ (Mimura *et al.,* 2018; Bazhin *et al.,* 2018). As we have previously described, triggering of the TCR results in the production of these cytokines. These cytokines have been implicated in upregulating the expression of PD-L1 on tumour cells. This in turn leads to the inhibition of interacting lymphocytes and contributes to tumour immune evasion. Therapies targeting both the PD-1 receptor and its ligand, PD-L1 have shown great success in several cancer types (Table 1.2).

1.4.3 Alternative immune checkpoints

The success of these immune checkpoint inhibitors for the treatment of patients with various cancer types has led to the interest in identifying and characterising alternative immune checkpoints (Figure 1.5). Other well characterised immune checkpoints include lymphocyte activation gene-3 (LAG-3), T cell immunoglobulin and mucin domain 3 (TIM-3) and V-domain immunoglobulin-containing suppressor of T-cell activation (VISTA) (Wei *et al.,* 2018). One such immune checkpoint that has been studied in relation to cancer immune evasion is CD200.

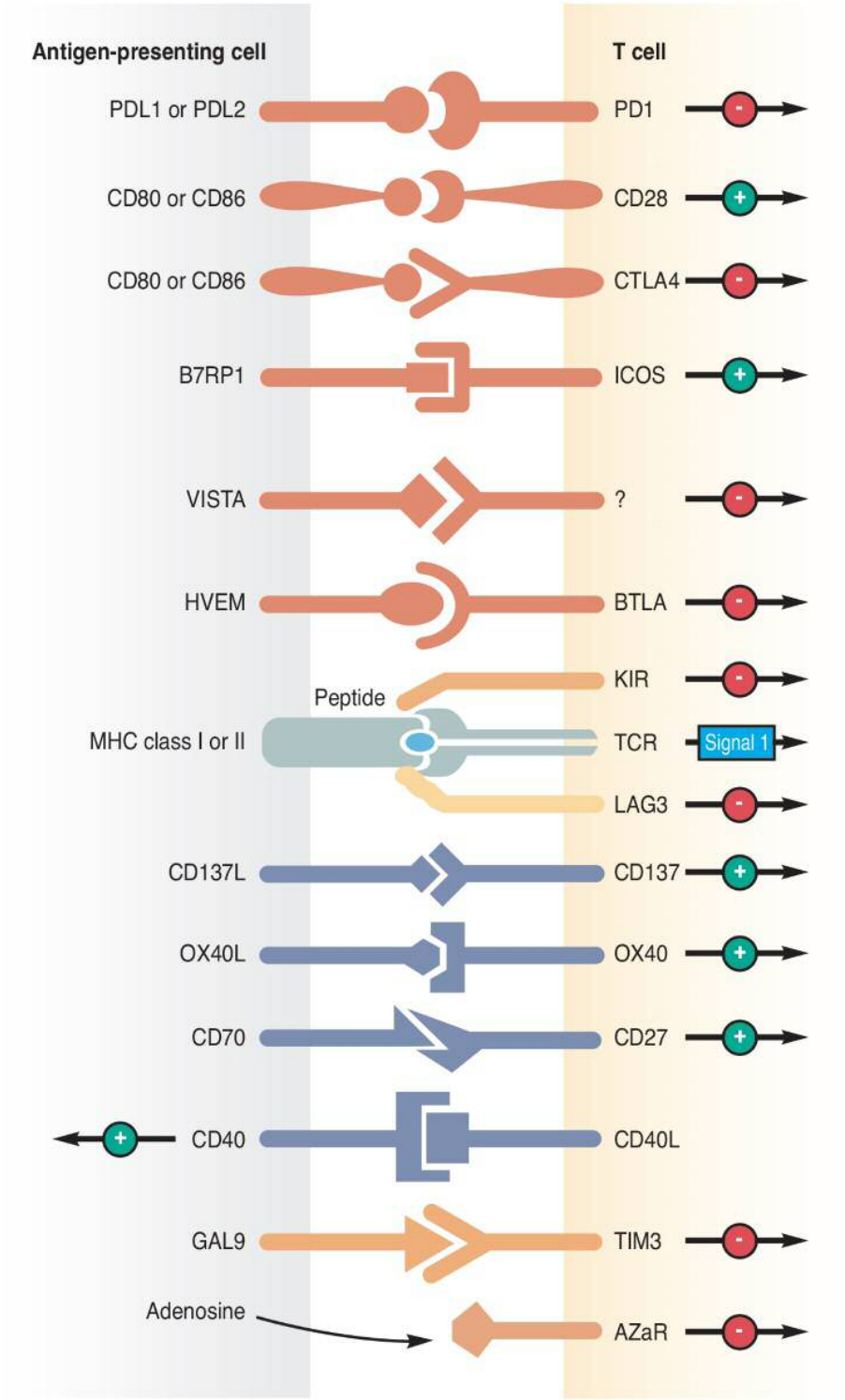

Figure 1.7: The various ligand-receptor interactions between T cells and antigen presenting cells. In addition to TCR binding, T cell activation is regulated by a balance of co-stimulatory and co-inhibitory signals, collectively referred to as immune checkpoints. Adapted from (Pardoll, 2012).

1.5 OX-2 membrane glycoprotein, CD200

1.5.1 CD200 ligand

OX-2 membrane glycoprotein, also named CD200 (cluster of differentiation 200), is a highly conserved transmembrane glycoprotein and member of the Ig superfamily (IgSF) of protein. It contains two intracellular immunoglobulin domains and a small 19 amino acid intracellular domain, with no known signalling motifs. CD200 was first characterised in rat in 1982, as a 41- to 47-kDa cell-surface glycoprotein (Barclay and Ward, 1982). Its expression was reported on multiple cell types including thymocytes, B cells, activated T cells, follicular dendritic cells, skin and cells in the central nervous system (CNS), and reproductive organs. Subsequent studies showed that its distribution was relatively conserved across species consistent with the molecule having an important biological function. Production of a of recombinant human OX-2 protein, its use in raising a mAb (OX-104) that recognizes native human OX-2 was used to generate an anti-humanCD200 monoclonal antibody, which was used to show that patterns of CD200 expression are highly conserved between rodents and humans and is thought to be expressed in "immune-privileged" sites (Wright *et al.,* 2003). CD200 is structurally similar to co-stimulatory molecules B7.1 and B7.2, and it was therefore suggested that CD200 may play both stimulatory and tolerogenic roles in antigen presentation (Boriello *et al.,* 1997).

1.5.2 CD200 Receptor

The lack of any signalling motif in the CD200 protein suggested that CD200 functions through engaging a receptor. The cell surface CD200 receptor (CD200R) was identified through studies using an antibody that blocked CD200 binding to macrophages. CD200R has a similar structure to CD200, containing two IgSF domains, but has a longer cytoplasmic domain and thus has a potential signalling capacity. Other members of the CD200R family have also been identified, however these homologues were found to have short, non-signalling cytoplasmic tails, though may bind ligands.

The identification of CD200R in humans came from analysing the NCBI database for the sequence encoding for the rat CD200R and has been confirmed in subsequent studies. The human CD200R gene was found to share 53% amino acid identity with rCD200R,

and 52% identity with mCD200R1. Two isoforms of CD200R were transcribed due to the insertion of exon 5, with one encoding a cell surface receptor, and one a truncated soluble protein. Each transcript was also alternatively spliced at exon 2 resulting in the generation of four different CD200R isoforms. mRNA transcripts for the four CD200R isoforms were identified in the thymus, spleen, liver and placenta (Vieites *et al.,* 2003). Only CD200R1 expressed the long cytoplasmic tail, with alternate CD200Rs containing a short cytoplasmic region (Wright *et al.,* 2003; Gorczynski *et al.,* 2004). It was felt that the alternate CD200Rs might use a different ligand (to CD200) and thus exert a different function to CD200R1 (Hatherley *et al.,* 2005).

This protein also contains two immunoglobulin domains, but unlike CD200, has a large cytoplasmic tail that contains tyrosines. Unlike most other inhibitory receptors, CD200R does not contain an ITIMs. ITIMs mediate cellular inhibition through the phosphorylation-dependent recruitment of the protein tyrosine phosphatases, which in turn suppress cell activation by promoting dephosphorylation of activating receptors and downstream signalling molecules. Instead, CD200R contains an NPXY sequence in its cytoplasmic domain (Smith *et al.,* 2006). This motif has been shown to be a binding site for proteins with a phosphotyrosine-binding (PTB) domain. The CD200R cytoplasmic tail contains three tyrosine residues, Y286, Y289, and Y297 that can be phosphorylated (Zhang and Phillips, 2006). The third most membrane distal residue (Y297) contains the NPXY sequence. CD200R is expressed several immune subtypes including those of the myeloid lineage, T cells, neutrophils, monocytes, basophils and NK cells. In the CNS, expression is restricted to microglia and PBMCs.

1.5.3 CD200 Receptor Signalling

The specificity of CD200 binding to CD200R was determined using an anti-CD200R antibody and CD200 has been shown to bind CD200R with a binding affinity of ~0.5 µM (Wright *et al.,* 2003). The CD200 receptor signalling pathway has been well characterised for myeloid cells (Zhang *et al.,* 2004; Zhang and Phillips, 2006). Upon CD200:CD200R binding, the third tyrosine residue becomes phosphorylated, which in turn binds the PTB domain proteins Dok1 and Dok2. Dok proteins have been shown to mediate inhibitory signalling by recruiting inhibitory effectors such as RasGAP, SHIP, and Csk. In CD200R,

Dok proteins recruit RasGAP and SHIP. This signalling leads to an inhibition of the Ras/MAPK pathways, as early as one minute after ligation. An inhibition of the p38 MAPK and JNK activation can also be seen upon ligation of CD200R, however, the molecules involved in this remain unclear. This inhibition ultimately leads to the functional reduction in mast cell degranulation and cytokine secretion.

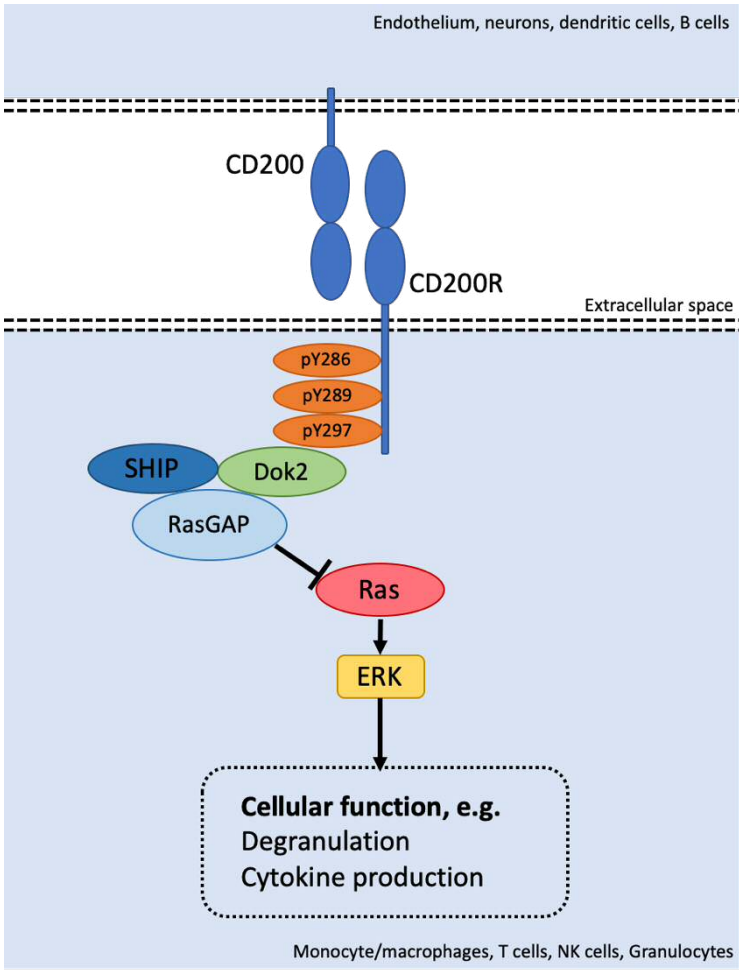

Figure 1.8: Illustration of CD200R signalling upon binding its cognate ligand CD200. Both proteins transverse the cell membrane with a single transmembrane domain and express two extracellular IgSF domains. CD200 has no known signalling motif but the CD200R has three conserved tyrosine residues in its cytoplasmic tail. Upon ligand binding the third tyrosine, pY297, becomes phosphorylated and recruits Dok2, which signals by recruiting inhibitory effectors RasGAP and SHIP. This signalling leads to an inhibition of the Ras/MAPK pathways and reduces immune cell function.

1.5.4 Immunosuppressive activities of CD200

Evidence that CD200 demonstrated immunosuppressive properties *in vivo* came from CD200 knock out mice studies (Hoek *et al.,* 2000). The first reported the *CD200*$^{-/-}$ mouse was found to have a normal appearance, fertility and lifespan. The importance of this protein in immune regulation was highlighted by the elevation in activated macrophages and aggregates of activated microglia (the macrophages of the CNS) in the *CD200*$^{-/-}$ mice. These mice were found to have phenotypic changes in the microglia of the brain that were suggestive of increased endogenous activation. It was suggested that the lack of CD200 led to the persistent activation of myeloid cells. This immunological role was further highlighted in these knock out mouse models using a facial nerve transection model. Facial nerve transection results in microglial activation in healthy animals but this activation is markedly accelerated in *CD200*$^{-/-}$ mice. In these mice there was also an increased incidence and more severe pathology of collagen-induced arthritis (CIA), a murine model of rheumatoid arthritis, suggesting a hyperactivation of T cells, the principal initiators of these diseases (Wright *et al.,* 2000).

The CD200:CD200R interaction is now considered a mechanism by which macrophage activity is controlled, that ultimately prevents severe inflammatory responses. In highly antigenic areas, such as the alveolar, murine macrophages were found to express higher basal levels of CD200R (Snelgrove *et al.,* 2008). These macrophages rapidly upregulate CD200R expression in response to stimulation by IL-10 and TGFβ and during influenza infection. Lung epithelial cells from the alveolar space express CD200, which induced excessive cytokine secretion from *CD200R1*$^{-/-}$ alveolar macrophages in comparison to those from wild-type (WT) mice. Upon influenza infection, the level of CD200 expressed by CD4+ and CD8+ T cells in both the lung and in the lymph nodes increased. These mice also suffered a greater pathology and severity of disease, associated with greater inflammation and macrophage and T cell activity. Interestingly, the viral tire was similar between WT and *CD200R1*$^{-/-}$ mice. Conversely, administering soluble CD200:Fc protein to WT animals reduced disease severity and infiltrating numbers of T cells.

The CD200:CD200R interaction has also been investigated in lymphocytes. Differential expression of the CD200R has been found on T cell subsets (Rijkers *et al.,* 2007). In both mice and humans, CD4+ T cells were observed to express higher amounts of the receptor that CD8+ T cells. The greatest amounts of CD200R1 expressed on memory cells and upregulation of expression on both CD4+ and CD8+ T cells after stimulation *in vitro*. CD200R was also observed on mouse and human B cells, however, knockout of CD200 did not appear to affect their function upon an antigenic challenge. The functional implications of B cell expression of the CD200R therefore remains unclear (Gorczynski, 2012). CD200 is now considered an immunosuppressive ligand, regulating the activity of various immune cell types.

1.5.5 Soluble CD200

Many cell surface molecules with inflammatory functions are also found as a soluble form in serum. The soluble forms of these cell-surface receptors and ligands may be generated by alternative splicing at the mRNA level or following either release as exosomes from the cell surface or by enzymatic cleavage by membrane-anchored proteins disintegrin and metalloprotease domains (ADAMs). The existence of a soluble form of CD200 (sCD200) has been identified in proliferative diabetic retinopathy, type 2 diabetes and several cancer types (Xu *et al.,* 2015; Wong *et al.,* 2009). The existence of a soluble form of CD200 (sCD200), with immunosuppressive properties, was found in the serum of patients with chronic lymphocytic leukaemia (CLL). Increased sCD200 in patients correlated with tumour burden, late stage disease, and disease aggressiveness. Subsequent studies in CLL identified that CD200 was shed from the cell surface, with ADAM28 playing an important role in the ectodomain shedding of the protein (Wong *et al.,* 2016). Using CD200R stably transfected Hek293 cells, it was demonstrated that the sCD200 detected in CLL patient plasma lacked the cytoplasmic domain of CD200 but retained the functional extracellular domain required for binding to, and phosphorylation of, CD200R. This data demonstrated that functionally active CD200 can be shed from the surface of cells.

1.5.6 Soluble recombinant CD200 proteins

Much of the data generated on the properties and function of CD200 are based on observations of the activities of CD200Fc fusion proteins. The fusion of proteins to the Fc domain of human immunoglobulin G1 (IgG1) molecule is used therapeutically to confer a longer half-life of the protein (Kamei *et al.,* 2005). The fusion protein however often has a reduced biological activity when compared to the native protein at the same concentration *in vivo*. In murine CIA models, repeated infusion of mCD200Fc fusion protein demonstrated a marked inhibition of the disease (Gorczynski *et al.,* 2001). This protein reduced cytokine secretion, including TNFα and IFNγ, and a reduction in the expression of IL-1β, TNFα and IL-10 mRNA transcripts in the mCD200R1-expressing synovium. Addition of the CD200Fc protein had no effect on the numbers of circulating T cells, indicating a specific role rather than general suppression of inflammation. The use of a CD200Fc protein has become an invaluable tool in the study of CD200:CD200R signalling.

1.5.7 CD200 in health and disease

CD200:CD200R signalling is involved in the regulation of inflammation in various pathologies including autoimmune diseases, infections and cancer.

1.5.7.1 Autoimmune diseases

The CD200:CD200R signalling pathway is well recognised as a modulator or immunological suppression, however, neither *CD200*$^{-/-}$ or *CD200R*$^{-/-}$ mice demonstrate a compromised central tolerance and do not succumb to spontaneous autoimmune disease (Hoek *et al.,* 2000; Boudakov *et al.,* 2007). Evidence for the role of CD200:CD200R signalling in autoimmune conditions comes from various mouse models. *CD200*$^{-/-}$ mice were shown to be more susceptible to the induction of autoimmune diseases such as experimental autoimmune encephalomyelitis (EAE), murine model of multiple sclerosis (Hoek *et al.,* 2000). In addition, CD200Fc is not only successful in suppressing transplant rejection but also potently inhibits collagen-induced arthritis (CIA) in rodents (Gorczynski *et al.,* 2001). CD200 expression has also been shown to regulate inflammation in the hair follicles of the skin (Rosenblum *et al.,* 2004). CD200 is expressed on Langerhans cells and keratinocytes in mouse epidermis. *CD200*$^{-/-}$ mice

were more susceptible to hair follicle inflammation and immune-mediated alopecia and suggests that the CD200:CD200R signalling pathways is a mechanism by which epidermal stem cells are protected from autoimmune destruction (Rosenblum *et al.,* 2006). The role of this pathway has since been implicated in the development of several human diseases, particularly of the nervous system.

1.5.7.1a Multiple Sclerosis

The role of the CD200:CD200R signalling pathways has been extensively studied in relation to the CNS. The interaction between CD200 and its receptor is postulated to be a mechanism involved in controlling the microglial inflammatory response in healthy brain tissue (Valente *et al.,* 2017). The effect of CD200 expression on EAE has been previously discussed, whereby *CD200*$^{-/-}$ mice develop more severe disease than WT (Hoek *et al.,* 2000). A more recent study in mouse EAE, CD200 and CD200R expression has been shown to be altered at both pre-symptomatic and symptomatic phases in the CNS (Valente *et al.,* 2017). This suggested a compromised control of the microglial inflammatory response from early pathological stages and hereby stimulating the inflammatory response and contributing to the development of the pathology.

1.5.7.1b Alzheimer's Disease

An investigation suggested evidence for altered CD200:CD200R expression in Alzheimer's disease (AD) (Walker *et al.,* 2009). A decrease in both protein and mRNA expression of CD200 and CD200R in AD hippocampus and inferior temporal gyrus was demonstrated. Low expression of CD200R was also seen in microglia when compared to blood-derived macrophages. Expression of CD200R significantly increased in these microglia upon treatment with IL-4 and IL-3, cytokines not normally detectable in the human brain. It was suggested from this study that mechanisms aimed at increasing levels of CD200 and CD200R could have therapeutic potential for controlling inflammation in human neurodegenerative diseases.

1.5.7.2 CD200 expression in cancer

The CD200:CD200R signalling pathway has been proposed to play an opposing role in tumour development, inhibiting a required immune response. The first indication that the CD200:CD200R pathway may be of relevance to the progression of tumour development came from studies using mouse transplantable thymoma (EL4) in C57BL/6 mice (Gorczynski *et al.,* 2001). It was found that all manipulations used to attenuate tumour growth were inhibited by infusion of an excess of soluble CD200Fc. Subsequent studies have confirmed CD200 expression in various cancer types, particularly in haematologic malignancies such as acute myeloid leukaemia, chronic lymphocytic leukaemia, and multiple myeloma (Tonks *et al.,* 2007; McWhirter *et al.,* 2006; Moreaux *et al.,* 2006). More recent studies have investigated the role of CD200 expression in solid tumour types, including subsets of melanomas, breast cancer, ovarian tumours, squamous cell carcinomas and renal cell carcinomas (Moreaux *et al.,* 2008). In addition to expression in tumour mass, CD200 expression has been linked to tumour initiating, or cancer-stem cell, populations (Colmont *et al.,* 2013; Zhang *et al.,* 2016).

1.5.7.2a Acute myeloid leukaemia

The role of tumour CD200 expression has been extensively characterised in acute myeloid leukaemia (AML). Expression of CD200 has been associated with a poor prognosis with patients with high CD200 expression levels significantly associated with a worse prognosis and an increased risk of relapse (Tonks *et al.,* 2007). Stratifying patients based on CD200 expression, $CD200^{high}$ patients saw changes in both the innate and adaptive response. There was a suppression in memory T cell function, with a suppression in Th1 cytokine (TNFa, IL2 and IFNγ) producing cells (Coles *et al.,* 2012). The cytotoxic memory T cell function was also compromised in these patients, with a significant reduction in CD107a+CD8+ memory T cells. This reduction was also evident in the frequencies of TNFa, IL2 and IFNγ producing CD4+ memory T cells. No difference was observed in TNFα-, IL-2- and IFNγ-producing CD8+ memory cells between $CD200^{high}$, $CD200^{low}$ and healthy donors. Conversely, the number of immunosuppressive lymphocytes increased. In addition to directly inhibiting an immune response, it was shown that CD200 has the potential to induce an immunosuppressive response via the formation of CD4+CD25+FoxP3+ Treg cells, with $CD200^{high}$ patients demonstrating an

increased frequency of these cells (Coles *et al.,* 2012). CD200 expression was also shown to inhibit the innate immune response. In $CD200^{high}$ patients, there was a twofold reduction in NK cell frequency, with a significant reduction in the cytolytic NK cell populations (Coles *et al.,* 2011). This was in addition to a reduction in NCR expression on NK cells, with NKp30, NKp44 and NKp46 expression reduced in all subpopulations, as well as a decrease in NK degranulation and IFNy production. It was shown that blocking the CD200 signal in AML was sufficient to restore both memory T cell and NK cell function. Subsequent studies have analysed the correlation of CD200 expression with other known prognostic markers for AML and confirms the negative prognostic role of CD200 in AML and identifies subgroups of patients in which CD200 significantly reduces survival probability (Damiani *et al.,* 2015). High CD200 expression is associated with poor prognosis in cytogenetically normal acute myeloid leukaemia (Tiribelli *et al.,* 2017). In AML, CD200 is emerging as both a prognostic factor and potential therapeutic target.

1.5.7.2b Chronic lymphocytic leukaemia

Overexpression of CD200 has been identified on primary tumour cells of patients with Chronic lymphocytic leukaemia (CLL) when compared to expression on normal B cells (McWhirter *et al.,* 2006). CD200 is now widely used as a marker of CLL when discriminating between other lymphoproliferative disorders such as mantle cell lymphoma (Palumbo *et al.,* 2009). Several studies have demonstrated that CD200 functions as a suppressive signal in this cancer type. An *in vitro* study demonstrated that blocking CD200 using both anti-CD200 mAab and CD200-specifc siRNAs augmented killing of a poorly immunogenic CD200+ lymphoma cell line and freshly obtained cells from CLL patients by effector PBMCs (Wong *et al.,* 2010). A similar result was seen inn a xerograph model that demonstrated that tumour expressed CD200 inhibited the ability of lymphocytes to eradicate tumour cells. Administration of an anti-CD200 mAb to mice bearing CD200 expressing tumour resulted in the near complete tumour growth inhibition (Kretz-Rommel, 2007).

1.5.7.2c Breast Cancer

The role of CD200 in regulating the growth of breast cancer cells was first established using the EMT6 mouse breast cancer cell line (Gorczynski *et al.,* 2010). The transplantable EMT6 mouse breast cancer line growing in vitro were shown to express low levels of CD200, which increased markedly during growth in immunocompetent mice. This increase in expression did not occur in NOD-SCID.IL-$2^{\gamma r-/-}$ mice or mice with generalized over-expression of a CD200 transgene ($CD200^{tg}$). This altered CD200 expression in control versus transgenic mice was accompanied by changes in tumour infiltrating cells (CD4+/CD8+ T cells). Neutralisation of expressed CD200 by anti-CD200mAbs led to decreased tumour growth and improved cytotoxic anti-tumour infiltrate in immunocompetent mice. Meanwhile, tumour growth and metastasis were further enhanced using $CD200^{tg}$ EMT6 tumour cells. The notion that the CD200:CD200R signalling pathway was a mechanism by which tumours evade the immune system was highlighted further in *CD200R*$^{-/-}$ mice, which demonstrated reduced tumour growth and metastasis, while optimal tumour immunity (and suppression of metastasis) was seen in *CD200R*$^{-/-}$ mice receiving inoculate of CD200-EMT6 tumour cells (Podnos *et al.,* 2012). The effect of breast cancer CD200 expression, however, is not clear. In an alternative mouse breast cancer model, the highly aggressive 4THM murine-breast carcinoma cell line was used in either $CD200^{tg}$ or *CD200R*$^{-/-}$ mice (Erin *et al.,* 2015). In this study, CD200 overexpression in the host attenuated tumour growth and was associated with decreased primary tumour growth and metastasis. Meanwhile, the lack of CD200R1 expression by host cells was associated with enhanced visceral metastasis and a decrease in the tumour-infiltrating-cytotoxic T cells and increased the release of inflammatory cytokines, such as TNF-α and IL-6. These results support the hypothesis that CD200 expression can alter the tumour immune response but highlight the complexity in the effect of CD200:CD200R interaction on tumour growth and progression.

1.5.7.2d CD200 cancer stem cells

Tumours are composed of a heterogenous populations that include highly differentiated cells, transit-amplifying cells and the quiescent cancer stem cells (Moore and Lyle, 2011). Cancer stem cells (CSCs) are a rare population that give rise to the other more differentiated cells of the tumour. These CSCs are thought to play a role in immune evasion, a hallmark of cancer. Having identified the immunosuppressive properties of CD200 in various cancer types, expression was analysed in CSCs. Expression of CD200 was found on CSCs of several cancer types, including prostate, breast, brain and colon cancers (Kawasaki and Farrar, 2008). In addition to the above cancer types, CD200 was reported to identify a subpopulation of basal cell carcinoma (BCC) with the capacity to recreate tumour growth *in vivo* (Colmont *et al.,* 2013). This rare population accounts for only 1.63 ± 1.11% of all BCC cells but *in vivo* growth was achieved with as few as 10,000 CD200+ cells, whilst CD200- BCC cells were unable to form tumours. Expression of CD200 has since been proposed as a cancer stem cell marker in colorectal cancer (Zhang *et al.,* 2016). CD200+ colorectal cells were found to have strong self-renewal and invasive abilities when compared to their CD200- counterparts. Expression of CD200 on CSCs remains a and design of therapies that target CSCs and the prevention of relapse.

1.5.8 Targeting CD200 as a novel anti-cancer therapeutic

Identifying expression of CD200 in these cancers and elucidating the mechanisms by which is affects tumour development has made CD200 a promising therapeutic target. Results from the first-in-human study of the novel recombinant humanized monoclonal antibody targeting CD200, Samalizumab, has recently been reported (Mahadevan *et al.,* 2019). This study investigated the therapeutic benefit of this immune checkpoint inhibitor in CLL and multiple myeloma (MM). Samalizumab produced dose-dependent decreases in CD200 expression on CLL cells and a decrease in tumour burden was observed in 14 of the 23 patients. One CLL patient achieved a durable partial response and 16 patients had stable disease. All MM patients had disease progression. The drug was reported to have a good safety profile and positive preliminary results support further development of Samalizumab as an immune checkpoint inhibitor.

1.5.9 Identifying other CD200 expressing tumour targets

Exploring the role of tumour CD200 expression has long been of interest. The promise of targeting this as a novel therapeutic has led to the interest in identifying expression of this ligand in other cancer types. A study analysing *CD200* expression in various tumour using publicly available gene expression data and revealed that CD200 mRNA is overexpressed in at least eight cancers compared to their normal counterparts (Moreaux *et al.,* 2008). Overexpression was seen in head and neck carcinomas, testicular cancer, malignant mesothelioma, colon carcinoma, smouldering myeloma, chronic lymphocytic leukaemia, and renal cell carcinoma. It was also demonstrated that CD200 could be associated with tumour progression in other cancer types such as in invasive bladder carcinoma compared to superficial bladder carcinoma, advanced lung cancer stages (stages II, III and IV) compared to stage I, metastatic melanoma compared to primary melanomas and normal melanocytes, as well as in the accelerated phase of chronic myelogenous leukaemia compared to the chronic phase, which is upregulated during disease progression. This study highlighted the breadth of tumour CD200 expression and that targeting the protein may be of therapeutic interest in a very wide panel of malignancies.

One the cancer types to demonstrate overexpression CD200 is renal cell carcinoma (RCC), the main type of kidney cancer. In addition to overexpression at mRNA level, CD200 expression has been identified at protein level in a number of small-scale studies (Siva *et al.,* 2008; Love *et al.,* 2017). The functional role of CD200 expression in RCC has not yet been explored.

1.6 Kidney Cancer

Kidney cancer is the 7th most common cancer in the UK, accounting for 4% of all new diagnosed cases (Cancer Research UK, 2016). The disease is most commonly diagnosed in men, with over 60% of the cases. Kidney cancer is the 13th most common cause of cancer death in the UK, accounting for 3% of all cancer deaths is 2017.

Kidney cancer includes renal cell carcinoma (formed in the lining of kidney tubules) and renal pelvis carcinoma (formed in the renal pelvis and ureter) (Figure 1.7). The most common form of kidney cancer is renal cell carcinoma, which encompass around 85% of all primary renal neoplasms (Hsieh *et al.,* 2017). The remaining 15% of kidney cancers include transitional cell carcinoma (8%), nephroblastoma or Wilms' tumour (5–6%), collecting duct tumours (<1%), renal sarcomas (<1%), and renal medullary carcinomas (<1%) (Nabi *et al.,* 2018).

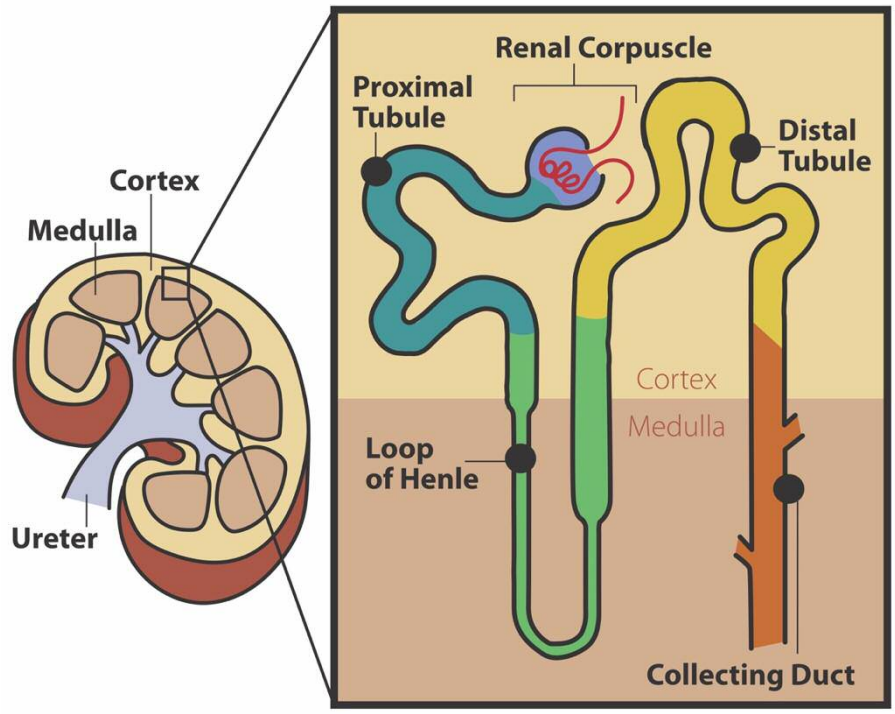

Figure 1.9: The kidney. RCC arises from the nephron, the functional unit of the kidney.

1.6.1 Renal Cell Carcinoma

Renal cell carcinoma (RCC) is a group of heterogeneous cancers that arise from distinct parts of the nephron. Each subtype is derived from the epithelial cells of renal tubules, but each are characterised by unique morphological and genetic characteristics (Hsieh *et al.,* 2017). The most common types of epithelial renal tumours include clear-cell renal carcinoma (75%), papillary RCC that is subdivided into type I (5%) and Type II (10%), chromophobe RCC (5%), and oncocytoma (5%). The remaining 15% of kidney tumours consist of translational cell carcinoma (8%), nephroblastoma or Wilms' tumour (5-6%), collecting duct tumours (<1%), renal sarcomas (<1%) and renal medullary carcinomas (<1%). The remaining subtypes are very rare (each with ≤1% total incidence) (Muglia and Prando, 2015).

1.6.1.1 Clear Cell Renal Cell Carcinoma

Clear cell renal cell carcinoma (ccRCC) is the most common type of RCC. It is characterised by a specific morphology and genetic background. ccRCC is thought to arise from the epithelium of the proximal tubule (Riazalhosseini and Lathrop, 2016). It is histologically characterised by optically-clear cells arranged in nests, surrounded by delicate "chicken wire" vasculature. The clear cell name reflects the observation that the cytoplasm is commonly filled with lipids and glycogens, which are dissolved during routine histological processing, which creates a clear cytoplasm surrounded by a distinct cell membrane. These tumours, however, often appear cystic, with large eosinophilic cell populations. Most ccRCCs are sporadic, however a percentage of cases are associated with heredity syndromes. The most common genetic alterations associated with ccRCC is loss of the short arm of chromosome 3 and include alterations in several key genes, with *VHL* mutations considered the key driver.

1.6.1.2 Papillary Renal Cell Carcinoma

Papillary renal cell carcinoma (pRCC) is the second most common type of renal carcinoma following clear cell renal cell carcinoma. pRCC is thought to arise from the epithelium of the proximal tubule (Cairns, 2011). The subtype is named after its papillary or tubulopapillary architecture. pRCC is divided histologically into two main types: type I (characterised by a single layered small cell and scanty cytoplasm) and type II

(characterised by large pseudostratified cells and eosinophilic cytoplasm). Type II is associated with more aggressive disease and a worse patient outcome prognosis (Kim *et al.,* 2012). Each subtype can also be characterised by specific genetic alterations, with type I being associated with alterations in the MET pathway and type II being associated with the activation of the NRF2-ARE pathway (Linehan *et al.,* 2016). Both hereditary and sporadic forms of pRCC have been observed and mutations in the MET oncogene are also thought to be an essential step into the pathogenesis of the hereditary pRCC forms (Linehan *et al.,* 2007) Other abnormalities associated with pRCC subtype include trisomies of chromosomes 3, 7, 12, 16, 17 and 20, as well as the loss of the Y chromosome (Low *et al.,* 2016).

1.6.1.3 Chromophobe Renal Cell Carcinoma

Chromophobe RCC (chRCC) cells are well circumscribed and highly lobulated (Vera-Badillo *et al.,* 2012). Histologically, chRCC cells grow in large nests and have flocculent cytoplasm that condenses around the edges. chRCC is thought to arise from the distal nephron, probably from the epithelium of the collecting tubule (Cairns, 2011). This subtype has been associated with a low risk of tumour progression, metastasis and a better survival rate than both ccRCC and pRCC (Volpe *et al.,* 2012). Cytogenetic abnormalities associated with chromophobe RCC include loss of multiple chromosomes such as 1, 2, 6, 10, 13, 17 and 21 (Prasad *et al.,* 2006; Low *et al.,* 2016).

1.6.1.4 Oncocytoma

Oncocytoma is an uncommon subtype, composed of oncocytes, which are uniform, round or polygonal neoplastic cells that exhibit a granular eosinophilic cytoplasm (Alamara *et al.,* 2008). Oncocytoma is also thought to arise from the distal nephron, probably from the epithelium of the collecting tubule (Cairns, 2011). The disease is often benign, and exclusion from RCC classification has often been recommended.

1.6.2 Disease Staging

The extent of cancer at the time of diagnosis is one of the key factors that defines prognosis and in determining the most appropriate treatment. The purpose of developing a grading system is to collate past experience and outcomes of groups with

similar disease stage between treatment centres, using a method that is clear and easy to convey, at both national and international level. The most commonly used cancer staging is the tumour-node-metastasis (TNM) stage grouping system (Brierley *at al.,* 2016). This system is maintained by the American Joint Committee on Cancer (AJCC) and is based on data obtained from large multicentre studies and is regularly monitored and updated. The TNM system classifies cancers by the size and extent of the primary tumour (T), involvement of reginal lymph nodes (N), and the presence or absence of metastases (M). This staging system is now globally recognised and used to classify extent of disease and is used for many solid tumours. The criteria for defining extent of disease are specific for tumour at different anatomic sites and of different histological types. This, the criteria for T, N and M are defined separately for each cancer type. The most recent primary tumour staging for RCC is reported in the 8th AJCC cancer staging manual and is described below (Table 1.3) (Swami *et al.,* 2019).

Table 1.3: TNM system of RCC classification according to AJCC 8th edition

Primary Tumour (T)	
TX	**Primary tumour cannot be assessed**
T0	**No evidence of primary tumour**
T1	**Tumour 7 cm or less in greatest dimension, limited to the kidney**
T1a	Tumour ≤ 4 cm, limited to the kidney
T1b	Tumour > 4 cm and ≤ 7 cm, limited to the kidney
T2	**Tumour more than 7 cm in greatest dimension, limited to the kidney**
T2a	Tumour > 7 cm and ≤ 10 cm, limited to the kidney
T2b	Tumour > 10 cm, limited to the kidney
T3	**Tumor extends into major veins or perinephric tissues but not into the ipsilateral adrenal gland and not beyond Gerota's fascia**
T3a	Tumour invades renal vein / branches, perirenal fat, renal sinus fat or pelvicaliceal system
T3b	Tumor extends into vena cava below the diaphragm
T3c	Tumor extends into vena cava above the diaphragm or invades vena cava wall
T4	**Tumor invades beyond Gerota's fascia (including contiguous extension into the ipsilateral adrenal gland)**
Regional Lymph Nodes (N)	
N0	No regional lymph node metastasis
N1-3	Increasing number or extent of regional lymph node involvement
NX	Regional lymph nodes cannot be assessed
Distant Metastasis (M)	
M0	No distant metastases
M1	Distant metastases present

1.6.3 Epidemiology

Globally, the incidence of RCC varies widely from region to region, with the highest rates found in North America, followed by Western Europe and Australia and New Zealand (Capitanio *et al.,* 2019). There has been an increase in the incidence of RCC worldwide, which is thought to be partly due to an increase in incidental detection of renal masses during nonspecific abdominal imaging. Whilst the majority of the lesions detected are

small, up to 17% of patients were found to harbour distant metastases at the time of diagnosis (Capitanio and Montorsi, 2016). This late diagnosis has been linked to late presentation as the disease is characteristically asymptomatic.

1.6.4 Aetiology

There are a number of risk factors described for RCC. Cigarette smoking is one of the most well studied factors linked to increased RCC risk (Theis *et al.,* 2008). The risk increased more in men than women, with a 50 and 20% increase in risk, respectively (Hunt *et al.,* 2005). This risk demonstrated a dose-dependent pattern. Cigarette smoking has since been linked to the increased likelihood of advanced disease (Tsivian *et al.,* 2011). Smoking cessation reduces the risk, but only among long-term quitters of ten or more years (Hunt *et al.,* 2005). Obesity is another risk factor associated with RCC, with excess body weight being estimated to account for over 40% of RCCs in the United States and over 30% in Europe (Calle and Kaaks, 2004). Similar to cigarette smoking, weight-related risks of RCC increased in a dose-dependent manner (Adams *et al.,* 2008). Hypertension is another significant risk factor for RCC. Several studies conducted show a dose-dependent increase in RCC with increasing blood pressure measurement taken at baseline clinic visit (Macleod *et al.,* 2013). Several other factors have been reported to affect risk of RCC, such as alcohol consumption, however, these often have conflicting or limited evidence to support them.

In addition to external conditions, there are a number of genetic and hereditary risk factors associated with RCC. Hereditary conditions that can predispose people to developing RCC account for approximately 3% of cases (Menko and Maher, 2016). These hereditary conditions have provided valuable insight into the genetic and molecular mechanisms leading to RCC development. For example, the most common genetic alteration associated with the development of ccRCC is loss of the short arm of chromosome 3 and is seen in 95% of ccRCC cases (Nabi *et al.,* 2018). The most common genes involved in the pathogenesis of ccRCC to include *VHL*, *PBRM-1*, *SETD2*, *BAP-1*, *KDM5C*, and *MTOR.* The evolutionary history of sporadic ccRCC in 10 individuals was investigated by exome sequencing multiregional samples from primary ccRCC and metastases (Gerlinger *et al.,* 2014). The study highlighted the intratumour heterogeneity

in all tumours (Hsieh *et al.,* 2017). Whilst heterogeneity is seen amongst individuals, the most common genetic event of ccRCC is the loss of function of the VHL gene.

1.6.5 Molecular alterations associated with RCC

Renal cell carcinoma is made up of a number of different types of cancer that are often characterised by different genetic drivers. Some of the most common genetic aberrations are discussed below.

1.6.5.1 Von Hippel-Lindau (VHL) gene

VHL is a tumour suppressor gene that encodes a multifunctional protein that forms complexes with several other proteins in the cell, including elongin B, elongin C, and cellulin 2 (Kibel *et al.,* 1995). The resulting complex (called the VBC complex) helps in the proteasomal degradation of several intracellular proteins. This VHL gene product functions by regulating the levels of several other intracellular proteins, including the hypoxia-inducible factor 1 alpha and 2 alpha (HIF1-α and HIF2-α). When bound to each other, these intracellular proteins serve as transcription factors for several growth factors, including vascular endothelial growth factor (VEGF), platelet-derived growth factor beta (PDGFB), and transforming growth factor alpha (TGFA). These growth factors have been implicated in the development of highly vascular tumours (such as ccRCC) associated with VHL alterations. The transcription factor complex also results in the regulation of proteins and enzymes responsible for controlling proteins in the extracellular matrix.

In ccRCC, *VHL* alteration is the hallmark of disease, with the VHL tumour suppressor gene being the most frequently mutated gene (Gnarra *et al.,* 1994; Creighton *et al.,* 2013). The complete loss of this gene through genetic (point mutations, indels and 3p25 loss) and/or epigenetic (promoter methylation) mechanisms constitutes the earliest, truncal oncogenic driving event. Germline mutations of *VHL* cause a rare familial tumour syndrome that can predispose an individual to developing RCC.

The von Hippel–Lindau disease is an inherited autosomal dominant condition caused by the epigenetic mutation of the VHL gene (Kim and Zschiedrich, 2018). VHL disease is

characterised by the formation of multiple benign and malignant tumours, as well as cysts in multiple organs. Affected individuals frequently develop retinal and central nervous system hemangioblastomas, pheochromocytomas, pancreatic neuroendocrine tumours, endolymphatic sac tumours and RCCs. A "two-hit" hypothesis has been described and validated in patients with VHL disease that go on to develop RCC (and other tumours) (Nabi *et al.,* 2018). Individuals born with VHL disease are heterozygous, born with one inactivated copy of the VHL gene whilst the other is normal. For tumorigenesis to take place, there must be a second event that leads to the inactivation of the second gene copy. This usually takes place as a result of somatic mutation or deletion of the allele (Varshney *et al.,* 2017).

Whilst VHL alterations are an established marker of ccRCC, mutations in pRCC, chRCC and oncocytoma have also been observed, however, they are much less common in these subtypes (Büscheck *et al.,* 2020). A recent study demonstrated no significant association between *VHL* mutation/deletion and tumour grade, stage, and clinical outcome (Büscheck *et al.,* 2020).

1.6.5.2 The mammalian target of rapamycin signalling pathway

The mammalian target of rapamycin (mTOR) signalling pathway is implicated in the regulation of cell growth, differentiation, survival and metabolism and has been linked to the regulation of angiogenesis. The mTOR-PI3K pathway starts with the binding of several growth factors to the cell surface, resulting in the activation of the phosphatidylinositol-3-kinase (PI3K) protein (Nabi *et al.,* 2018). These are lipids kinases that regulate diverse cellular processes. Activated PI3K in turn activates mTOR, creating mTOR complexes 1 and 2 (mTORC1 and mTORC2). This leads to the phosphorylation of P70S6K and 4E-BP1/eukaryotic translation initiation factor 4E (4E-BP1/eIF4E). The phosphorylated P70SK migrates to the nucleus and initiates the transcription of the HIFA protein, which, as mentioned above, has the ability to increase the production of angiogenic proteins such as VEGF, PDGF, and TGFB.

It has been shown that mTOR is frequently deregulated in human tumours, including RCC (Pópulo *et al.,* 2012). In particular, the mTOR pathway has been shown to be

upregulated in over 60% of ccRCC patients (Robb *et al.,* 2007). In a study investigating the association between single nucleotide polymorphisms (SNPs) of the mTOR pathway and the risk of developing RCC found that of the 190 SNPs in the 22 genes investigated, six SNPs located in the AKT3 gene were correlated with risk of RCC (Shu *et al.,* 2013). Genetic mutations that lead to the constitutive increase in mTOR activity increase the incidence of metastatic RCC. For example, loss-of-function mutations in PTEN, a negative regulator of mTOR through the PI3K/Akt pathway, are found in approximately 5% of patients with RCC. The link between mTOR pathway and RCC development can also be seen in patients with tuberous sclerosis, who have a predisposition to RCC. These patients have loss-of-function mutations of genes encoding either TSC1 or TSC2 lead to the inactivation of the TSC, a negative regulator of mTOR.

Alterations to the mTOR pathway have been observed in most RCC subtypes, with the majority of patients demonstrating at least one impacted mTOR pathway component (Chen *et al.,* 2016). Proteomic analysis revealed increased activation of this pathway in ccRCC and pRCC when compared to chRCC.

1.6.5.3 Other pathways

Polybromo 1 (PBRM1) is the second most frequently mutated gene and is mutated in approximately 45% of ccRCC (Varela *et al.,* 2011). *PBRM1* is on the same chromosome arm as VHL and the second allele is frequently co-deleted with *VHL*. *PBRM1* encodes BAF180, a component of a nucleosome-remodelling complex. *PBRM1*-mutant ccRCCs are enriched for genes in pathways implicated in the cytoskeleton and cell motility, however, how its loss promotes tumorigenesis is poorly understood (Kapur *et al.,* 2013). The BRCA1 associated protein-1 (*BAP1*) gene is mutated in 10% to 15% of patients with ccRCC (Peña-Llopis *et al.,* 2012). BAP1 is a two-hit tumour suppressor gene located on chromosome 3p between the *VHL* and *PBRM1* genes. BAP1-deficient ccRCCs are characterised by enrichment of pathways implicated in growth factor and phosphatidylinositol 3-kinase (PI3K) signalling. Consistent with this, BAP1-deficient tumours exhibit increased mTOR complex 1 activation. The gene encoding SET domain containing protein 2 (SETD2) is somatically mutated in approximately 10% to 15% of ccRCCs (Sato *et al.,* 2013). Like VHL and PBRM1, SETD2 is a two-hit tumour suppressor

gene and is located on chromosome 3p. How inactivation of this gene leads to ccRCC remains unclear.

VHL, *PBRM1*, *SETD2*, and *BAP1* are within a 50 Mb stretch on chromosome 3p, in a region that is lost in approximately 90% of sporadic ccRCCs (Peña-Llopis *et al.,* 2013). Deletion of this region simultaneously inactivates one allele of four ccRCC tumour-suppressor genes, leaving cells vulnerable to the loss of the remaining allele (Brugarolas, 2014). The discovery of the genetic background of ccRCC has provided insight into the development of the disease and have provided the foundation for the generation of molecularly targeted therapies.

1.6.6 Treatment

The treatment course for patients with RCC depends on metastatic status of the disease.

1.6.6.1 Surgery

Surgery (full or partial nephrectomy) is considered the mainstay treatment for RCC. In patients with localised, stage I disease, removal of the primary tumour has been shown to be curative in over 90% of patients (Chin *et al.,* 2006). Patients with metastatic disease may also receive surgery for different reasons, including palliative nephrectomy for symptomatic patients in whom cure is not achievable, cytoreductive nephrectomy before systemic therapy, or consolidative nephrectomy after systemic therapy (Ball, 2017). For patients with advanced RCC, additional treatment options are considered.

1.6.6.2 Targeted Therapies

The development in our understanding of RCC biology has resulted in the development of several targeted therapies. The VHL mutations associated with ccRCC (as described above) cause the accumulation of hypoxia-inducible factors in cells and activation of many downstream hypoxia-driven genes, including VEGF and other genes involved in angiogenesis, cell growth or survival. Several VEGF-receptor (VEGFR) tyrosine kinase inhibitors (TKI) have now been developed that target and deactivate these downstream pathways and inhibitors of VEGF are now typically used as first-line therapy for the treatment of metastatic ccRCC. Other drugs that target the mTOR pathway have also

been developed. The targeted therapies for advanced RCC currently approved by NICE and used in the NHS are summarised in below (Table 1.4).

Table 1.4: Approved targeted therapies for the treatment of advanced and/or metastatic RCC

Name	Target	Reccomended use
First-line treatment		
Sunitinib	Multiple RTKs (including VEGFR and PDGF)	RCC who are suitable for immunotherapy and have an ECOG performance status of 0 or 1
Cabozantinib	VEGFR as well as c-MET and AXL	Untreated RCC that is intermediate- or poor-risk
Tivozanib	Multiple RTKs (VEGFR 1-3, c-Kit and PDGF)	Untreated RCC
Pazopanib	Multiple RTKs (VEGFR 1-3 and PDGF)	Not received prior cytokine therapy and have an ECOG performance status of 0 or 1
Second-line treatment		
Lenvatinib with Everolimus	Multiple RTKs (VEGFR 1-3, c-Kit and PDGF)	Adults who have had 1 previous VEGF-targeted therapy and their ECOG performance status score is 0 or 1
Cabozantinib	VEGFR as well as c-MET and AXL	Option for treating advanced renal cell carcinoma in adults after VEGF-targeted therapy
Everolimus	mTOR	RCC that has progressed during or after treatment with vascular endothelial growth factor targeted therapy
Axitinib	Multiple RTKs (including VEGFR, c-Kit and PDGF)	RCC after failure of treatment with a first-line tyrosine kinase inhibitor or a cytokine

While these treatments have improved palliative outcomes, they are limited by both innate and acquired resistance which typically occurs within the first year of treatment (Choueiri and Motzer, 2017).

1.6.6.3 Immunotherapies

Prior to the introduction of targeted therapies cytokines, including high-dose IL-2 and IFN-α, were the standard of care for advanced ccRCC. The severe toxicity and low response rates led to the interest in identifying alternative immunotherapies.

1.6.6.3.1 Rational for Immunotherapy in RCC

Removal of primary RCC lesions has been shown to result in the spontaneous regression in metastasis, particularly in the lungs (Vogelzang *et al.,* 1992). This observation has been linked the immune rich infiltrates seen in RCC and is thought to be the result of "resetting" the host immune system that had been overwhelmed by the tumour burden. For many decades, RCC has been known to be susceptible to immune therapy, showing particular response to cytokine therapy. While numerous cytokines showed anti-tumour activity against mRCC, IL-2 and IFN-α were the most promising (Gill *et al.,* 2016). High dose IL-2 improved overall response rate to 15-20%, with 7-9% of patients demonstrating complete responses (Rosenberg *et al.,* 1994). IFN-α demonstrated a more modest overall response rate (ORR) of 10–15% without long-term responses (Fosså, 2000). Combination therapy of both these cytokines had a slightly improved overall response rate (Negrier *et al.,* 1998).

These cytokines have pleiotropic effects on the immune system, regulating development, survival and function of immune cells. Both drugs work by generating a robust T cell response that non-specifically targets RCC cells. Whilst this resulted in anti-tumour activity, the unspecific mechanism of action of these cytokines would stimulate numerous pro-inflammatory cytokines including IL-1, INF-γ, and tumour TNF-α that were linked to severe toxicity. (Mier *et al.,* 1988; Numerof *et al.,* 1988). Capillary leak syndrome was one of the most common forms of toxicity from IL-2 treatment, which can result in life-threatening hypotension, oedema and pulmonary congestion (Schwartz *et al.,* 2002). Whilst cytokine therapy, particularly IL-2, demonstrated curative potential, this was only found in a subset of patients and the associated toxicity was severe. For that reason, cytokine therapy is rarely used and is reserved for younger patients without significant comorbidities. The most recent optimisation of immunotherapies for the treatment of advanced and metastatic RCC (mRCC) has now moved on to immune checkpoint inhibitors.

1.6.6.3.2 Immune Checkpoint Inhibitors

Immune checkpoint inhibitors account for the majority of immunotherapies in use today, with CTLA-4, PD-1 and PD-L1 the principal drug targets, as previously discussed (Topalian *et al.,* 2015). Over recent years, a multitude of clinical trials have investigated the efficacy of drugs targeting these pathways in the treatment of advanced RCC.

1.6.6.3.2a PD-1 Inhibitors

Nivolumab (Bristol-Myers Squibb) is a fully human monoclonal IgG4 antibody that is specific for PD-1 and has received FDA and EMA approval in non-small cell lung cancer, RCC and head and neck cancers. Patients with RCC were included in the first in-human phase I study of nivolumab, where is demonstrated responses and a favourable toxicity profile (Brahmer *et al.,* 2010). These favourable responses were supported in subsequent trials (Motzer *et al.,* 2015). Nivolumab was finally approved for previously treated patients with advanced ccRCC based on the phase III CheckMate 025 study, which demonstrated overall survival (OS) and ORR benefits compared with everolimus

in patients who had prior antiangiogenic therapy (Motzer *et al.,* 2015). However, there was no progression free survival (PFS) advantage with nivolumab.

1.6.6.3.2b CTLA-4 Inhibitors

Several studies into the efficacy of utilising the monoclonal antibody targeting CTLA-4, ipilimumab, have been carried out. A phase II study of ipilimumab as a monotherapy demonstrated only a 10% ORR, with a third of patients experiencing severe toxicity (Yang *et al.,* 2007). For toxicity reasons, the use of ipilimumab as a monotherapy for RCC was not taken into further trials, however, within the cohort of patients who responded some had significant durable responses. Ipilimumab has since been studied as a combination therapy for RCC.

1.6.6.3.3 Combination Therapy

While the results from the Checkmate 025 study were encouraging, only 1% of patients receiving nivolumab achieved complete responses (CRs), and 31% of patients achieved durable responses greater than 12 months (Motzer *et al.,* 2015). Combination strategies that combine immune checkpoint inhibitors or angiogenesis inhibitors are currently being investigated in multiple trials.

1.6.6.3.3a Combination regimens – immune checkpoint inhibitors and angiogenesis inhibitors

The tumour microenvironment is complex and its importance on tumour development and drug efficacy is becoming increasingly recognised. As described above, VEGF plays a key role in advanced RCC and has been targeted successfully with significant therapeutic efficacy. The rationale behind combining therapies targeting this pathway with checkpoint inhibitors is that angiogenic activity seen in RCC interacts with the immune status.

The CheckMate 016 study was the first trial to explore the safety and tolerability of combination immunotherapy in the setting of advanced RCC (Hammers *et al.,* 2014). This phase I study, in addition to exploring different dose combinations of nivolumab and ipilimumab, explored the combination of nivolumab with either the TKIs, sunitinib

or pazopanib, or with the immunotherapy, ipilimumab. The addition of standard doses of sunitinib or pazopanib to nivolumab resulted in a high incidence of high-grade toxicities (Amin *et al.,* 2018). This most favourable outcome was seen in the combination of nivolumab and ipilimumab, which led to the phase III CheckMate 214 trial.

1.6.6.3.3b Combination regimens – immune checkpoint inhibitors

When administered as monotherapy in clinical studies, CTLA-4 and PD-1 blockers have demonstrated impressive durable response rates, increased survival time of responding patients significantly and have had a manageable safety profile across various cancer types. The response rates for these monotherapies are often low, with only a fraction of patients responding to therapy (Rotte, 2019). Combination of CTLA-4 and PD-1 blockade was thus proposed to increase the response rates and survival rates of the patients.

The phase III trial, CheckMate 214, tested the combination of ipilimumab and nivolumab over sunitinib in previously untreated patients with intermediate/poor risk metastatic or locally advanced ccRCC (Motzer *et al.,* 2018). The combination resulted in a significant OS benefit (median overall survival not reached versus 26.0 months with sunitinib) in this population of patients. In addition, ORR was significantly better in the combination arm (42% with 9% of CR) compared to sunitinib (27% with 1% of CR). CR rate was 9% versus 1%. This superior efficacy of nivolumab plus ipilimumab over sunitinib was maintained in an extended follow-up, showing long-term benefits of this combination for patients with all risk category advanced RCC (Motzer *et al.,* 2019).

1.6.6.3.4 Future directions for RCC management

Developments in our understanding of RCC biology has led to the development of several effective treatments. Whilst these current treatments have shown significant improvement in ORR, they are rarely curative. Immunotherapies have shown great promise in the treatment of RCC, both historically with IL-2 treatment, and more recently with the use of immune checkpoint inhibitors. For that reason, novel immunotherapeutic approaches for the treatment of RCC are still being investigated.

1.7 Hypothesis and Aims

Targeting immune checkpoints has become an active and successful area of cancer research. Immune checkpoint therapy has shown promising results in a number of cancers, including RCC. Efficacy of current immune checkpoint therapies, however, is limited to a subset of patients and thus, there remains an unmet clinical need to identify additional therapeutic targets for these patients. CD200 is an immune checkpoint with known immunosuppressive properties in cancer. Preliminary genomic studies have identified possible overexpression of this inhibitory ligand in RCC. The purpose of this study was to explore the role of CD200 in the immune evasion of RCC and ultimately, the possibility of targeting CD200 as a novel therapeutic target for patients with this disease.

Hypothesis:

Renal cell carcinoma patients may benefit from CD200 immune checkpoint inhibition

Aims:

1. Define CD200 expression in renal cell carcinoma
2. Define inflammatory infiltrate in CD200+ and CD200- renal cell carcinomas
3. Determine if human CD200+ renal cancer cells inhibit the natural killer cells and whether this can be reversed by blocking CD200 signalling

Chapter 2:

Materials and methods

Chapter 2: Materials and methods

2.1 Human tissue samples

Normal skin, normal kidney and renal cell carcinoma sections were obtained from the Welsh Cancer Bank (WCB Application Number 17/008).

2.2 Cell Lines

The cell lines that have been utilised for this project and are summarised in Table 2.1. Renal cell carcinoma cell lines, A498, UMRC-2, UMRC-3, UOK-121 and UOK-143 were kindly provided by the Francis Crick Institute, Kings College London. The renal carcinoma cell line SN12C were kindly provided by Lab Genomica Funzionale, Università di Padova. The cervical adenocarcinoma cell line HeLa (CCL-2™) and the natural killer cell line NK92-MI (CRL-2408™) were obtained from the American Type Culture Collection (ATCC).

2.2.1 Maintenance of cell lines

2.2.1a Adherent cells

RCC and HeLa cell lines were maintained in a T75 flask with 15mL media at 37°C in either 5 or 10% $C0_2$ (summary of cell line culture conditions in table 2.1). To subculture adherent cells, media was aspirated, and cells were washed once with pre-warmed PBS (Gibco, UK). Either Trypsin (0.05%), TrypLe or Versene were added to the cells, and incubated at 37°C for 5 mins, or until the cells became detached from the culture flask. Four volumes of media containing FBS was added to the cells to inhibit the enzymatic activity and the cell suspension was transferred to a 15mL falcon tube. Cells were then pelleted by centrifugation at 120xg for 5 mins at room temperature. The supernatant was removed, and the cell pellets re-suspended in fresh media. When required for assay, cells were counted using a haemocytometer. Cells were seeded into appropriate cell culture plates/flasks depending on the assay being performed. Cells were incubated at 37°C (5% CO_2) until 80-90% confluent (typically 3-5 days) before being split.

2.2.1b Non-adherent/suspension cells

The NK92MI cell line was maintained in a T150 flask with 25mL media at 37°C in 5% $C0_2$. The NKL cell line was maintained in a T75 flask with 15mL media at 37°C in 5% $C0_2$. To subculture suspension cells, cells in media were transferred to a falcon tube as above and pelleted by centrifugation at 120xg for 5 mins at room temperature. The supernatant was removed, and the cell pellets re-suspended in fresh media. Cells were seeded into appropriate cell culture plates/flasks depending on the assay being performed. Cells were incubated until 80-90% confluent, forming large clusters (typically 3-5 days).

2.2.2 Cryopreserving cell lines

All cell lines were prepared for cryopreservation in the same manner as sub-culturing, with the exception that they are re-suspended in freezing medium following centrifugation. As freezing can be lethal to cells, freezing medium contains a cryoprotectant, DMSO. For RCC and HeLa cells, the freezing medium was 90% growth medium + 10% DMSO. For the NK92MI cell lines, the freezing medium was 90% FBS + 10% DMSO. All cell lines were frozen at a concentration of $2\text{-}3\times10^6$ cells/mL. Cells were transferred to 2ml cryovials and placed in a CoolCell Biocision cryopreservation container (Dutscher Scientific) and stored at -80°C overnight, before being transferred to liquid nitrogen.

Table 2.1: List of cell lines and their culture conditions

Cell Line	Cell Details	Growth Media	%CO_2	Split Ratio
A498	Human renal carcinoma	EMEM + 10% FCS + NEAA + Pyruvate	5%	1:10
UMRC-2	Human renal carcinoma	DMEM + 10% FCS + NEAA	10%	1:10
UMRC-3	Human renal carcinoma	DMEM + 10% FCS + NEAA	10%	1:10
UOK-121	Human clear cell renal carcinoma	DMEM + 10% FCS	10%	1:10
UOK-143	Human sporadic clear cell renal carcinoma	ISCOVES + 10% FCS	5%	1:10
SN12C	Human renal carcinoma	DMEM + 10% FBS + L-Glut	5%	1:20
HeLa	Human cervical adenocarcinoma	RPMI + 10% FBS + L-Glut	5%	1:10
NK92-MI	Natural killer cells from malignant non-Hodgkin's lymphoma	RPMI 1640 + L-Glut + 10% HI-HS + 10% HI-FBS	5%	1:5
NKL	Natural killer cells	RPMI 1640 + 10% FBS + IL2	5%	1:5

2.2.3 Cell culture functional assays

2.2.3a Tumour and NK cell co-incubation

Tumour cells were detached from flask using Versene, sub-cultured and counted as above (2.2.1). Tumour cells were plated (20,000 cells) were plated in a white walled 96-well plate and left to adhere overnight. The following day, sample wells were detached and counted to determine the number of cells in each well. Various numbers of NK92MI cells were added to the tumour cells at different effector:target ratios. Co-incubations were left for four hours, after which the suspension NK cells, and the supernatant were removed and the remaining tumour cells at the bottom of the well were washed thoroughly with PBS. Tumour cell death was measured relative to untreated tumour cell wells by analysing and comparing luminescence using CellTiter-Glo® viability assay (see 2.8).

2.2.3b CD200 peptide treatment of NK92MI cells

NK92MI cells were plated in either a 96 – or 24-well plate. A CD200 Fc chimera protein (R&D) was added to the cells at a concentration of 4μg/10^6 cells for indicated time points, after which cell viability and/or protein and RNA was extracted. Various inhibitors were added to the co-cultures (Table 2.2).

Table 2.2: List of inhibitors added to CD200 peptide treatment of NK cells

Inhibitor	Concentration(s) used	Source	Cat #
Caspase inhibitors (Z-VAD-FMK, Z-IETD-FMK, Z-LEHD-FMK)	50 μM	R&D	FMKSP01
Fas Neutralising Ab (ZB4)	10-100 ng	Enzo Life Sciences	ADI-AAM-227-E
PPAR-γ antagonist (GW9662)	1-100 μM	Abcam	ab141125

2.2.4 Collection of Cell Conditioned Media

Conditioned media was harvested from cultured cells. This media contains the cell secretome, and refers to the collection of proteins, metabolites and growth factors secreted by cultured cells.

2.2.4a Cell conditioned media of cell lines

Cells were subcultured and plated as above (2.2.1). Cells were allowed to grow to 60-70% confluency, after which, media was replaced with 15mL of fresh media. Cells were left to grow for 48 hours, after which the conditioned media/supernatant was collected and placed into Pierce™ concentrators with a molecular weight cut off of 3K MWCO (ThermoFisher). These are disposable ultrafiltration centrifugal devices with a polyethersulfone (PES) membrane for the concentration of biological samples. Samples were centrifuged at top speed for 1-2 hours, until a 10x concentration is remaining. This concentrated media was then transferred to an Eppendorf and stored at -80°C. The number of cells within each flask was counted using a haemocytometer, for which a concentration per number of cells can be determined.

2.2.4b Cell conditioned media of co-cultures

Tumour cells were seeded in a 96-well plate and co-incubated with 200µL of either an effector cell line (NK92MI) or with a CD200 peptide, as a positive control, as above (2.2.3). Cells were co-incubated for the indicated periods of time, after which the suspension NK9MI cells and the conditioned media/supernatant were transferred to a 96-well round bottom plate. This plate was then centrifuged at 200xg for 5 mins to pellet the NK92MI cells at the bottom of the well. To separate and remove only the cultured media/supernatant, 150µL from the top of the well was transferred to another plate, careful not to suck up NK cells. This plate was then sealed and stored at -80°C. Cell numbers for each assay was recorded as to determine concentration per number of cells.

2.3 Immunofluorescence

Immunofluorescence was performed on paraffin embedded sections. Slides were heated at 60°C for 30 mins, then deparaffinised with xylene (2 x 10 mins) and decreasing concentrations of ethanol (100 – 75%) for 5 mins each, followed by a 5 min wash in PBS. For antigen retrieval, samples were submerged in citrate buffer (pH6.0) and heated in a microwave for 10 mins in a pressure cooker and allowed to cool to room temperature gradually. A hydrophobic barrier was drawn around the tissue sample. To block non-specific staining between the primary antibodies and the tissue, samples were incubated in blocking buffer (10% donkey serum in PBS) for 1 hour at room temperature. Primary antibodies (Table 2.4a) were diluted in 5% donkey serum and incubated overnight at 4°C. Samples were washed 4 x 5 mins in PBS Tween-20 (0.5%) before incubating with fluorescence-conjugated secondary antibodies (Table 2.4b) for 1 hour in the dark at room temperature. Samples were again washed 4 x 5 mins in PBS Tween-20 (0.5%) before mounting with Vectashield mounting solution (Vector Labs). Samples were visualised, and pictures acquired on a DMI6000B Inverted fluorescent microscope (Leica Biosystems, England). Microscope settings were unchanged between samples. Samples were also scanned on a Zeiss Axioscan Z1 slide-scanner. Slides were stored at 4°C.

2.3.1 Scoring CD200 expression

Using immunofluorescence, samples were stained for CD200, vimentin and DAPI. Slides were photographed then re-stained with haematoxylin and eosin (H&E) and photographed again. The level of CD200 positivity was determined within H&E demonstrable clear cell RCC regions, using a 5-point grading system: 0 = <1% cells positive, 1 = 1-25% cells positive, 2 = 25-50% cells positive, 3 = 51-75% cell positive and 4 = >75% cell positive. The intensity was also semi quantitatively analysed using the common scoring method: 0 = absent, 1 = weak, 2 = moderate and 3 = strong staining intensity.

2.3.2 Characterising immune infiltrate

Using serial sections of the same TMA, the immune infiltrate for each core was characterised. Cells were counted manually using Fiji Image J and counts were repeated three times on different days to ensure reproducibility. Total leukocyte number was measure by the presence of CD45+ cells. Immune subpopulations were characterised by co-expression of respective markers (summary in table 2.3). Immune cell density was calculated as cells per tumour tissue mm^2. The relative frequency of each immune population infiltrate was characterised as a percentage of the CD45+ cells.

Table 2.3: Markers used for characterising immune subpopulations

Cell Type	Markers
All leukocytes	CD45+
T cells	CD45+ CD3+
Cytotoxic T cells	CD45+ CD8+
T helper cells	CD45+ CD3+ CD4+
T regulatory cells (Tregs)	CD4+ CD25+ FOXP3+
Natural killer cells (NK)	CD45+ NKp46+

Table 2.4a: Primary antibodies used in immunofluorescence

Antibody	Dilution	Source	Cat #	Species
CD200	1:100	R&D	AF2724	Gt
NaDC3	1:200	Proteintech	26184-1-AP	Rb
K14	1:500	Thermo Scientific	RB-9020-P1	Rb
CD45	1:100	Sigma	HPA000440	Rb
CD45	1:200	R&D	MAB1430	Ms
CD3	1:100	abcam	Ab16669	Rb
CD8	1:100	Dako	M7103	Ms
CD4	1:100	R&D	AF-379-NA	Gt
CD25	1:50	R&D	MAB623	Ms
FOXP3	1:100	Cell Signalling	98377	Rb
NKp46	1:200	R&D	AF1850	Gt

Table 2.4b: Secondary antibodies and stains used in immunofluorescence

Antibody	Fluorochrome (nm)	Dilution	Source	Cat #
Dk anti Gt	488	1:500	Invitrogen	A11055
Dk anti Rb	568	1:500	Invitrogen	A10042
Dk anti Ms	647	1:500	Life technologies	A31571
DAPI		1:500		

2.4 Haematoxylin and eosin (H&E)

Haematoxylin and eosin staining was performed on sections previously stained for immunofluorescence. After removal of cover slips, sections were deparaffinised and re-hydrated in a series of xylene and ethanol. Sections were submerged in haematoxylin solution for 5 mins and once stain is considered strong enough, was washed under running water. Sections were then stained with eosin and washed before dehydrating in a series of ethanol and xylene. Sections were mounted and imaged.

2.5 Flow Cytometry

2.5.1 CD200 expression

Cells in culture were collected and counted. Adherent cells in culture were detached using either Trypsin, TrypLe, Versene (Gibco) or by scraping. Cells were washed with FACS buffer (0.05% sodium azide and 0.5% BSA in PBS) before antibody staining. All antibody incubations were carried out for 30 min at 4°C. Antibodies used are summarised in table 2.4. Excess antibodies were removed by washing twice by centrifugation. All centrifugations were performed at 250×g for 5 min at 4°C. Samples were gated on the basis of forward- and side-scatter. Doublets and dead cells were excluded. Single stained samples were used as compensation controls and use of an isotype control was used to determine background fluorescence. Data was processed using FlowJo analysis software.

2.5.2 NK cell degranulation assay

One of the methods used to measure NK cell activity is through analysing degranulation. During degranulation, CD107a becomes expressed on the cell surface. NK92MI cells were co-cultured with tumour cells as described above at an effector:target ratio of 5:1 (2.2.3a). As a positive control for degranulation, NK cells were treated with a combination of PMA and ionomycin, 100ng/mL and 2µg/mL, respectively and as described in (Lorenzo-Herrero *et al.,* 2019). Untreated NK cells were used for baseline expression. The CD107a antibody was added at the beginning of the co-culture. Isotype control for CD107a was also added to the co-culture duration. After 30 mins of co-culture, 1x monensin was added to the well to prevent the reinternalization of the protein. The suspension NK92MI cells were removed from the co-culture and pelleted by centrifugation at 200xg for 5 mins. Cells were washed with FACS buffer (0.05% sodium azide and 0.5% BSA in PBS) before CD56 antibody staining. Antibodies used are summarised below (Table 2.5). Excess antibodies were removed by washing twice by centrifugation. All centrifugations were performed at 250×g for 5 min at 4°C. Samples were gated on the basis of forward- and side-scatter, and CD56 positivity. Doublets and dead cells were excluded. Single stained samples were used as compensation controls and use of an isotype control was used to determine background fluorescence. Data was processed using FlowJo analysis software.

Table 2.5: Fluorescent antibodies and stains used in flow cytometry analysis.

Antibody	Fluorochrome	Dilution	Source	Cat #	Species
CD200	AF647	1 µg/106	R&D	FAB27241R	Ms
CD56	PE	5 µl/10^6	BioLegend	362507	Ms
CD107a	AF647	5 µl/10^6	BD	562622	Ms
CD200R	PE	1µg/10^6	BioLegend	329306	Ms
DAPI		1:500			
AF647 isotype	AF647	Same as target antibody	AbDSerotec	MCA1209A647	Ms
PE isotype	PE	Same as target antibody	BioLegend	400112	Ms

2.6 Protein analysis

2.6.1 Protein extraction

Cells in culture were collected and counted. Adherent cells in culture were detached using Versene (Gibco). Cells were centrifuged at 150 g for 5 mins and the resulting pellet was washed with cold PBS, and again pelleted. PBS was removed, and the pellet was resuspended in 100µL per 10^6 cells of RIPA buffer (compositions of RIPA buffer found in Table 2.6) containing complete protease inhibitors (1 tablet/5mL RIPA buffer; Roche) and incubated on ice for 30 mins. Samples were then homogenised by pipetting before incubating for a further 30 mins on ice. Following incubation, samples were centrifuged at 10,000 g for 10 mins at 4°C and the supernatant was collected and stored at -80°C.

Table 2.6: Buffers used for protein extraction

RIPA BUFFER	**Amount (for 100mL)**
1M Tris pH 7.4	5mL
10% Nonidet-P40 (Sigma)	10mL
Sodium Deoxycholate	0.25g
5M NaCl	3mL
0.25M EGTA	0.4mL
Water pH 7.4	Make up to 100mL

2.6.2 Quantifying protein concentration

The BCA assay kit (Pierce, ThermoFisher Scientific) was used to determine protein concentrations of total proteins. BCA assay was set up in a 96- well clear flat-bottomed plate with each sample ran in duplicate for accuracy. 15µL of sample or BSA standard was added to 200µL BCA reagent (BCA reagent was made using 50 parts of BCA reagent A to 1 part of BCA reagent B) and incubated at 37°C for 30min. Standards of 25, 125, 250, 500, 750, 1000, 1500, 2000µg of BSA per mL were diluted in RIPA buffer to produce a standard curve from which sample protein concentration can be extrapolated. Following incubation, protein concentrations were determined by running the plate on a CLARIOstar plate reader (BMG LABTECH), and protein concentration was calculated.

2.6.3 Western Blotting

Samples were diluted in RIPA buffer to equal concentrations. Laemmli buffer (4x) was added to the samples, which were then heated at 95°C for 4 mins. TGX™ FastCast™ premixed acrylamide solutions (BioRad) was used to cast gels. 20-30 µL (10-20ug of protein) of prepared samples were loaded into the wells in addition to a molecular weight marker (PageRuler Plus, ThermoFisher). Once the samples were loaded, the electrophoresis tank was connected to a power pack and gels were run at 300V until the desired marker separation was achieved. Trans-Blot® Turbo™ Transfer System (BioRad) was used to transfer to PDVF membrane. Protein transfer was confirmed using ponceau red. Following confirmation of transfer and washing steps in TBST, membranes were incubated with gentle agitation in blocking buffer of 10% milk or BSA (depending on antibody) in TBST for 1 hour at room temperature. Following incubation, membranes were incubated in the desired primary antibody (see Table 2.7b) diluted in 5% BSA or milk (depending on the antibody used) in TBST and incubated overnight at 4°C on a roller. Following incubation, the membrane was washed 4 x 5 mins in TBST before incubating in horseradish peroxidase (HRP)-conjugated secondary antibody (Abcam) diluted 1:5000 in TBST for 1 hour at room temperature (see Table 2.7c). Membranes were washed again for 4 x 5 mins in TBST before antibody binding was detected by incubating Illumina Forte chemiluminescence reagent (Millipore) on the membrane for 30-60 seconds (less for endogenous controls) and membrane transferred to the ChemiDoc MP Imaging System (BioRad) and chemiluminescence was detected and imaged. Where necessary, membranes were stripped and re-probed to detect another protein of interest. Western blot data was quantified by densitometry, in which the ImageLab software (BioRad) was used. The pixel density over the selected areas was quantified and compared. A full list of reagents used can be seen in the table below (Table 2.7a).

Table 2.7a: Buffers used in western blotting

Solution	Composition
4x Laemmli (Loading) Buffer	60mM Tris-Cl pH 6.8, 2% SDS, 10% glycerol, 5% β-mercaptoethanol, 0.01% bromophenol blue
TBST	1xPBS solution: 5 tablets 500mL dH_2O with 0.5mL Tween (Sigma)
Resolving Gel	Made using TGXTM FastCastTM Acrylimide Kit, 7.5% #161-0171
Stacking Gel	Made using TGXTM FastCastTM Acrylimide Kit, 7.5% #161-0171
1x SDS-PAGE Running Buffer	3.62g Trizma (Sigma), 14.4g Glycine (Sigma) pH6.8 and add H_2O up to 1 L
Trans-Blot Turbo Transfer Buffer	Add 200mL 5x Trans-Blot Turbo Transfer Buffer to 800mL of dH_2O
Blocking Buffer	10% w/v non-fat dry milk powder (Marvel): 0.75g in 15mL TBST 10% w/v BSA powder (Sigma): 0.75g BSA in 15mL TBST
Antibody Dilution Buffer	5% w/v non-fat dry milk powder (Marvel): 0.1g in 2mL TBST 5% w/v BSA powder (Sigma): 0.1g BSA in 2mL TBST
Stripping Buffer	15 g glycine, 1 g SDS, 10 mL Tween-20 to 1 L dH_2O. pH 2.2

Table 2.7b: Primary antibodies used for western blot

Antibody	Dilution	Source	Cat #	Species	Target Size
CD200	1:500	R&D	AF2724	Gt	~47
Phospho-p44/42 MAPK (Erk1/2) (Thr202/Tyr204)	1:1000	Cell Signalling	9101	Rb	42, 44
PARP	1:1000	Cell Signalling	9532	Rb	116, 89
Caspase 8	1:1000	Cell Signalling	9746	Ms	18, 43, 57
Caspase 9	1:1000	Cell Signalling	9502	Rb	35, 37, 47
Fas	1:1000	Cell Signalling	8023	Ms	40-50
FasL	1:1000	Cell Signalling	4273	Rb	26, 40
FADD	1:1000	Cell Signalling	2782	Rb	28
GAPDH	1:5000	Millipore	MAB374	Ms	38

Table 2.7c: Secondary antibodies used for western blot

Antibody	Dilution	Source	Cat #
Goat pAb to Rb IgG (HRP)	1:5000	Abcam	ab97051
Goat pAb to Ms IgG1 (HRP)	1:5000	Abcam	ab98693
Goat pAb to Ms IgG2a (HRP)	1:5000	Abcam	ab97245
Rb pAb to Gt IgG (HRP)	1:5000	Abcam	ab97100

2.7 ELISAs

Enzyme-linked immunosorbent assay (ELISA) is a plate-based assay used to detect and quantify substances such as proteins, peptides, antibodies and hormones. Plates were coated with a capture antibody and left to adhere overnight. Plates were washed and blocked to prevent unspecific binding. Plates were then washed again and incubated with the solution of interest. The capture antibody will immobilise the antigen of interest. The plate was washed further to remove excess and then incubated with a capture antibody. This capture antibody is further conjugated to biotin and streptavidin-HRP and the signal was measured using the CLARIOstar plate reader. For each ELISA, a standard curve is generated using serial dilutions of the protein of interest with a known concentration. This standard curve is used to determine the concentration of our test samples. Wells containing media/diluent served as a blank.

2.7.1 Soluble CD200 ELISA

Soluble CD200 in cell line supernatant was determined using the Sino Biological solid phase sandwich ELISA (SEK10886), following manufacturer's guidelines. Preparation of cell culture supernatant can be found above (2.2.4a). The capture antibody was diluted to a working concentration of 2µg/mL in PBS before coating a 96 well and leaving to incubate overnight at 4°C. The following day, wells were washed with wash buffer before blocking with blocking buffer for one hour at room temperature. Summary of solutions used can be found in table (2.8a). Wells were again washed before samples and standards were added and incubated for two hours at room temperature. A seven-point standard curve using 2-fold serial dilutions in sample dilution buffer, and a high standard of 3000 pg/mL was used. Following washing, wells were then incubated with the detection antibody diluted to working concentration of 0.5µg/mL in detection antibody dilution buffer and left to incubate for one hour at room temperature. Wells were washed for a final time before 200µL substrate solution was added for 20 mins at room temperature and out of direct light. To stop the reaction, 50µL of stop solution was added to each well and the plate was tapped gently to ensure thorough mixing. The optical density was measured immediately, using the CLARIOstar platereader set to 450nm. Wells containing concentrated media of each respective cell types served as the blank. Supernatant was collected from each cell line in replicates of four.

Table 2.8a: Solutions required for Sino Biological sCD200 ELISA

Solution	Components
PBS	136.9 mM NaCl, 10.1 mM Na2HPO4, 2.7 mM KCl, 1.8 mM KH2PO4, pH 7.4, 0.2µm filtered
TBS	20mM Tris, 150 mM NaCl, pH 7.4
Wash Buffer	0.05% Tween20 in TBS, pH 7.2 - 7.4
Blocking Buffer	2% BSA in Wash Buffer
Sample dilution buffer	0.1% BSA in wash buffer, pH 7.2 - 7.4, 0.2µm filtered
Detection antibody dilution buffer	0.5% BSA in wash buffer, pH 7.2 - 7.4, 0.2µm filtered
Substrate Solution	For each plate dilute 250µl substrate stock solution in 25ml substrate dilution buffer and then add 80µl 0.75% H2O2, mix it well
Substrate stock solution	10mg/ml TMB (Tetramethylbenzidine) in DMSO
Substrate dilution buffer	0.05M Na2HPO4 and 0.025M citric acid; adjust pH to 5.5
Stop Solution	2N H_2SO_4

2.7.2 CCL4 ELISA

CCL4 in the supernatant of NK92MI and tumour co-cultures was determined using the R&D Human CCL4/MIP-1 beta DuoSet ELISA, following manufacturers guidelines (DY271). Preparation of cell culture supernatant can be found (2.2.4b). The capture antibody was diluted to a working concentration of 120µg/mL in PBS before coating a 96 well and leaving to incubate overnight at room temperature. The following day, wells were washed three times with wash buffer before blocking with reagent diluent for one hour at room temperature. Summary of solutions used can be found in table (2.8b). Wells were again washed before samples and standards were added and incubated for two hours at room temperature. A seven-point standard curve using 2-fold serial dilutions in sample dilution buffer, and a high standard of 1000 pg/mL was used.

Following washing, wells were then incubated with the detection antibody diluted to working concentration of 3µg/mL in reagent diluent buffer and left to incubate for two hours at room temperature. Wells were washed a further time before adding 100µL of the working dilution of Streptavidin-HRP for 20 mins. Wells were washed for a final time before 200µL substrate solution was added for 20 mins at room temperature and out of direct light. To stop the reaction, 50µL of stop solution was added to each well and the plate was tapped gently to ensure thorough mixing. The optical density was measured immediately, using the CLARIOstar platereader set to 450nm. Wells containing concentrated media of each respective cell types served as the blank. Supernatant was collected from each assay in replicates of four.

Table 2.8b: Solutions required for Sino Biological CCL4 ELISA

Solution	Components
PBS	137 mM NaCl, 2.7 mM KCl, 8.1 mM Na2HPO4, 1.5 mM KH2PO4, pH 7.2-7.4, 0.2µm filtered
Wash Buffer	0.05% Tween® 20 in PBS, pH 7.2-7.4
Reagent diluent	1% BSA in PBS, pH 7.2-7.4, 0.2µm filtered
Substrate Solution	1:1 mixture of Colour Reagent A (H2O2) and Colour Reagent B (Tetramethylbenzidine), (R&D Systems, Catalogue #DY999)
Stop Solution	2N H_2SO_4

2.7.3 sFasL ELISA

sFasL in the supernatant of NK92MI and tumour co-cultures was determined using the R&D Human Fas Ligand/TNFSF6 DuoSet ELISA, following manufacturers guidelines (DY126). Preparation of cell culture supernatant can be found (2.2.4b). The capture antibody was diluted to a working concentration of 2µg/mL before coating a 96 well and left to incubate overnight at room temperature. The following day, wells were washed three times with wash buffer before blocking with reagent diluent for one hour at room temperature. Summary of solutions used can be found in table (2.8b). Wells were again washed before samples and standards were added and incubated for two hours at room

temperature. A seven-point standard curve using 2-fold serial dilutions in sample dilution buffer, and a high standard of 2000 pg/mL was used. Following washing, wells were then incubated with the detection antibody diluted to working concentration of 50ng/mL in reagent diluent buffer and left to incubate for two hours at room temperature. Wells were washed a further time before adding 100µL of the working dilution of Streptavidin-HRP for 20 mins. Wells were washed for a final time before 200µL substrate solution was added for 20 mins at room temperature and out of direct light. To stop the reaction, 50µL of stop solution was added to each well and the plate was tapped gently to ensure thorough mixing. The optical density was measured immediately, using the CLARIOstar platereader set to 450nm. Wells containing unspent media served as the blank. Supernatant was collected from each assay in replicates of three.

2.8 Cell Viability Assay - CellTiter Glo

The CellTiter-Glo® Luminescent Cell Viability Assay is a homogeneous method to determine the number of viable cells in culture based on quantitation of the ATP present. Cells were plated (20,000 cells in 100µL) in an opaque-walled 96 well plate and left overnight to adhere. The following day, an estimate of the number of cells in the wells was determined by detaching a swith Trypsin and counting. Tumour cell count was used to determine effector-target ratio. Media was removed and NK cells were added to the wells at various effector-target ratios. Co-incubations were left for 4 hours, after which NK cells and media were removed and the adherent tumour cells in wells were washed thoroughly with PBS. Fresh media was added to the wells and an equal amount of CellTiter-Glo® reagent was added to each well (100µL). Contents were mixed on an orbital shaker for 2 minutes to induce cell lysis before incubating in the dark at room temperature for 10 minutes. Luminescence was recorded using a CLARIOstar plate reader with wells containing only media serving as a blank. Blank corrected values were used to calculate the percentage of cell death when compared to untreated tumour cells.

2.9 RNA analysis

2.9.1 RNA extraction

Cells in culture were collected and counted. Cells were pelleted by centrifugation at 120 g for 5 mins. RNA was isolated using the Qiagen RNeasy Plus Mini Kit (Qiagen, UK) per manufacturer's instructions. This process begins by disrupting the cells followed by the addition of ethanol to the lysate, which promotes selective binding of RNA to the RNeasy membrane. The sample is then applied to the RNeasy Mini spin column where total RNA binds to the membrane and contaminants are washed away. The retained RNA is then eluted in RNase-free water. The quality of the extracted RNA was assessed using the Agilent RNA 6000 Nano kit. The Nano kit assesses RNA quality quantitatively within the range of 25- 500 ng/µl of total RNA (i.e. RNA from whole tissue or cell cultures). Agilent Nano chips were run on the Agilent 2100 Bioanalyzer according to manufacturer's guidelines. RNA integrity was assessed on the 28S to 18S rRNA ratio, and several other characteristics of the RNA electropherogram trace, to generate an RNA Integrity Number (RIN). RIN assigns an electropherogram a value of 1 to 10, with 10 being the least degraded. RNA concentration was determined using a NanoDrop 2000 (Thermo Scientific).

2.9.2 Preparation of cDNA for quantitative analysis

cDNA synthesis was performed using the Quantitect Reverse Transcription Kit (Qiagen, UK) in 0.2ml PCR tubes as per manufacturer's guidelines. This process begins with the elimination of genomic DNA (gDNA) using a gDNA Wipeout buffer. After gDNA elimination, the RNA is reverse transcribed using a master mix containing a reverse transcriptase, reverse transcriptase primers and a buffer. The reverse transcription takes place at 42°C and is then inactivated at 95°C. To help normalise the cDNA output, an equal amount of RNA was reverse transcribed.

2.9.3 Quantitative real-time PCR (qPCR)

For qPCR gene expression studies, all reactions were performed using the TaqMan assay. Pre-designed TaqMan primer/probes were obtained from Applied Biosystems (see table 2.9). Reactions were run using the TaqMan Universal Master Mix II, with UNG (Applied Biosystems) according to the manufacturer's guidelines. Housekeeping genes

(usually GAPDH and beta actin) were used as a reference gene for each plate run. All reactions were run in three technical triplicates. All reactions were run on the QuantStudio 7 Flex Real-Time PCR system (Applied Biosystems) supplemented with the QuantStudio software. Gene expression analysis of qPCR data was analysed using the 2ΔΔCt method to calculate fold change relative to control or for analysis of expression levels, arbitrary units were calculated.

Table 2.9: Probes used for qPCR

Gene Symbol	Assays on demand reference	Dye
CD200	Hs01033303_m1	FAM-MGB
FAS	Hs00236330_m1	FAM-MGB
FASLG	Hs00181225_m1	FAM-MGB
FADD	Hs00538709_m1	FAM-MGB
ADAM17	Hs01041915_m1	FAM-MGB
ADAM28	Hs00248020_m1	FAM-MGB
ACTB	Hs00357333_g1	FAM-MGB
GAPDH	Hs02758991_g1	FAM-MGB

2.9.4 Microarray

RNA for microarray was extracted as outlined in 2.9.2 and RNA quality was checked. RNA was amplified, and cDNA was prepared using the Illumina TotalPrep RNA Amplification Kit, which is used to generate biotinylated amplified RNA for hybridisation with Illumina Sentrix arrays. Samples were applied to the Illumina HumanHT-12 v4 Expression BeadChip, which provided genome-wide transcriptional coverage of well-characterized human genes. 9 samples (3x untreated NK, 3x 2-hour treatment and 3x 4-hour treatment with CD200 peptide) were applied to the chip using the Direct Hybridization assay protocol. A full protocol and reagent list can be found on the Illumina website. The labelled cRNA generated was hybridised to the BeadChip containing the complementary gene specific sequence. The cRNA samples were first preheated to 65°C for 5 mins and then allowed to cool to room temperature before adding the appropriate amount each cRNA sample into each hybridisation tube (750ng worth of cRNA for 12-sample chip)

and made up to 5µL using nuclease free water. Finally, to each cRNA sample tube, 10µL of HYB solution was added (15µL total). Next 15µL of the sample was loaded onto the ports of the BeadChip, which was loaded into a Hyb chamber insert. The BeadChip chamber lid was closed and placed in the Hyb chamber into a 58°C Illumina Hybridization Oven for at least 14 hours. Following incubation in the Hyb Chamber the BeadChip was washed in E1BC solution before being blocked with Block E1 buffer for 10 mins. The final stage before scanning the BeadChip was detection of the signal, which involves the addition of Cy3-SA to bind to the analytical probes that were hybridised to the BeadChip, which allowed for differential detection of signals upon scanning the BeadChip. Cy3-Streptavidin was diluted 1:1000 in Block E1 buffer and the BeadChip was incubated in the solution for 10 mins. After the incubation, the BeadChip was washed with fresh Wash E1BC buffer. After incubation, the BeadChip was dried by placing it in a centrifuge and spinning at 1,400rpm for 4 min at room temperature. After the centrifuge was complete, the dried BeadChip was stored in a dark environment until ready to be scanned. The BeadChip was imaged in the iScan system.

2.9.5 Bioinformatic analysis of the data

Microarray data were analysed using the Bioconductor packages in the R statistical program for data processing for all the subsequent steps. For analysing Illumina microarray data, the 'Lumi' package was used for assessing quality control of the samples. Outliers were removed, before transforming the data using variance stabilising transformation (vst) and normalising the data using the conditional quantile normalisation method. Finally, genes were annotated and mapped at the probe level using 'lumiHumanAll.db' and 'luminHumanIDMapping' programs respectively. Genes/probes whose expression was absent between the samples were then filtered out. Comparisons between the treated groups and the untreated group were performed using the Limma program again in the Bioconductor package to calculate the level of gene differential expression. The fold change and standard errors were estimated by fitting a linear model for each gene using 'lmFit' and the empirical Bayes smoothing was applied to the standard errors using 'eBayes'. A list of differentially expressed genes (DEGs) at a p value <0.05 was obtained. Expression values of DEGs were used to perform pathway analysis using NIH DAVID Tools (NCBI), and Gene Set Enrichment Analysis

(GSEA; Broad Institute) by exporting the DEGs in a format accepted by GSEA software. Bioinformatic analysis was performed with the help of members of Cardiff University School of Biosciences data clinic.

2.10 Statistical Analysis

An unpaired student's T-test was used to establish statistical significance between experimental sample sets. All sample sets were analysed for equal variance and on at least sample sizes of n=4. A Mann-Whitney U test was used to establish statistical difference between immune phenotype variables as normal distribution was not detected. Correlation between CD200 tumour area and intensity score was determined using Spearman's rank correlation. Error bars on bar graphs represent standard deviation and bar and whisker plots were used to demonstrate the range in TMA samples. Statistical tests were carried out using GraphPad. Results were taken to be significant if the calculated p value was equal to or less than 0.05.

Chapter 3:

Characterising CD200 expression

in renal cell carcinoma

Chapter 3: Characterising CD200 expression in renal cell carcinoma

3.1 Introduction

CD200 is a highly conserved transmembrane glycoprotein normally expressed by neurons, endothelial cells, follicular dendritic cells, lymphocytes, macrophages, and granulocytes (Wright *et al.,* 2001). CD200 expression has been well studied in many haematopoietic malignancies. CD200 has also been linked to a number of solid tumours such as melanoma, basal cell carcinoma and breast cancer, and has shown some link to prognosis (Moreaux *et al.,* 2008). This report demonstrated a particular overexpression of CD200 in RCC when compared to normal kidney at mRNA level. CD200 expression has not been extensively studied in RCC and the aim of this study is to characterise expression in this cancer type. In this chapter, we analysed the expression of CD200 at protein level in RCC patient samples, analysing the three main subtypes.

3.2 Expression of CD200 for immunofluorescent analysis

We first determined the specificity of our CD200 antibody. CD200 is a marker for the human hair follicle bulge. Optimisation of the CD200 primary antibody was performed using human hair-bearing skin samples (n=3) (Figure 3.1). As expected, CD200 expression was in the hair follicle bulge (arrow).

Sections that were stained using the secondary antibody alone served as a negative control and did not yield any staining. We observed autofluorescence in the hair shaft of both samples. These results demonstrate the specificity of our CD200 antibody and that CD200 expression on paraffin-embedded sections could be detected by immunofluorescence staining protocol.

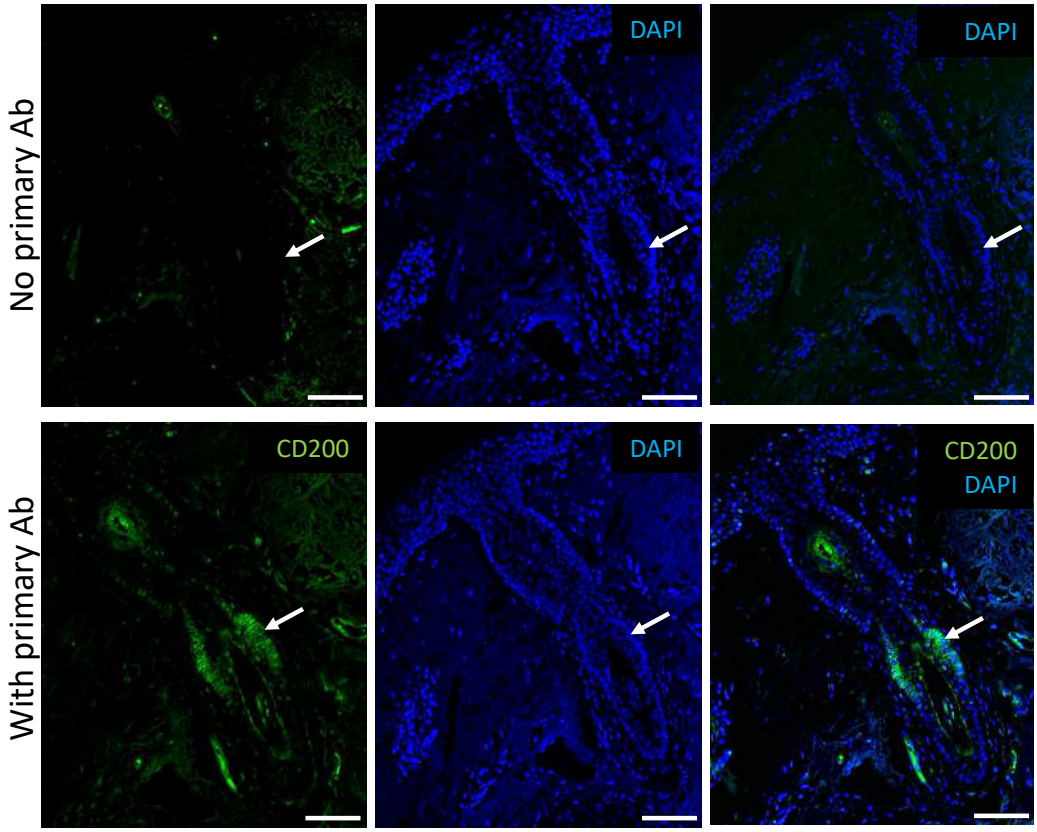

Figure 3.1: Optimisation of CD200 antibody labelling using human skin. Human hair bearing skin sections were labelled by immunofluorescence for CD200 and stained with DAPI. Section were stained with only secondary antibody as a negative control. Representative image of n=3. Scale bar represents 100 µm.

3.3 CD200 expression in normal kidney

As above, a kidney section without CD200 primary antibody were used as a negative control and did not yield any staining, demonstrating specificity of our antibody in our kidney tissue samples (data not shown). Having determined that the antibody specifically identified CD200 positive cells, we analysed CD200 expression in normal kidney.

Each kidney can be divided into two sections, the inner medulla and the outer cortex, both differentiated by the structure within them. The medulla consists of loops of Henle and collecting ducts and can be further divided that structural differentiation of the tubules that form the loops of Henle. The cortex consists of convoluted tubules together with the renal corpuscles, the functional filtration units of the kidney. The renal corpuscle is the most distinctive microscopic feature of the kidney and is clearly visible in our samples using H&E (Figure 3.2, A). Each renal corpuscle consists of an epithelial cup called Bowman's capsule enclosing a knot of capillaries and other elements called the glomerulus. To confirm the structure of the kidney and the corpuscles, we used vimentin. Vimentin is an intermediate filament protein ubiquitously expressed by mesenchymal cells. Expression of vimentin in the kidney is reported in the mesenchymal cells, including blood vessels. Glomeruli also shown extensive expression of vimentin, whereas the epithelial cells constituting tubules are negative. Immunofluorescence analysis of vimentin expression in our kidney samples demonstrates specific staining localised to the corpuscles, with no expression observed in the tubules (Figure 3.2, B). Having identified these filtration structures, we analysed CD200 expression within them. We observed CD200 expression both within the glomeruli and on the bowman’s capsule.

Renal tubules make up the majority of the cortex. Cells of the proximal tubules stain more intensely eosinophilic than those the comprising distal tubules, with nuclei spaced further apart. The proximal convoluted tubule is lined by a simple cuboidal epithelium. The apical end of each cell has a brush border of microvilli, which are often visible in histological staining. The distal convoluted tubule is also lined by a simple cuboidal epithelium but do not have a brush border. The lumens of distal tubules commonly appear more open and clear than those of the proximal tubules. Because the proximal

convoluted tubule is considerably longer than the distal convoluted tubule, a typical section of the renal cortex includes many more profiles of proximal tubules than of distal tubules. Using the H&E staining of our kidney samples, we were able to identify both proximal and distal tubules based on the appearance of nuclei and the presence of the brush border (Figure 3.2, A). Immunofluorescent analysis demonstrated moderate expression of CD200 across the tubules, both in the distal and proximal tubules, with latter demonstrating stronger staining. This finding is important to note as RCC is a kidney cancer that originates from the lining of the renal tubules.

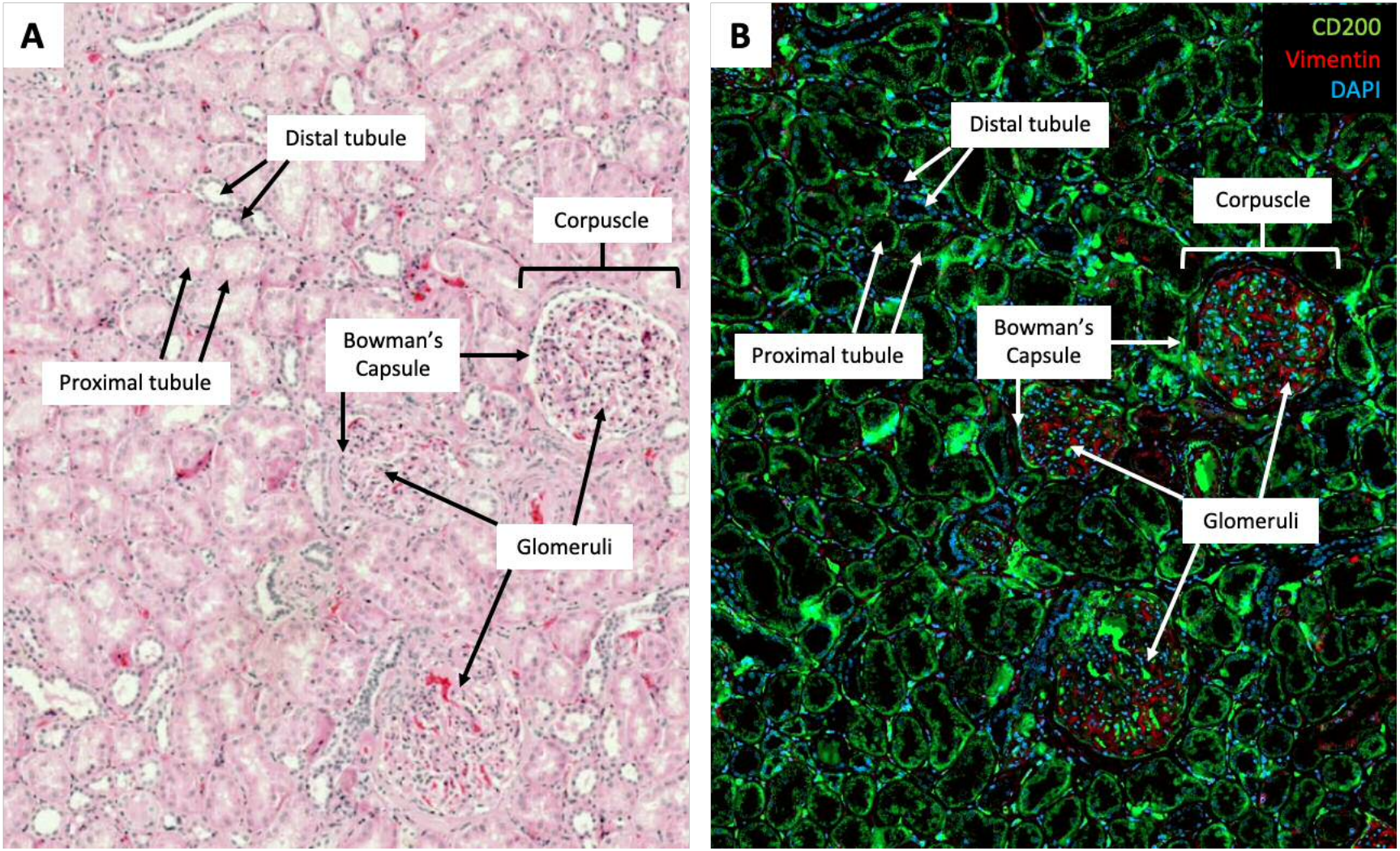

Figure 3.2: CD200 expression in normal human kidney. Human normal kidney sections were stained with H&E (A) and by immunofluorescence for CD200 and vimentin and stained with DAPI (B). Structural features of the kidney are annotated.

3.4 CD200 expression in renal cell carcinoma

Having identified that CD200 is expressed in the tubules of the kidney, we next analysed whether expression was retained in RCC. RCC is a heterogeneous group of cancers arising from renal tubular epithelial cells and the most common subtypes are clear cell RCC (ccRCC), papillary RCC (pRCC), and chromophobe RCC (chRCC). A total of 91 paraffin-embedded tissues of RCC patients were analysed determining CD200 expression by immunofluorescence (Figures 3.3 – 3.5). Of the 91 samples, 10 were chRCC, 13 were pRCC and 68 were ccRCC. The ccRCC samples were made up of cores taken from patients with different stage disease (T1-T4). The area of tumour that was positive for CD200 was calculated semi-quantitively using a scoring system and the intensity of the expression was also scored. Scoring was performed as described in the materials and methods.

3.4.1 Analysing the presence of CD200 expression

Of the 91 RCC samples, 84 (92.3%) scored positive for CD200 expression, where positivity >25% of the sample. Within each subtype, 90% of the chRCC, 100% of the pRCC and 91.2% of ccRCC samples scored positive (Table 3.1). Within ccRCC, the number of positive samples increased with disease stage.

Table 3.1: Summary of CD200 positive RCC samples

Disease	Positive (%)
RCC	**84/91 (92.3)**
chRCC	9/10 (**90**)
pRCC	13/13 (**100**)
ccRCC	62/68 (**91.2**)
T1	*18/21 (**85.7**)*
T2	*13/15 (**86.7**)*
T3a	*11/12 (**91.7**)*
T3b/T4	*20/20 (**100**)*

3.4.2 Analysing the distribution of CD200 expression

We analysed the distribution of CD200 expression within our samples. Where samples demonstrated CD200 positivity, the samples would be positive across the entire tumour section. Therefore, upon using our area of CD200 expression scoring system, we observed no significant difference in CD200 expression coverage between the RCC subtypes or between the disease stages in ccRCC.

3.4.3 CD200 expression intensity

In addition to analysing the presence and area coverage of CD200 expression, we also characterised the intensity of the expression. The majority of the RCC samples demonstrated weak staining for CD200 (44.9%). This remained the case for ccRCC, with the majority of the samples demonstrating weak staining, however a number of samples demonstrated both moderate and strong CD200 expression (Figure 3.3). In pRCC, over half of the samples (53.8%) demonstrated strong CD200 staining intensity (Figure 3.4), whilst chRCC demonstrated mainly weak intensity (60%) (Figure 3.5). Several samples demonstrated unspecific binding, which was determined by analysing respective H&E staining. Areas demonstrating unspecific binding were ignored in calculating overall intensity of each core. A summary of expression can be seen below (Table 3.2).

Upon comparing the CD200 expression between the RCC subtypes, it was observed that the average CD200 expression intensity was significantly greater in ccRCC when compared to chRCC (p=0.0349) but not when compared to pRCC. We also observed a significantly greater CD200 intensity in pRCC when compared to chRCC (p=0.0098).

Table 3.2: Summary of CD200 expression intensity score in RCC

	CD200 Intensity			
Disease	**Absent (%)**	**Weak (%)**	**Moderate (%)**	**Strong (%)**
RCC	**4/91 (5.1)**	**35/91 (44.9)**	**22/91 (28.2)**	**30/91 (33.0)**
chRCC	1/10 (10)	6/10 (60)	3/10 (30)	0/10 (0)
pRCC	0/13 (0)	4/13 (30.8)	2/13 (15.4)	7/13 (53.8)
ccRCC	3/68 (5.5)	27/68 (49.1)	19/68 (34.5)	19/68 (27.9)
T1	*0/21 (0)*	*9/21 (64.3)*	*3/21 (21.4)*	*9/21 (42.9)*
T2	*2/15 (13.3)*	*7/15 (46.7)*	*4/15 (26.7)*	*2/15 (13.3)*
T3a	*1/12 (8.3)*	*5/12 (41.7)*	*4/12 (33.3)*	*2/12 (16.7)*
T3b/T4	*0/20 (0)*	*6/20 (42.9)*	*8/20 (57.1)*	*6/20 (30)*

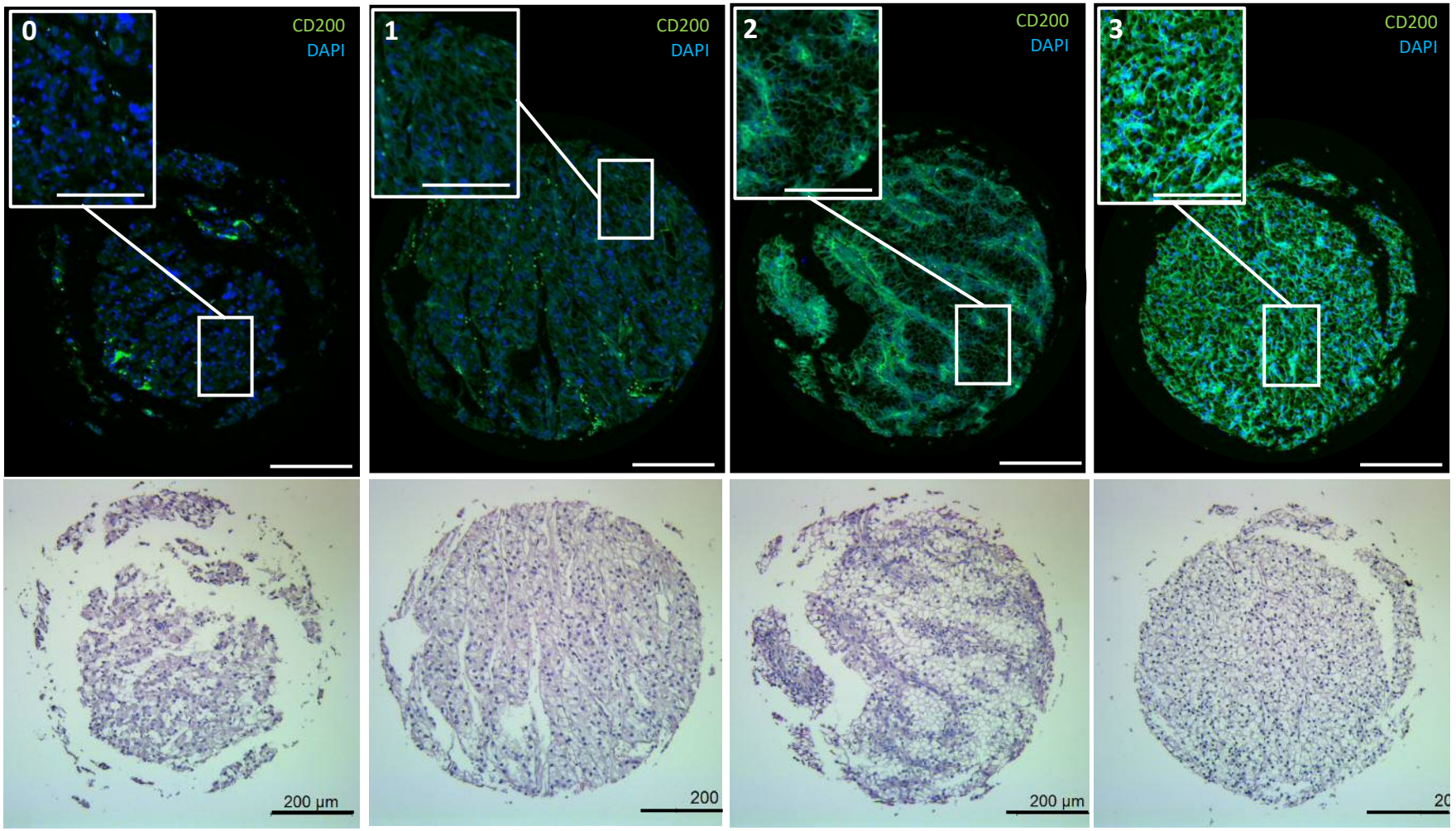

Figure 3.3: Differential CD200 expression intensity in ccRCC. Representative images from patients with different intensity of CD200 expression: absent (0), weak (1), moderate (2) and strong (3). Scale bar represents 200 µm.

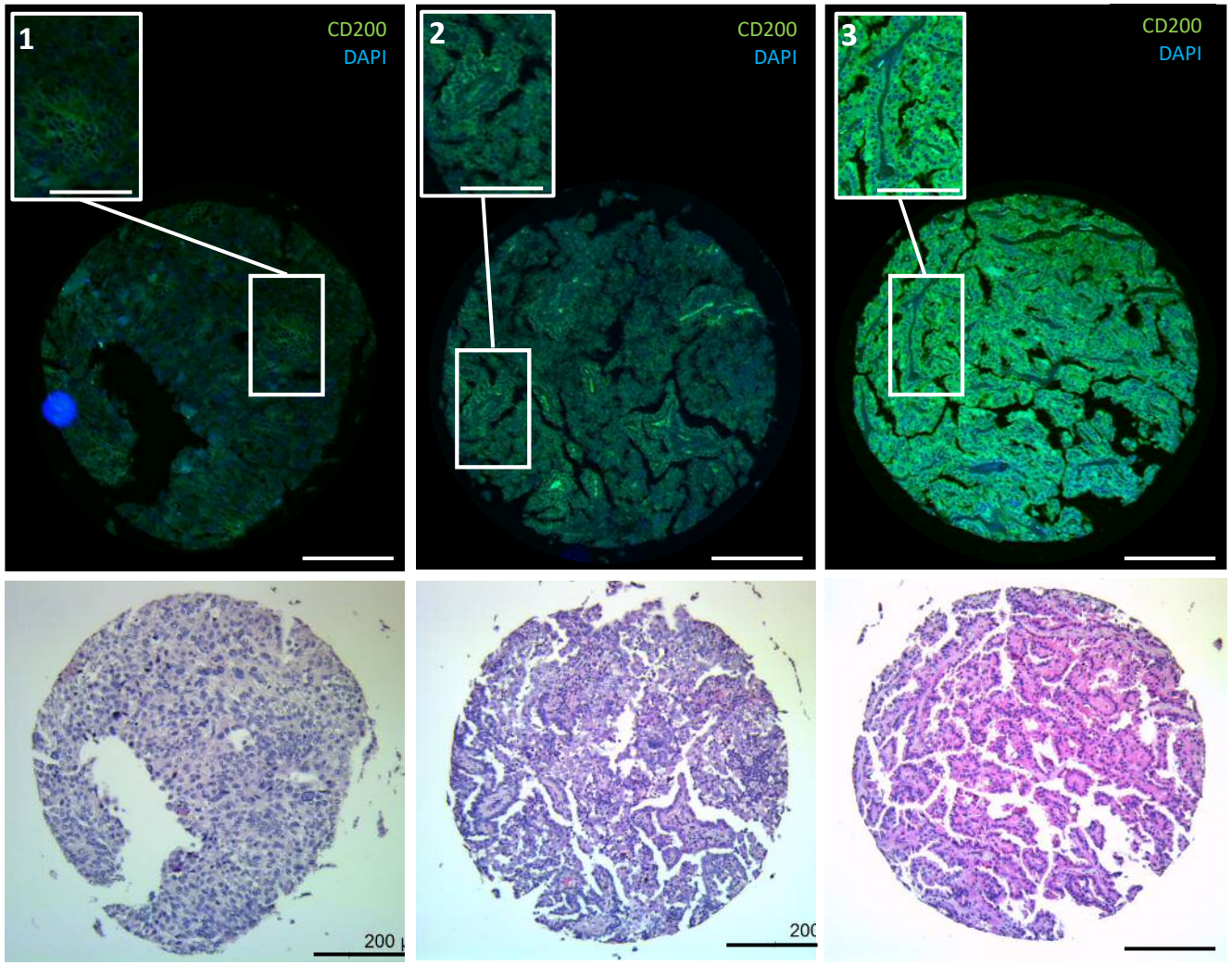

Figure 3.4: Differential CD200 expression intensity in pRCC. Representative images from patients with different intensity of CD200 expression: weak (1), moderate (2) and strong (3). Scale bar represents 200 µm.

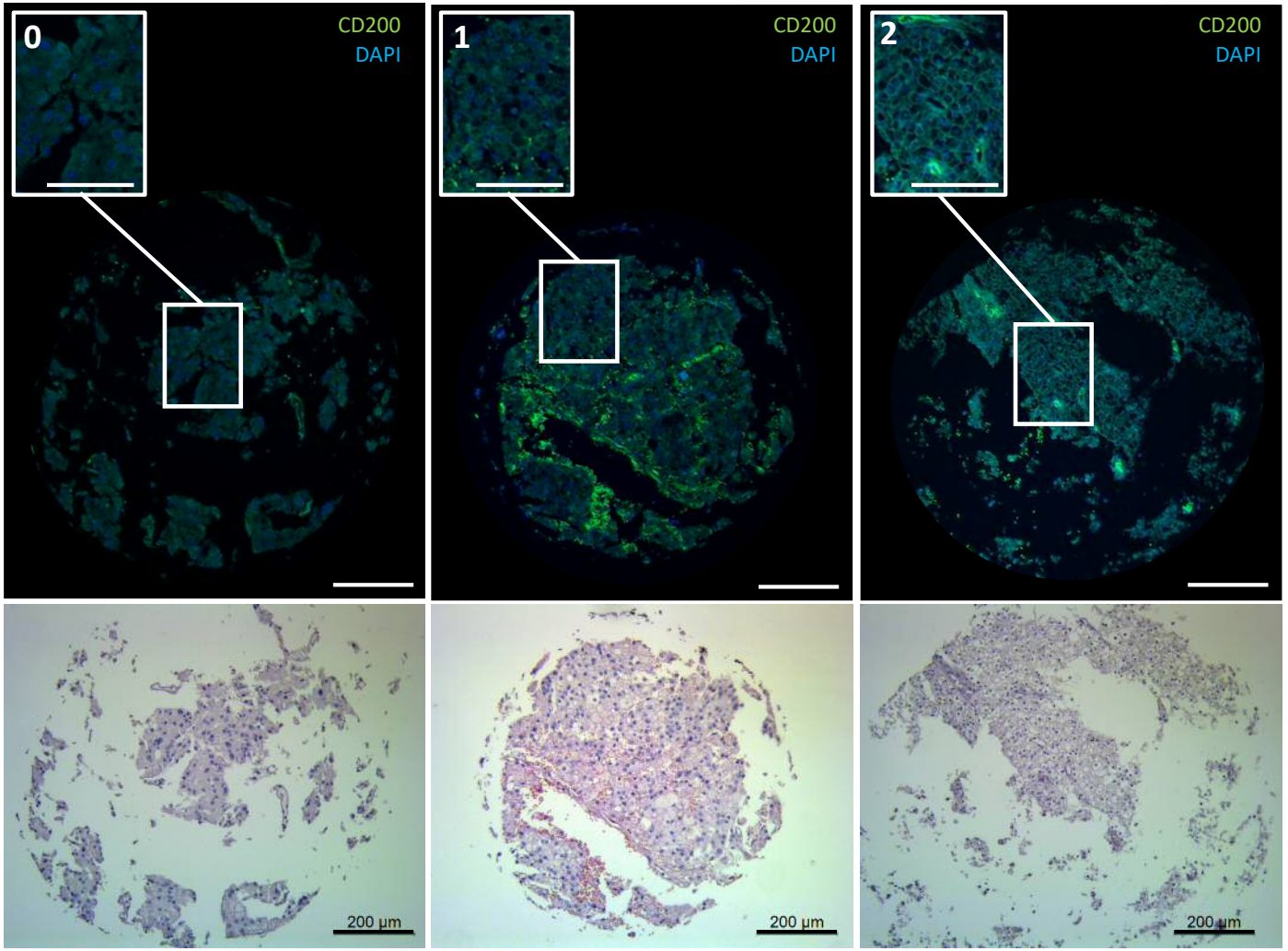

Figure 3.5: Differential CD200 expression intensity in chRCC. Representative images from patients with different intensity of CD200 expression: absent (0), weak (1), moderate (2). Scale bar represents 200 µm.

3.5 Localising CD200 expression in renal tubules

Having identified a stronger CD200 expression in ccRCC and pRCC compared to chRCC, we hypothesised that the renal tubules from which they originate demonstrate differential CD200 expression level.

Solute carrier family 13 member 3 also called sodium-dependent dicarboxylate transporter (NaDC3) transports important metabolic intermediates, including succinate and citrate into cells. This transporter has been shown to play an important role in handling citrate in the kidneys, with expression shown in the basolateral membrane of proximal tubules. We immunoassayed for this transporter as a marker for proximal tubules within our kidney samples to identify whether CD200 expression was limited to a specific tubule.

We observe CD200 expression in across the kidney, with moderate to strong expression seen in the tubules (Figure 3.6). NaDC3 expression is localised to the basolateral membrane of the proximal tubules. Co-localisation of NaDC3 and CD200 can be seen, however, CD200 expression is also observed in the tubules negative for NaDC3. We do however observe stronger CD200 expression in the tubules that stain positive with the proximal tubule marker, which corresponds to the stronger CD200 expression seen in the RCC that originate from these tubules.

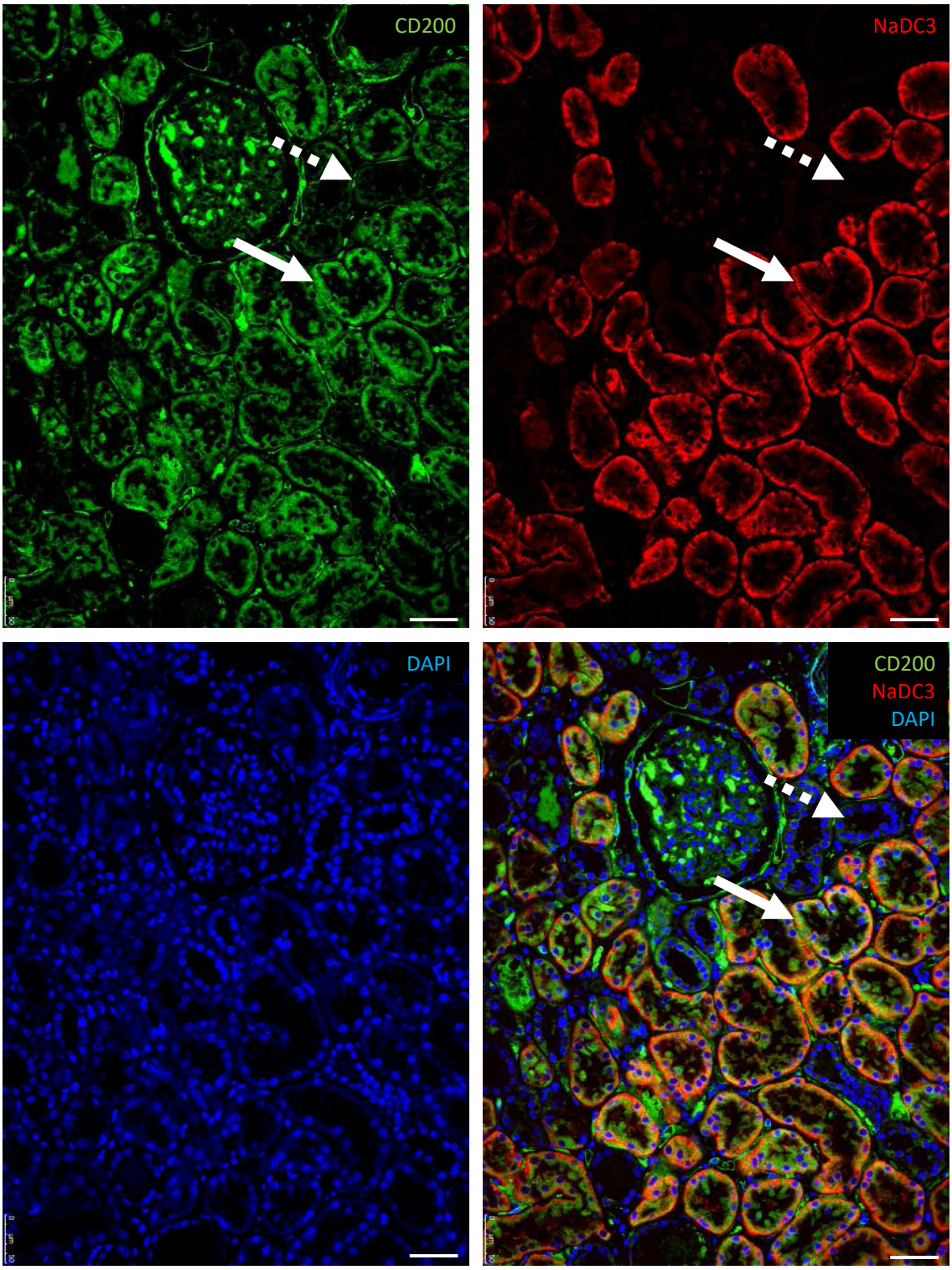

Figure 3.6: CD200 expression in normal kidney. Human normal kidney sections were labelled by immunofluorescence for CD200 and the proximal tubule marker NaDC3, and stained with DAPI. Kidney contains tubules that either co-stain for CD200 and NaDC3 (full arrow) or stain with neither marker (dashed arrow). Scale bar represents 50 µm.

3.6 Summary

CD200 is a highly conserved transmembrane glycoprotein that functions as a negative regulator of the immune system. CD200 is expressed in normal tissue, including reports of expression on the cells of kidney glomeruli (Wright *et al.,* 2001). We first assessed whether CD200 was expressed in normal kidney tissue, where we observed expression both in components of the glomeruli as well as the renal tubules.

Previous microarray studies have highlighted RCC as a cancer type that demonstrates upregulation of CD200 gene expression when compared to normal tissue (Lenburg *et al.,* 2003; Moreaux *et al.,* 2008). We demonstrate that the CD200 expression seen in the tubules was conserved in all three RCC subtypes, a kidney cancer that originates from the lining of the renal tubules. Using immunofluorescence, we confirm CD200 expression in RCC at protein level in the majority of our RCC samples. Upon analysing the intensity of CD200 expression, we observed higher levels of CD200 in ccRCC and pRCC when compared to chRCC. We were able to link this to a stronger CD200 expression in their cell of origin, demonstrating a stronger CD200 expression in the proximal tubules than seen in the distal tubules.

As an immune checkpoint, CD200 functions by providing an inhibitory signal to interacting immune cells. The role of this protein is therefore dependent on the presence and interaction with immune cells that infiltrate the tumour bed. Having identified CD200 expression in RCC, we next sought to explore how expression of this immunosuppressive ligand influenced the immune infiltrate in our samples.

Chapter 4:

Defining the inflammatory response in renal cell carcinoma

Chapter 4: Defining the inflammatory response in renal cell carcinoma

4.1 Introduction

As an immune checkpoint, CD200 functions by providing an inhibitory signal to interacting immune cells. The role of this protein is therefore dependent on the presence and interaction with immune cells that infiltrate the tumour bed. RCC has historically been characterised as a highly immune rich cancer type, with high levels of tumour infiltrating lymphocytes common to the disease. Immune response has been closely associated with clinical outcome in RCC, with tumour infiltrating immune cells forming part of the tumour microenvironment that is known to regulate caner progression. Both cytotoxic CD8+ T cells and CD4+ T helper cells can target antigenic tumour cells. In addition to cells that function to inhibit tumour development, immune cells found within the TME can also inhibit T cell response. One of the most well studied is Treg cells, which secrete immunosuppressive cytokines that can lead to T cell dysfunction. In addition to T cells, NK cells play an important role in the early detection and clearance of tumours. We sought to determine whether tumour expression of CD200 had any impact on the immune infiltrate phenotype by analysing the number and proportion of the key immune cell types for each core.

4.2 Characterising the immune infiltrate

Using serial sections of the same TMA we analysed CD200 expression, we analysed the leukocyte infiltrate in each core and the relationship between immune phenotype and (i) RCC subtype, (ii) disease stage of ccRCC, (iii) CD200 expression in RCC as a whole, and (iii) CD200 expression in ccRCC.

4.2.1 Characterising the immune infiltrate in RCC subtypes

4.2.1.1 Tumour infiltrating leukocytes

We first characterised and compared the immune infiltrate composition between the RCC subtypes. We first analysed the CD45+ immune cell infiltration in our RCC samples. CD45 (leukocyte common antigen) is expressed by most haematopoietic cells and therefore represent the immune cells. RCC samples were stained for CD45 and the number of positive cells were counted, and the density of cells within the tumour core was calculated (cells/mm^2). Representative image for CD45 staining can be found (Appendix; Figure 1). There were significantly more tumour infiltrating CD45+ cells in ccRCC when compared to both pRCC (200.8 ± 288.5 versus 72.6 ± 151.5, p=0.0039) and chRCC (200.8 ± 288.5 versus 15.4 ± 28.0, p=<0.0001) (Figure 4.1). The level of variation in immune cell density seen within ccRCC subtype raises the prospect that variation may relate to immune evasion. We focused our study on the tumour infiltrating lymphocytes, analysing the presence of the main subtypes: T cells and NK cells.

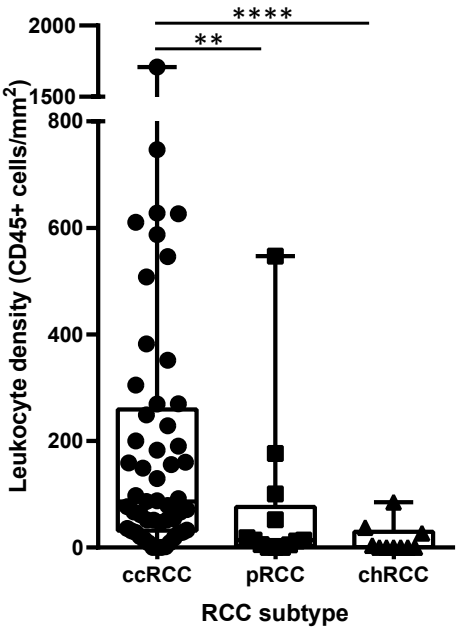

Figure 4.1: Tumour infiltrating CD45+ cells within RCC subtypes. The number of CD45+ cells were counted within each core and the cells/mm^2 was calculated to give immune cell density. The difference in immune cell numbers between each subtype was analysed using a Mann-Whitney test, where ** and ** represents p<0.01 and p<0.0001, respectively.**

4.1.1.2 T cell infiltrate

The density and relative frequency of tumour infiltrating T cells (CD3+) was analysed. Representative image for CD3 staining can be found (Appendix; Figure 1). Although no difference was seen in the relative frequency of the T cell compartment, we saw significant differences in the density of T cells between RCC subtypes. As seen by the increased total CD45+ immune cell infiltrate, there was a significantly higher density of T cells in the ccRCC tumours when compared to both pRCC (170 ± 257.2 versus 64.6 ± 130.2, p=0.0046) and chRCC (170 ± 257.2 versus 13.7 ± 25.5, p=<0.0001). As seen in the density of CD45+ cells, a variation in T cell density was seen within ccRCC.

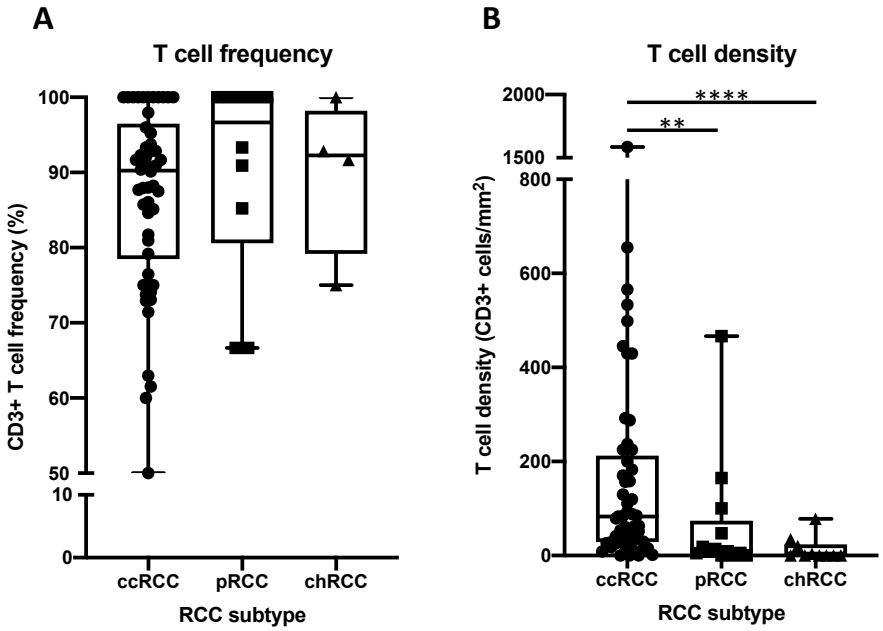

Figure 4.2: Tumour infiltrating T cells within RCC subtypes. The relative percentage of T cells was calculated by calculating the number of the CD45+ cells that were also CD3+ (A). The number of CD3+ cells were counted within each core and the cells/mm^2 was calculated (B). The difference in CD3+ T cell infiltrate between each subtype was analysed using a Mann-Whitney test, where ** and ** represents p<0.01 and p<0.0001, respectively.**

4.1.1.3 T cell subpopulations

T cells are subdivided into two main subtypes based on their expression of CD4 and CD8. T helper cells are CD45+ CD3+ CD4+ lymphocytes. Representative image for CD4 staining can be found (Appendix; Figure 1). There was no difference in the relative frequency of these T helper cells between RCC subtypes (Figure 4.2, A), however, as seen by the increased total number of T cells, the density of T helper cells was also significantly greater in ccRCC when compared to both pRCC (60.4 ± 63.1 versus 21.1, p=0.0034) and chRCC (60.4 ± 63.1 versus 7.8 ± 22.3, p=<0.0001) (Figure 4.2, B).

Cytotoxic T cells are CD45+ CD3+ CD8+ lymphocytes. Unfortunately, triple staining for cytotoxic T cell was not possible, therefore they were identified as CD45+ CD8+. Representative image for CD8 staining can be found (Appendix; Figure 2). As seen in the T helper cells, there was no difference in the relative frequency of CD8+ cytotoxic T cells between the subtypes (Figure 4.2, C). The increased number of T cells was also reflected in the density of cytotoxic T cells, which was significantly greater in ccRCC when compared to both pRCC (102.2 ± 123.8 versus 164.8 ± 377.8, p=0.0173) and chRCC (102.2 ± 123.8 versus 2.0 ± 4.9, p=<0.0001) (Figure 4.2, D). There were also significantly more cytotoxic T cells present in pRCC compared to chRCC (164.8 ± 377.8 versus 2.0 ± 4.9, p=0.0359).

The interactions between CD4 and CD8 T cells are crucial in immunity and the proportion of CD4+ T helper cells to CD8+ cytotoxic T cells is a measure of immune system health, with a CD4:CD8 ratio of 1.5-2.5 in normal blood. We observed no significant difference in the CD4:CD8 ratio between the RCC subtypes (Figure 4.2, E). This result demonstrates that despite the difference in T cell density, the composition of the T cell infiltrate remains consistent between the RCC subtypes and suggests that subtype influences the infiltrate density.

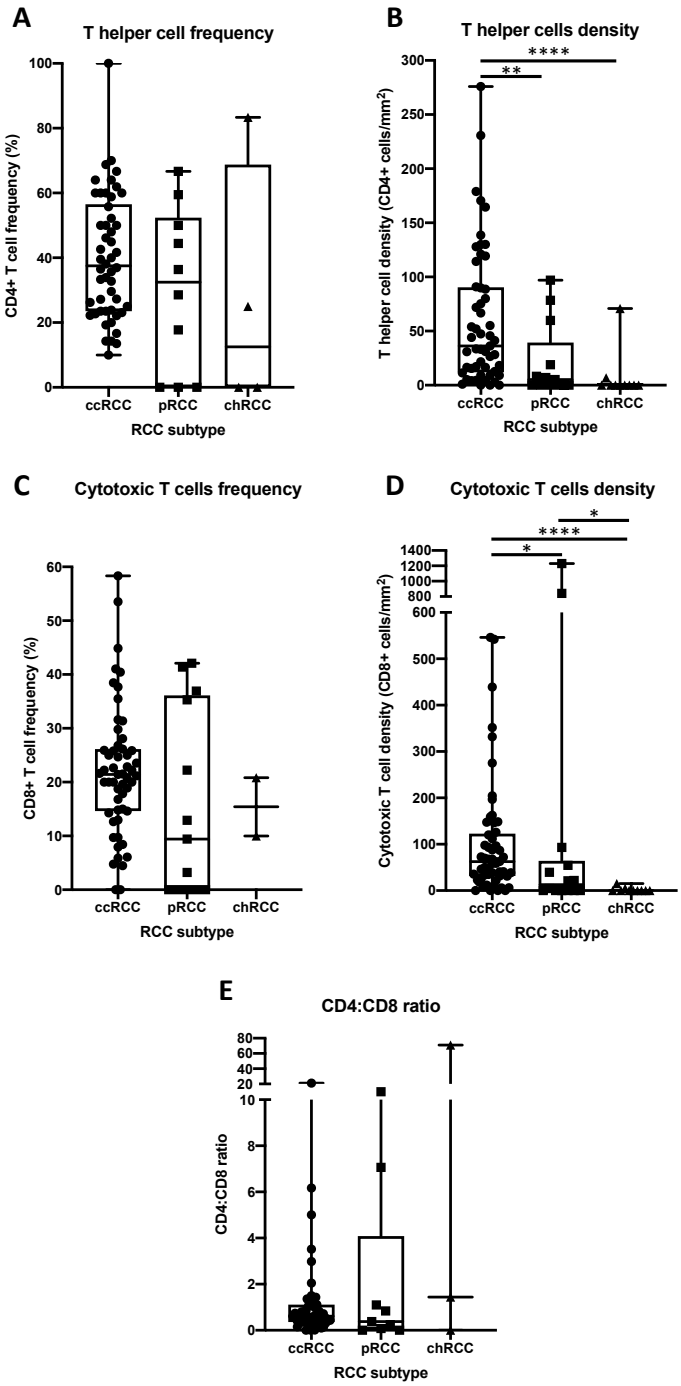

Figure 4.3: Tumour infiltration of T cell subsets within RCC subtypes. The relative percentage was calculated by calculating the number of the CD45+ cells that were also either CD4+ or CD8+ (A, C). The density of CD4+ and CD8+ cells were counted within each core with cells/mm^2 calculated (B, D). The CD4:CD8 ratio was calculated (E). The difference in T cell subset numbers between each subtype was analysed using a Mann-Whitney test, where *, ** and ** represents p<0.05, p<0.01 and p<0.0001, respectively.**

4.1.1.4 Tregs cells

CD4+ T cells are commonly divided into regulatory T (Treg) cells and conventional T helper cells. Treg cells are and have been implicated in downregulating an anti-tumour immune response by inhibiting the function of cytotoxic cells. Presence of these cells has been associated with a poor prognosis for many can cancer types, including RCC. Classical Treg cells are CD4+ CD25+ and are defined by the expression of the nuclear transcription factor, FoxP3. Representative image for Treg staining can be found (Appendix; Figure 3). We observed very few Treg cells within our samples and observed no significant difference in the frequency of these Treg cells between the RCC subtypes (Figure 4.4).

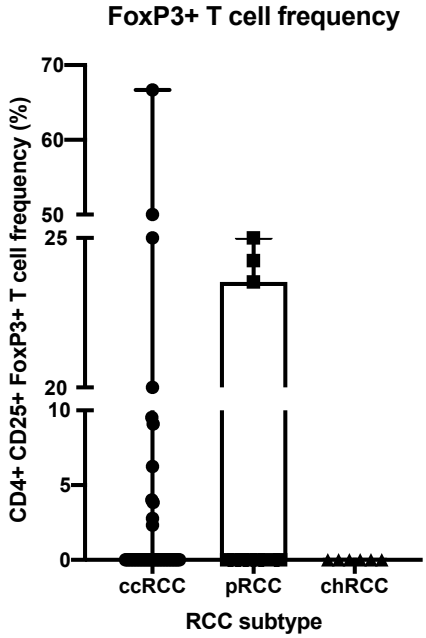

Figure 4.4: Tumour infiltration of Treg cells within RCC subtypes. The relative frequency of Treg cells was calculated by calculating the number of the CD4+ CD25+ lymphocytes were also FoxP3+. The difference in lymphocyte numbers between each subtype was analysed using a Mann-Whitney test.

4.1.1.5 NK cells

NK cells are crucial in the early detection and destruction of emerging tumours. Traditionally, human NK cells are defined as CD56+ and CD3-, with the intensity of CD56 seen as an indicator of function. CD56 is also expressed by other immune cell subtypes, such as NKT cells. NKp46 is uniquely expressed on all NK cell subsets and has been suggested as a pan NK cell marker (Hadad *et al.,* 2015). For this reason, we used NKp46 as a marker of NK cells in our immunohistochemical analysis. Representative image for NKp46 staining can be found (Appendix; Figure 4). The relative frequency of NK cells in the CD45+ immune infiltrate was highest in ccRCC when compared to both pRCC (12.8 ± 12.9 versus 5.8 ± 10.4, p=0.0022) and chRCC (12.8 ± 12.9 versus 1.1 ± 2.9, p<0.0001) (Figure 4.5, A). In keeping with the increased number of CD45+ cells observed in ccRCC, NK cell density was higher in this subtype when compared to chRCC, where NK cells were almost absent (34.6 ± 38.9 versus 0.3 ± 1.0, p<0.0001) (Figure 4.5, B). Less NK cells were also observed in pRCC when compared to ccRCC, however the difference was not significant. As seen with T cells, variation in NK cell density was seen within ccRCC.

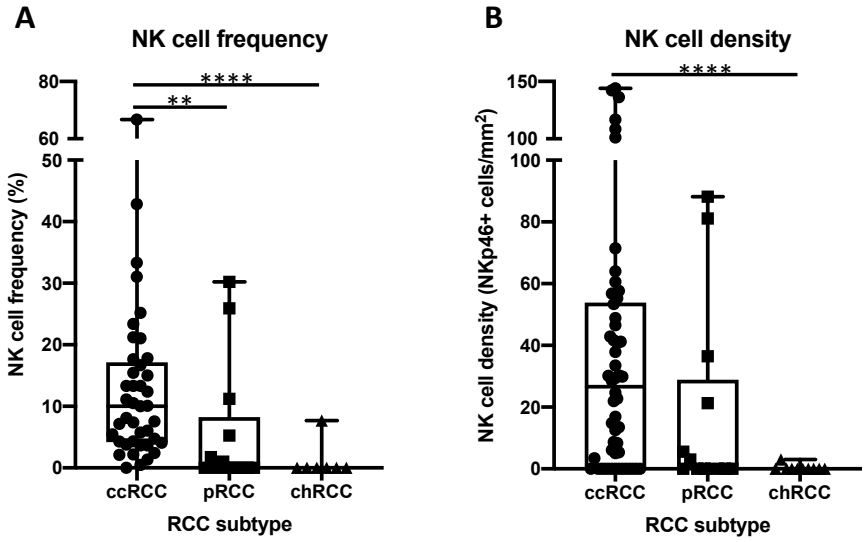

Figure 4.5: Tumour infiltration of NK cells within RCC subtypes. The relative frequency of NK cells was calculated by calculating the number of the CD45+ cells that were also NKp46+ (A). The density of NKp46+ cells was calculated as cells/mm^2 (B). The difference in NK cell numbers between RCC subtypes was analysed using a Mann-Whitney test, where ** and ** represents p<0.01 and p<0.0001, respectively.**

4.1.1.6 Immune phenotype summary of RCC subtypes

Tumour infiltrating lymphocytes (TILs) are the most widely studies immune infiltrate populations. Several studies have analysed those composition of TILs within RCC and the differences between the subtypes. We demonstrated that ccRCC harbours a more dense immune infiltrate, with higher proportions of effector T cells that seen in both pRCC and chRCC. We also observed a higher frequency of NK cells in ccRCC. The average frequency of TIL is presented below (Table 4.1). We observed variation within each subtype, particularly ccRCC, which suggests the possibility that the variation may be linked to immune evasion.

Table 4.1: Immune phenotype summary for each RCC subtype

	Mean ± SD		
Lymphocyte	**ccRCC**	**pRCC**	**chRCC**
T cells (CD3)	**86.8%** ± 12.2	**90.3%** ± 13.4	**89.9%** ± 10.6
Cytotoxic T (CD8)	**22.0%** ± 12.1	**15.7%** ± 17.5	**15.4%** ± 7.7
T helper (CD4)	**40.1%** ± 19.1	**30.3%** ± 25.2	**27.1%** ± 39.3
CD4:CD8 ratio	**1.4** ± 3.1	**3.2** ± 6.3	**24.1%** ± 40.5
Treg (FoxP3)	**4.1%** ± 12.4	**6.6%** ± 11.3	**0.0%** ± 0.0
NK cells (NKp46)	**12.8%** ± 12.9	**5.8%** ± 10.4	**1.1%** ± 2.9

4.1.2 Immune infiltrate changes by disease stage in ccRCC

We have shown that ccRCC is a the most immune-rich RCC subtype when compared to both pRCC and chRCC. ccRCC is the most common subtype within RCC and within our TMA, samples from various disease stage were included. We next sought to determine whether this immune infiltrate changed with disease stage, which would provide an insight into the immune phenotype associated with advanced disease.

4.1.2.1 Tumour infiltrating leukocytes

We previously demonstrated that the total number of tumour-infiltrating cells was greatest in ccRCC. Within this subtype, we observed an increased density of tumour infiltrating CD45+ cells as disease stage increased (Figure 4.6). There was a significant increase in the T3a/T4 stage when compared to stages T1 (319.2 ± 227.6 versus 92.8 ± 133.9, p=0.0027), T2 (319.2 ± 227.6 versus 152.2 ± 214.3, p=0.0469), and T3a (319.2 ± 227.6 versus 227.2 ± 472.4, p=0.0414). This suggests that higher number of tumour infiltrating CD45+ cells is associated with a more advanced disease.

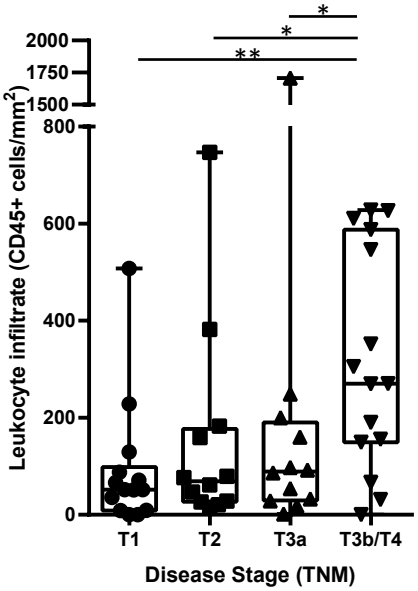

Figure 4.6: Tumour infiltrating CD45+ cells within ccRCC disease stages. The number of CD45+ cells were counted within each core and the cells/mm^2 was calculated to give immune cells density. The difference in CD45+ cell numbers between each subtype was analysed using a Mann-Whitney test, where * and ** represents p<0.05 and p<0.01, respectively.

4.1.2.2 T cell infiltrate

T cells are the most prevalent type of lymphocyte and play an important role in tumour development and progression. We next analysed whether the relative frequency and density of T cells was affected by RCC disease stage. The frequency of T cell lymphocytes demonstrated a general decrease with progressing stage (Figure 4.7, A). There was a significant decrease of CD3+ T cell percentage in the T3a/T4 stage when compared to stages T1 (76.7 ± 10.6 versus 90.2 ± 13.8, p=0.0013), T2 (76.7 ± 10.6versus 90.6 ± 9.6, p=0.0024), and T3a (76.7 ± 10.6 versus 91.6 ± 7.6, p=0.0001). As seen with the overall number of tumour infiltrating CD45+ immune cells, the total number of T cells seen in the tumour increased with disease stage, with a significant increase seen in the number in the late stage T3a/T4 when compared to the early stage T1 (254.9 ± 194.5 versus 81.6 ± 114.3, p=0.0079) (Figure 4.7, B).

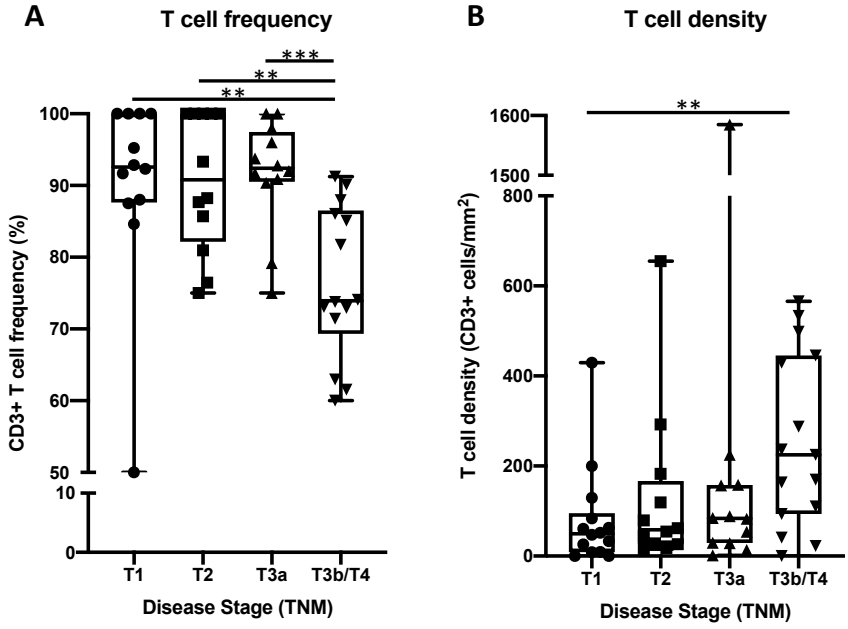

Figure 4.7: Tumour infiltrating T cells within ccRCC disease stages. The relative percentage of T cells was calculated by calculating the number of the CD45+ cells that were also CD3+ (A). The number of CD3+ cells were counted within each core and the cells/mm^2 was calculated (B). The difference in lymphocyte numbers between each subtype was analysed using a Mann-Whitney test, where ** and * represents p<0.01 and p<0.001, respectively.**

4.1.2.3 T cell subpopulations

Having demonstrated that T cell number and frequency is different between disease stages, we next analysed whether either of the two T cell subpopulations demonstrated a similar change. We observed a decrease in the relative frequency of CD4+ T helper cells in the late T3a/T4 stage ccRCC samples when compared to the early stage T1 samples (26.8 ± 8.0 versus 42.4 ± 26.5, p=0.0451), to T2 samples (26.8 ± 8.0 versus 45.8 ± 19.1, p=0.0131), and T3a samples (26.8 ± 8.0 versus 44.7 ± 18.2, p=0.0054) (Figure 4.8, A). Conversely, as seen in the increase in the number of infiltrating T cells, we observed an increase in the number of CD4+ T cells with progressive disease stage (Figure 4.8, A). There was a significant increase in the number of CD4+ T cells in the T3a/T4 stage when compared to stages T1 (88.2 ± 63.1 versus 33.5 ± 39.3, p=0.0173). (Figure 4.8, B).

Unlike the frequency of CD4+ T cells, the frequency of CD8+ cytotoxic T cells increased in the late stage disease (Figure 4.8, C). The relative frequency of CD8+ T cells was significantly greater in the T3a/T4 stage when compared to stage T1 (25 ± 9.2 versus 14.0 ± 10.6, p=0.0096). Similar to the number of T helper cells, the density of CD8+ T cells increased with disease stage (Figure 4.8, D). There was a significant increase in the number of these cytotoxic cells in the T3a/T4 stage when compared to stages T1 (175.6 ± 146.2 versus 67.2 ± 141.4, p=0.0006), T2 (175.6 ± 146.2 versus 78.1 ± 83.5, p=0.0141), and T3a (175.6 ± 146.2 versus 83.0 ± 87.1, p=0.0222). There was also a significant increase in CD8+ cells in stage T3a when compared to stage T1 (83.0 ± 87.1 versus 67.2 ± 141.4, p=0.0388). There was no change seen in the CD4:CD8 ratio between the disease stage (Figure 4.8, E). These results suggest that increased density of T cells, of both subtypes, is associated with a more advanced disease, which may also influence T cell infiltrate composition.

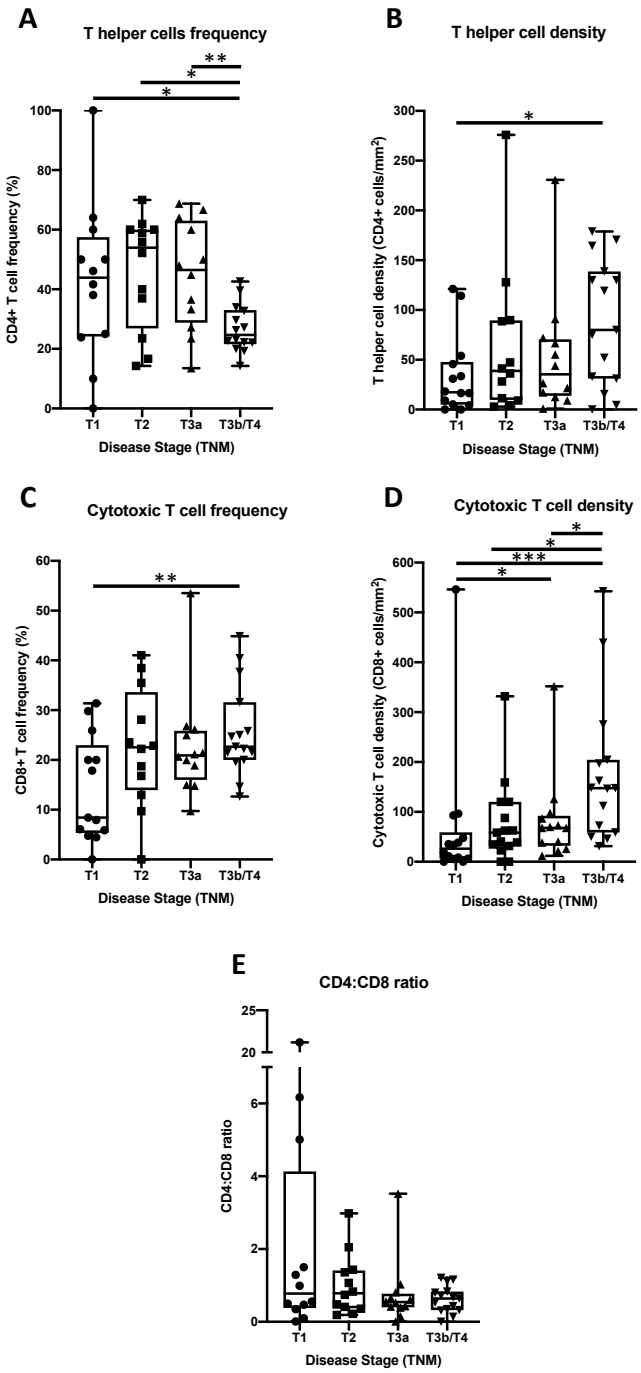

Figure 4.8: Tumour infiltration of T cell subsets within ccRCC disease stages. The relative percentage was calculated by calculating the number of the CD45+ cells that were also either CD4+ or CD8+ (A, C). The density of CD4+ and CD8+ cells were counted within each core with cells/mm^2 calculated (B, D). The CD4:CD8 ratio was calculated (E). The difference in T cell subset numbers between each subtype was analysed using a Mann-Whitney test, where *, ** and * represents p<0.05, p<0.01 and p<0.001, respectively.**

4.1.2.4 Treg cells

We also analysed the frequency of Treg cells, which are often associated with more advanced disease and worse prognosis. We observed no difference in the frequency of classic Treg (CD4+CD25+FoxP3+) cells between the stages of ccRCC (Figure 4.9).

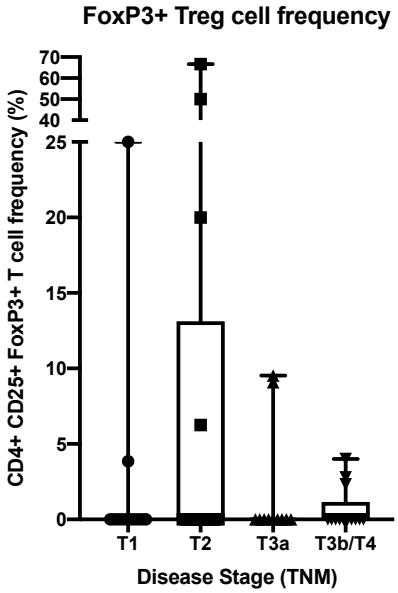

Figure 4.9: Tumour infiltration of Treg cells within ccRCC disease stages. The relative frequency of Treg cells was calculated by calculating the number of the CD4+ CD25+ lymphocytes were also FoxP3+. The difference in lymphocyte numbers between each subtype was analysed using a Mann-Whitney test.

4.1.2.5 NK cells

In addition to T cell lymphocytes, we analysed whether NK cell infiltrate varied with disease stage in ccRCC. Whilst we observed no significant difference in either the frequency or density of NK cells as the ccRCC disease stage increased (Figure 4.10, A and B, respectively). We did, however, observe a trend of increasing NK cell numbers with disease stage.

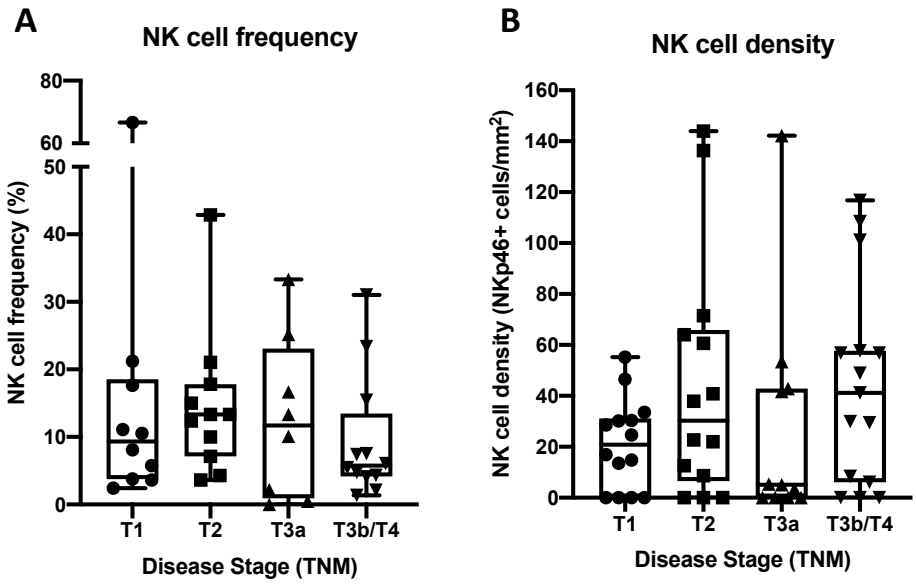

Figure 4.10: Tumour infiltration of NK cells within ccRCC stages. The relative frequency of NK cells was calculated by calculating the number of the CD45+ cells that were also NKp46+ (A). The density of NKp46+ cells was calculated as cells/mm^2 (B). The difference in NK cell numbers between RCC subtypes was analysed using a Mann-Whitney test.

4.1.2.6 Immune phenotype summary for ccRCC disease stages

Having demonstrated that ccRCC is the most immune-rich RCC subtype, we analysed whether disease stage within ccRCC affected the TIL composition. We observed an increase in CD45+ cell density as disease progression. Whilst the density increased with stage, the relative frequency of overall T cells decreased. Interestingly, we saw a decrease in the frequency of T helper cells but an increase in frequency of cytotoxic T cells. The frequency of NK cells appeared to be unaffected by disease stage. The average frequency of TILs is presented below (Table 4.2). These results highlight immune phenotypes that are associated with more advanced disease.

Table 4.2: Immune phenotype summary for ccRCC disease stages

	Mean ± SD			
Lymphocyte	**T1**	**T2**	**T3a**	**T3b / T4**
T cells (CD3)	**90.2%** ± 13.6	**90.6%** ± 9.6	**91.6%** ± 7.6	**76.6%** ± 10.6
Cytotoxic T (CD8)	**14.0%** ± 10.6	**22.5%** ± 12.1	**22.8%** ± 10.9	**25.7%** ± 9.2
T helper (CD4)	**42.4%** ± 26.5	**45.8%** ± 19.1	**44.7%** ± 18.2	**26.8%** ± 8.0
CD4:CD8 ratio	**3.2** ± 6.0	**1.0** ± 0.8	**0.8** ± 0.9	**0.6** ± 0.4
Treg (FoxP3)	**2.4%** ± 7.2	**11.0%** ± 22.1	**1.7%** ± 3.8	**0.7%** ± 1.4
NK cells (NKp46)	**15.1%** ± 19.1	**14.6%** ± 10.8	**12.6%** ± 12.1	**9.4%** ± 9.2

4.2 Relationship between tumour CD200 expression and the immune infiltrate

4.2.1 CD200 expression in all RCC subtypes

Having demonstrated that CD200 is expressed by all three RCC subtypes studied, we analysed whether there was any relationship between CD200 expression in RCC as a whole and the immune infiltrate phenotype. As we observed CD200 expression in the majority of our samples, we analysed the immune phenotype for the CD200 expression intensity. Given that only four of our samples scored negative for CD200, they were not included in the analysis.

4.2.1.1 Tumour infiltrating leukocytes

We have shown that the number of CD45+ tumour-infiltrating cells is influenced by the subtype of RCC as well as the disease stage in ccRCC. We next analysed whether the CD45+ cell infiltrate was affected by RCC expression of CD200. We observed significantly less CD45+ cells in the samples that expressed strong intensity of CD200 when compared to those that weakly expressed CD200 (66.1 ± 184.1 versus 152.4 ± 185.7, p=0.0012) (Figure 3.17). These results suggest that RCC expression of CD200 does influence the density of the tumour lymphocyte infiltrate.

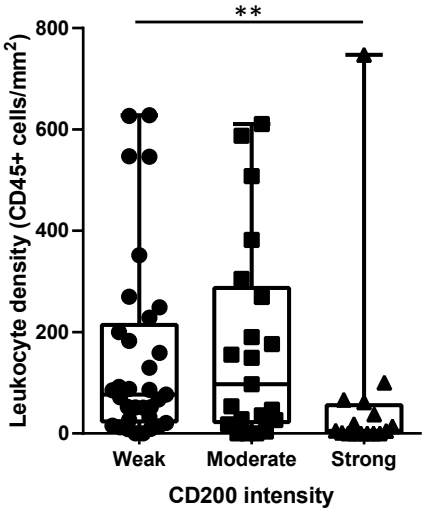

Figure 4.11: CD45+ immune cell infiltrate relative to RCC CD200 expression. RCC samples were grouped according to their CD200 expression intensity. The number of CD45+ cells were counted for each core as before. The difference in CD45+ cell numbers between each CD200 expression grouping was analysed using a Mann-Whitney test, where ** p<0.001.

4.2.1.2 T cell infiltrate

We analysed whether RCC expression of CD200 had any impact on the T cell infiltrate. We observed no significant different in the relative frequency of these cells within the immune infiltrate (Figure 4.12, A). We did, however, observe a decrease in T cell density with the increase in CD200 expression intensity, where we observed a significant decrease in the number of these cells in the samples that expressed strong intensity of CD200 when compared to those that weakly expressed CD200 (59.1 ± 161.6 versus 131.1 ± 162.2, p=0.0016) as well as those that stained moderately for CD200 (59.1 ± 161.6 versus 137.3 ± 150.7, p=0.0155) (Figure 4.12, B). This result suggests that CD200 expression somehow affects T cell infiltration to the tumour.

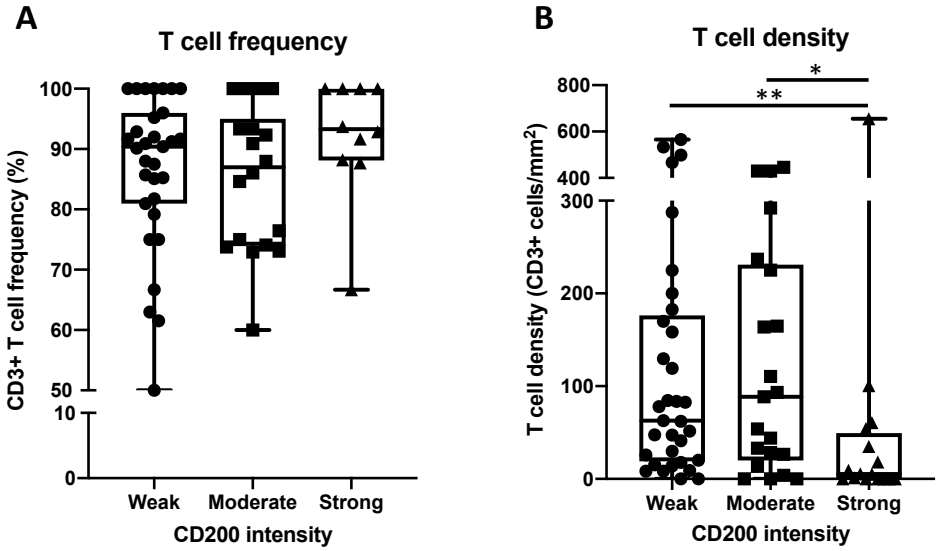

Figure 4.12: T cell infiltrate relative to RCC CD200 expression. RCC samples were grouped according to their CD200 expression intensity. The relative frequency of T cells was calculated by calculating the number of the CD45+ cells that were also CD3+ (A). The number of CD3+ cells were counted within each core and the cells/mm^2 was calculated (B). The difference in CD3+ T cell numbers between each CD200 expression intensity group was analysed using a Mann-Whitney test, where * and ** represents $p<0.05$ and $p<0.01$, respectively.

4.2.1.3 Helper T cells

We analysed whether RCC expression of CD200 had any impact on the helper T cell infiltrate. We observed a significant decrease in the relative frequency of CD4+ T cells in the RCC samples that stained moderately for CD200 when compared to those that stained weakly (30.2 ± 14.8 versus 45.5 ± 20.9, p=0.009) (Figure 4.13, A). As seen in the decrease in the number of overall T cell numbers, the number of CD4+ T cells decreased as the CD200 expression intensity increased, where we observed a significant decrease in the number of these cells in the samples that expressed strong intensity of CD200 when compared to those that weakly expressed CD200 (24.7 ± 69.1 versus 54.8 ± 53.1, p=0.0002) as well as those that stained moderately for CD200 (24.7 ± 69.1 versus 47.1 ± 49.0, p=0.0085) (Figure 4.12, B).

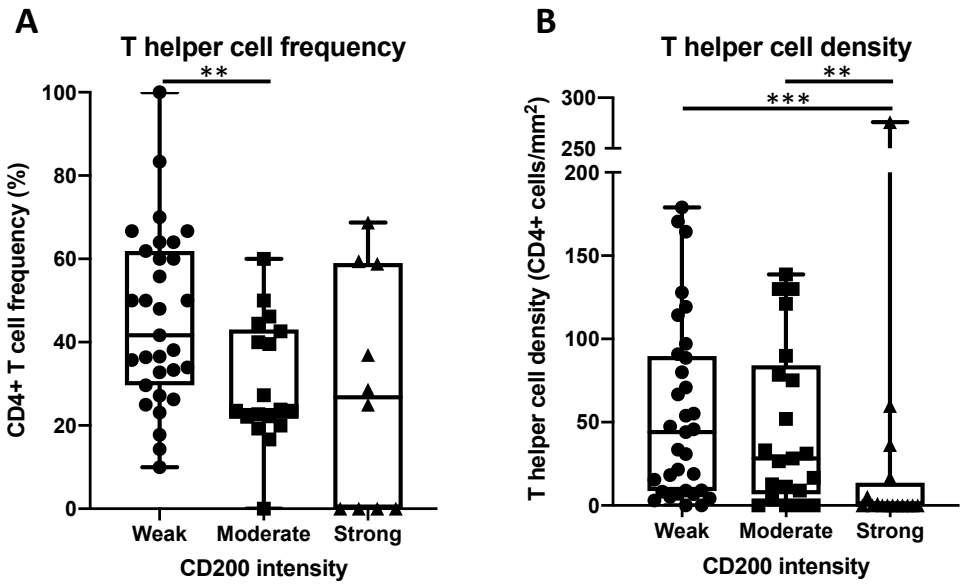

Figure 4.13: T helper cell infiltrate relative to RCC CD200 expression. RCC samples were grouped according to their CD200 expression intensity. The relative frequency of T helper cells mwas calculated by calculating the number of the CD45+ cells that were also CD4+ (A). The number of CD4+ cells were counted within each core and the cells/mm^2 was calculated (B). The difference in CD4+ T cell numbers between each CD200 expression intensity group was analysed using a Mann-Whitney test, where ** and * represents p<0.01 and p<0.001, respectively.**

4.2.1.4 Cytotoxic T cells

We also analysed whether RCC expression of CD200 had any impact on the cytotoxic T cell infiltrate. We observed no difference in the relative frequency of these CD8+ T cells between the CD200 expression intensity groups (Figure 14.4, A). We did, however, observe a difference in the density of cytotoxic cells. As seen in the decrease in the number of overall T cell and the number of CD4+ T cells, the number of CD8+ cells decreased as the CD200 expression intensity increased, where we again observed a significant decrease in the number of these cells in the samples that expressed strong intensity of CD200 when compared to those that weakly expressed CD200 (37.4 ± 82.0 versus 110.9 ± 224.0, p=0.0122) as well as those that stained moderately for CD200 (37.4 ± 82.0 versus 145.3 ± 211.3, p=0.0017) (Figure 4.14, B). These results, taken together with the reduction in CD4+ T cell density, suggest that increased CD200 expression reduces the presence and/or infiltration of T cells to the tumour site.

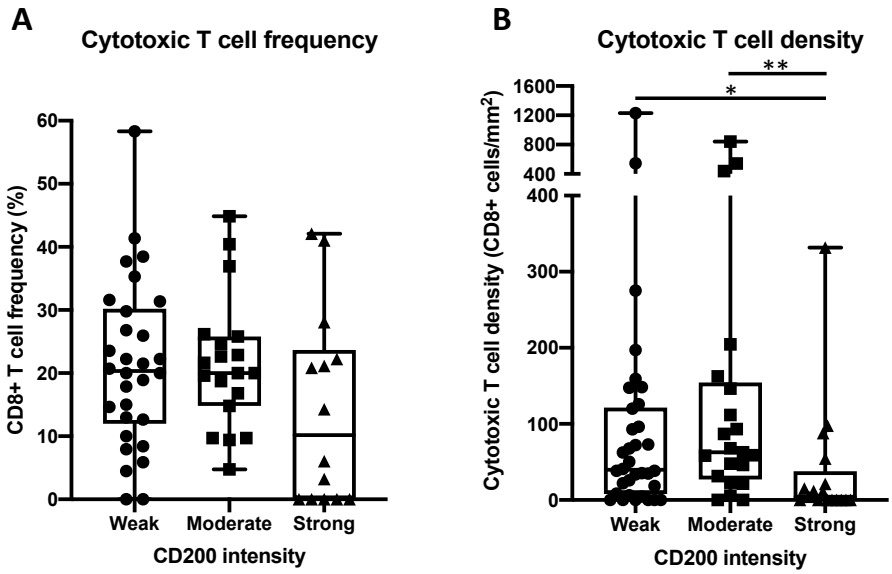

Figure 4.14: Cytotoxic T cell infiltrate relative to RCC CD200 expression. RCC samples were grouped according to their CD200 expression intensity. The relative frequency of cytotoxic T cells was calculated by calculating the number of the CD45+ cells that were also CD8+ (A). The number of CD8+ cells were counted within each core and the cells/mm^2 was calculated (B). The difference in CD8+ T cell numbers between each CD200 expression intensity group was analysed using a Mann-Whitney test, where * and ** represents $p<0.05$ and $p<0.01$, respectively.

4.2.1.5 The CD4:CD8 T cell ratio

We demonstrated that increasing RCC CD200 expression intensity was associated with a decrease in the density of both CD4+ T helper and CD8+ cytotoxic T cells. The relationship between the presence of these two subtypes has been linked to prognosis in various cancers. We analysed the ratio between these T cell subtypes. We observed a significant decrease in the CD4:CD8 T cell ratio in the samples that stained moderately for CD200 when compared to the samples that scored weakly for CD200 (1.6 ± 4.8 versus 4.1 ± 12.7, p=0.0320) (Figure 4.14). This result reflects the significant decrease in CD4+ T cell frequency in the moderate CD200 expression group.

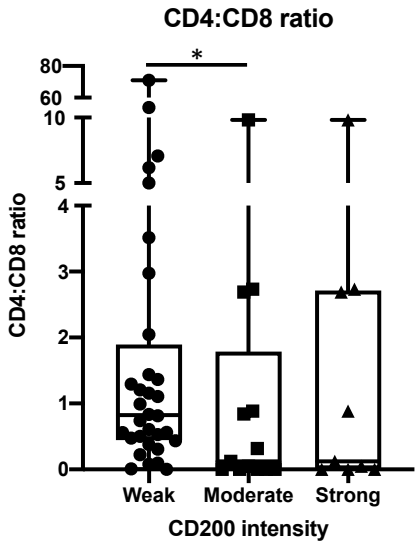

Figure 4.15: The CD4:CD8 T cell ratio relative to RCC CD200 expression. RCC samples were grouped according to their CD200 expression intensity. The number of CD4+ and CD8+ cells were counted for each core. The CD4:CD8 T cell ratio was calculated by dividing the number of CD4+ cells by the number of CD8+ cells. The difference in ratio between each CD200 expression intensity group was analysed using a Mann-Whitney test, where * represents p<0.05.

4.2.1.6 Treg cells

We analysed whether RCC expression of CD200 had any impact on the Treg cell infiltrate. We observed a lower frequency of Treg cells in the RCC samples that scored moderately and strongly for CD200 that in those that stained weakly, however, we observed no significant difference between the groups (Figure 4.16).

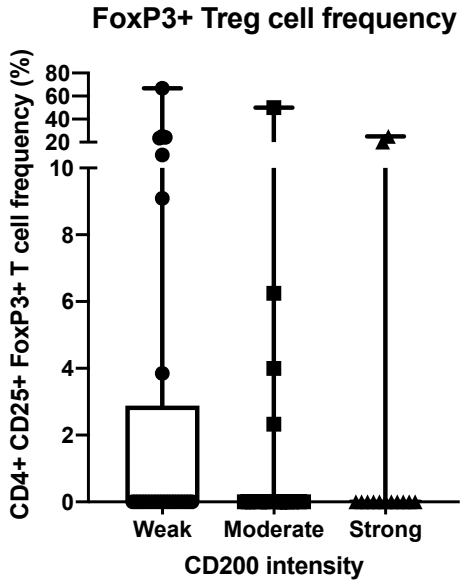

4.16: Tumour infiltration of Treg cells relative to RCC CD200 expression. The relative frequency of Treg cells was calculated by calculating the number of the CD4+ CD25+ lymphocytes were also FoxP3+. The difference in lymphocyte numbers between each subtype was analysed using a Mann-Whitney test.

4.2.1.7 NK cells

We demonstrated that NK cell numbers vary according to RCC subtype, however, unlike T cells, we demonstrated that NK cell number and frequency was not affected by disease stage in ccRCC. We wanted to determine whether NK cell infiltrate was affected by RCC expression of CD200. The frequency of lymphocytes that were NKp46+ demonstrated a decrease as CD200 intensity increase but this was not significant (Figure 4.17, A). There was also no difference in the density of NK cells between the CD200 intensity groups (Figure 4.17, B). Of interest, exclusion of the 2 samples with the highest NK cell numbers in the strongly expressing group would render both the frequency and density of NK cells significantly lower than both the weak and moderate group ($p<0.05$). It is also important to note here that many of the samples are absent of any NK cells.

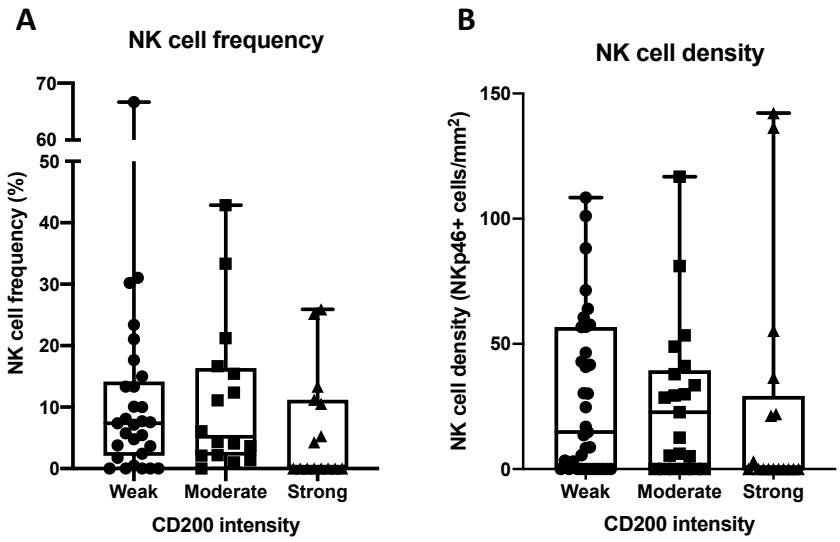

Figure 4.17: NK cell infiltrate relative to RCC CD200 expression. RCC samples were grouped according to their CD200 expression intensity. The relative frequency of NK cells was calculated by calculating the number of the CD45+ cells that were also NKp46+ (A). The density of NKp46+ cells was calculated as cells/mm^2 (B). The difference in NK cell numbers between RCC subtypes was analysed using a Mann-Whitney test.

4.2.1.8 Immune phenotype summary for RCC based on CD200 expression intensity

The purpose of this study was to analyse whether RCC expression of CD200 was associate with any immune phenotype. Upon grouping all RCC samples based on their CD200 expression intensity, we observed a number of associations. We demonstrated that strong CD200 expression was associated with fewer CD45+ infiltrating cells, in which the T cell frequency was reduced. We also observed a decrease in the frequency of T helper cells in the stronger CD200 expressing RCC samples. CD200 expression appeared to have little effect on the NK cell infiltrate. The average frequency of TIL is presented below (Table 4.3). These results suggest that RCC expression of CD200 is associated with a decrease in T cell lymphocyte density and frequency of CD4+ T cells.

Table 4.3: Immune phenotype summary for RCC based on CD200 expression intensity

	Mean ± SD		
Lymphocyte	**Weak**	**Moderate**	**Strong**
T cells (CD3)	**86.7%** ± 12.8	**85.2%** ± 12.0	**92.1%** ± 10.2
Cytotoxic T (CD8)	**21.2%** ± 13.2	**21.6%** ± 10.5	**14.2%** ± 15.3
T helper (CD4)	**45.5%** ± 20.9	**30.2%** ± 14.8	**27.8%** ± 27.8
CD4:CD8 ratio	**4.1** ± 12.7	**1.3** ± 2.7	**1.8** ± 3.2
Treg (FoxP3)	**6.0%** ± 14.3	**3.1%** ± 11.2	**3.5%** ± 8.5
NK cells (NKp46)	**11.0%** ± 13.8	**11.1%** ± 12.4	**6.4%** ± 9.1

4.2.2 CD200 expression in ccRCC

Our previous results demonstrate that ccRCC is the most immune-rich RCC subtype, which demonstrates variation amongst individual samples. We wanted to determine whether this rich infiltrate was affected by CD200 expression in this subtype.

4.2.2.1 Tumour infiltrating leukocytes

We demonstrated that our ccRCC samples contained an increased number of infiltrating CD45+ cells when compared to pRCC and chRCC. We wanted to determine whether CD200 expression within ccRCC had any effect on the number of the CD45+ cells observed. The density of CD45+ cells did not change between samples of varying CD200 expression intensity (Figure 4.18). These results suggest that CD200 expression does not affect the number of CD45+ immune cells that infiltrate the tumour bed in ccRCC.

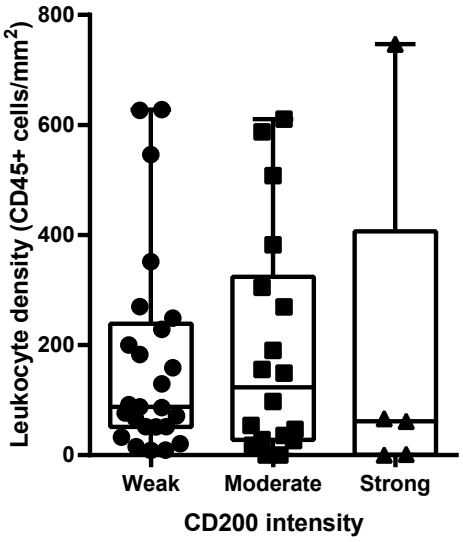

Figure 4.18: CD45+ immune cell infiltrate relative to ccRCC CD200 expression. RCC samples were grouped according to their CD200 expression intensity. The number of CD45+ cells were counted for each core as before. The difference in CD45+ cell numbers between each CD200 expression grouping was analysed using a Mann-Whitney test.

4.2.2.2 T cell infiltrate

We next analysed the relationship between T cell compartment of immune infiltrate and ccRCC CD200 expression. We observed no significant difference in the T cell frequency between the CD200 intensity groups (Figure 4.19, A). We observed no significant difference in the T cell density between CD200 expression intensity groups despite observing a lower average density in the strong CD200 group (Figure 4.19, B). This is likely due to a single outlier that demonstrated a high density of T cells. These results suggest that in ccRCC, CD200 expression levels have little impact on overall T cell infiltrate.

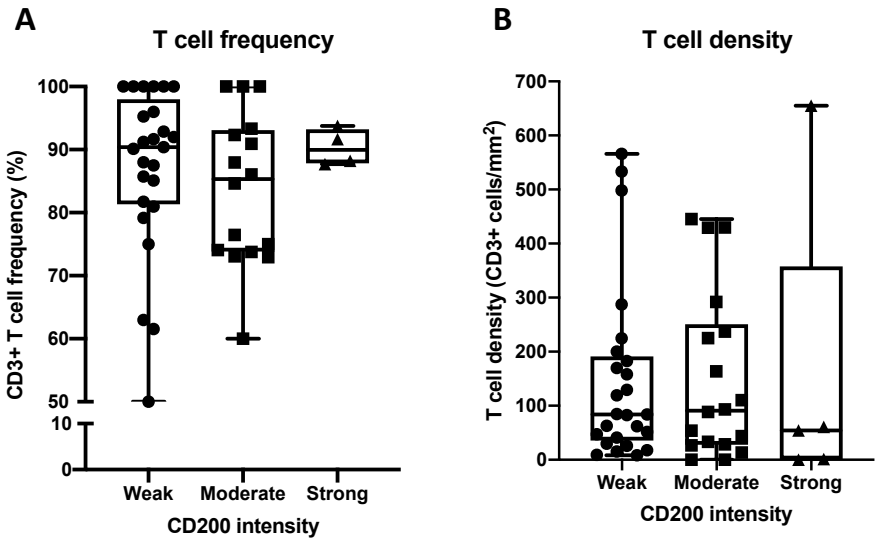

Figure 4.19: T cell infiltrate relative to ccRCC CD200 expression. cRCC samples were grouped according to their CD200 expression intensity. The number of CD3+ cells were counted within each core and the cells/mm^2 was calculated (A). The relative percentage was calculated by calculating the number of the CD45+ cells that were also CD3+ (B). The difference in CD3+ T cell numbers between each CD200 expression intensity group was analysed using a Mann-Whitney test.

4.2.2.3 T helper cells

We have shown that RCC expression decreases the number and frequency of CD4+ T helper cells. We next analysed whether this relationship was also seen in the highly infiltrated ccRCC. When analysing the frequency of CD4+ lymphocytes, we observed a significant decrease in the samples that stained moderately for CD200 when compared to those that stained weakly (37.5 ± 15.1 versus 51.0 ± 19.8, p=0.0152) (Figure 4.20, A). An increase in T helper frequency was seen in the samples that stained strongly for CD200, which may be due to the small sample size. A decrease in the density of CD4+ T cells was observed as the CD200 expression intensity increased; however, no significant difference was observed between each group (Figure 4.20, B). These results suggest that CD200 expression does affect the presence of CD4+ T helper cells, however, to a lesser extent than when considering all RCC samples as a whole.

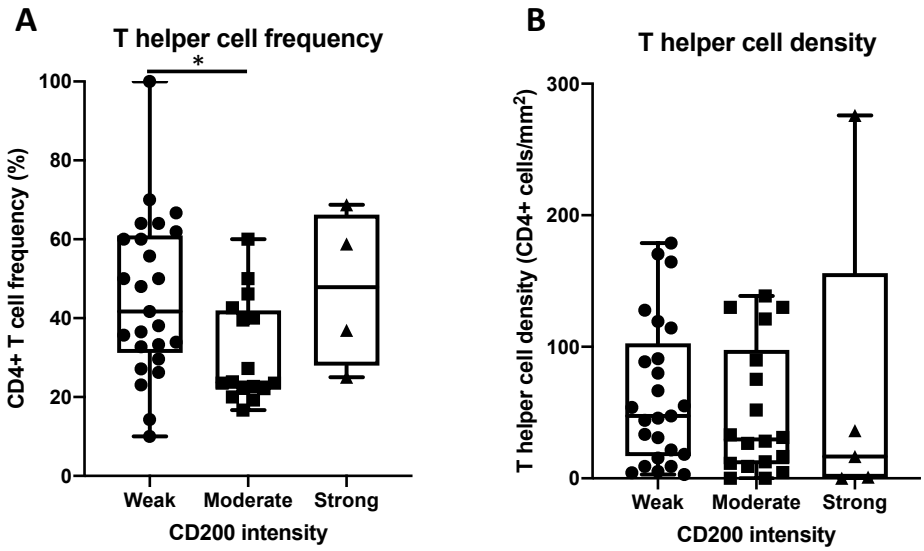

Figure 4.20: T helper cell infiltrate relative to ccRCC CD200 expression. cRCC samples were grouped according to their CD200 expression intensity. The number of CD4+ cells were counted within each core and the cells/mm^2 was calculated (A). The relative percentage was calculated by calculating the number of the CD45+CD3+ cells that were also CD4+ (B). The difference in CD4+ T cell numbers between each CD200 expression intensity group was analysed using a Mann-Whitney test, where * represents p<0.05.

4.2.2.4 Cytotoxic T cells

We wanted to determine whether CD200 expression levels in ccRCC had any effect on the infiltrate of cytotoxic T cells. We observed no difference in the number or CD8+ lymphocytes between CD200 expression intensity groupings (Figure 3.26, A). Interestingly, we did observe a significant decrease in the relative frequency of these cytotoxic cells between those samples that were absent of CD200 and those that stained weakly (44.5 ± 12.8 versus 21.1 ± 12.4, p=0.0476) and those that stained moderately (44.5 ± 12.8 versus 21.4 ± 10.0, p=0.0468) for CD200, however, it is important to note the small sample number that scored absent for CD200 expression. These results suggest that the presence of CD200 does affect the frequency of these CD8+ cytotoxic T cells but the intensity at which CD200 is expressed does not.

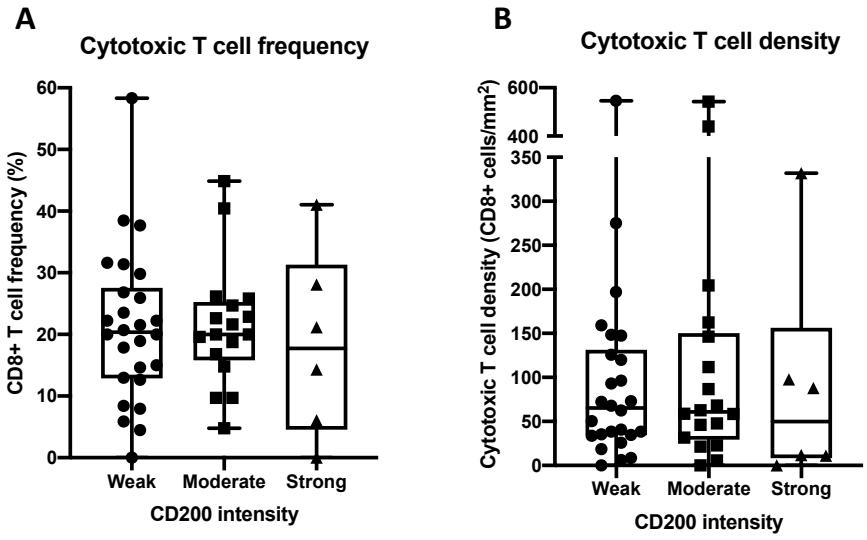

Figure 4.21: Cytotoxic T cell infiltrate relative to ccRCC CD200 expression. cRCC samples were grouped according to their CD200 expression intensity. The relative frequency of cytotoxic T cells was calculated by calculating the number of the CD45+ cells that were also CD8+ (A). The number of CD8+ cells were counted within each core and the cells/mm^2 was calculated (B). The difference in CD8+ T cell numbers between each CD200 expression intensity group was analysed using a Mann-Whitney test.

4.2.2.5 CD4:CD8 T cell ratio

We demonstrated that increasing ccRCC CD200 expression intensity was associated with a decrease in the number CD4+ T helper cells. Whilst we observed a decrease in the CD4:CD8 ratio in the moderate CD200 expression group when compared to the weak CD200 group, this did not reach significance (Figure 4.22). We observed an increase in the CD4:CD8 ratio in the strong CD200 intensity group, which again may be due to the smaller sample size and the outlier. This result suggests that stronger CD200 expression is associated with a decreased CD4 infiltrate, however due to the variability seen in each grouping, the association is not significant.

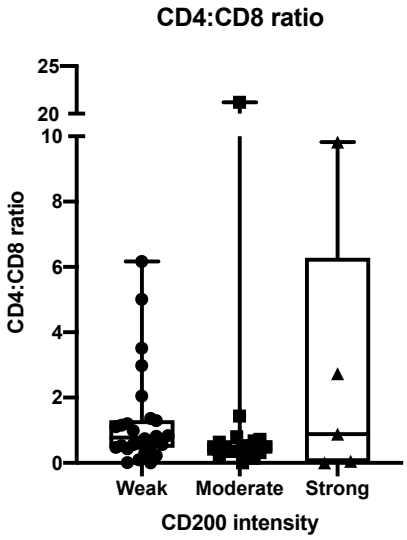

Figure 4.22: CD4:CD8 ratio relative to ccRCC CD200 expression. cRCC samples were grouped according to their CD200 expression intensity. The number of CD4+ and CD8+ cells were counted for each core. The CD4:CD8 T cell ratio was calculated by dividing the number of CD4+ cells by the number of CD8+ cells. The difference in ratio between each CD200 expression intensity group was analysed using a Mann-Whitney test.

4.2.2.6 Treg cells

We analysed whether ccRCC expression of CD200 had any impact on the Treg cell infiltrate. We observed no significant difference between the intensity groups (Figure 4.16).

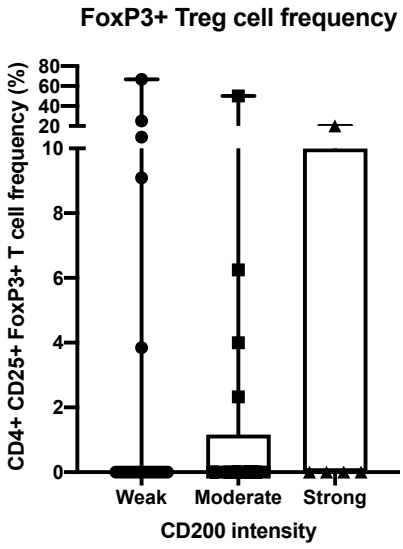

Figure 4.23: Tumour infiltration of Treg cells relative to ccRCC CD200 expression. The relative frequency of Treg cells was calculated by calculating the number of the CD4+ CD25+ lymphocytes were also FoxP3+. The difference in lymphocyte numbers between each subtype was analysed using a Mann-Whitney test.

4.2.2.7 NK cells

We analysed whether CD200 expression affects the presence of NK cells in ccRCC. When analysing the effect of CD200 expression intensity on NK cell frequency in RCC as a whole, we see a slight decrease in the frequency of these cells. In ccRCC, we observed the opposite effect, with the average frequency of NK cells in the CD45+ infiltrate increased with the increasing CD200 expression intensity, however this was not significant (Figure 4.24, A). We did not observe any significant difference in the density of the NK cells based on CD200 expression intensity in ccRCC (Figure 4.24, B). This result suggests that CD200 expression in ccRCC has little impact in the infiltrate of NK cells.

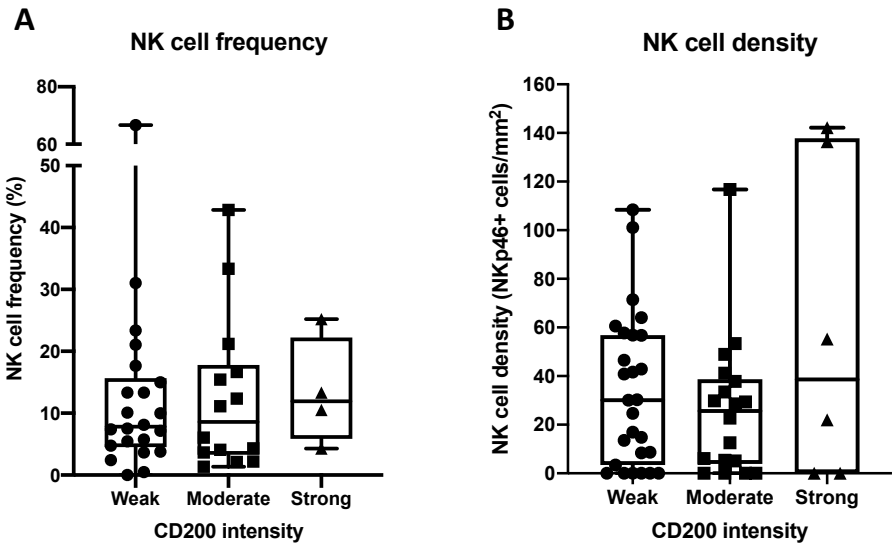

Figure 4.24: NK cell infiltrate relative to ccRCC CD200 expression. RCC samples were grouped according to their CD200 expression intensity. The relative frequency of NK cells was calculated by calculating the number of the CD45+ cells that were also NKp46+ (A). The density of NKp46+ cells was calculated as cells/mm^2 (B). The difference in NK cell numbers between RCC subtypes was analysed using a Mann-Whitney test.

4.2.2.8 Immune phenotype summary for ccRCC based on CD200 expression intensity

Our results so far demonstrate that ccRCC is the most immune-rich subtype, with immune phenotypes associated with disease stage. We analysed whether CD200 expression within ccRCC had any effect on the immune infiltrate phenotype. The intensity of CD200 did not affect the immune phenotype to such an extent as seen when all RCC subtypes were analysed together. We did, however, observe a reduction in T helper cell frequency. We observed no association between ccRCC expression of CD200 and NK cell infiltrate. The average frequency of TIL is presented below (Table 4.4). These results reinforce the suggestion that RCC expression of CD200 is associated with a decrease frequency of CD4+ T cells.

Table 4.4: Immune phenotype summary for ccRCC based on CD200 expression intensity

	Mean ± SD		
Lymphocyte	**Weak**	**Moderate**	**Strong**
T cells (CD3)	**87.1%** ± 13.2	**83.8%** ± 12.0	**90.3%** ± 2.9
Cytotoxic T (CD8)	**21.1%** ± 12.4	**21.4%** ± 10.0	**18.4%** ± 15.0
T helper (CD4)	**45.3%** ± 20.3	**31.2%** ± 13.1	**47.4%** ± 20.0
CD4:CD8 ratio	**1.3** ± 1.5	**1.7** ± 5.0	**2.7** ± 4.2
Treg (FoxP3)	**5.2%** ± 14.8	**3.7%** ± 12.1	**4.0%** ± 8.9
NK cells (NKp46)	**12.6%** ± 14.4	**12.6%** ± 12.6	**13.3%** ± 8.8

4.3 Summary

Renal cell carcinoma is a highly vascularised and immune rich cancer type. Immune infiltration of tumours is thought to be closely associated with clinical outcome in RCC. Having identified CD200 expression in our RCC samples, we sought to analyse whether expression of this immunosuppressive ligand was associated with an immune phenotype. Using serial sections of the same TMA, we were able to characterise the immune infiltrate of each core and relate this to their relative CD200 expression.

We began by analysing the immune phenotype of each RCC subtype, where we demonstrate that ccRCC samples contain a significantly denser tumour CD45+ infiltrate. This result corroborates other similar studies and may be linked to the subtype driver mutation, the loss of VHL activity, leading to a highly vascularised and immune dense environment. We also characterised the immune phenotypes associated with more advanced disease in ccRCC. We observed a higher density of T cells in samples from later stage disease, which was reflected in the increase density of overall CD45+ cell numbers. Within the T cells, we observed that late-stage disease samples included a lower frequency of T helper cells and an increased frequency of cytotoxic T cells. These results suggest that ccRCC is capable of eliciting an immune response but that the activity of immune cells is inhibited upon reaching the tumour bed. We observed no association between disease stage or NK cell frequency. Together, these results provided us with an immune phenotype characteristic of advanced disease for ccRCC.

Having observed CD200 expression in all three RCC subtypes, we analysed whether expression of this immunosuppressive ligand had an overarching effect on RCC immune phenotype. We observed a decrease in CD45+ cells with stronger CD200 expression, which was mirrored by a decrease in both CD4+ and CD8+ T cell frequency. No significant difference was seen in NK cell infiltrate. We did however observe a trend in decreasing NK frequency and density as CD200 expression increased, an observation that may become clearer with increased sample size. We also analysed the effect of CD200 expression on immune phenotype in ccRCC. We demonstrate that CD200 expression had no effect on the density of the CD45+ cells but did demonstrate an effect on T helper cells, whose frequency decreased in the moderate CD200 expressing samples. Again, no

significant difference was seen in the cytotoxic cell infiltrate, both CD8+ cytotoxic T cells and NK cells. We also analysed the presence of immunosuppressive cells. Tregs contribute to suppressing anti–tumour T cell responses. We observed very few of these cells within our samples, which may contribute to the why we observed any difference in frequency of these cells in any of our analyses.

Using serial sections of patient tumour tissue, we were able to characterise an immune phenotype and begin exploring the relationship between this and patient tumour CD200 expression. In addition to demonstrating that RCC expression of CD200 has some impact on the immune phenotype, the presence of an immune compartment highlights the concept that RCC is an immunogenic disease. We demonstrate this by the increased immune compartment in later stage ccRCC samples. Several reports indicate that lymphocytes within RCC tumours are often rendered dysfunctional, suggesting that RCC tumours possess a potent regional ability to impair host anti-tumour immunity. Elucidating the mechanisms responsible for immune dysfunction within the TME may provide useful to improve immunotherapeutic approaches to the treatment of RCC. We hypothesise that RCC expression may play a role in rendering these immune cells incapable of eliciting an effecting tumour killing response upon entering the tumour bed and may therefore be a possible therapeutic target.

Chapter 5:

Functional characterisation of CD200 expression towards NK cells

Chapter 5: Functional characterisation of CD200 expression towards NK cells

5.1 Introduction

Tumours escape the immune system by a variety of mechanisms, all of which result in a significant barrier to conventional anti-cancer and single agent immunotherapy. One of the most well studied is tumour manipulation of immune checkpoints (Postow *et al.,* 2015). Therapies aimed at blocking these pathways and preventing the inhibition of an immune response have since been developed (Darvin *et al.,* 2018). These immune checkpoint blockade therapies function by blocking the inhibitory effect of immune checkpoints, restoring immune cell anti-tumour activity. Immune checkpoint blockade therapies are now approved for the treatment of many cancer types and this success has led to the interest in identifying novel targets (Qin *et al.,* 2019).

CD200 is one such checkpoint that has gained interest in our lab. CD200 is a transmembrane protein with no known signalling motif (Barclay and Ward, 1982). It functions through engaging its receptor, found on various immune cell types. CD200 interaction with its receptor is reported to induce an inhibitory response. CD200 has been well characterised in haemopoietic malignancies, such as acute myeloid leukaemia (Coles *et al.,* 2011). In this cancer, CD200 was associated with the reduced cytotoxicity of effector immune cells, including natural killer cells is impaired. In CD200 high patients, NK cell activity was impaired, with cytolytic function and pro-inflammatory cytokine production reduced. Having identified CD200 expression in the RCC tissue samples, we explored whether this expression may have a similar effect on the tumour infiltrating NK cells that we observed in those same tumours.

In this chapter, we analysed the effect of RCC tumour cell line expression of CD200 on NK cell activity, both their cytotoxic and effector activities. The aim of this chapter was to determine the effect of RCC expression of CD200 on the activity of NK cells.

5.2 Characterising CD200 expression in renal cancer cell lines

In vitro human cell line models have been widely used for cancer pharmacogenomic studies to predict clinical response, to help generate pharmacogenomic hypothesis for further testing, and to help identify novel mechanisms associated with variation in drug response (Niu and Wang, 2015). To explore the role of tumour CD200 expression on immune evasion and the possibility of blocking this signal, we utilised cRCC cell lines.

5.2.1 Optimisation of cell isolation

5.2.1.1 Predicting possible cleavage sites

Our group has previously developed a CD200 tumour model, transducing the cervical cancer cell line, HeLa cells, to constitutively express CD200. This provided us with a CD200 positive and CD200 negative epithelial tumour model. Like HeLa cells, RCC cell lines are adherent and in order to analyse CD200 expression, it is necessary to detach the cells from the flask. The most common method of detaching cells in conventual tissue culture is the use of Trypsin. Trypsin is a member of the serine protease family and is the most commonly used proteolytic enzyme to detach adherent cells. Whilst tolerated by many cell types, it is advised not to use in proteomic studies as can cleave membrane proteins. To determine whether Trypsin would have any effect on CD200 we used ExPASy PeptideCutter tool. PeptideCutter can be used to predict potential cleavage sites cleaved by proteases, like Trypsin, for a given peptide sequence.

CD200 protein sequence (FASTA sequence) was inputted into the ExPASy PeptideCutter tool. The number and position of potential cleavage sites are given. Trypsin was predicted to cleave CD200 at a possible 23 sites within the protein, which of these 18 were in the extracellular domain of the protein (Figure 5.1). This possible cleavage may affect both the function of CD200 as well as antibody binding to the protein.

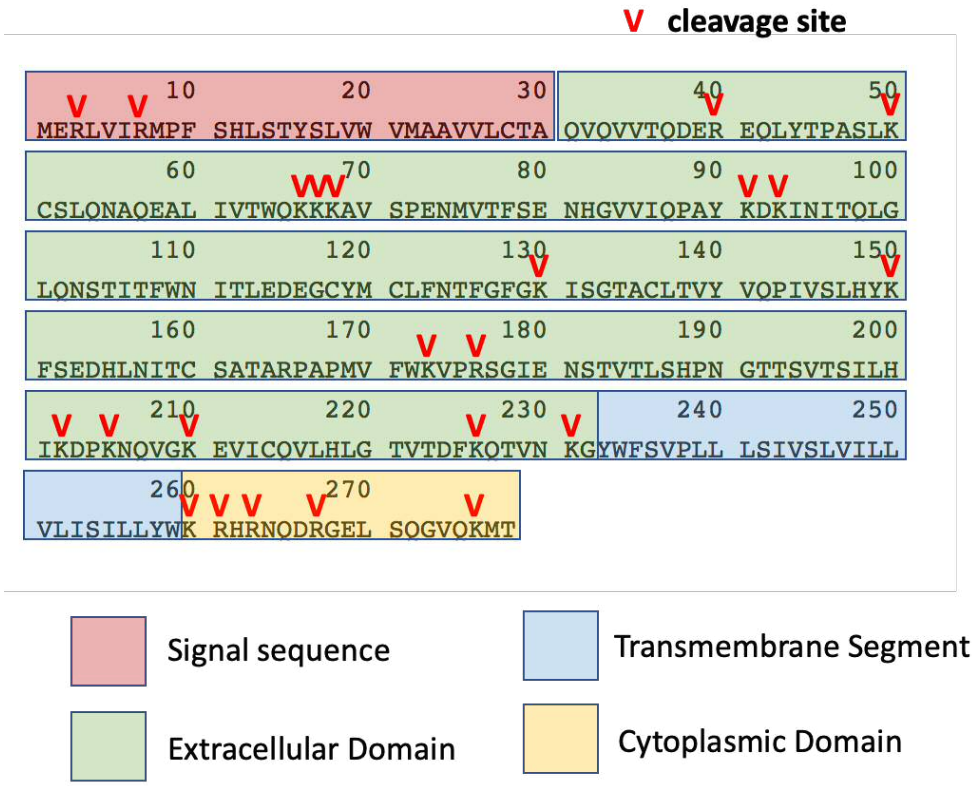

Figure 5.1: Predicted cleavage sites of Trypsin within CD200 protein. The 278 amino acid CD200 FASTA sequence was inputted into ExPASy PeptideCutter tool, which identifies the possible cleavage sites of Trypsin (v).

5.2.1.2 Identifying alternative cell culture detachment methods

Having identified that Trypsin may theoretically cleave CD200 and affect expression on the cell surface, alternative methods of detaching the cells were analysed for their effect on CD200. Using our HeLa CD200+ cell line, Trypsin, TrypLE, Versene and cell scraping methods were used to detach the cells. These cells were analysed for CD200 expression using flow cytometry and the percentage of CD200+ cells were analysed (Figure 5.2). We saw an increase in the percentage of CD200+ HeLa cells in those cells detached with TrypLE, Versene and by scraping when compared to detachment by Trypsin, with a significant increase seen in cells detached with Versene ($p<0.05$). Detachment using Versene was therefore used in subsequent analysis of adherent cell lines.

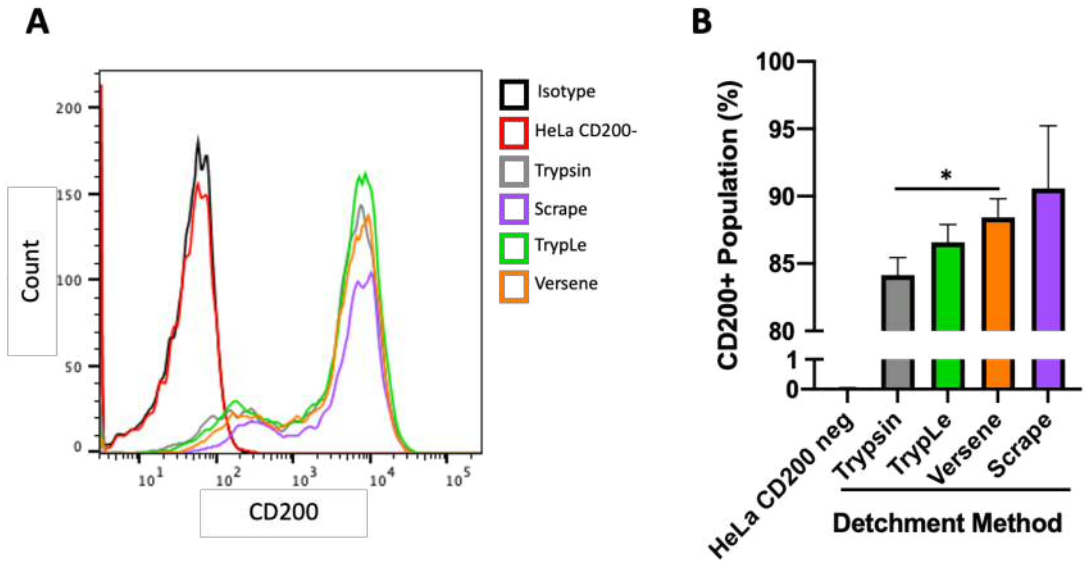

Figure 5.2: Frequency of CD200+ expression with different cell isolation methods. CD200 transduced HeLa cells were detached from culture using either Trypsin, TrypLE, Versene or by scraping. Cells were labelled with a fluorochrome conjugated anti-CD200 antibody and subject to flow cytometry analysis. CD200- HeLa cells were used as a negative control (A). Cells were gated for live single cells. Unlabelled and isotype controls were also used for each cell line to determine background fluorescence. Percentage of CD200+ cells were analysed, and values were obtained from an average over 3 independent experiments (B). * represents $p<0.05$.

5.2.2 Characterising CD200 expression in RCC cell lines

Having identified CD200 expression in our RCC patient samples, we next wanted to investigate the role of this expression in immune evasion. Human cancer-derived cell lines are crucial in the study of tumour biology, and to test the therapeutic benefit of novel anti-cancer agents. In order to explore the effect of RCC CD200 expression on immune evasion, we first characterised CD200 expression in six available cRCC cell lines: A498, SN12C, UOK 121, UOK 143, UMRC2 and UMRC3. We focused our *in vitro* analysis on ccRCC as we observed both variable CD200 expression as well as variable immune infiltrate phenotype this subtype. The aim of using several cell lines with possible differential expression of CD200 was to explore the link between CD200 expression and immune function in more detail.

A498 is part of the NCI-60 cancer cell line panel. This panel is a group pf 60 cell lines that are used by the National Cancer Institute for the screening of novel cancer therapies. The A498 therefore is widely used in RCC studies and has become one of the most highly cited RCC cell lines. A498 have a mutated *VHL*, and xenograft tumours are consistent with the classical appearance of ccRCC, with nests of malignant epithelial cells with clear cytoplasm. This cell line has been reported to be both p53 wild type (Warburton *et al.,* 2005) p53 mutated (Brodaczewska *et al.,* 2016). SN12C is also part of the NCI-60 cancer cell line panel. Uncharacteristic for ccRCC, SN12C is wild type *VHL* (Pan *et al.,* 2006). In a copy number alteration analysis of cell line databases, SN12C was found to cluster on their own as outliers, not conforming to the well described RCC subtypes but shares some similarities with pRCC (Sinha *et al.,* 2017). SN12C does not cluster with ccRCC, which might be due to it having been established from an RCC with extensive invasion of perinephric fat and displaying a mix of clear cell and poorly differentiated RCC. UOK 121 and UOK 143 are cell lines from sporadic ccRCC. Both have one hyper-methylated copy and one silent copy of *VHL.* UMRC2 and UMRC3 cell lines are both part of the European Collection of Authenticated Cell Cultures (ECACC). Both UMRC2 (ECACC 08090511) and UMRC3 (ECACC 08090512) are continuous cell line established from a primary renal adenocarcinoma. The mutational status of *VHL* is unknown for these cell lines. They exhibit a loss of contact inhibition and produces tumours in nude mice. The patient had metastatic disease at the time of their nephrectomy.

5.2.2.1 CD200 mRNA expression

To determine expression of CD200 in our RCC cell lines, we first determined mRNA transcript expression. CD200 gene expression has been associated with tumour progression and prognosis in various cancer types, including in RCC (Moreaux *et al.*, 2008). These mRNA levels have been reported to correlate with CD200 protein expression (Siva *et al.,* 2008; Li *et al.,* 2016). CD200 mRNA levels were evaluated across our panel of six RCC cell lines as well as our CD200+ and CD200- HeLa cells. The highest levels were found in our transduced HeLa CD200+ cell line, demonstrating over a $4x10^5$ fold increase in expression when compared to the CD200- HeLa cells (not shown). All six of the RCC cell lines expressed CD200 at some level, with the highest CD200 levels found in the SN12C cell line and the lowest found in the UOK 143 cell line (Figure 5.3). This result suggests that CD200 expression is retained in cell lines, showing differential expression.

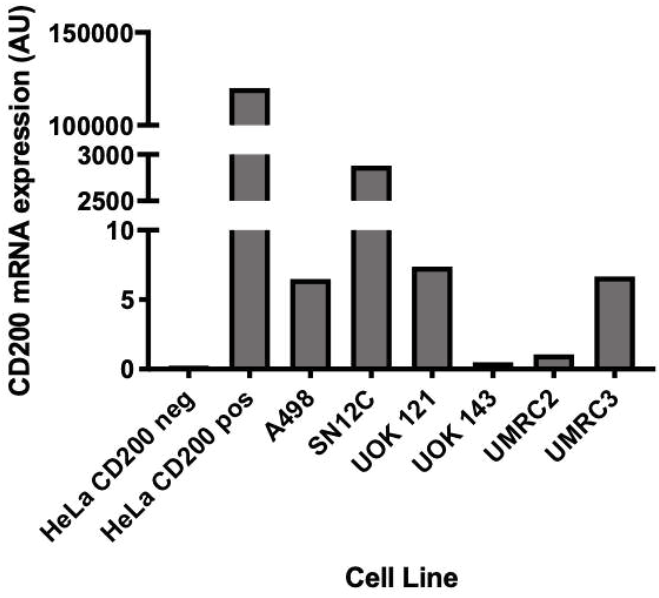

Figure 5.3: CD200 mRNA levels in cell lines. RNA was extracted from transduced HeLa and six RCC cell lines and CD200 gene expression was determined by RT-PCR. Expression was normalised to β -Actin and CD200 expression was calculated according to the 2^-delta Ct method and is shown as arbitrary units (AU).

5.2.2.2 CD200 protein expression

Measuring mRNA levels is an indicator of gene regulation, however, this mRNA undergoes various post-translational modification steps that may affect the resulting protein. This means that mRNA levels do not necessarily translate into protein levels. To determine whether CD200 mRNA levels correlated with expression of CD200 at protein level, whole protein lysate was extracted from each cell line and probed for CD200 by western blot analysis (Figure 5.4). The CD200 transfected HeLa cells results in over a 100-fold increase in protein expression compared to the CD200- HeLa cells. As found at mRNA level, the SN12C cell line was found to have greatest levels of CD200 protein of the six RCC cell lines.

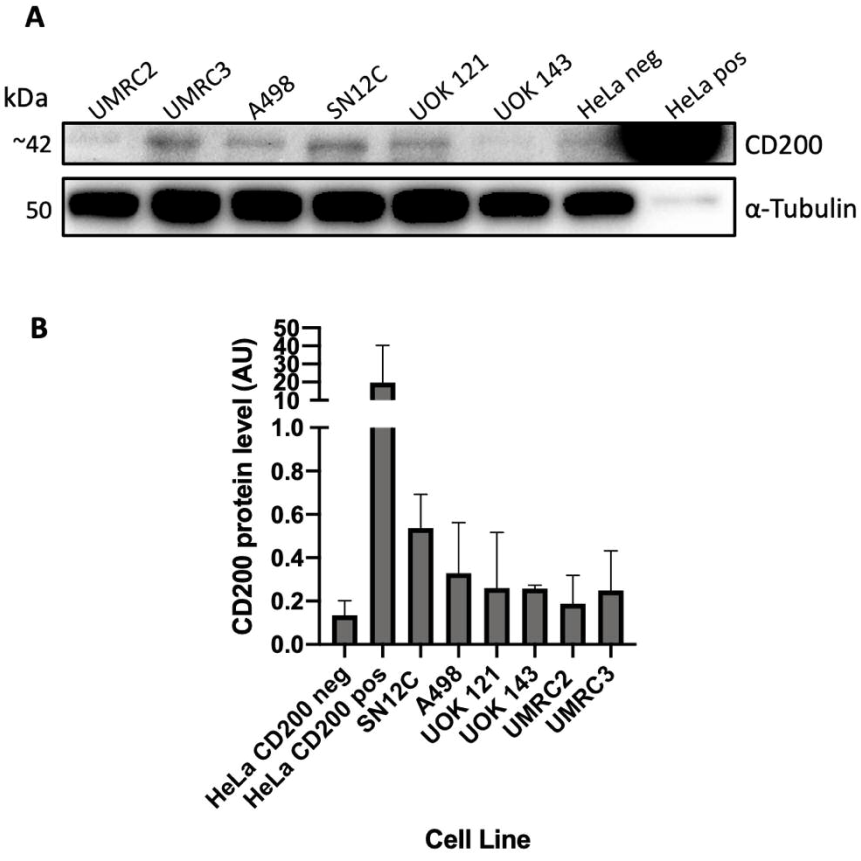

Figure 5.4: Western blot analysis of CD200 protein expression. Whole cell lysate was extracted from our HeLa and six RCC cell lines and immunoblotted for CD200. (A) is a representative image. (B) Expression was normalised to α-tubulin and CD200 protein level is shown as arbitrary units (AU) where values were obtained from an average over 3 independent experiments.

5.3 Cytotoxic assessment of NK cells

CD200 is reported to exert its function through engaging its receptor, CD200R. Expression of this inhibitor immune receptor is found on cells of the myeloid lineage as well B and T cells, and NK cells. Binding of CD200 to its receptor is generally thought to induce an immunosuppressive response in these cell types. Having evaluated the expression of CD200 in our cell lines, we next wanted to explore how this expression affects an immune response. In particular we focus on the effect on NK cell activity. NK cells are crucial in the early detection and destruction of emerging tumours. It has been previously shown that NK activity is impaired in CD200 high AML patients (Coles *et al.,* 2011). We set out to determine whether RCC cell line expression affected NK cell activity.

5.3.1 Characterising CD200R expression in NK cell lines

To determine the specificity of CD200 signalling pathway in these assays we assessed expression of the CD200R in NK cell lines, NK92MI and NKL. The NK92MI is an IL-2 independent cell line derived from the well characterised NK92 cell line by transfection. This line has demonstrated broad and consistent high cytotoxicity activity towards cancer cells (Gong *et al.,* 1994). The NKL cell line is also capable of natural killing and has demonstrated *in vitro* cytotoxicity against a variety of malignant target cells (Robertson *et al.,* 1996).

The cytotoxic capacity of both NK92MI and NKL cell lines toward tumour cells make them good candidates to use in tumour co-culture assays. Both cell lines were first analysed for CD200R expression by flow cytometry, where we demonstrate expression in the NK92MI cell line but little to no expression in the NKL cell line (Figure 5.5).

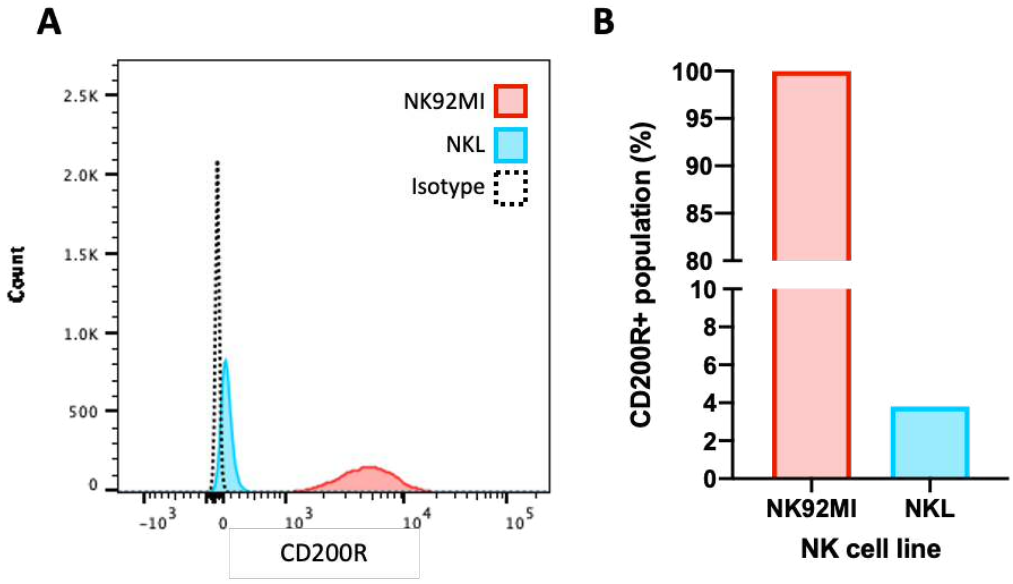

Figure 5.5: CD200R expression in NK cell lines. NK92MI and NKL cells were labelled with CD200R and subject to flow cytometry analysis for expression (A). Cells were gated for live single cells. Unlabelled and isotype controls were used for each cell line to determine background fluorescence. Percentage of CD200R+ cells were analysed (B).

5.3.2 HeLa tumour cell killing by NK92MI and NKL cells

Having characterised CD200R expression in our NK cell lines, we sought to determine the effect of tumour expression of the ligand, CD200, on their activity. One of the main objectives of NK cells is to eradicate emerging tumour cells, therefore we analysed the effect of CD200 on their ability to kill target tumour cells. The CD200+ and CD200- HeLa cells were co-incubated for four hours with either the CD200R+ NK92MI or CD200R- NKL cell lines at different effector:target ratios. The four-hour incubation period was used as previous results have demonstrated that this period was sufficient to observe NK92MI killing of target tumour (data not shown). We see that tumour CD200 expression reduces the CD200R+ NK92MI cell line's ability to kill those cells, with significant difference in the percentage of tumour cell death between the two HeLa populations at both effector:target ratios of 1:1 and 2:1 ($p<0.05$ and $p<0.001$, respectively) (Figure 5.6). Meanwhile, CD200 expression had no significant effect on the CD200R- NKL cell lines ability to kill the target tumour cells, where there was little difference in tumour cell death between the two HeLa cell lines.

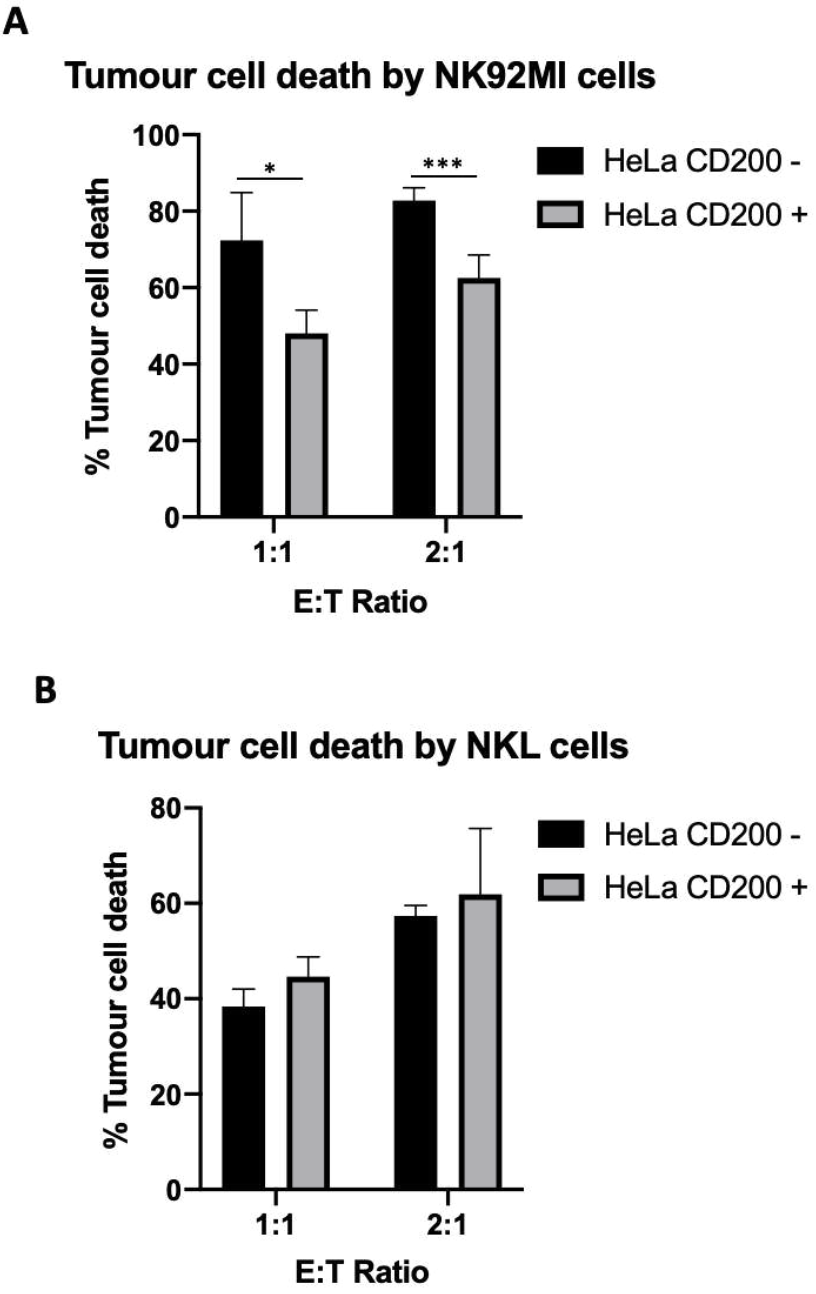

Figure 5.6: HeLa CD200 expression confers immune protection against CD200R expressing NK cells. HeLa CD200+ and HeLa CD200- cell lines were co-incubated with either NK92MI (A) or NKL (B) cells for a period of 4 hours at effector:target ratios of 1:1 and 2:1. The percentage of tumour cell death was calculated relative to untreated cells. Values were obtained from an average over 4 independent experiments. Students t test was used to determine difference between cell death, * and * represents $p<0.05$ and $p<0.001$.**

5.3.3 RCC tumour cell killing by NK92MI

Having determined that HeLa CD200 expression affected the CD200R+ NK92MI cell line activity, we set out to determine whether RCC CD200 expression had a similar immunosuppressive effect. We first looked at whether CD200 expression of our RCC cell lines could be used to determine how effective NK cells are at killing those tumour cells. RCC cell lines were co-incubated with our NK cells at an E:T ratio of 1:1 and 2:1 for a period of 4 hours, after which time the NK cells are removed and the percentage of tumour cell death is calculated relative to untreated tumour cells (Figure 5.7). We saw the greatest death in the SN12C cell line, which we previously demonstrated the greatest CD200 expression. Meanwhile, little death was seen in the low CD200 expressing A498 cell line. This assay suggests a possible reverse affect to what we observed with CD200 expression in the HeLa cells and demonstrates that CD200 expression alone is not sufficient to predict NK cell response.

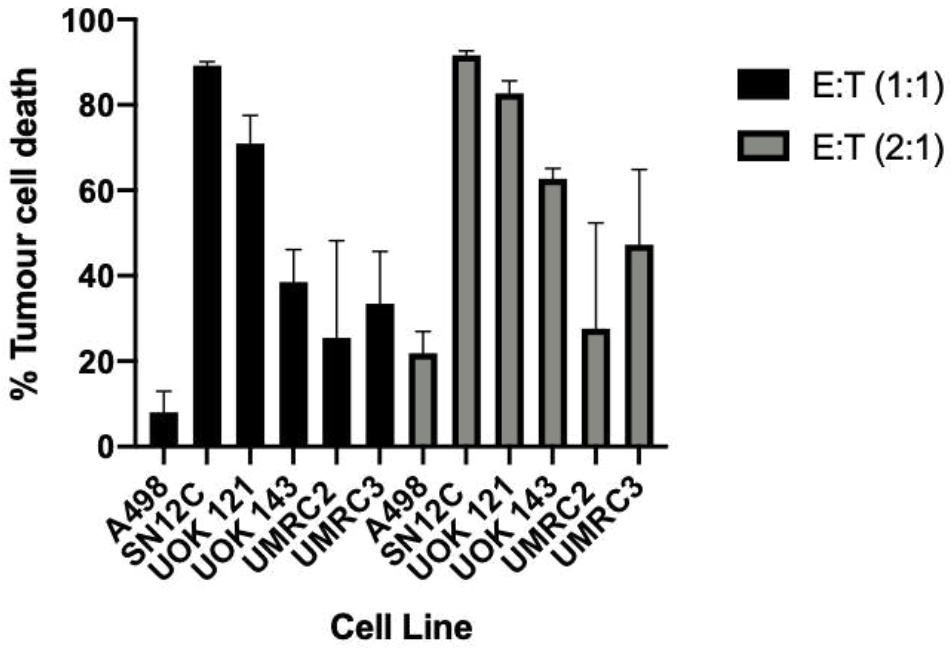

Figure 5.7: NK92MI cell line killing of RCC cell lines. RCC cell lines were co-incubated with NK92MI cells for a period of 4 hours at effector:target ratios of 1:1 and 2:1. The percentage of tumour cell death was calculated relative to untreated cells. Values were obtained from an average over 4 independent experiments.

5.3.4 CD200+ HeLa tumour cell killing by NK92MI with anti-CD200 antibody

Individual RCC cell line killing by NK cells could not be defined on the basis of CD200 expression. To determine how CD200 expression of each cell line affects NK cell killing, we used the transduced HeLa cells to evaluate the effect of blocking CD200 signalling. Our CD200+ HeLa cells were co-incubated with NK9MI cells at E:T of 1:1 and 2:1 as before, this time with the addition of a CD200 blocking antibody (60 μg/10^6 cells) or a mouse IgG isotype control at the same concentration. We see a significant increase in tumour cell death in the CD200+ HeLa cells co-incubated with NK cells in the presence of our CD200 blocking antibody at both E:T ratios ($p<0.05$ and $p<0.001$) (Figure 5.8). There was no significant difference in the tumour cell death when CD200+ HeLa cells were co-incubated in the presence of the isotype control antibody. This confirms that blocking the CD200 signal is sufficient to restore NK92MI activity towards our CD200+ tumour model.

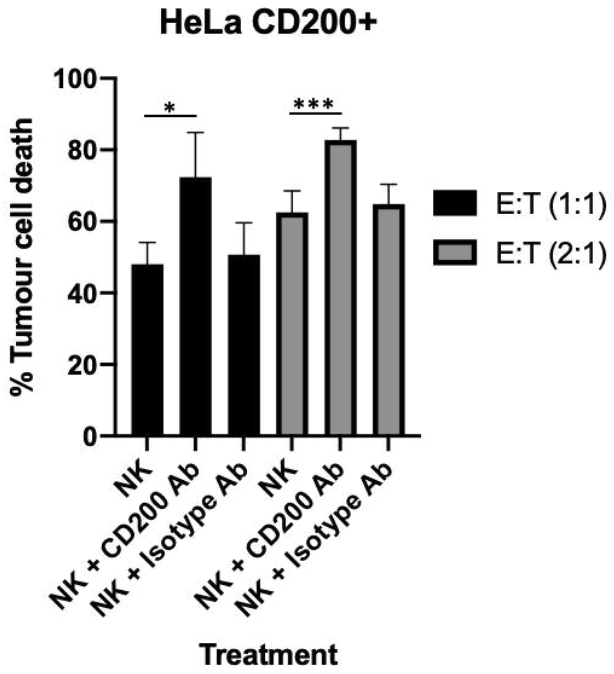

Figure 5.8: Blocking CD200 restores NK92MI cell activity. HeLa CD200+ cells were co-incubated with NK92MI cells for a period of 4 hours at effector:target ratios of 1:1 and 2:1. The percentage of tumour cell death was calculated relative to untreated cells. Values were obtained from an average over 4 independent experiments. Students t test was used to determine difference between cell death, * and * represents $p<0.05$ and $p<0.001$.**

5.3.5 RCC tumour cell killing by NK92MI with anti-CD200 antibody

Having demonstrated that our anti-CD200 blocking antibody is sufficient to inhibit the CD200:CD200R binding and immunosuppressive signal in our CD200+ HeLa model, we set out to determine whether blocking the CD200 signal in our RCC cell lines would demonstrate a similar response. As above, RCC cell lines were co-incubated with NK92MI cells at E:T ratios of 1:1 and 2:1 for a period of four hours with or without the addition of our CD200 blocking antibody. Tumour cell death was calculated (Figure 5.9). Only in the SN12C cell line did we see a significant increase in tumour cell death with the addition of the CD200 blocking antibody, at both 1:1 and 2:1 ($p<0.01$ and $p<0.001$, respectively). This corresponds to our previous findings that SN12C expresses greater levels of CD200. Thus, as expected, blocking CD200 signalling in the CD200 positive cell line, SN12C, increased NK cell killing. For unclear reasons, the UOK 143 and UMRC3 cell line, the addition of the CD200 blocking antibody had the opposite effect, reducing the tumour cell death by the NK cells at the 2:1 effector:target ratio ($p<0.05$).

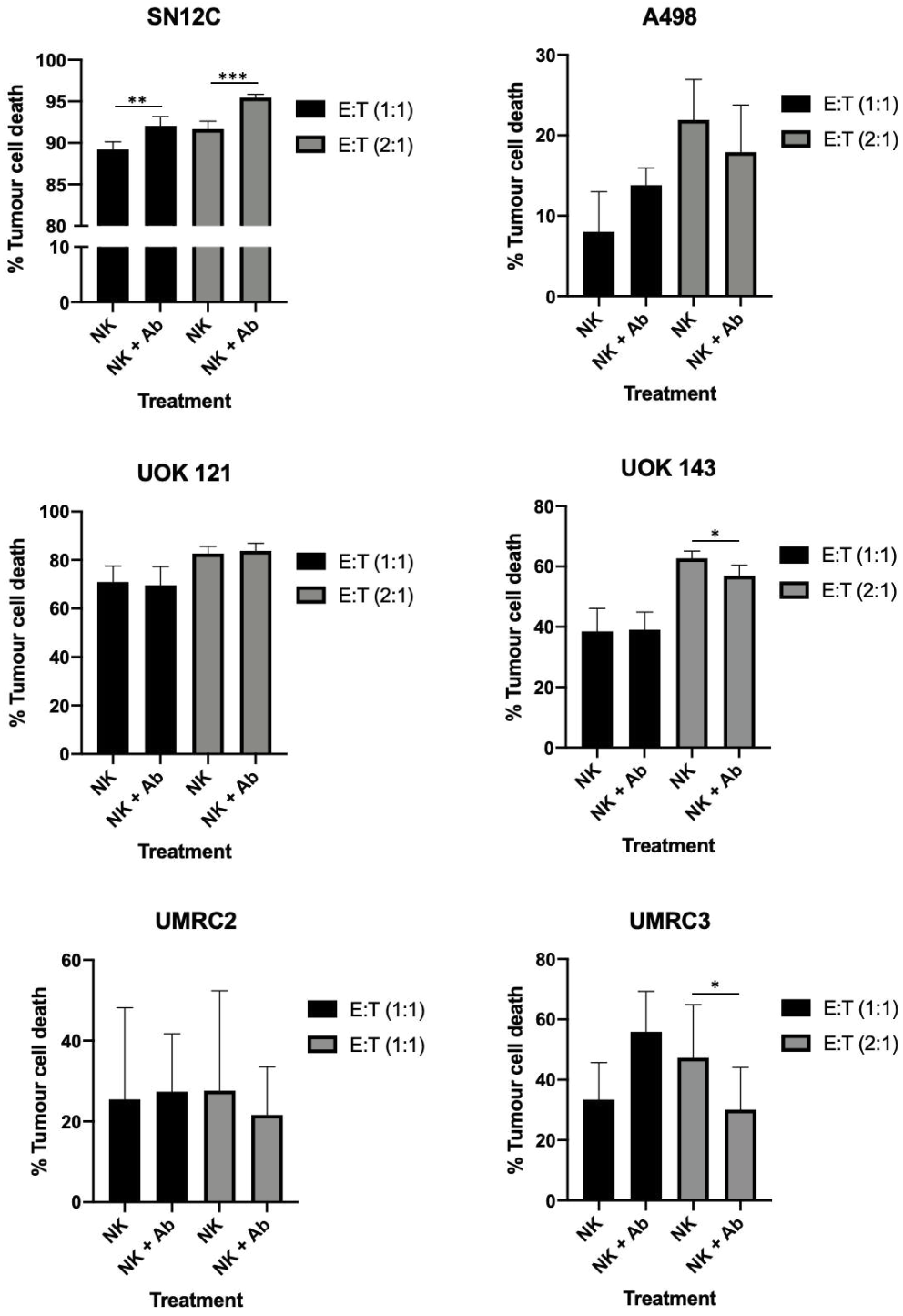

Figure 5.9: Blocking CD200 in RCC. HeLa CD200+ cells were co-incubated with NK92MI cells for a period of 4 hours at effector:target ratios of 1:1 and 2:1 in the presence of a CD200 blocking antibody. The percentage of tumour cell death was calculated relative to untreated cells. Values were obtained from an average over 4 independent experiments. Students t test was used to determine difference between cell death, *, **and * represents p<0.05, p<0.01 and p<0.001.**

5.3.6 CD200+ HeLa tumour cell killing by NK92MI with additional sCD200 Fc peptide

Our characterisation of CD200 expression in the six cell lines demonstrated low levels of CD200. To explore whether we could recapitulate the effect of CD200 expression in our RCC cell lines, we utilised our co-incubation assay, this time with the addition of a CD200 peptide. This human Fc chimera protein is reported to bind to CD200R in a functional ELISA assay. We sought to determine whether the presence of additional CD200 was capable of increasing the inhibitory signal in our NK cells. We observed a heterogeneous response in tumour cell death in the presence of the CD200 peptide, both between cell lines and between the E:T ratios. At an E:T of 1:1, the CD200 peptide decreased the NK tumour cell killing in 5/6 of the cell lines and also resulted in a significant reduction seen in the killing of the UOK 143 cell line at 2:1 ($p<0.05$) (Figure 5.10). However, at an E:T of 2:1, addition of the CD200 peptide had little effect on NK cell killing and increased NK cell killing of the UMRC3 cell line, however, this was not significant. This assay suggests that the addition of a sCD200 peptide may not contribute to blocking NK cell tumour cell killing.

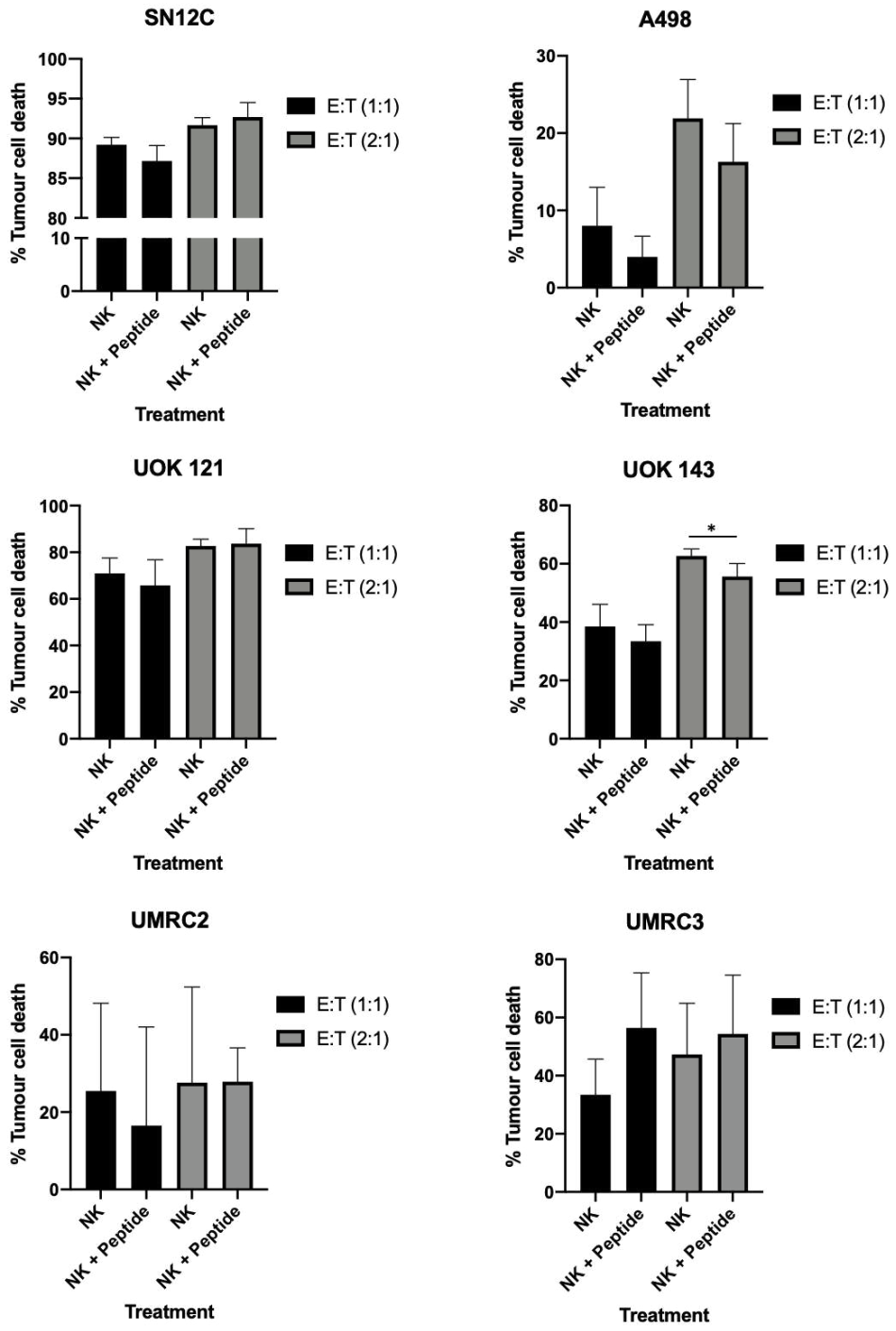

Figure 5.10: Recapitulating CD200 expression in RCC. HeLa CD200+ cells were co-incubated with NK92MI cells for a period of 4 hours at effector:target ratios of 1:1 and 2:1 in the presence of a soluble CD200 peptide. The percentage of tumour cell death was calculated relative to untreated cells. Values were obtained from an average over 4 independent experiments. Students t test was used to determine difference between cell death, * represents $p<0.05$.

5.3.7 Optimisation of NK92MI degranulation assay

Having demonstrated that blocking CD200 was sufficient to restore NK92MI ability to induce tumour cell death, we wanted to also look at the activity of our NK9MI cells. Tumour CD200 expression has been linked to do a decrease in NK cell activity, through a reduction in cytokines interferon gamma secretion as well as a reduced degranulation capacity (Coles *et al.,* 2011).

Expression of CD107a is considered a marker for NK cell degranulation. In AML, NK expression of CD107a was reduced in $CD200^{high}$ patients suggesting that CD200 inhibits degranulation. We determined whether RCC expression acted in a similar manner, preventing the degranulation of our NK92MI cells. First, we set out to determine whether our NK92MI cells were responsive to degranulation. Cells were stimulated with PMA/ionomycin and treated with monensin for a period of four hours. CD107a surface expression was analysed on our CD56+ NK92MI cells by flow cytometry (Figure 5.11). Stimulation increased the average NK CD107a expression by 3-fold when compared to baseline, with an average frequency of 60% ($p<0.0001$). These data demonstrate that CD107a is significantly upregulated on the surface of NK cells following activation.

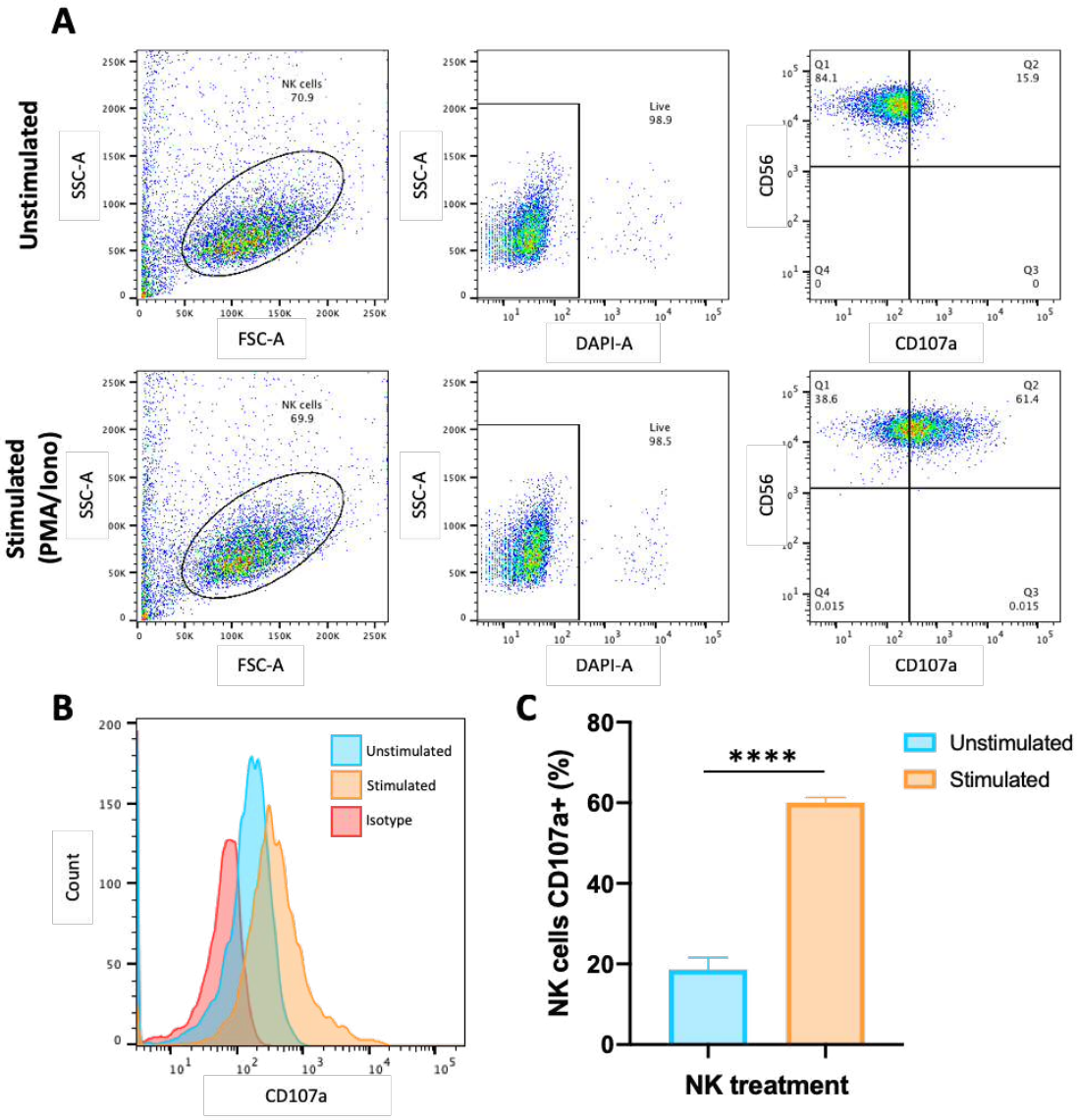

Figure 5.11: Stimulating degranulation in NK92MI cell line. The NK92MI cell line was stimulate to with of PMA and Ionomycin for 4 hours. Unstimulated NK92MI cells were used as a baseline. The expression of CD107a was analysed in live, CD56+ NK92MI cells by flow cytometry (A/B). These data are representative of 3 independent experiments. (C) Average CD107a positivity was calculated. Students t test was used to determine difference between CD107 population positivity, ** represents p<0.0001.**

5.3.8 Degranulation of NK92MI cells in response to HeLa tumour cells

Having demonstrated that NK92MI cells are susceptible to activation and CD107a expression, we sought to determine whether tumour CD200 expression affected NK92MI CD107a expression. Both CD200- and CD200+ HeLa cells were co-incubated with NK92MI cells at an effector:target ratio of 5:1 and NK expression of CD107a was analysed (Figure 5.12). Whilst incubation with both CD200- and CD200+ HeLa cells increased cell surface CD107a expression ($p<0.0001$), the CD200+ HeLa CD200 resulted in significantly less CD107a+ NK cells when compared to the CD200- HeLa cells ($p<0.05$), however, the percentage change of CD107a+ NK cells was small.

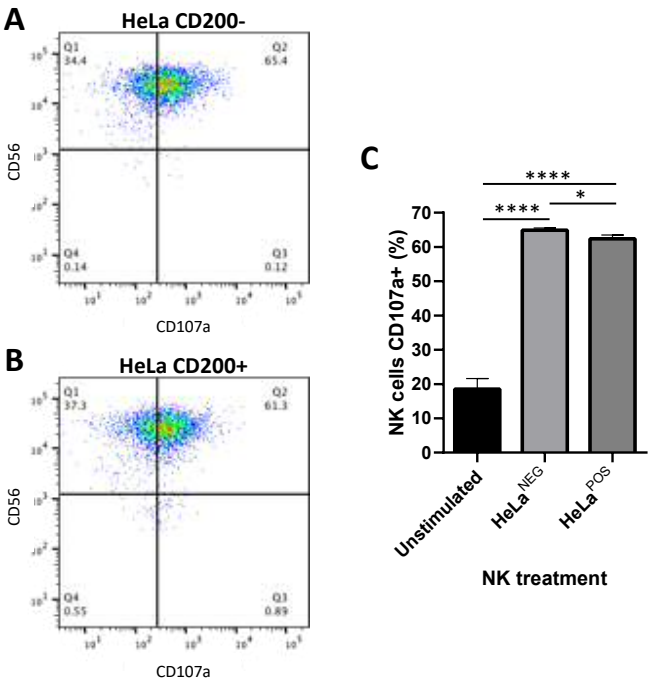

Figure 5.12: HeLa CD200 expression reduces CD107a expression. The NK92MI cell line was co-incubated with either CD200- or CD200+ HeLa cells at 5:1 for 4 hours. Unstimulated NK92MI cells were used as a baseline. The expression of CD107a was analysed in live, CD56+ NK92MI cells by flow cytometry (A/B). These data are representative of 3 independent experiments. (C) Average CD107a positivity was calculated. Students t test was used to determine difference between CD107a population positivity, * and ** represents $p<0.05$ and $p<0.0001$, respectively.**

5.3.9 Degranulation of NK92MI cells in response to treated HeLa tumour cells

Having shown that CD200 expression reduces CD107a expression, we next looked at whether soluble CD200 had a similar effect on NK activity, and whether we could recapitulate this immunosuppressive effect in our CD200- HeLa cells. NK92MI cells were co-incubated with CD200- HeLa cells in the presence of the soluble CD200 peptide and their CD107a expression was analysed (Figure 5.13). As we saw in our killing assays, the addition of the peptide reduced NK cell activity, however the reduction in CD107a expression did not reach significance. We next looked at whether blocking the CD200 signal had the opposite effect and was able to increase expression of the activity marker, CD107a. We previously demonstrated that blocking CD200 in our CD200+ HeLa cells was sufficient to restore NK92MI capacity to kill target cells, however blocking CD200 had no effect on NK cell CD107a expression. Important to note here that NK cells were co-incubated here at an effector:target ratio of 5:1, suggesting the efficacy of blocking the CD200 signal is somewhat dependent on the effector:target ratio.

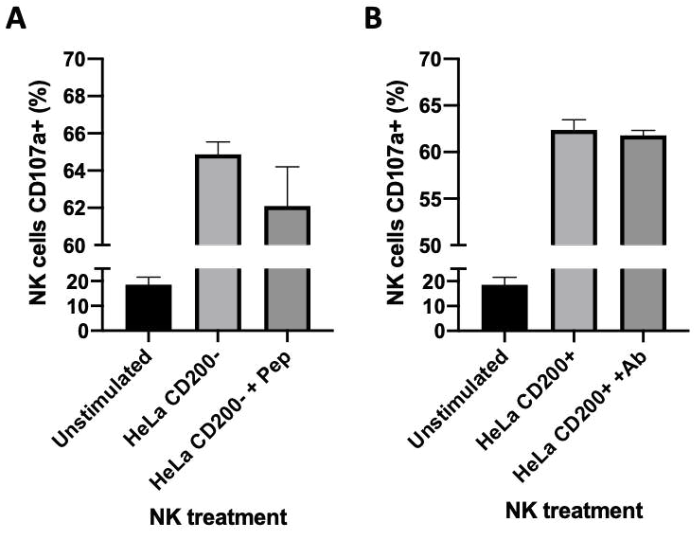

Figure 5.13: NK92MI CD107a expression in response to different stimulus. The NK92MI cell line was co-incubated with CD200- HeLa cells with the addition of a soluble CD200 peptide (A) and with CD200+ HeLa cells and the addition of a CD200 blocking antibody (B). Co-incubations were at 5:1 for 4 hours. Unstimulated NK92MI cells were used as a baseline. The expression of CD107a was analysed in live, CD56+ NK92MI cells by flow cytometry. These data are representative of 3 independent experiments. Average CD107a positivity was calculated.

5.3.10 Degranulation of NK92MI cells in response to SN12C tumour cells

We have shown that RCC expression of CD200 also has an effect on our NK92MI activity. In our CD200+ RCC cell line, SN12C, we saw that blocking CD200 was sufficient to restore NK cell cytotoxicity as we saw an increase in tumour cell killing. As above, we analysed CD107a expression on our NK cells after co-incubation with the SN12C cell line (Figure 5.14). We observed that the NK cells are activated in the presence of the SN12C cells, with around a 3.5-fold increase in expression and an average frequency of 65%. As before, we observed a decrease in NK cell activity with the addition of the soluble CD200 peptide, however this did not reach significance. Addition of the CD200 blocking antibody had no effect on NK CD107a expression.

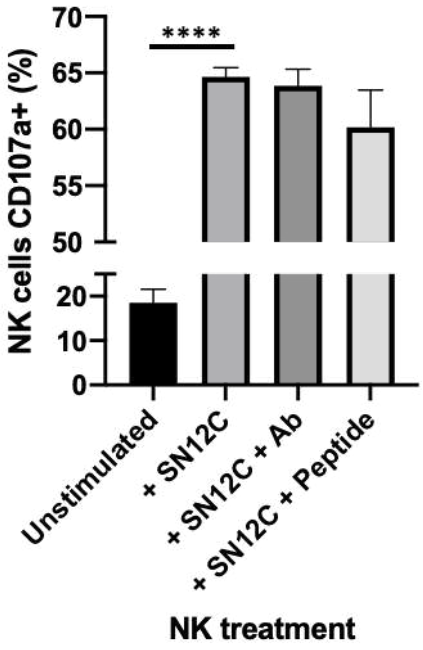

Figure 5.14: NK92MI CD107a expression in response SN12C. The NK92MI cell line was co-incubated with SN12C cells with the addition of a soluble CD200 peptide or a CD200 blocking antibody. Co-incubations were at 5:1 for 4 hours. Unstimulated NK92MI cells were used as a baseline. The expression of CD107a was analysed in live, CD56+ NK92MI cells by flow cytometry. These data are representative of 3 independent experiments. Average CD107a positivity was calculated. Students t test was used to determine difference between CD107 population positivity, **** p<0.0001.

5.4 Immunoregulatory assessment of NK cells

So far, we have analysed the cytotoxic activity of NK cells. NK cells are also involved in regulating the immune response and are capable of immunoregulatory functions, secreting various cytokines and chemokines. Chemokine (C-C motif) ligands 4 (CCL4) is a chemoattractant for a variety of immune cells, including NK cells. CCL4 is one of the many chemokines that NK cells produce upon activation. This production in turn augments their cytolytic activity whilst simultaneously recruiting other effector cells during immune responses. We looked at whether tumour CD200 expression and the subsequent interaction with the CD200R affects NK secretion of CCL4.

5.4.1 NK cell secretion of CCL4 in response to HeLa populations

To determine whether tumour CD200 effects NK cell production of CCL4, NK92MI cells were co-incubated with either CD200- or CD200+ HeLa cells as before, at E:T ratios of 1:1 and 2:1 over a period of 4 hours. Supernatant from the co-cultures was analysed for CCL4 by ELISA. We observed a significant decrease in the concentration of CCL4 in supernatant taken from NK92MI cells co-incubated with CD200+ HeLa cells when compared to the CD200- HeLa cells at both 1:1 and 2:1 E:T ratios ($p<0.01$ and $p<0.05$, respectively) (Figure 5.15).

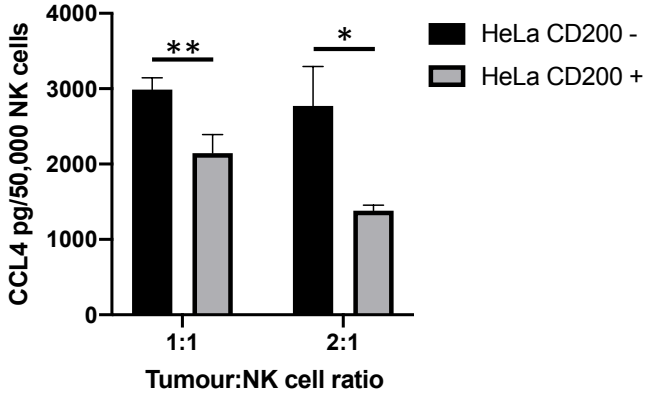

Figure 5.15: HeLa CD200 expression reduces NK92MI secretion of CCL4. HeLa CD200+ and HeLa CD200- cell lines were co-incubated with NK92MI cells for a period of 4 hours at effector:target ratios of 1:1 and 2:1. Co-culture supernatants were analysed for CCL4. Values were obtained from an average over 4 independent experiments. Students t test was used to determine difference between co-culture supernatant CCL4 concentrations, * and ** represent $p<0.05$ and $p<0.01$.

5.4.2 Restoring NK92MI cell secretion of CCL4 in response blocking CD200

Having demonstrated that blocking the CD200 signal was sufficient to restore NK cell activity in killing CD200+ target tumour cells, we analysed whether blocking CD200 also restored CCL4 secretion from our NK cells. HeLa CD200+ cells were co-incubated with NK92MI cells as before and the supernatant from the co-cultures was analysed for CCL4 by ELISA. Addition of the CD200 blocking antibody restored NK secretion of CCL4 and both E:T ratios, however only reached significance at 2:1 ($p<0.05$) (Figure 5.16). Unlike in the tumour killing assay, addition of the isotype control antibody also restored NK cell secretion of CCL4, reaching significance in 2:1 ($p<0.01$).

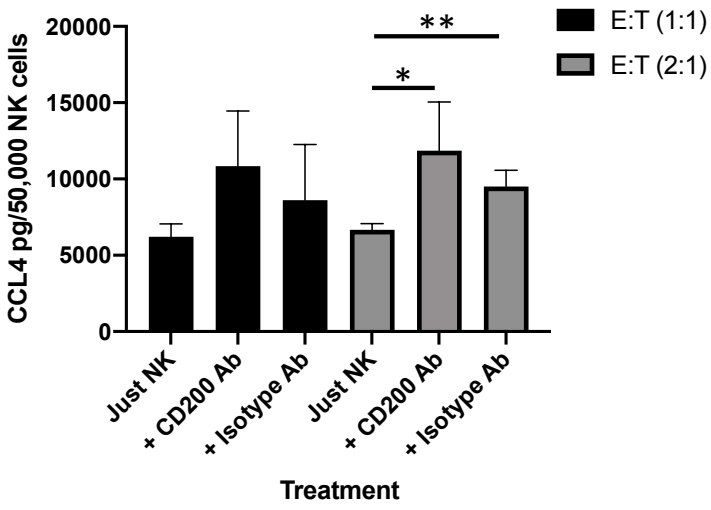

Figure 5.16: Blocking CD200 restores NK92MI secretion of CCL4. The HeLa CD200+ cell lines were co-incubated with NK92MI cells for a period of 4 hours at effector:target ratios of 1:1 and 2:1 wither the addition of either a CD200 blocking antibody (60μg/10^6 cells) or an isotype control antibody at the same concentration. Co-culture supernatants were analysed for CCL4. Values were obtained from an average over 4 independent experiments. Students t test was used to determine difference between co-culture supernatant CCL4 concentrations, * and ** represents $p<0.05$ and $p<0.01$.

5.4.3 NK92MI cell secretion of CCL4 in response to RCC cell lines

To determine whether CD200 expression in RCC and its subsequent blocking had a similar effect on NK cell chemokine activity, supernatant from the same co-incubations were analysed for CCL4 levels (Figure 5.17). The RCC cell lines SN12C, A498 and UOK143 significantly stimulated NK cell secretion of CCL4 at both 1:1 and 2:1, whilst the UOK 121 significantly increased CCL4 secretion only at 1:1. Meanwhile, at 2:1, the UOK 121 and the UMRC cell lines decreased CCL4 secretion from NK cells when compared to their baseline. Addition of the CD200 peptide had no significant impact on NK secretion of CCL4. Addition of the CD200 blocking antibody significantly increased CCL4 secretion in NK cells incubated with the A498 cell line ($p<0.01$) but no effect on CCL4 secretion of our NK cells incubated with our CD200+ SN12C cell line. These results suggest that a number of factors affect NK secretion of CCL4, such as the cell line and the E;T ratio. This assay, however, suggests that RCC expression of CD200 has limited effect on NK secretion of CCL4.

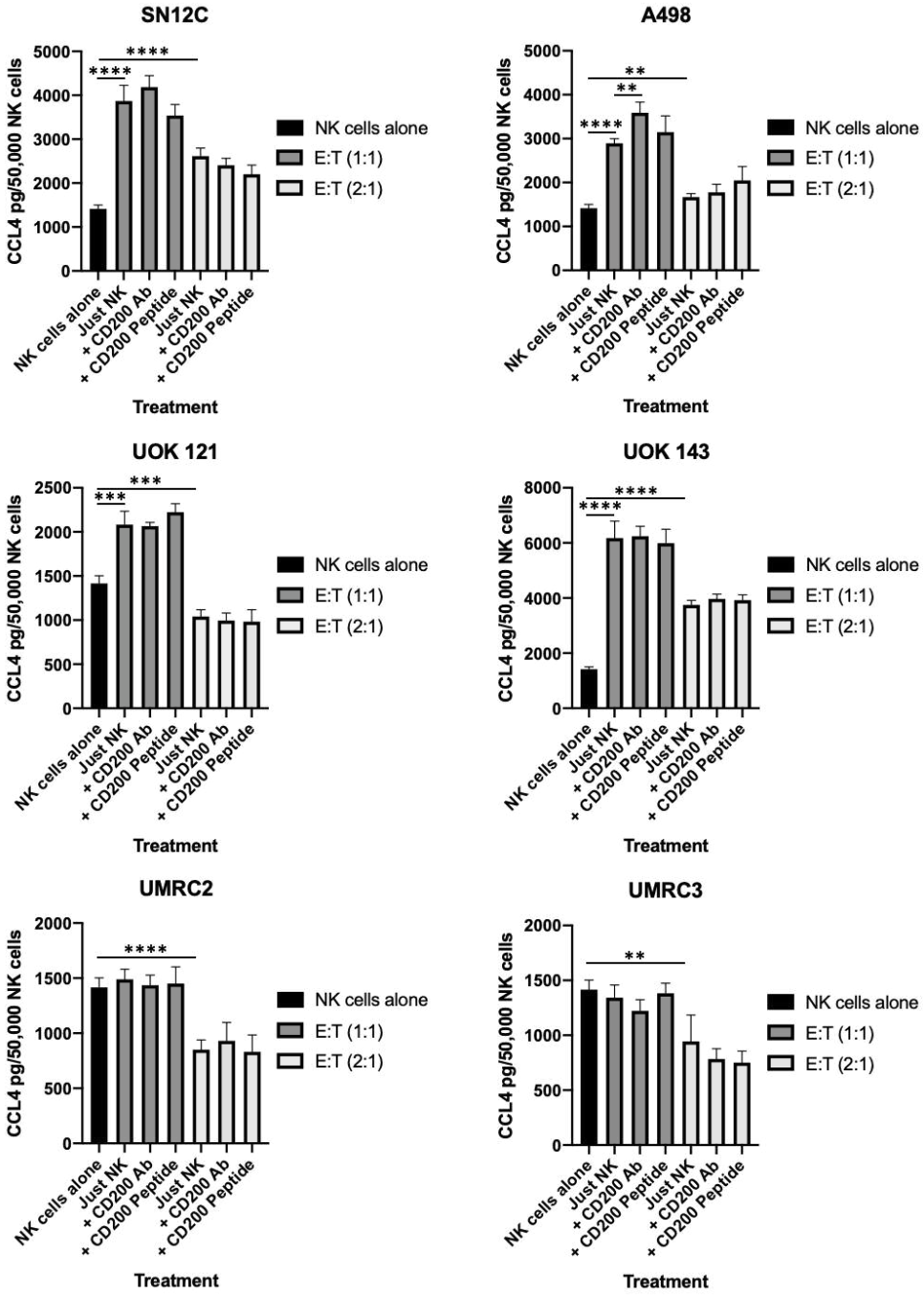

Figure 5.17: Secretion of CCL4 by NK92MI in co-culture with RCC cell lines. The six RCC cell lines were co-incubated with NK92MI cells for a period of 4 hours at effector:target ratios of 1:1 and 2:1 wither the addition of either a CD200 blocking antibody (60μg/10^6 cells) or a CD200 peptide (4μg/10^6 cells). Co-culture supernatants were analysed for CCL4. Values were obtained from an average over 4 independent experiments. Students t test was used to determine difference between co-culture supernatant CCL4 concentrations, * and ** represents p<0.05 and p<0.01.

5.5 Characterising secretion of the soluble form of CD200

It has previously been reported that CD200 exists in a soluble form (sCD200), which has since been detected in a number of cancer types. In chronic lymphocytic leukaemia (CLL) presence was attributed to ectodomain shedding of the membrane form, with the sCD200 being confirmed as functionally active.

5.5.1 CD200 is present in the supernatant of RCC supernatant

We have shown in our co-incubation assays that addition of the soluble CD200 peptide can confer an element of immune evasion towards NK cells. To determine whether CD200 is shed from our RCC cells, we collected supernatant from these cell lines after 48 hours. The number of cells at the end of this period was counted to determine concentration of sCD200 per number of cells. sCD200 levels in cell line supernatants were determined by ELISA. We saw the presence of sCD200 at varying levels in all but one of our cell lines (Figure 5.18). We observed the highest sCD200 concentration, in the supernatant of the A498 cell line, with an average 616.2pg/10^6 cells. No sCD200 was detected in the supernatant collected from any of the UMRC2 cell line replicates, which is consistent with the low CD200 mRNA and protein levels seen.

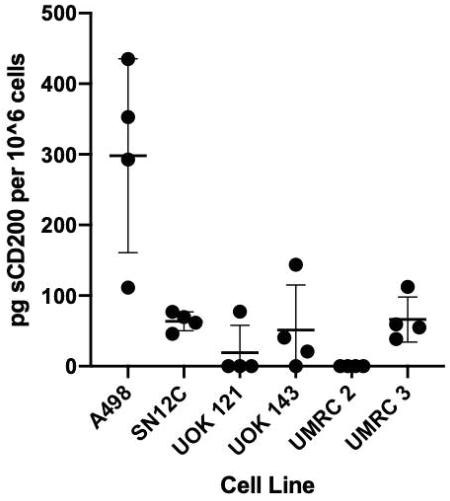

Figure 5.18: sCD200 levels in RCC cell line supernatant. Supernatant of RCC cell lines were collected after 48 hours of culture. The number of tumour cells in the flask at the end of this period was counted. sCD200 concentration was measured by ELISA. Values were obtained from an average over 4 independent experiments.

5.5.2 The role of ADAM enzymes in shedding of CD200 in RCC cell lines

Ectodomain shedding is ADAM (a disintegrin and metalloproteinase) enzymes have been implicated in the shedding of membrane proteins. In CLL patients, overexpression of several ADAMs correlated with shedding of CD200 correlated, including ADAM17 and ADAM28, with the latter demonstrating the strongest association. To determine whether ADAM expression was correlated to the sCD200 secretion we saw from our RCC cell lines, mRNA expression of ADAM17 and ADAM28 was analysed by RT-PCR (Figure 5.19). Unfortunately, we were unable to obtain an expression value of ADAM28 for the SN12C cell line.

Expression of ADAM17 was seen at various levels across the six RCC cell lines, with the greatest expression seen in UOK 121. ADAM28 was seen at various levels across the six cell lines, with the A498 cell line demonstrating particularly high expression. Both ADAM17 and ADAM28 expression remained consistent in the two HeLa populations. In order to determine if expression of ADAM17 and/or ADAM 28 was responsible for the sCD200 in our RCC cell lines, we plotted their expression against sCD200 levels. Spearman's rank correlation demonstrated no significant correlation between either ADAM17 or ADAM28 and sCD200. This may be due to the small sample number.

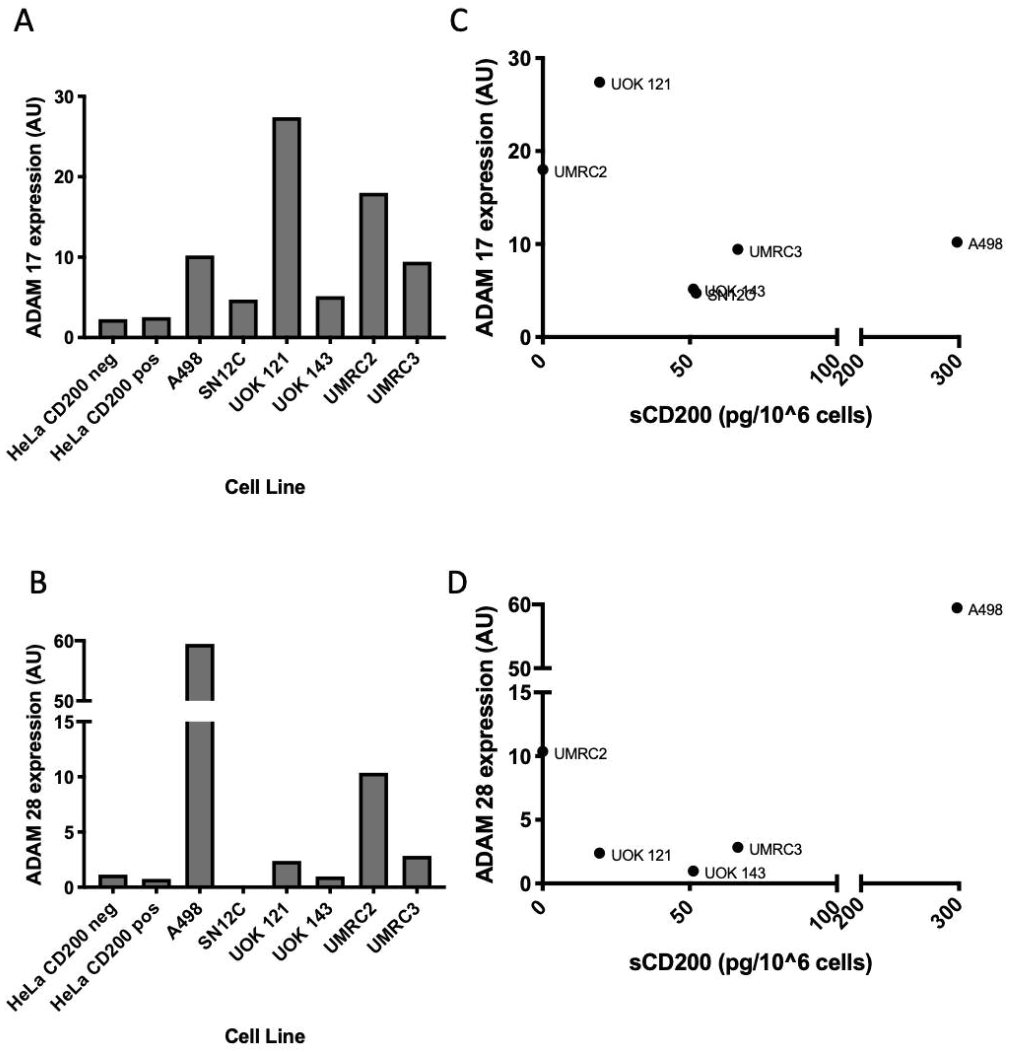

Figure 5.19: ADAM18 and ADAM28 mRNA and supernatant sCD200 in RCC cell lines. RNA was extracted from our HeLa and six RCC cell lines and probed for ADAM17 and ADAM28 gene expression by RT-PCR. Expression was normalised to β-Actin and ADAM expression was calculated according to the 2^-delta Ct method and is shown as arbitrary units (AU).

5.6 Summary

Immune checkpoint therapy for cancer encompasses strategies that target these regulatory pathways in order to enhance immunity activity against tumour cells. CD200 has previously been shown to inhibit immune cell activity, including the anti-tumour activity of NK cells. More promisingly, blocking the tumour CD200 signal has been shown to reverse this effect.

To explore the possibility of targeting CD200 as a novel therapeutic in RCC, we first set out to analyse the effect of expression of this immunosuppressive ligand on immune cell activity, focusing on NK cells. As innate cells, NK cells play pivotal functions in cancer immune surveillance. They are capable of eliminating aberrant cells, including cancer cells, without prior sensitisation. This capacity makes them a good model to explore how tumour expression of CD200 affects initial detection and destruction. Using a CD200 stably transduced HeLa model, we were able to demonstrate that CD200 expression alone was sufficient to reduce the cytotoxic capacity of our CD200R+ NK92MI cells. The specificity of this signal was demonstrated by the CD200R- NKL cell line, where no difference in the cytotoxicity towards either the CD200+ and CD200- HeLa cell lines was observed. The clinical relevance of CD200 expression was demonstrated by the ability to restore cytotoxicity of the NK92MI towards the CD200+ cells using an anti-CD200 antibody, which led to an increase in tumour cell killing. This model highlighted the potential relevance of CD200 expression on the immune evasion of NK cells in solid tumours.

Having demonstrated the immunosuppressive capacity of CD200 expression towards CD200R+ NK cells, we analysed whether CD200 expression in RCC demonstrated a similar protective property. We observed differential expression of CD200 in our cell line panel, with the SN12C cell line demonstrating greatest expression levels. This is interesting as this cell line has been reported to have a wild type *VHL*, the most common oncogenic driver of ccRCC. This cell line has also been reported to cluster with pRCC. The increased CD200 expression level we observed in this cell line would reflect the slightly higher CD200 expression intensity we observed in the pRCC samples by immunohistochemical analysis.

CD200 is just one of the many factors that contribute to how immunogenic a tumour may be. We demonstrate this in our co-culture killing assay with NK92MI cells, where we observed that CD200 alone was not sufficient to predict NK capacity to detect and kill that target tumour cell. We do, however, demonstrate that blocking the CD200 signal in the CD200-expressing SN12C cell line restores tumour cell killing. In an attempt to recapitulate tumour CD200 expression, we analysed the effect of addition of a sCD200 Fc chimera peptide. This sCD200 had a mixed result but generally decreased the NK cell mediated tumour cell killing, significantly so in the UOK 143 cell line that had previously demonstrated lowest levels of CD200. This result suggests that CD200 may function both as a membrane and as a soluble form in RCC, however, further studies are needed to confirm this.

In addition to their cytotoxic capacity, NK cells release a variety of cytokines that play a role in regulating the immune response. We analysed the secretion of the chemokine CCL4, which contributes to the migration of other immune cells. We demonstrated a significant reduction in NK92MI secretion of this chemokine when incubated with our CD200+ HeLa cells when compared to our CD200- control, suggesting that CD200 expression not only inhibits NK cytotoxic function, but may also their effector immunoregulatory capacity. Addition of the anti-CD200 blocking antibody restored NK secretion of CCL4. Expression of CD200 in our ccRCC cell lines demonstrated more heterogenous responses. In our RCC cell line panel, CD200 expression alone did not predict the effector capacity of the NK92MI cells. As seen in the killing assay, co-culture with the SN12C cell line resulted in a significant upregulation of CCL4 secretion at both effetor:target ratios, with a similar observation seen in the A498 and UOK143 cell lines. Whilst we observed an increase in CCL4 concentration at 1:1 in the UOK121 co-culture, a decrease in CCL4 concentration was seen at 2:1, which would suggest that the effector:target ratio of NK cells to tumour cells plays a crucial role in their effector capacity. This was also true for NK cells co-culture with both the UMRC2 and UMRC3 cell line, which suggests a mechanism by which these tumour cells are able to downregulate the production and secretion of CCL4 by interacting NK cells. Further analysis would be required to determine this. We did, however, observe an increase in NK92MI secretion

of CCL4 upon addition of the anti-CD200 blocking antibody. Surprisingly, whilst we observed an increase in the CCL4 in the SN12C it did not reach significance. We did, however, observe a significant increase in the concentration of CCL4 from the NK co-culture with the A498 cell line upon the addition of the anti-CD200 antibody, suggesting a possible additional benefit of targeting CD200 in RCC.

Having demonstrated that tumour CD200 expression can alter the TME through the regulation of cytokines, we next analysed whether CD200 itself also had any other additional mechanisms by which it could create an immunosuppressive environment. The presence of a soluble form of CD200 (sCD200) has been reported. We demonstrate differential capacity of our cell lines to shed CD200, with the A498 cell line demonstrating the highest concentration of sCD200 in its supernatant. The ectodomain shedding of CD200 has been linked to ADAMs, in particular ADAM28 and to a lesser extent, ADAM17. We analysed whether there was any relationship between the sCD200 concentrations we observed and the expression of both ADAMs in each cell line. Whilst no significant correlations were observed, the A498 cell line that demonstrated the highest sCD200 concentrations demonstrated particularly higher ADAM28 expression. This would be consistent with prior observations in shedding of sCD200, however, further studies would be required to confirm this relationship.

In this chapter, we demonstrate that tumour CD200 expression is capable of interfering with the NK cell anti-tumour response, reducing both their cytotoxic and effector capacity. This ties in with our immunohistochemical analysis, where we demonstrate an NK cell infiltrate that suggests its dysfunction. We demonstrate that blocking this signal is capable of restoring NK cell activity in CD200+ tumour cells but demonstrates a mixed result in RCC cell lines, particularly those with lower CD200 levels. The heterogeneity observed between cell lines may be reflective of the heterogeneity observed in our patient tissue samples and highlights the possibility that it may be necessary to determine CD200 expression on a patient-by-patient basis in future CD200 therapeutic studies for RCC.

In addition to surface CD200 expression, we demonstrate the presence of sCD200 in the supernatant of some of our RCC cell lines. This is important to note, as sCD200 has been shown to retain functional properties, including our studies where we demonstrate that addition of a sCD200 peptide may contribute to an immune-protective capacity, particularly in low CD200 expressing cell lines. The effect of sCD200 on NK cells warrants further analysis, which we undertook in the next chapter.

Chapter 6:

CD200 signalling results in the apoptosis of interacting NK cells

Chapter 6: CD200 signalling results in the apoptosis of interacting NK cells

6.1 Introduction

An immune response is tightly regulated by a balance between co-stimulatory and co-inhibitory molecules, called immune checkpoints. Expression of these checkpoints is essential for maintaining self-tolerance and well as impeding autoimmunity. Immune checkpoints differ in their mechanisms of action and understanding their mode of action and at which immune activation level they act is important when developing therapeutics that target these pathways.

In the previous chapter, we have shown that the CD200:CD200R signalling pathway is a potent regulator of NK cell activity and potentially relevant in CD200+ RCC tumours. In this chapter, we sought to determine the effect of CD200 ligand signal transduction on NK cells. CD200 is a cell surface glycoprotein with no known intracellular signalling motif (Minas and Liversidge, 2006). This ligand functions through engaging its receptor, CD200R, whose expression is found on many leukocyte subsets. The early events following ligation of CD200 to the CD200R has been previously characterised (Zhang *et al.,* 2004). The receptor has a 67-aa cytoplasmic tail containing three tyrosine residues, with the third tyrosine residue located within the NPXY motif. This tyrosine becomes phosphorylated upon ligation of the CD200R, which leads to the recruitment and phosphorylation of Dok-1 and Dok-2 that in turn bind to RasGAP and SHIP (Zhang and Phillips, 2006; Mihrshahi R and Brown, 2010). This signalling pathway has been well characterised in macrophages and mast cells. Phosphorylation of the receptor and the consequent recruitment of adapter proteins have been shown to mediate the inhibition of the Ras/MAPK pathways. Phosphorylation and the subsequent inhibition of the MAPK pathway can be detected as early as one minute after receptor engagement, with a decrease in phosphorylation seen up to 30 minutes after initial engagement. This reduced activation of MAPKs is thought to be responsible for the reduction in immune cell degranulation and cytokine production, thus limiting inflammation. We therefore sought to determine the effect of CD200 signalling in our CD200R+ NK92MI cells.

6.2 CD200 binding to NK92MI CD200R results in the downregulation of the MAPK pathway

To confirm CD200:CD200R ligation and subsequent signalling in our NK92MI cell line, we looked at whether the MAPK pathway was inhibited. Our CD200R+ NK92MI cells were co-incubated with a CD200 peptide for various periods of time. To confirm the specificity of the CD200:CD200R interaction, the CD200R- NKL cells were also treated with the CD200 peptide.

Equal amounts of cell lysates were immunoblotted with anti-phosphorylated ERK antibody that recognises the phosphorylation of both ERK1 and ERK2 (Figure 6.1). In the CD200R+ NK92MI cells, addition of the CD200 peptide inhibits the activation of ERK1 and ERK2 in the first 30 minutes of co-incubation, with a downregulation in the presence of phosphorylated ERK1 and ERK2. Phosphorylation of ERK is restored after an hour. We do not see a decrease in the levels of phosphorylated ERK1 and ERK2 in our NKL cell line upon the addition of the CD200 peptide, thus suggesting that the MAPK pathway is not inhibited. This demonstrated that that the CD200 ligand initiates signal transduction in CD200R+ NK cells.

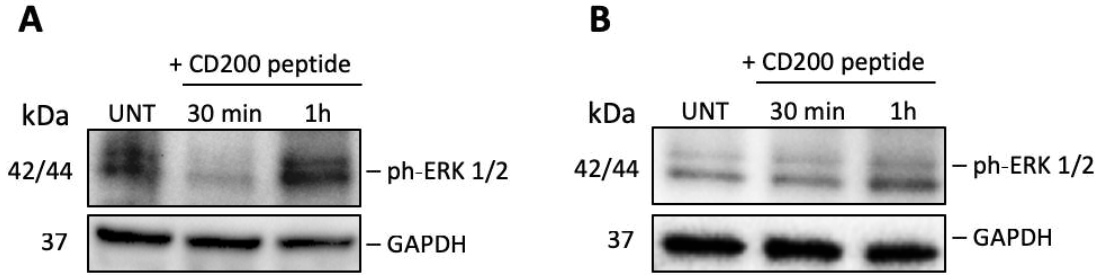

Figure 6.1: Inhibition of MAPK activation by CD200 peptide in CD200R+ NK cells. NK92MI cells were stimulated with a CD200 peptide (4 µg/10^6 cells) for indicated time periods (A). Activation of ERK was detected by immunoblotting whole cell lysates for phosphorylated ERK1 and ERK2 with the indicated Abs. NKL cells were treated with a CD200 peptide and immunoblotted as above (B). GAPDH was used as a loading control.

6.3 CD200 peptide induces cell death of NK92MI cells

An initial observation within the lab demonstrated apoptosis of interacting NK92MI cells in co-culture assays with the CD200+ HeLa cell line, which was not observed in the CD200- HeLa cells (data not shown). We therefore wanted to determine whether CD200 signalling had any effect on the viability of interacting NK cells. The CellTiter-Glo® Luminescent Cell Viability Assay is a method of determining the number of viable cells based on the amount of ATP present. To determine whether CD200 had any effect on the viability of our CD200R+ NK92MI cells, NK92MI cells were incubated with a soluble CD200 peptide for up to 24 hours, after which time, CellTiter-Glo® reagent was added to the wells (Figure 6.2). The percentage of viable cells, based on luminescence, was calculated relative to untreated cells. We observed an increase in NK cell death after 8 hours incubation with the CD200 peptide, which continued to increase over time, reaching an average of 18.8% cell death at 24 hours. This suggests that in addition to providing an inhibitory signal to the CD200 NK92MI cells as previously reported, CD200 ligation to the CD200R triggers cell death.

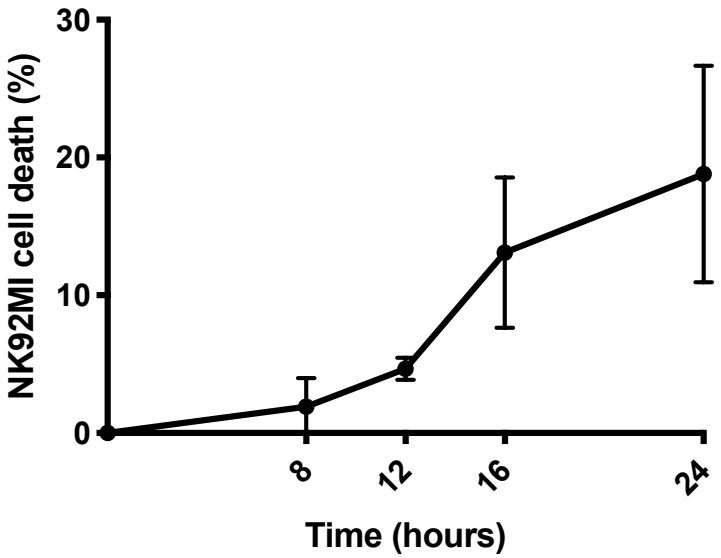

Figure 6.2 CD200 induces cell death of NK92MI cells. NK92MI cells were stimulated with a CD200 peptide (4 μg/10^6 cells) for indicated time periods. The apoptosis of NK cells was determined by analysing the ATP luminescence values between treated and non-treated NK cells. Values were obtained from an average over 4 independent experiments.

6.4 Characterising CD200 mediated cell death of NK92MI cells

There are two core pathways that exist to induce apoptosis: the extrinsic and intrinsic pathways. Whilst there is often substantial crosstalk between these pathways, they can function independently and are characterised by their mean of activation and the initiator caspases involved. Both pathways ultimately lead to the initiation of programmed cell death. Poly (ADP-ribose) polymerase (PARP) and is now used as one of the early indicators of apoptosis.

6.4.1 CD200 mediated cell death induces upregulation of caspase 8

NK92MI cells were stimulated with the CD200 peptide for various periods of time as before. Equal amounts of cell lysates were immunoblotted with either anti-caspase 8, caspase 9 or PARP antibodies (Figure 6.3). We see a progressive increase in cleaved PARP levels over the incubation period, which correlate with the increase in cell death seen above. We observed an increase in the cleavage of caspase 8 from as early as two hours, which continued throughout. No change was seen in the levels of cleaved caspase 9. The significant increase (p=0.0084) in the cleavage of caspase 8 when compared to caspase 9 suggests that CD200 ligand binding induces the extrinsic apoptotic signal.

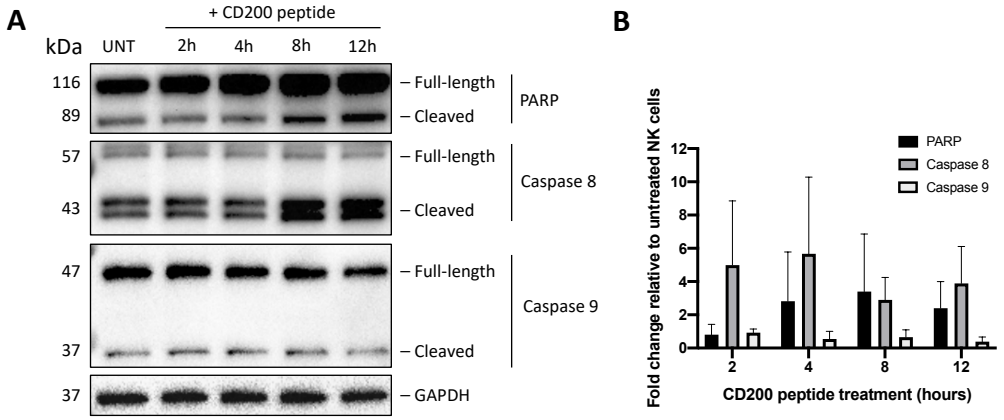

6.3: Apoptotic markers in CD200 treated NK92MI cell lines. NK92MI cells were stimulated with a CD200 peptide (4 μg/10^6 cells) for indicated time periods. Apoptosis of NK cells was detected by immunoblotting whole cell lysates for whole length and cleaved PARP, caspase 8 and caspase 9 (A). GAPDH was used as a loading control. Fold change in cleaved protein levels were quantified relative to untreated NK cells (n=3) (B).

6.4.2 Caspase 8 is required for the CD200-mediated apoptosis of NK cells

Having demonstrated a significant increase in cleaved caspase 8, we next wanted to confirm that CD200-mediated NK cell apoptosis was caspase dependent. Fluoromethyl ketone (FMK)-derivatized peptides are cell permeable irreversible caspase inhibitors with no cytotoxic effects. These peptides have become an essential tool in the study of caspase activity. To determine involvement of caspases in the apoptosis of our NK cells, caspase inhibitors preferentially targeting either caspase 8 or caspase 9 were used (Figure 6.4). The pan caspase inhibitor, Z-VAD-FMK, was used as a positive control. We observed reduced cleavage of apoptosis hallmark, PARP, as well as caspase 8 with Z-VAD-FMK. Selective inhibition of caspase 8 with the Z-IETD-FMK inhibitor reduced the CD200-mediated cleavage of both PARP and caspase 8. Inhibition of caspase 9 with the Z-LEHD-FMK inhibitor did not reduce the cleavage of PARP or caspase 8. These results suggest that the caspase 8 mediated extrinsic pathway is involved in CD200 mediated apoptosis of our NK92MI cells. Thus, CD200-mediated NK92MI cell death was dependent upon caspase 8 cleavage, a hallmark of the extrinsic apoptosis pathway.

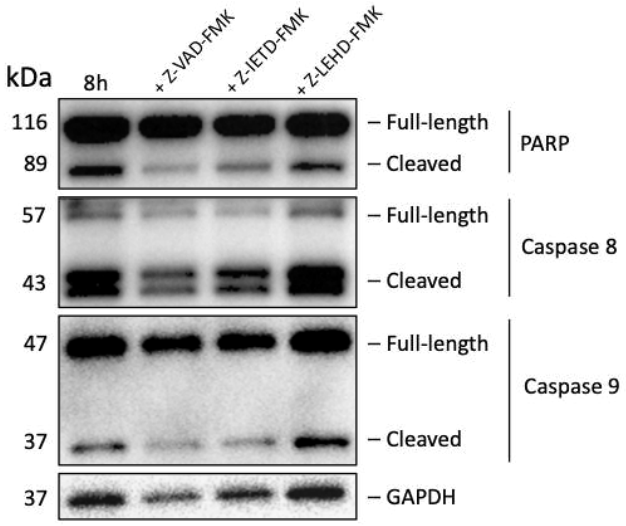

Figure 6.4: Caspase inhibition. NK92MI cells were stimulated with a CD200 peptide (4 µg/10^6 cells) for 8 hours with the addition of either Z-VAD-FMK, Z-IETD-FMK or Z-LEHD-FMK. Apoptosis of NK cells was detected by immunoblotting whole cell lysates for whole length and cleaved PARP, caspase 8 and caspase 9. GAPDH was used as a loading control.

6.4.3 CD200 peptide does not induce apoptosis in CD200R- NKL cells

We have shown that CD200 signalling results in the downstream downregulation of the MAPK pathway. We have also shown that in those same cells, incubation with the CD200 results in their death, through the caspase 8-mediated apoptosis pathway. To confirm that apoptosis is mediated via the CD200R, we analysed apoptosis markers in our CD200R- NKL cell line. As before, the NKL cells were incubated in the presence of a CD200 peptide for 8 hours and analysed for expression of apoptosis markers PARP, caspase 8 and caspase 9 (Figure 6.5). Unlike in our NK92MI cells, there was no induction of cleavage of either the apoptosis hallmark, PARP, or either of the caspases. Hence, NK cell apoptosis was dependent upon CD200 receptor-ligand interaction.

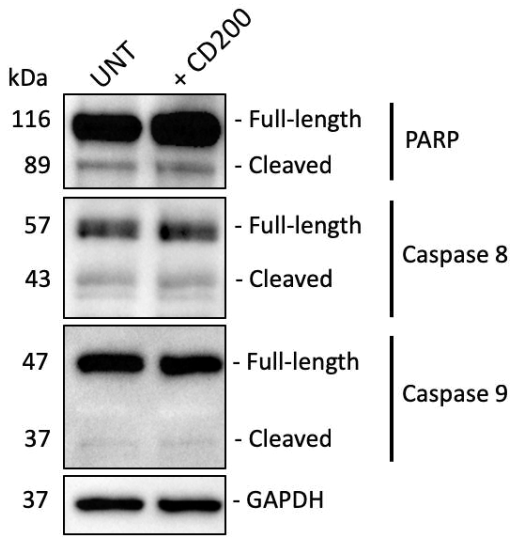

Figure 6.5: Apoptosis markers in CD200 treated NKL cell lines. NKL cells were stimulated with a CD200 peptide (4 μg/10^6 cells) for 8 hours. Apoptosis of NK cells was detected by immunoblotting whole cell lysates for whole length and cleaved PARP, caspase 8 and caspase 9. GAPDH was used as a loading control.

6.5 Microarray analysis of CD200 stimulated NK92MI cells

In order to define the intracellular signalling events after CD200:CD200R signalling that result in NK cell apoptosis, we undertook a microarray analysis of our NK92MI cell line treated with the CD200 peptide over a period of 2 and 4 hours, as well as untreated NK cells for comparison. NK92MI cells were incubated in the presence of CD200 peptide (4ug/10^6 cells) for 2 and 4 hours, after which RNA was extracted and stored at -80 °C. The quantity and quality of the RNA was determined by NanoDrop™ and Bioanalyser™, respectively. The three replicates of each treatment condition with the highest quality (RIN number) were chosen for further analysis by microarray. Each sample was determined to be of sufficient quantity and quality (RIN 9-10) for gene profiling by Illumina HT-12 v4 bead microarray chips. Bioconductor packages in the R statistical programme were used to transform and normalise the raw microarray data to be used in subsequent analysis.

6.5.1 Volcano plots

Illumina HT-12 v4 bead microarray chips are expression arrays that analyse differential gene expression. This chip allowed for the gene expression analysis of 16,192 genes, using multiple probes for each gene. Following transformation and normalisation of samples, differentially expressed genes were identified. Volcano plots using a cut off of an adjusted p-value of <0.5 identified 5 downregulated genes in the 4-hour CD200-stimulated NK cells when compared to the untreated (Figure 6.6). These genes include *THOC4*, *ALPP*, *LOC100134648*, *CDKN2AIPNL* and *DFFA*, which are involved in a range of process such as molecular chaperoning, enzymatic activity and DNA fragmentation during apoptosis. No differential gene expression was seen at these cut offs between 2-hour CD200-stimulated NK cells and the untreated. These genes did not signify an upregulation of any particular pathway and thus, we focused our analysis towards apoptosis gene sets.

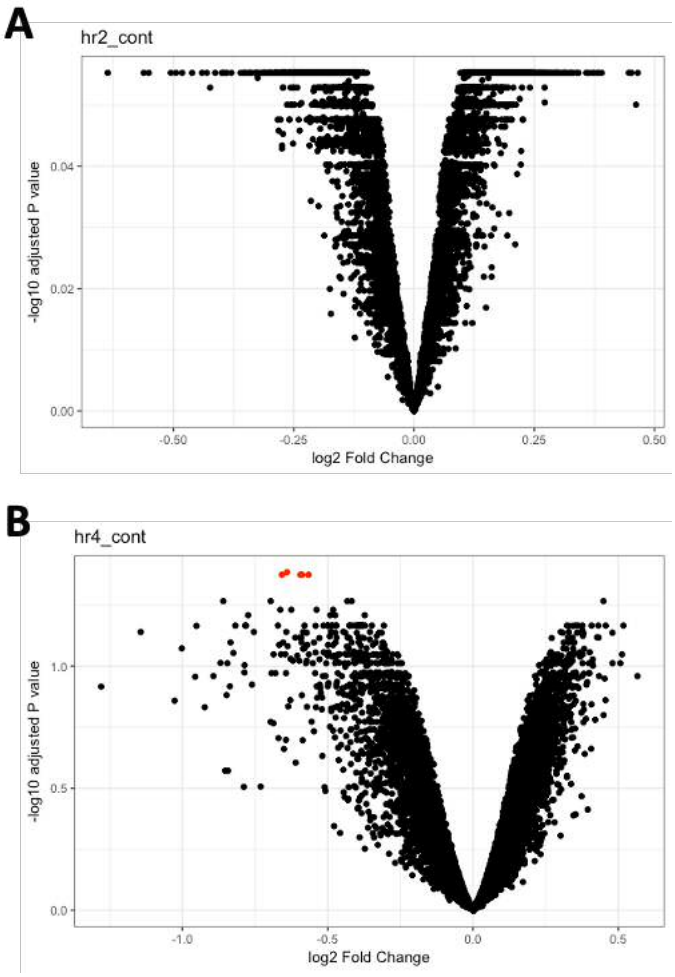

Figure 6.6: Volcano plots of differentially expressed genes. Volcano plot representation of the differentially expressed genes between 2-hour CD200 treatment (A) and 4-hour CD200 treatment (B) of NK92MI cells when compared to untreated cells. Statistically significant genes observed are highlighted in red (adj.P <0.05).

6.5.2 Gene set enrichment analysis

Gene set enrichment analysis (GSEA) is a method of identifying classes of genes or proteins that are over-represented in a large set of genes or proteins. This computational method determines whether a priori defined set of genes shows statistically, concordant differences between two biological states. GSEA utilises differentially expressed genes to highlight biological pathways or molecular functions that may be relevant to each sample and for further analysis. To identify the intracellular events leading to NK92MI cell apoptosis upon CD200 binding, GSEA analysis was conducted on relevant apoptotic gene sets within the Broad Institute.

6.5.2.1 Extrinsic apoptosis pathway

Having demonstrated that stimulation of our CD200R+ NK92MI cells with the soluble CD200 peptide results in NK cell death, we focused our gene expression search towards genes involved in the apoptosis pathway. In particular, we explored the extrinsic apoptosis pathway. We analysed the gene sets relating to extrinsic apoptosis within the Broad Institute, that passed the gene set size threshold for our gene set. We confirmed enrichment of the extrinsic pathway in our CD200 treated NK cells (Appendix; Figure 5). The extrinsic pathway is activated by extracellular ligand binding to cell surface death receptors and therefore we analysed gene sets specific to this pathway.

We analysed whether the Gene Ontology “regulation of extrinsic apoptosis signalling pathway via death domain receptors” gene set (GO:1902041) was enriched in our samples. This gene set is composed of 58 genes that are involved in any process that modulates the frequency, rate or extent of extrinsic apoptotic signalling pathway via death domain receptors. Of the 58 genes included in this gene set, our microarray covered 39 of the genes. This gene set was enriched in the NK92MI cells treated with the CD200 peptide for both 2 and 4 hours (ES=0.26, p=0.374 and ES=0.36, p=0.063, respectively), however, this did not reach significance (Figure 6.7). This finding confirms our previous analysis that the cell death we observe in our NK92MI cells upon the addition and binding of the soluble CD200 peptide results in the triggering of the extrinsic apoptosis pathway and suggests involvement of the death receptors.

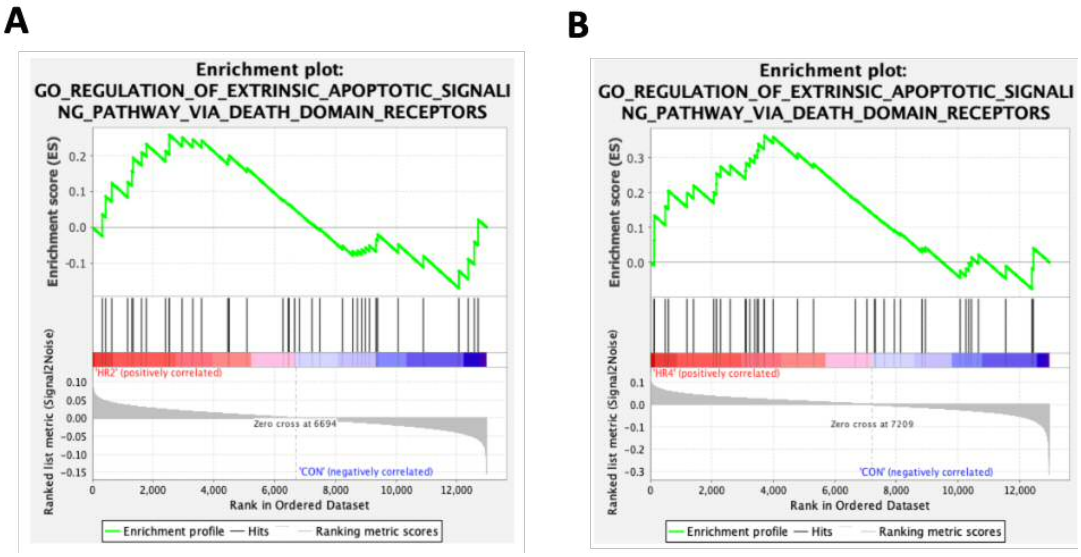

Figure 6.7: Death receptor extrinsic pathway enrichment in CD200 treated N92MI cells. GSEA reveals enrichment of the Gene Ontology "regulation of extrinsic apoptosis signalling pathway via death domain receptors" gene set in both the 2- (A) and 4- (B) hour treated NK92MI cells when compared to untreated cells. On the x-axis, the genes included in the gene set are ranked from the most upregulated (on the left) to the most downregulated (on the right), with each black line representing a gene. The y-axis represents the enrichment score (ES).

6.5.2.2 Genes involved in the regulation of extrinsic apoptosis signalling pathway via death domain receptors gene set

Apoptosis can be induced through the activation of death receptors, that include Fas, TNFαR (TNFRSF1A), DR3 (TNFRSF25), DR4 (TNFRSF10A or TRAILR1), and DR5 (TNFRSF10B or TRAILR2). These receptors are activated upon ligation to their respective ligands. To determine which of the death receptors was involved in the induction of the extrinsic apoptosis pathway observed in our NK92MI cells, we looked towards the genes included in the gene set. We looked at the genes that were annotated as being core enriched in our gene set. Core enrichment of genes using GSEA are genes that contribute to the leading-edge subset within the gene set and are the subset of genes that contribute most to the enrichment score. In the 2-hour treated cells, 11 genes demonstrated core enrichment. This included the death receptor DR4, but not its ligand, TRAIL. However, the FasL demonstrated core enrichment as well as the Fas associated death domain (FADD) (Figure 6.8, A). In the 4-hour treated cells, 19 genes demonstrated core enrichment. Including three of the death receptors: Fas, DR4 and DR5. In addition to the receptors, genes encoding the death receptor ligands FasL and TRAIL demonstrated a core enrichment (Figure 6.8, B). We also observe a core enrichment of FADD and the Fas-associated factor 1, FAF1. Of the death receptors, the Fas pathway demonstrates elements that are most consistently upregulated at both 2- and 4-hour CD200 treatment and thus, suggests that this pathway is key to the CD200-mediated apoptosis observed in our NK92MI cells.

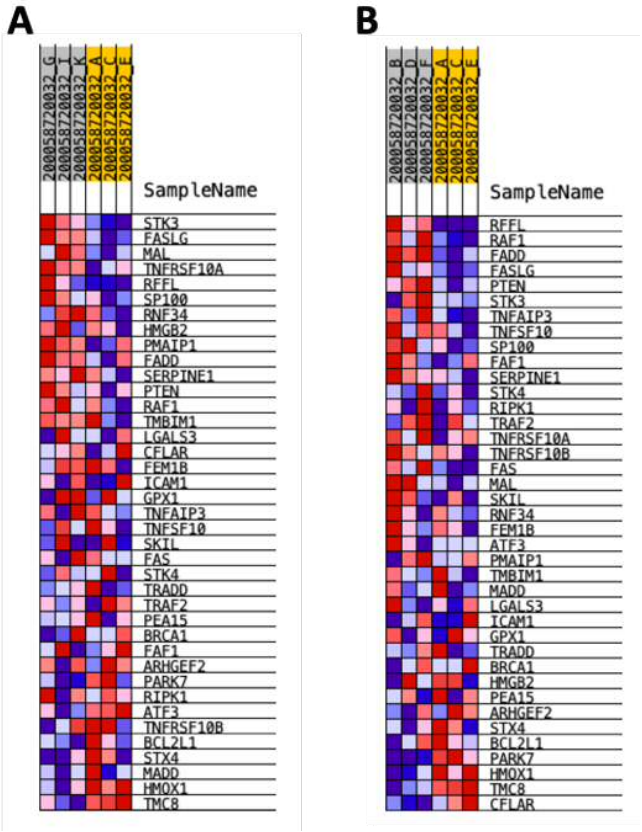

Figure 6.8: Genes involved in the Gene Ontology "regulation of extrinsic apoptosis signalling pathway via death domain receptors" gene set. A heat map of the genes involved with expression values for the 3 replicates shown as colours, where red is upregulated, and blue is downregulated in 2- (A) and 4- (B) treated NK cell compared to untreated.

6.6.2.3: Differential expression of death receptor pathway genes

Having identified that the death receptor pathways are enriched in our CD200 stimulated NK92MI cells, we next looked toward the relative fold change in expression of genes involved in these pathways. To isolate whether there was any particular death receptor involved in the apoptosis we observe in our NK cells, we analysed the fold change in gene expression. We observed very small changes in fold change gene expression. We saw an upregulation in the gene expression of the Fas and DR4 receptors at both 2- and 4-hour CD200 treatment (Figure 6.9, A). We saw an upregulation of FasL gene expression at both 2- and 4-hour CD200 treatment (Figure 6.9, B). Whilst these changes in gene expression are small, upregulation of both the receptor and ligand involved in the Fas death receptor pathway suggest the possibility that this death receptor is involved in the CD200 mediated apoptosis we observe in our NK92MI cells.

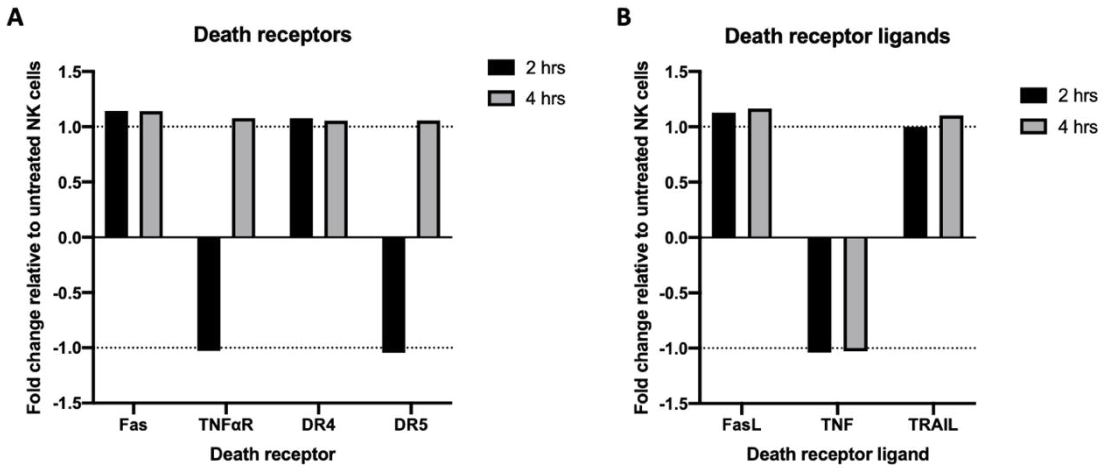

Figure 6.9: Differential expression of death receptor genes in CD200 stimulated NK92MI cells. The average fold change was calculated relative to untreated NK92MI cells.

5.5.2.4: Fas pathway gene set

Having observed a core enrichment in FasL and its receptor, Fas, as well as an upregulation in gene expression, we next analysed whether the Fas signalling pathway was significantly enriched in our CD200 treated samples. We observed an enrichment of the "BioCarta Fas pathway" in both our 2- and 4-hour CD200 treated NK92MI cells (ES=0.30, p=0.58 and ES=0.31, p=0.9, respectively), however these do not reach significance (Figure 6.10). Of the 30 genes within the gene set, and as seen in the previous death receptor gene set, the FasL gene demonstrated core enrichment. In the 4-hour treated cells, PARP1 gene also demonstrated core enrichment, coinciding with our western blot analysis. These results suggest that the Fas death receptor pathway may be upregulated upon CD200 ligand binding to the CD200R in our NK92MI cells and may play a role in the apoptosis we see in these cells.

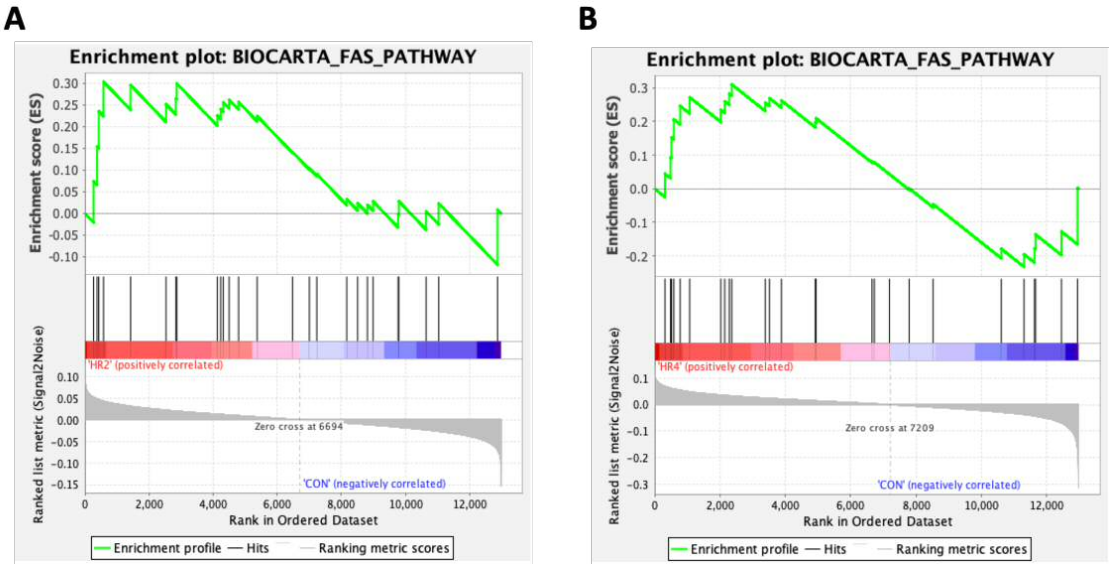

Figure 6.10: Fas pathway enrichment in CD200 treated N92MI cells. GSEA reveals enrichment of the Biocarta "Fas Pathway" gene set in both the 2- (A) and 4- (B) hour treated NK92MI cells when compared to untreated cells.

6.6 Involvement of the Fas death receptor pathway in CD200-mediated NK apoptosis

Our microarray analysis suggested an upregulation of death receptor pathways in our CD200 treated NK92MI cells. Further exploration of the enriched genes in our dataset suggested a particular upregulation of the Fas death receptor pathway. We sought to better characterise the involvement of this death receptor pathway in the CD200 apoptosis of our NK92MI cells.

6.6.1 Upregulation in gene expression of the Fas death receptor pathway

We hypothesised that the Fas death receptor pathway was involved in CD200 mediated apoptosis of our NK92MI cells. To confirm our findings in the microarray, we used RT-PCR to analyse mRNA expression of the three major components of the pathway: the Fas receptor (Fas), Fas ligand (FasL) and the FAS-associated death receptor domain (FADD). We saw an upregulation of all three genes after both 2- and 4-hour treatment when compared to untreated NK cells (Figure 6.11). This result confirms our microarray analysis that CD200 stimulation of our NK92MI cells leads to an upregulation of the Fas pathway components.

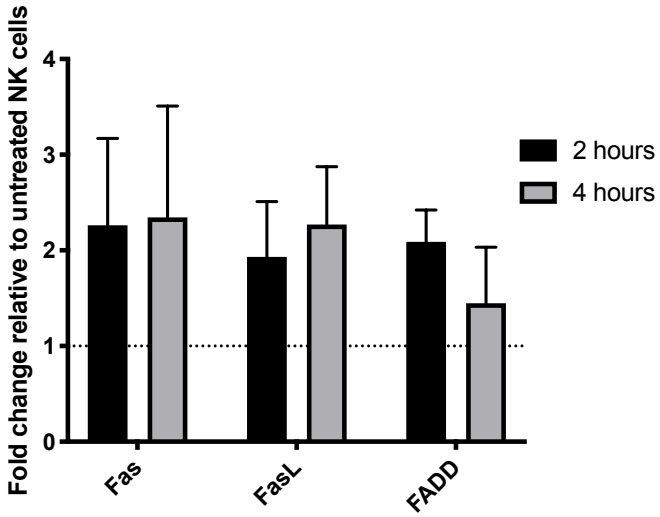

Figure 6.11: Upregulation of Fas death receptor pathway. RNA was extracted from NK92MI cells treated with a Fc chimera CD200 peptide for 2 and 4 hours and probed for Fas, FasL and FADD gene expression by RT-PCR. Expression was normalised to β-Actin. Fold change was calculated relative to untreated NK cells according to the 2^-delta Ct method.

6.6.2 Upregulation in Fas death receptor proteins

To determine whether the changes we see at mRNA level corresponded to changes in protein level changes, we validated our RT-PCR findings, we looked at whether there was an upregulation of Fas, Fas ligand and FADD at protein level using western blot (Figure 6.12). NK92MI cells were stimulated with our CD200 peptide for various periods of time as before. Equal amounts of cell lysates were immunoblotted for Fas, Fas ligand and FADD. As seen at mRNA level, there was an increase in all three components of the Fas pathway.

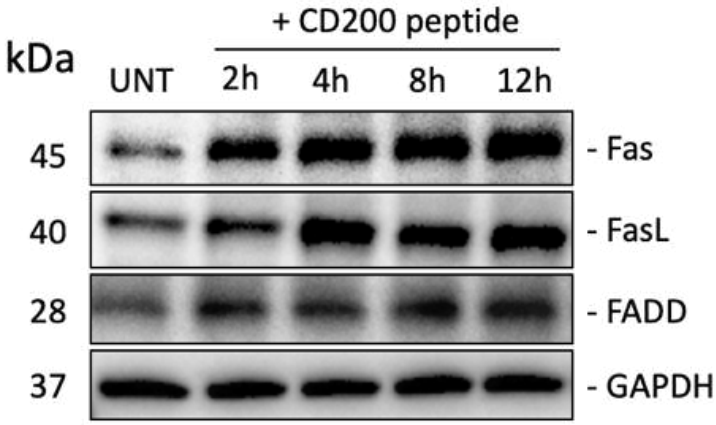

Figure 6.12: Upregulation of Fas death receptor proteins. NK92MI cells were stimulated with an Fc chimera CD200 peptide (4 μg/10^6 cells) for indicated time periods. Whole cell lysates were probed for the death receptors proteins Fas, FasL (membrane form) and FADD. GAPDH was used as a loading control.

6.6.3 Secretion of soluble FasL (sFasL)

FasL also exists as a soluble protein as it is cleaved from the cell surface. We sought to determine whether the increase in FasL we saw at protein level also resulted in the cleavage of the protein from the cell surface and an increase in the concentration of sFasL. Our NK92MI cells were incubated with a CD200 peptide over the indicated periods of time that we saw an increase in FasL protein levels. The supernatant of the cultures was analysed for sFasL by ELISA (Figure 6.13). We observed a small increase in the sFasL concentration in the first two hours of CD200 incubation, increasing from an average concentration of 53.4 to 58.1 pg/mL, an 8.8% increase. The concentration then decreases again at both 4 and 8 hours. Within the limits of this experiment, we did not detect a significant increase in the secretion of sFasL upon CD200:CD200R signalling.

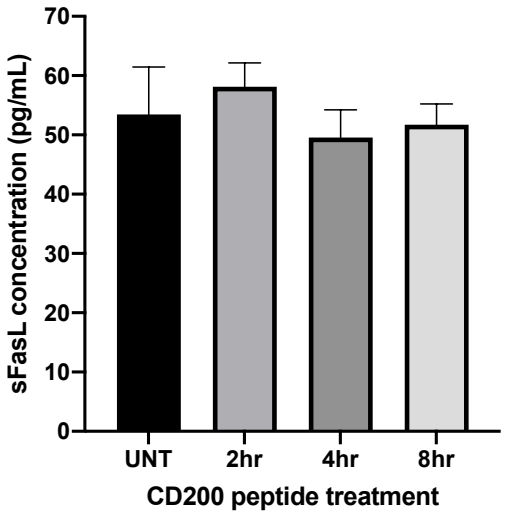

Figure 6.13: Secretion of FasL by NK92MI cells. NK92MI cells treated with a CD200 peptide for 2, 4 and 8 hours, after which the supernatant was analysed for soluble FasL by ELISA. Values were obtained from an average over 3 independent experiments. Students t test was used to determine difference between co-culture supernatant sFasL concentrations.

6.6.4 Blocking the Fas receptor signalling pathway

We have demonstrated that CD200 signalling lead to an upregulation of Fas death receptor components. To determine whether CD200-mediated apoptosis was dependent on Fas:FasL interaction, we incubated our NK92MI cells with the CD200 peptide in the presence of an antagonistic ZB4 clone anti-Fas monoclonal antibody. This antibody, without activating the receptor when bound, binds to the Fas receptor, preventing the ligation of the Fas ligand and the subsequent apoptosis signal.

NK92MI cells were treated with a CD200 peptide for 8 hours, which we have shown is long enough to induce cleavage of PARP and caspase 8. Various concentrations of the Fas blocking antibody was added to the cultures. As before, whole cell lysate was collected and probed for PARP, caspase 8 and caspase 9 and fold change in protein levels was analysed (Figure 6.14). We saw an increase in cleaved PARP and cleaved caspase 8 as before (1.55- and 1.32-fold change, respectively). Cleavage of PARP was reduced at all three antibody concentrations when compared to CD200 peptide treated NK cells, with the lowest concentration of 10ng demonstrating the greatest reduction in cleavage of caspase 8 and PARP. Fold change analysis demonstrated that cleavage of caspase 8 was also reduced at all three antibody concentrations when compared to CD200 peptide treated NK cells. The lowest concentration of the antibody reduced the cleavage of both PARP and caspase 8 proteins to levels below untreated cells (0.93- and 0.86-fold change compared to untreated NK, respectively). In keeping with our previous results, addition of the CD200 peptide had no effect on the cleavage of caspase 9, with the Fas blocking antibody also showing no effect on its cleavage. This result suggests that CD200-mediated apoptosis of the NK92MI cells is mediated by the Fas death receptor pathway. In conclusion, these results demonstrate that Fas:FasL interaction is necessary in the CD200-mediated apoptosis of our NK92MI cells.

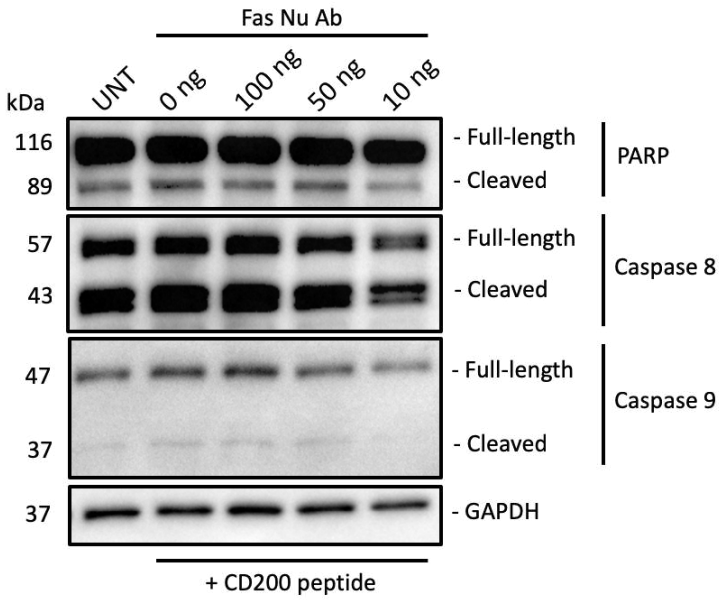

Figure 6.14: Fas neutralising antibody. NK92MI cells were stimulated with a CD200 peptide (4 µg/10^6 cells) for 8 hours with the addition of varying concentrations of the antagonistic ZB4 clone anti-Fas monoclonal antibody (10-100 ng). Whole cell lysates were probed for PARP, caspase 8 and caspase 9. GAPDH was used as a loading control.

6.7 Inhibition of PPAR-γ reduces CD200 mediated apoptosis

Peroxisome proliferator–activated receptor (PPAR)-γ is a ligand-activated transcription factor whose activation plays a role in controlling the inflammatory response, involved in the inhibition of pro-inflammatory gene expression. PPARγ has been reported to positively regulates the FasL gene expression (Bonofiglio *et al.,* 2009). We analysed whether PPARγ played a role in the CD200-mediated apoptosis of our NK cells.

GW9662 is a potent irreversible antagonist of PPAR-γ by binding to the ligand binding site. NK92MI cells were treated with a CD200 peptide for 8 hours, which we have shown is long enough to induce cleavage of PARP. Various concentrations of the GW9662 was added to the cultures. As before, whole cell lysate was collected and probed for PARP (Figure 6.15). We observed a decrease in the levels of cleaved PARP induces by CD200 binding in our NK92MI cells, with levels decreasing as the concentration of the antagonist increases. The higher GW9662 concentrations of 50 and 100uM decrease the levels lower than observed in untreated NK cells. This suggests that PPAR-γ plays some role in the CD200:CD200R signalling leading to NK cell death.

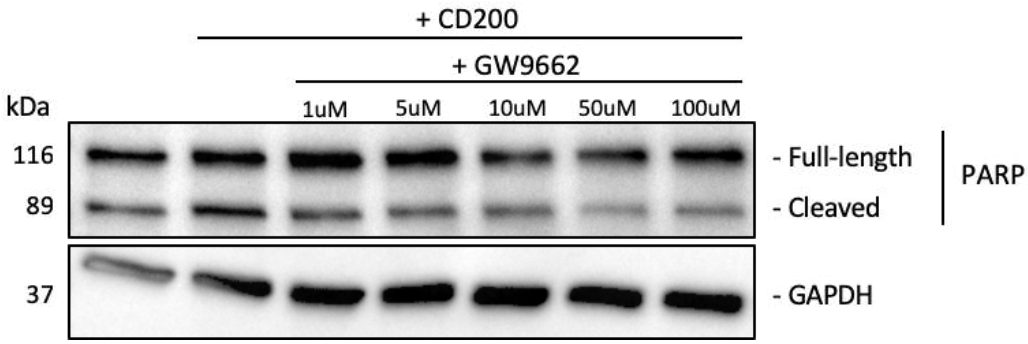

Figure 6.15: PPAR-γ antagonist reduces CD200 induced cleaved PARP. NK92MI cells were stimulated with a CD200 peptide (4 µg/10^6 cells) for 8 hours with the addition of varying concentrations of the PPAR-γ antagonist, GW9662 (1-100 µM). Whole cell lysates were probed for PARP. GAPDH was used as a loading control.

6.8 Summary

NK cells are characterised by their potential to kill tumour cells by different means without prior sensitisation. However, their efficacy against solid tumours is poor. This diminished response has been attributed to the immunosuppressive effect of the TME, where NK cells face a several factors, produced by both tumour and tumour-associated cells, that directly or indirectly inhibit their function. We have demonstrated that tumour CD200 expression directly inhibits both the cytotoxic and effector activity of our CD200R+ NK92MI cells. This observation correlates with previous studies that demonstrate an inhibition of circulating NK cell activity in CD200 positive AML patients (Coles *et al.,* 2011). In this chapter, we present an additional mechanism of CD200 mediated immune regulation. In our CD200+ NK92MI cells, we show that CD200 binding to the receptor leads to their death.

The initial event following CD200 ligand binding to the CD200R have been characterised (Zhang and Phillips, 2006; Mihrshahi R and Brown, 2010). We were able to confirm CD200 signalling within our cells, where the ERK 1/2 pathway was inhibited within the first 30 minutes of incubation. Following this initial signalling, we demonstrated that those NK cells undergo apoptosis, which we were able to attribute to induction of the caspase 8 dependent extrinsic apoptosis pathway. In an attempt to characterise this signalling pathway further we undertook microarray analysis of NK cells treated with a CD200 peptide for 2 and 4 hours. The purpose of analysing NK cell gene expression at these early time points was to identify transcriptional events that occurred before induction of apoptosis as our previous analyses suggested a time lag between ligand-receptor engagement occurring within the first 30 minutes of incubation to the apoptosis we observed 2-8 hours later. We observed very little changes in the differential gene expression of the treated NK cells compared to untreated, likely due to the short incubation periods being insufficient to induce large changes in their transcriptional profile. We did, however, observe an upregulation of the extrinsic apoptosis pathway which confirmed our western blot analyses. We also observed an enrichment in a gene set that suggested involvement of death receptors. Exploring this gene data set, we observed a particular upregulation of components of the Fas death receptor pathway, which we were able to conform in subsequent qPCR and western blot

experiments. We did not observe a marked increase in the soluble form of FasL, suggesting that the upregulation of Fas gene and protein expression leads to increase expression of FasL on the NK cell surface. This is unsurprising as native soluble FasL, a processed version of membrane FasL, does normally not activate Fas and can even inhibit apoptotic signalling (Suda *et al.,* 1997; Henkler *et al.,* 2005). This suggests that Fas:FasL signalling is induced either by the FasL on its own cell surface or by the FasL on another cell's surface. We confirm that CD200-mediated apoptosis is dependent on Fas signalling by demonstrating that blocking the Fas signalling pathway reduces the apoptosis we see in our NK92MI cells. We conclude by highlighting the possible role of the transcription factor, PPAR-γ, in the induction of the CD200-mediated apoptosis, however its precise role in this pathway needs further investigation. A schematic diagram of the CD200 induced apoptosis of NK92MI can be seen below (Figure 5.16).

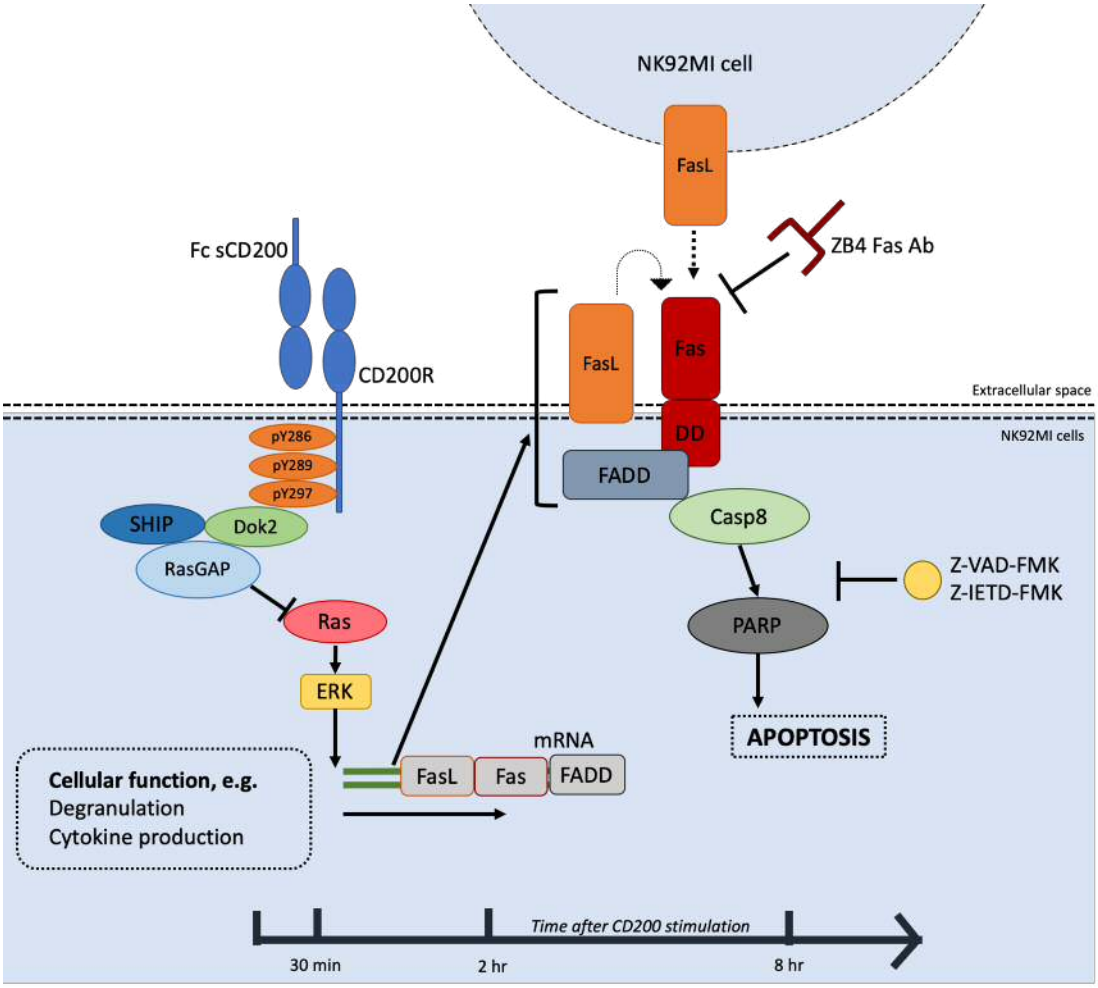

Figure 6.16: Proposed model of CD200 induced apoptosis of NK92MI cells.

Chapter 7: General discussion

Chapter 7: General Discussion

7.1 General Discussion

It is now well known that tumours evade immune surveillance and progress through different mechanisms that include activation of immune checkpoint pathways that supress anti-tumour immune responses. The discovery of immune checkpoint proteins and the mechanisms by which cancer cells utilise them to evade the immune system has transformed our approach to cancer therapy with the advent of immunotherapy (Ghahremanloo *et al.,* 2019). The aim of this study was to identify expression of the immunosuppressive ligand CD200 in RCC and to explore whether this expression had any influence on immune evasion. Using a combination of human tissue analysis and cell culture assays revealed, (i) that RCC demonstrates CD200 protein expression, (ii) that higher CD200 expressing patients demonstrated a significantly reduced T cell infiltrate but had little effect on NK cell numbers, (iii) that tumour CD200 expression diminished CD200R+ NK cell activity, which could be restored by blocking the CD200 signal and (iii), that CD200 signalling induced apoptosis of interacting NK cells. Together, these results suggest that CD200 may be a novel therapeutic target for the treatment of RCC.

CD200 is a highly conserved transmembrane protein thought to be expressed in "immune-privileged" sites (Minas and Liversidge, 2006). This ligand functions by engaging its receptor, CD200R, which results in an immunosuppressive signal and provides a regulatory mechanism by which an immune response is regulated. Several studies have demonstrated CD200 expression in cancer and has been associated with a mechanism of immune evasion. CD200 has been most extensively studied in haematological malignancies (Moreaux *et al.,* 2006; Tonks *et al.,* 2007). In contrast, CD200 expression in solid tumours has been less extensively studied. Microarray analysis has demonstrated that CD200 is overexpressed in a number of solid tumours, with RCC demonstrating significant overexpression when compared to normal tissue (Moreaux *et al.,* 2008). These studies, however, only demonstrated overexpression of CD200 at mRNA transcript level and thus, warrant further analysis of CD200 expression at protein level in this disease.

The aim of this study was to identify CD200 expression in RCC at protein level and to explore whether expression of this immunosuppressive ligand had any effect on tumour immune evasion. Through immunohistochemical analysis we were able to confirm RCC expression of CD200 at protein level. Immunofluorescence analysis provides an insight into the location and distribution of expression within a tumour and hence, is a common method used to identify immune checkpoint expression in cancers (Gorris *et al.,* 2018). To score CD200 positivity in our samples we used a positivity threshold used in previous immunohistochemical studies of CD200 expression (Dorfman and Shahsafaei, 2010). We found CD200 expression in the majority (92.3%) of our RCC samples. This finding is higher than previous immunohistological analysis of CD200 expression in RCC, which reported that 71% of RCC samples stained positive (Love *et al.,* 2017). The sample size in this study, however, was much smaller than ours. RCC is comprised of several histological cell types, of which we studied the most common subtypes: ccRCC, pRCC and chRCC. We observed expression of CD200 in all three subtypes, which demonstrated differential CD200 expression intensity between them. CD200 intensity analysis revealed a significantly weaker CD200 expression in chRCC when compared to both ccRCC and pRCC. Observation of CD200 expression in all three subtypes suggests that CD200 expression is not driven by the oncogenic drivers of these subtypes but more likely derives from the cell of origin of these tumours, cells of the renal tubules. We were able to provide evidence for this hypothesis, showing CD200 expression across the tubules in normal kidney tissue. This finding corresponds to previous immunohistological analysis of CD200 expression in normal kidney, which reported low-level reactivity in a subset of renal tubules (Love *et al.,* 2017). Both clear cell and papillary RCC are thought to arise from the epithelium of the proximal tubule, whilst chromophobe RCC is believed to arise from the distal nephron, probably from the epithelium of the collecting tubule (Cairns, 2011). Given the greater CD200 expression we observed in the ccRCC and pRCC subtypes, we attempted to analyse whether CD200 expression was stronger in their cells of origin, the proximal renal tubules. We did observe a slightly stronger expression in the renal tubules that expressed the proximal tubule marker, NaDC3, however, CD200 expression was not limited to these tubules. Additional evidence for the differential expression of CD200 expression in RCC based on tubule of origin comes from the histological analysis of neoplasm CD200 expression

where, of the nine samples analysed, the two CD200-negative renal tumours in their study were chRCC (Love *et al.,* 2017). We concluded from this analysis that expression of CD200 seen in the tubules of the kidney is retained in RCCs, which ultimately suggests that CD200 may play a role in the immune evasion in this set of diseases.

For many cancer types, CD200 has been associated with prognosis. CD200 is now commonly used as both a diagnostic and prognostic marker in several lymphoid malignancies, such as in AML where CD200 expression has been associated with a poor prognosis (Mora *at al.,* 2019; Tonks *et al.,* 2007). CD200 expression as a prognostic marker is not limited to haematological malignancies. Increased expression of CD200 was detected in the cutaneous squamous cell carcinoma (CSCC) tumour tissues compared with the corresponding normal tissues both at mRNA and protein level (Li *et al.,* 2016). CD200 expression level was associated with tumour differentiation grade and clinical stage, with patient with high levels of CD200 expression demonstrating a shorter OS than those with low expression. A similar link between higher CD200 expression and tumour progression was seen in another skin cancer, melanoma (Petermann *et al.,* 2007). Having demonstrated CD200 in RCC, we analysed whether the expression we observed had any link to disease progression. Of the RCC subtypes, ccRCC is by far the most common and accounts for the most cancer related deaths (Hsieh *et al.,* 2017). For this reason, we analysed this subtype in more detail. We explored the relationship between CD200 expression and progression in ccRCC with data available to us. Pathologic stage, based on the size of the tumour and the extent of invasion, is one of the most important prognostic indicators. Using the TNM staging of our ccRCC samples, we observed an increasing frequency of samples that scored positive for CD200; however, we did not observe any relationship between disease stage and CD200 expression intensity. Clinical data on the samples within our study may provide further insight into whether the CD200 expression we observed in our samples demonstrated any correlation with patient outcome.

The composition of the immune infiltrate has demonstrated a prognostic value for many cancer types. Using serial sections of our samples, we were able to analyse the effect of RCC CD200 expression on the immune infiltrate for each individual sample. The purpose

of characterising the immune infiltrate in our samples was to explore whether the immune phenotype associated with RCC expression could be linked to known prognostic value of immune cell type and highlight any cell types that may be rendered dysfunctional by CD200 in RCC. Using immunofluorescence, we analysed the main TILs: T cells and the two subtypes, T helper and cytotoxic T cells, as well as NK cells. We also analysed the presence of the immunoregulatory Treg cells. We observed a relationship between RCC expression of CD200 and the density of infiltrating T cells. This would suggest that RCC expression of CD200 impairs T cell migration to the tumour site. We observed a particular decrease in the frequency of T helper cells, which resulted in a reduced CD4:CD8 ratio. CD200 expression did not appear to affect the frequency of NK cells within our sample set. We observed very few Treg cells within our samples and did not observe any relationship between CD200 expression levels and Treg frequency. Using previous RCC immune phenotype studies, we were able to correlate the phenotype associated with CD200 to known prognostic markers.

Several studies have demonstrated phenotypic profiles of TIL in RCC lesions with correlated with clinicopathological parameters and survival of patients (Geissler *et al.,* 2015). In contrast to most other cancer types, increased TILs, both CD4+ and CD8+ T cells, appear to correlate with tumour recurrence and poor prognosis in renal cell carcinoma (Kolbeck *et al.,* 1992; Remark *et al.,* 2013). This may be in part due to the observation that patients with high CD8+ T cell infiltration often also have high densities of Tregs that may offset the anti-tumour activity of these cytotoxic cells (Xiong *et al.,* 2020). This is supported by the observation that patients with a higher T effector/Treg ratio are less likely to develop a recurrence following surgery (Ghatalia *et al.,* 2019). In addition to the influence of surrounding immune cells, tumour infiltrating lymphocytes in patients with high immune infiltrates often display an immunosuppressed phenotype, such as increase expression of PD1 (Kawashima *et al.,* 2020). Expression of inhibitory receptors is also associated with T cell exhaustion, which is a state of dysfunction that commonly occurs due the persistence of antigen and inflammation (Blank *et al.,* 2019). This can result in the progressive loss of T cell effector function.

Our results confirm the negative association of increased immune infiltrate, with higher numbers of TILs, including CD4+ and CD8+ cells, observed in samples of later stage disease in ccRCC. Conversely, we saw a decrease in the number of these T cell TILs with increasing tumour CD200 expression. This would suggest that RCC expression of CD200 is linked to a better prognosis if TIL density is used as a predictor of prognosis in our samples. This supports the survival analysis data for CD200 expression in the human protein atlas, which demonstrates a significant increase in ccRCC patient survival in those with high CD200 mRNA expression levels. A possible explanation for this may be that tumour CD200 expression reduces the immunogenicity of the tumour, which consequently reduces the number of tumour-infiltrating immune cells that migrate to the tumour bed. In turn, this may reduce the level of inflammation in the tumour microenvironment that can cause T cell exhaustion. More detailed analysis of the phenotypes of the immune cell subsets, such as analysing markers of exhaustion, may provide more insight whether there is any link between tumour CD200 expression and the infiltration of dysfunctional immune cells.

In addition to effector immune subtypes, the presence of inhibitory cell subtypes is an area of study for many cancers, including RCC. FoxP3+ Treg cells play a key role in inducing immune tolerance and in the limitation of the inflammatory response executed by T helper cells and as such, have been implicated as inhibitor of anti-tumour immunity (Whiteside, 2012). High numbers of FoxP3+ Tregs, both in the TME and the peripheral blood, have been associated with metastasis, short disease-free survival, and poor prognosis (Griffiths *et al.,* 2007; Liotta *et al.,* 2011). A previous meta-analysis demonstrated that a high level of infiltration of FoxP3+ Tregs in the majority of solid tumours is significantly associated with poor prognosis of patients with cancer, including RCC (Shang *et al.,* 2015). A recent study using CIBERSORT to analyse the composition of immune cells in RCC and normal tissues from The Cancer Genome Atlas (TCGA) cohort to determine the prognostic value of immune infiltrate in RCC confirmed the poor prognostic association demonstrated that the proportion of Tregs was associated with tumour grade and TNM classification (Zhu and Zhang, 2019). We observed very few FoxP3+ Treg cells in our samples. In our study, we analysed the frequency of these cells in the RCC subtypes and focused on ccRCC where Tregs accounted for around 4% of

CD4+ cells. We did not observe any correlation with TNM classification in ccRCC. This figure, however, is the same as observed in a previous study analysing Treg cells in ccRCC by immunofluorescence, which also demonstrated that only a quarter of samples contained Treg cells (Siddiqui *et al.,* 2007). This same study observed no association between the presence of these cells and prognosis. This result suggests that the prognostic role of FoxP3+ Treg cells is dependent on molecular subtype.

Tumour expression of CD200 has been linked to the frequency of these Treg cells. In AML, high CD200 expressing AML patients demonstrated a higher frequency of Treg cells, which has previously been associated with relapse in myeloid malignancy (Coles *et al.,* 2012; Nadal *et al.,* 2007). We analysed whether RCC expression of CD200 had any effect on Treg frequency, where did not observe any significant association. This result may reflect the observation that RCCs harbour very few of these cells, particularly in our study. In a phase-I study using anti-CD200 monoclonal antibody immunotherapy, blocking CD200 was shown to be sufficient to reduce the Treg frequency in chronic lymphocytic leukaemia patients, which was suggested may be therapeutically advantageous when Treg cells are associated with a worse prognosis (Mahadevan *et al.,* 2019).

In addition to T cells, NK cell lymphocytes play an important role in the recognition and elimination of emerging tumours. Several studies have correlated high numbers of tumour-infiltrating NK cells with a good prognosis in various cancers (Larsen *et al.,* 2014). Multiple independent studies have associated intratumoral NK cell infiltration with increased survival of metastatic RCC patients (Donskov and von der Maase, 2006; Geissler *et al.,* 2015). We observed differential frequency of NK cells between RCC subtypes. Interestingly, the frequency of NK cells within ccRCC was similar to the levels seen in normal healthy blood, a frequency that did not change between samples of different TNM stages. We also observed no significant association between NK cell infiltrate and RCC CD200 expression. We did observe a trend of decreasing NK cell frequency and density with increasing RCC CD200 expression, which became significant upon excluding outliers. The observation that exclusion of two samples alone was sufficient to cause this change suggests that the small sample size may be impacting the

associations made and that increasing the cohort may clarify results. Despite the NK cell infiltration, tumours are able to grow, indicating that the TME negatively affects NK cell functionality (Terrén *et al.,* 2020). Several reports have indicated that NK cells infiltrated in ccRCC have an altered phenotype and poor degranulation activity compared with circulating NK cells and with those from non-tumour kidney tissue (Prinz *et al.,* 2014). Links between NK cell function and tumour CD200 expression have been made, again most extensively studied in AML (Coles *et al.,* 2011). It was found that highly expressing CD200 patients showed a 50% reduction in the frequency of activated NK cells. Analysis of activation markers in our panel may provide further insight into whether the NK cells we observe in our samples are functional and whether CD200 expression in RCC plays any role in this observation.

Given that NK cells are still present in our RCC samples, it would suggest that they are in some way rendered dysfunctional. Given that CD200 expression is known to inhibit an immune response, we focused our attention on analysing the effect of RCC expression of CD200 on NK cell activity. We were able to utilise a solid tumour CD200 model using the NK-sensitive HeLa cell line, which were transduced to stably express CD200. We analysed the activity of the highly cytotoxic NK cell line, NK92MI, towards our HeLa-CD200+ cells compared with HeLa-CD200− controls. NK92MI is an IL-2 independent NK cell line that is characterised as $CD56^{bright}$ CD16-. NK92MI cells are known to be very effective NK cell line with multiple lytic granules that are capable for killing large amount of target cells (Xu *et al.,* 2017). We demonstrated decreased degranulation, using CD107a expression to monitor NK cell cytolytic activity, of these CD200R+ NK cells towards the HeLa-CD200+ cells compared with HeLa-CD200− controls. This result is consistent with that observed in an AML model, which in a similar study to ours. Tumour CD200 expression was analysed in co-incubation assays where NK cells from healthy patients were shown to degranulate less in response to CD200+ K562 targets cells compared with CD200− controls (Coles *et al.,* 2011). These results suggest that tumour CD200 expression alone is sufficient to impair NK cell degranulation. We also analysed NK capacity to kill target tumour cells. Unsurprisingly, the decrease degranulation was coupled with a decreased ability to kill those HeLa CD200+ target cells. These results support our hypothesis, that despite NK cells presence in the tumour bed, CD200

expression on tumour cells render them unable to degranulate and effectively kill those target cells, ultimately conveying a mechanism of immune evasion. We found that we could recover a significant proportion of NK cell activity toward CD200+ tumour targets using a CD200-blocking antibody.

We made a similar observation in relation to CD200 expression in RCC cell lines. Differential expression of CD200 within our RCC cell line did not prove to be a predictor of NK cell ability to kill target tumour cells, likely due to the multitude of other factors involved in tumour cell recognition. For example, loss of MHC class I is common in cancer and it was reported to be partially or fully lost in 39% and 6% of ccRCC patients, respectively (Romero *et al.,* 2006). Loss of MHC class I would normally result in an activating signal mediated by lack of MHC binding to the inhibitory receptors, tipping the NK cell towards an activated state. In cancer, however, NK activity is reduced. As NK cell activation is regulated by a balance between both activating signals, such as loss of MHC class I, and inhibitory signals, it is possible that the contribution of inhibitory signals outweigh and override any activating signals. Tumour expression of CD200 may contribute towards the overall inhibitory signal, which ultimately disables NK cell activation towards target tumour cells. Our results support this hypothesis as we demonstrate that use of a CD200 blocking antibody was sufficient to induce NK cell activation and restore NK cell activity toward the CD200+ cell line, SN12C. This result suggests that blocking CD200 signal reduces the inhibitory signal, tipping the NK towards a state of activation. Addition of the antibody restored both NK cytotoxic and effector activity towards our CD200+ tumour models, including the SN12C cell line. Efficacy of the antibody appeared to be dependent on the E:T ratio. This may be unsurprising as the NK:tumour ratio has been associated with prognosis in various cancer types (Larsen *et al.,* 2014). Whilst additional studies would be required to clarify this observation, this result suggests that stratification of patients based on CD200 expression and even NK:tumour cell ratio may be required for successful application of anti-CD200 therapies in RCC.

In addition to their cytotoxic function, NK cells have an important immune-regulatory role through the secretion of cytokines. NK cells are endowed with immunoregulatory

functions since they secrete cytokines such as IFN-γ, which favour the development of Th1 cells, and chemokines such as CCL3/MIP-1α and CCL4/MIP-1β, which recruit various inflammatory cells into sites of inflammation (Maghazachi, 2010). Studies analysing the effect of tumour CD200 expression on NK secretion of IFN-γ and has already been reported, demonstrating a diminished response (Coles *et al.,* 2011). We analysed the effect of tumour CD200 expression on NK chemokine secretion, which have been shown to regulate cancer cell migration and contribute to cancer cell proliferation and survival (Chow and Luster, 2014). To fit in with our co-culture experiments, we analysed the secretion of the CCL4 chemokine, shown to be released from NK cells as early as one hour after stimulation (Fauriat *et al.,* 2010). CCL4 is a chemokine produced by many immune cells, including NK cells. Having demonstrated a reduced cytotoxic capacity of our NK92MI cells in response to CD200+ tumour cells, we analysed whether a similar effect was seen in their effector function, measured by their production and secretion of CCL4. We demonstrate a diminished production of CCL4 by NK cells in response to our CD200+ HeLa model when compared to the CD200- control. Blocking CD200 signalling was sufficient to restore NK effector activity and increased their secretion of CCL4, including in our CD200+ SN12C cell lines. As discussed, NK cells are crucial in the early detection of tumour cells and are often some of the first immune cells at the tumour site. In addition to eradicating the aberrant cells, NK cells also play a role in signalling and the recruitment of other immune cells through secretion of cytokines such as CCL4 (Marcus *et al.,* 2014; Paul and Lal, 2017). The CD200 mediated inhibition of CCL4 production may play a part in the immune infiltrate phenotype, such as the reduced number of T cells seen associated with the increase in CD200 expression in our RCC samples. Evidence to support this suggestion are seen in oesophageal squamous cell carcinoma, where CCL4 expression has been shown to be positively correlated with the expression of CTL markers, CD8 and Granzyme B (Liu *et al.,* 2015). Ultimately, this result demonstrates that tumour CD200 expression inhibits both the cytotoxic and effector function activity of NK cells and possibly contributing to an immunosuppressive TME.

The TME consists of several components and soluble factors that contribute to tumour development (Bhome *et al.,* 2015). In addition to the receptors and ligands of immune checkpoints on cell membranes, a series of soluble immune checkpoints have also been

analysed, and their plasma levels have been measured (Gu *et al.,* 2018). These soluble checkpoints have been shown to be involved in the development and prognosis of cancer and are considered to be potential biomarkers and therapeutic targets. A soluble form of CD200 (sCD200) has been identified and analysis of the human CD200 gene suggested that, unlike CTLA-4, alternative splicing is an unlikely mechanism responsible for the production of sCD200, as the only reported isoform of CD200 is a truncated form lacking amino acids at the N-terminal (Chen *et al.,* 2008). The presence of sCD200 has since been linked to ectodomain shedding by ADAM proteases (Twito *et al.,* 2013). Several proteolytic ADAM species, including ADAM8, ADAM9, ADAM12, ADAM15, ADAM17, ADAM19, and ADAM28, are overexpressed in human cancers and are associated with tumour growth and progression, including in RCC (Mochizuki and Okada, 2007; Roemer *et al.,* 2004). Of these proteases, ADAM28 has been associated with the ectodomain shedding of CD200 (Twito *et al.,* 2013). Our cell culture assays suggest the possibility that ADAM28 may be responsible for the presence of sCD200 in our culture supernatant, as high mRNA levels of this protease were seen in the A498 cell line that demonstrated highest levels of shedding. Further knockdown studies would be required to validate this finding. The sCD200 shed from CLL was also found to be capable of interacting with the CD200R, resulting in its phosphorylation (Wong *et al.,* 2016). It would be interesting to determine whether the sCD200 shed from our RCC cells is also capable of interacting with CD200R, which would indicate an additional layer of immune evasion.

Under normal conditions, immune checkpoints are involved in balancing efficient recognition and destruction of aberrant cells, whilst preventing tissue damage by excessive or inappropriate immune reactions. In addition to inhibitory signals, lymphocyte apoptosis is believed to maintain homeostasis and self-tolerance in the immune system and this process has been linked to characteristics of the tumour immune infiltrate (Xu and Shi, 2007). It has been suggested that a number of human tumours considered as immune desert were in fact previously infiltrated by T cells that have disappeared through apoptosis (Zhu *et al.,* 2019). Evidence for this is seen in the activation-induced cell death (AICD). AICD is a mechanism of peripheral T cell tolerance that depends upon an interaction between Fas and FasL. A model whereby TCR ligation

leads to the transcription of FasL, which translocate to the plasma membrane and interacts with Fas and initiates the apoptosis caspase cascade has been reported (Zhang *et al.,* 2000). A similar observation was made in NK cells, where tumour cells were shown to induce apoptosis of NK cells by engaging the NCRs NKp30, NKp44, and NKp46 (Poggi *et al.,* 2005). As seen in TCR engagement, the engagement of NCR induced up-regulation of FasL, which in turn interacts with Fas at NK cell surface and causing NK cell apoptosis. Having shown that CD200:CD200R signalling in our NK92MI cells results in a reduction in both cytotoxic and effector functions, we explored whether this signalling also had any effect on their viability. We demonstrate a similar apoptotic process seen in the activation induced cell death described above, whereby CD200 ligations results in the upregulation of the Fas death receptor pathway and consequently, activation of the caspase 8 extrinsic pathway. We therefore present an additional method in which CD200 generates immune tolerance, where the inhibitory signal not only inhibits function of the interacting NK cell, but confers an apoptotic signal. This process may demonstrate an additional mechanism by which tumours evade destruction by the immune system. Indeed, given the breadth of CD200 expression in tumours, it may be in part responsible for the reduced frequency of NK cells seen in the TME reported for several cancers, including in our samples, where the strongly expressing CD200 samples contained fewer NK cells in the infiltrate. Having demonstrated this apoptosis with a sCD200 ligand, it may be hypothesised that the sCD200 shed from RCC that we observed may also contribute to inducing apoptosis in the TME. Mediating the apoptosis of lymphocytes has already been observed in RCC, with the overexpression of several apoptosis inducing genes (Uzzo *et al.,* 1999). Overexpression of the cytokine CD70 in RCC has been shown to promote lymphocyte apoptosis through the interaction with its receptor CD27 (Diegmann *et al.,* 2006). It was found that blocking CD27 and CD70 partially reduced lymphocyte apoptosis within the TME. Given that CD200R expression is also observed on T cells, it would be interesting to analyse whether CD200:CD200R signalling also leads to T cell apoptosis. This may also provide insight into the reduced frequencies of both CD4+ and CD8+ T cells we observed in our more intense CD200-expressing samples.

In conclusion, our identification of CD200 expression in RCC represents a possible novel therapeutic target, with our results highlighting the possibility that targeting CD200 may be of therapeutic benefit for patients with RCC. We have demonstrated that CD200 is expressed by RCC and in cell culture assays, blocking this ligand enhances NK cell activity towards the RCC target. Our results suggest that blocking CD200 may increase cytotoxicity of NK cells and result in increased tumour cell killing. Targeting CD200 may also influence the tumour immune infiltrate, either by enhancing recruitment of TILs or by preventing the apoptosis of TILs already in the tumour bed. Taken together, our data provide evidence for NK cell suppression mediated by CD200 expression on RCC tumours. Whilst our *in vitro* analysis suggests a negative on cytotoxic activity, our immunofluorescence analysis suggests that tumour CD200 expression is associated with a better prognosis due to an associated reduction in tumour infiltrating immune cells. Whilst it is possible that therapeutically blocking CD200 may induce a higher immune infiltrate that is characteristic of a worse prognosis, it may also enable the immune cells that are in the tumour bed to detect the tumour cells as the inhibitory signal is removed.

Further study is required to fully characterise the effect of CD200 expression in RCC and to determine whether anti-CD200 therapy is a safe and viable approach for patients with RCC. As CD200 is expressed on normal healthy tissue, including the kidney, adverse immune reactions may occur. Results from the first-in-human study of the novel recombinant humanised monoclonal antibody targeting CD200, Samalizumab, have demonstrated some positive results for patients with CLL and have shown limited immune related adverse events (Mahadevan *et al.,* 2019). If anti-CD200 antibody therapies are found to be viable, similar trials in RCC patients could be explored.

7.2 Future Directions

Future analysis would be to validate our immunohistological analysis of human samples, by analysing both CD200 expression and immune phenotype in another cohort. We observed a trend of decreasing NK cell frequency and density as CD200 expression increased, which became significant upon removing outliers. Increasing sample size would increase the power of this analysis and determine whether RCC expression of CD200 does indeed impact NK cell infiltrate. We have already acquired funding as part of an ASTRA grant to access additional samples from the Welsh Cancer Bank for this purpose (WCB Application 19/002).

In addition to analysing the presence of NK cells, it would be interesting to analyse the expression of the CD200R on these NK cells. We have shown that CD200 ligand binding induces apoptosis to CD200R+ NK cells. Analysis of CD200R would identify whether there was a depletion in NK cells that express this receptor. This could be done in conjunction with analysis of whether the sCD200 shed from our RCC cell lines induce apoptosis of NK92MI cells in a similar manner as the sCD200 chimera peptide used in the experiments. This would reveal a possible mechanism by which CD200 inhibits and causes the death of NK cell both in close proximity to the tumour and those that are further afield. This finding may be applicable to other CD200 expressing cancer types.

Appendices

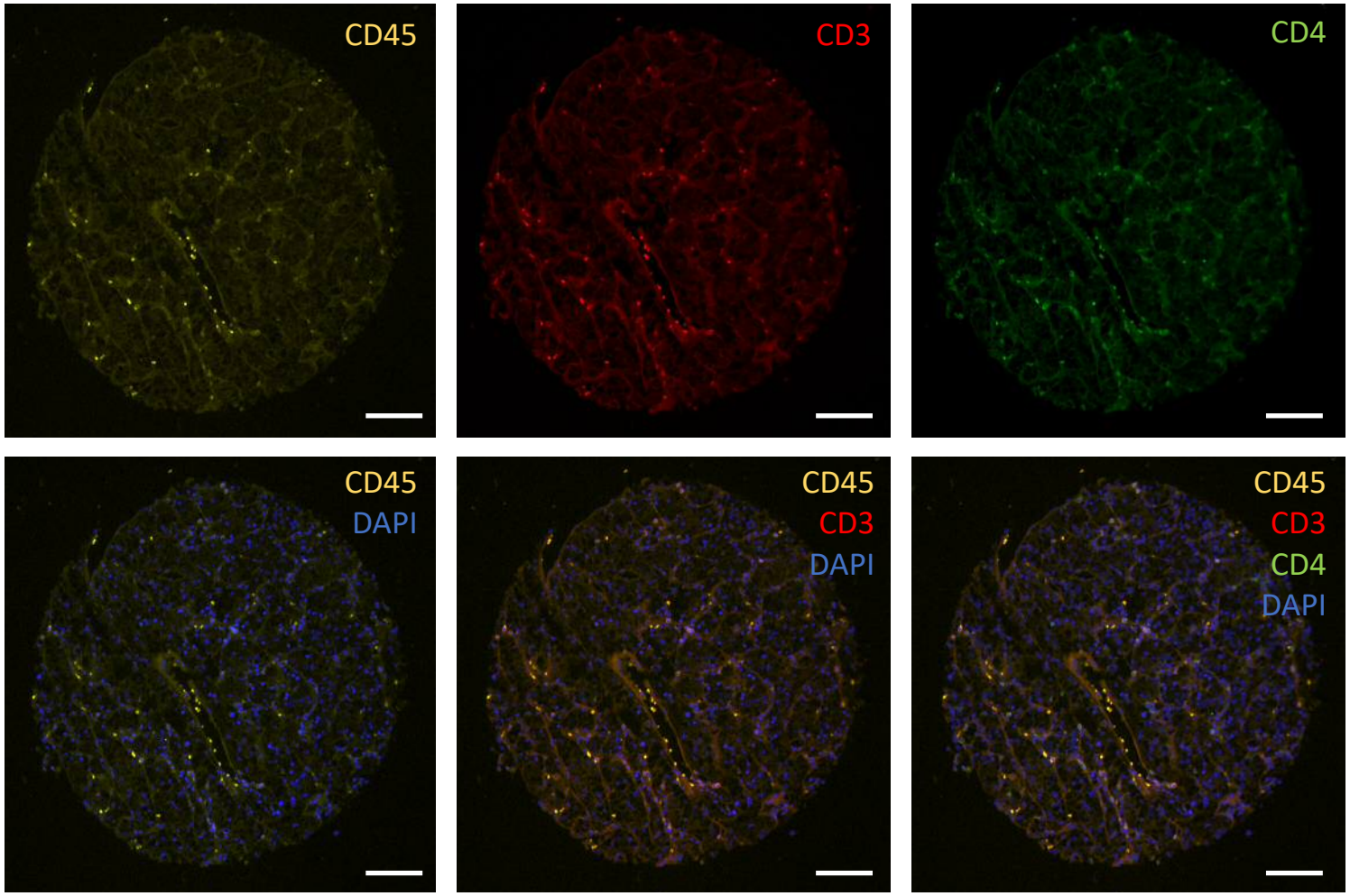

Appendix; Figure 1: Representative immunofluorescence staining for T helper cells. Human RCC sections were labelled by immunofluorescence for CD45, CD3, CD4 and stained with DAPI. Scale bar represents 100 µm.

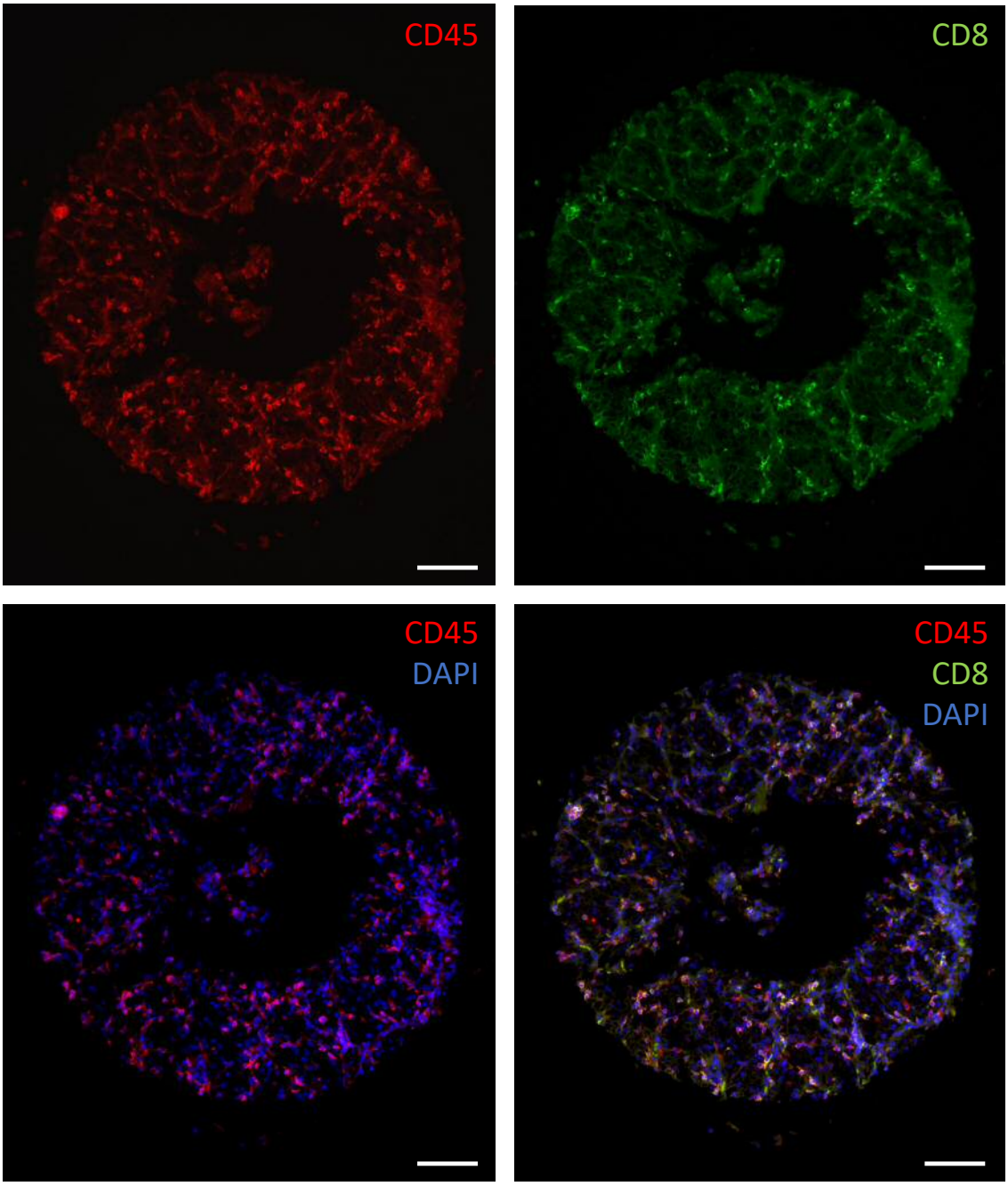

Appendix; Figure 2: Representative immunofluorescence staining for cytotoxic T cells. Human RCC sections were labelled by immunofluorescence for CD45, CD8 and stained with DAPI. Scale bar represents 100 µm.

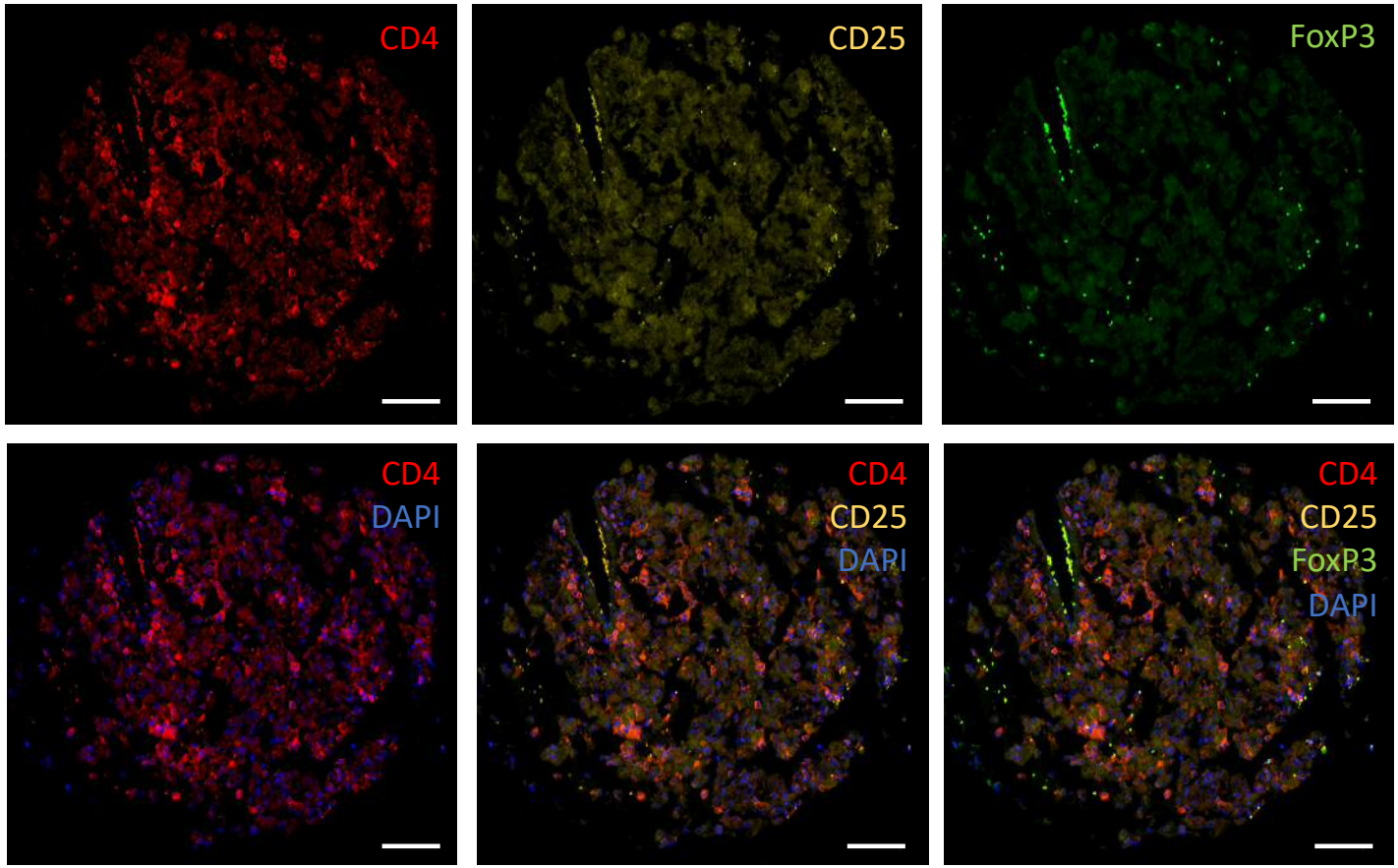

Appendix; Figure 3: Representative immunofluorescence staining for Treg cells. Human RCC sections were labelled by immunofluorescence for CD4, CD25, FoxP3 and stained with DAPI. Scale bar represents 100 µm.

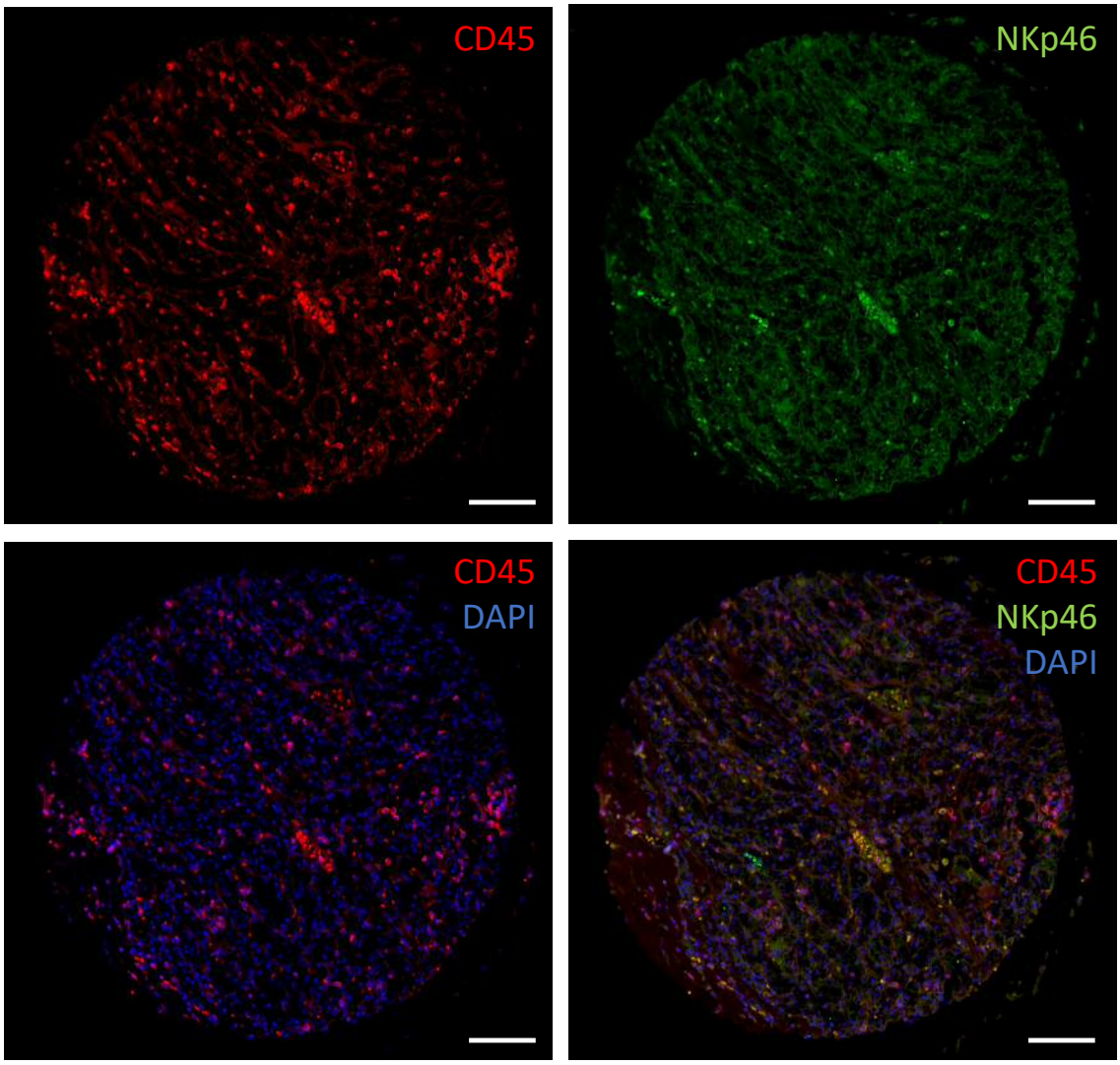

Appendix; Figure 4: Representative immunofluorescence staining for NK cells. Human RCC sections were labelled by immunofluorescence for CD45, NKp46 and stained with DAPI. Scale bar represents 100 µm.

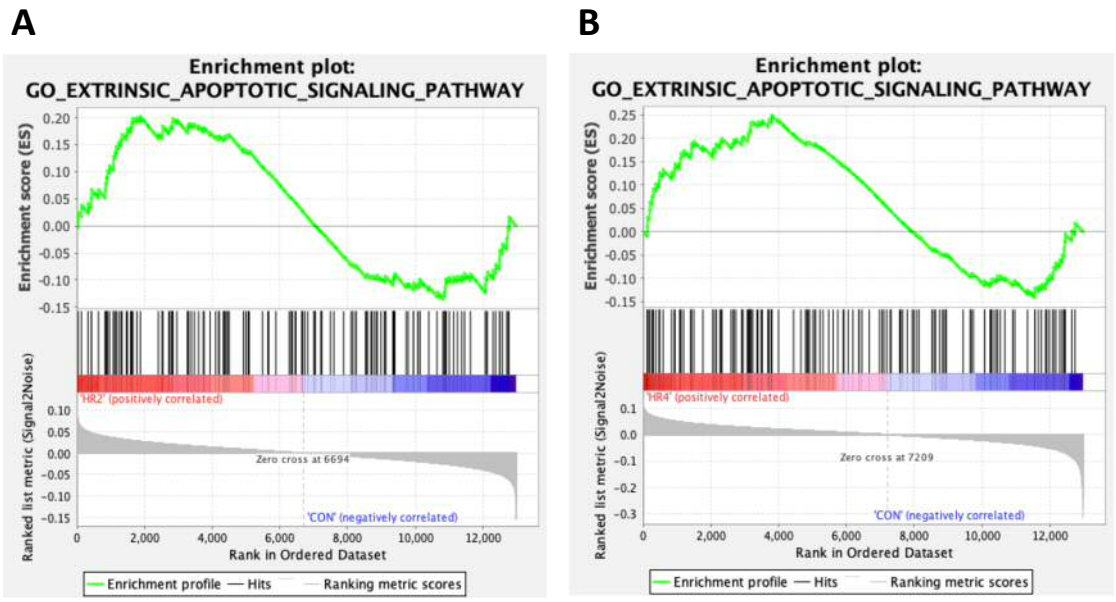

Appendix; Figure 5: Extrinsic pathway enrichment in CD200 treated N92MI cells. GSEA reveals enrichment of the Gene Ontology "Extrinsic apoptotic signalling pathway" gene set in both the 2- (A) and 4- (B) hour treated NK92MI cells when compared to untreated cells. Enrichment and nominal-P value for 2- and 4- hour CD200 treatment of NK cells: ES=0.20, p=0.52 and ES=0.25, p=0.084, respectively.

References

Abel AM, Yang C, Thakar MS, Malarkannan S. (2018) Natural Killer Cells: Development, Maturation, and Clinical Utilization. *Frontiers in Immunology*. **9**: 1869

Adams KF, Leitzmann MF, Albanes D, Kipnis V, Moore SC, Schatzkin A, Chow WH. (2008) Body size and renal cell cancer incidence in a large US cohort study. *American Journal of Epidemiology*. **168**(3): 268-77

Alamara C, Karapanagiotou EM, Tourkantonis I, Xyla V, Maurer CC, Lykourinas M, Pandha H, Syrigos KN. (2008) Renal oncocytoma: A case report and short review of the literature. *European Journal of Internal Medicine*. **19**: e67–9

Almishri W, Santodomingo-Garzon T, Le T, Stack D, Mody CH, Swain MG. (2016) TNFα Augments Cytokine-Induced NK Cell IFNγ Production through TNFR2. *Journal of Innate Immunity*. **8**(6): 617-29

Alsaab HO, Sau S, Alzhrani R, Tatiparti K, Bhise K, Kashaw SK, Iyer AK. (2017) PD-1 and PD-L1 Checkpoint Signaling Inhibition for Cancer Immunotherapy: Mechanism, Combinations, and Clinical Outcome. *Frontiers in Pharmacology*. **8**: 561

Amin A, Plimack ER, Ernstoff MS, Lewis LD, Bauer TM, McDermott DF, Carducci M, Kollmannsberger C, Rini BI, Heng DYC, Knox J, Voss MH, Spratlin J, Berghorn E, Yang L, Hammers HJ. (2018) Safety and efficacy of nivolumab in combination with sunitinib or pazopanib in advanced or metastatic renal cell carcinoma: the CheckMate 016 study. *Journal for Immunotherapy of Cancer*. **6**(1): 109

Asada N, Takeishi S, Frenette PS. (2017) Complexity of bone marrow hematopoietic stem cell niche. *International Journal of Hematology.* **106**(1): 45-54

Balkwill FR, Capasso M, Hagemann T. (2012) The tumor microenvironment at a glance. *Journal of Cell Science*. **125**(Pt 23): 5591-6

Ball MW. (2017) Surgical management of metastatic renal cell carcinoma. *Discovery Medicine*. **23**(129): 379-87

Barclay AN and Ward HA. (1982) Purification and chemical characterisation of membrane glycoproteins from rat thymocytes and brain, recognised by monoclonal antibody MRC OX 2. *European Journal of Biochemistry*. **129**(2): 447-58

Barrow AD, Martin CJ, Colonna M. (2019) The Natural Cytotoxicity Receptors in Health and Disease. *Frontiers in Immunology*. **10**: 909

Bazhin AV, von Ahn K, Fritz J, Werner J, Karakhanova S. (2018) Interferon-α Up-Regulates the Expression of PD-L1 Molecules on Immune Cells Through STAT3 and p38 Signaling. *Frontiers in Immunology*. **9**: 2129

Bellone G, Aste-Amezaga M, Trinchieri G, Rodeck U. (1995) Regulation of NK cell functions by TGF-beta 1. *Journal of Immunology*. **155**(3): 1066-73

Bhome R, Bullock MD, Al Saihati HA, Goh RW, Primrose JN, Sayan AE, Mirnezami AH. (2015) A top-down view of the tumor microenvironment: structure, cells and signaling. *Frontiers in Cell and Developmental Biology*. **3**: 33

Blank CU, Haining WN, Held W, Hogan PG, Kallies A, Lugli E, Lynn RC, Philip M, Rao A, Restifo NP, Schietinger A, Schumacher TN, Schwartzberg PL, Sharpe AH, Speiser DE, Wherry EJ, Youngblood BA, Zehn D. (2019) Defining 'T cell exhaustion'. *Nature Reviews. Immunology*. **19**(11): 665-74

Borriello F, Iannone R, Marone G. (2017) Histamine Release from Mast Cells and Basophils. *Handbook of Experimental Pharmacology*. **241**: 121-39

Borriello F, Lederer J, Scott S, Sharpe AH. (1997) MRC OX-2 defines a novel T cell costimulatory pathway. *Journal of Immunology*. **158**(10): 4548-54

Bossi G and Griffiths GM. (1999). Degranulation plays an essential part in regulating cell surface expression of Fas ligand in T cells and natural killer cells. *Nature Medicine*. **5**(1): 90-6

Boudakov I, Liu J, Fan N, Gulay P, Wong K, Gorczynski RM. (2007) Mice lacking CD200R1 show absence of suppression of lipopolysaccharide-induced tumor necrosis factor-alpha and mixed leukocyte culture responses by CD200. *Transplantation*. **84**(2): 251-7

Brahmer JR, Drake CG, Wollner I, Powderly JD, Picus J, Sharfman WH, Stankevich E, Pons A, Salay TM, McMiller TL, Gilson MM, Wang C, Selby M, Taube JM, Anders R, Chen L, Korman AJ, Pardoll DM, Lowy I, Topalian SL. (2010) Phase I study of single-agent anti-programmed death-1 (MDX-1106) in refractory solid tumors: safety, clinical activity, pharmacodynamics, and immunologic correlates. *Journal of Clinical Oncology*. **28**(19): 3167-75

Brierley J, Gospodarowicz M, O'Sullivan B. (2016) The principles of cancer staging. *Ecancermedicalscience*. **10**: ed61

Brillantes M and Beaulieu AM. (2019) Transcriptional control of natural killer cell differentiation. *Immunology*. **156**(2): 111-9

Brugarolas J. (2014) Molecular Genetics of Clear-Cell Renal Cell Carcinoma. *Journal of Clinical Oncology*. **32**(18): 1968-76

Burkhardt JK, Hester S, Lapham CK, Argon Y. (1990) The lytic granules of natural killer cells are dual-function organelles combining secretory and pre-lysosomal compartments. *The Journal of Cell Biology*. **111**(6 Pt 1): 2327-40

Burnet M. (1957) Cancer—A Biological Approach. *British Medical Journal*. **1**(5022): 779-86

Büscheck F, Fraune C, Simon R, Kluth M, Hube-Magg C, Möller-Koop C, Sarper I, Ketterer K, Henke T, Eichelberg C, Dahlem R, Wilczak W, Sauter G, Fisch M, Eichenauer T, Rink M. (2020) Prevalence and clinical significance of VHL mutations and 3p25 deletions in renal tumor subtypes. *Oncotarget*. **11**(3): 237-49

Carson WE, Giri JG, Lindemann MJ, Linett ML, Ahdieh M, Paxton R, Anderson D, Eisenmann J, Grabstein K, Caligiuri MA. (1994) Interleukin (IL) 15 is a novel cytokine that activates human natural killer cells via components of the IL-2 receptor. *The Journal of Experimental Medicine.* **180**(4): 1395-403.

Cairns P. (2011) Renal Cell Carcinoma. *Cancer Biomarkers*. **9**(1-6): 461-73

Calle EE and Kaaks R. (2004) Overweight, obesity and cancer: epidemiological evidence and proposed mechanisms. *Nature Reviews. Cancer*. **4**(8): 579-91

Capitanio U, Bensalah K, Bex A, Boorjian SA, Bray F, Coleman J, Gore JL, Sun M, Wood C, Russo P. (2019). Epidemiology of Renal Cell Carcinoma. *European Urology*. **75**(1): 74-84

Capitanio U and Montorsi F. (2016) Renal Cancer. *Lancet*. **387**(10021): 894-906

Carrelha J, Meng Y, Kettyle LM, Luis TC, Norfo R, Alcolea V, Boukarabila H, Grasso F, Gambardella A, Grover A, Högstrand K, Lord AM, Sanjuan-Pla A, Woll PS, Nerlov C, Jacobsen SEW. (2018) Hierarchically related lineage-restricted fates of multipotent haematopoietic stem cells. *Nature*. **554**(7690):106-11

Casey TM, Meade JL, Hewitt EW. (2007) Organelle proteomics: identification of the exocytic machinery associated with the natural killer cell secretory lysosome. *Molecular and Cellular Proteomics*. **6**(5): 767-80

Chaplin DD. (2010) Overview of the Immune Response. *The Journal of Allergy and Clinical Immunology.* **125**(2 Suppl 2): S3-23

Chen DS and Mellman I. (2013) Oncology meets immunology: the cancer-immunity cycle. *Immunity*. **39**(1): 1-10

Chen DS and Mellman I. (2017) Elements of cancer immunity and the cancer-immune set point. *Nature*. **541**(7637): 321-30

Chen F, Zhang Y, Şenbabaoğlu Y, Ciriello G, Yang L, Reznik E, Shuch B, Micevic G, De Velasco G, Shinbrot E, Noble MS, Lu Y, Covington KR, Xi L, Drummond JA, Muzny D, Kang H, Lee J, Tamboli P, Reuter V, Shelley CS, Kaipparettu BA, Bottaro DP, Godwin AK, Gibbs RA, Getz G, Kucherlapati R, Park PJ, Sander C, Henske EP, Zhou JH, Kwiatkowski DJ, Ho TH, Choueiri TK, Hsieh JJ, Akbani R, Mills GB, Hakimi AA, Wheeler DA, Creighton CJ. (2016) Multilevel Genomics-Based Taxonomy of Renal Cell Carcinoma. *Cell Reports*. **14**(10): 2476-89

Chen L and Flies DB. (2013) Molecular mechanisms of T cell co-stimulation and co-inhibition. *Nature Reviews Immunology*. **13**(4): 227-42

Chen W, Jin W, Wahl SM. (1998) Engagement of cytotoxic T lymphocyte-associated antigen 4 (CTLA-4) induces transforming growth factor beta (TGF-beta) production by murine CD4(+) T cells. *The Journal of Experimental Medicine*. **188**(10): 1849-57

Chen X, Allan DSJ, Krzewski K, Ge B, Kopcow H, Strominger JL. (2006) CD28-stimulated ERK2 phosphorylation is required for polarization of the microtubule organizing center and granules in YTS NK cells. *Proceedings of the National Academy of Sciences of the USA.* **103**(27): 10346-51

Chen Z, Chen DX, Kai Y, Khatri I, Lamptey B, Gorczynski RM. (2008) Identification of an expressed truncated form of CD200, CD200tr, which is a physiologic antagonist of CD200-induced suppression. *Transplantation*. **86**(8): 1116-24

Cheng H, Zheng Z, Cheng T. (2020) New paradigms on hematopoietic stem cell differentiation. *Protein & Cell*. **11**(1): 34-44

Chin AI, Lam JS, Figlin RA, Belldegrun AS. (2006) *Reviews in Urology*. **8**(1): 1-7

Chiu YM, Tsai CL, Kao JT, Hsieh CT, Shieh DC, Lee YJ, Tsay GJ, Cheng KS, Wu YY. (2018) PD-1 and PD-L1 Up-regulation Promotes T-cell Apoptosis in Gastric Adenocarcinoma. *Anticancer Research.* **38**(4): 2069-78

Choueiri TK and Motzer RJ. (2017) Systemic Therapy for Metastatic Renal-Cell Carcinoma. *The New England Journal of Medicine*. **376**(4): 354-66

Chow MT and Luster AD. (2014) Chemokines in cancer. *Cancer Immunology Research*. **2**(12): 1125-31

Clark RH, Stinchcombe JC, Day A, Blott E, Booth S, Bossi G, Hamblin T, Davies EG, Griffiths GM. (2003) Adaptor protein 3-dependent microtubule-mediated movement of lytic granules to the immunological synapse. *Nature Immunology*. **4**(11): 1111-20

Coles SJ, Hills RK, Wang EC, Burnett AK, Man S, Darley RL, Tonks A. (2012) Expression of CD200 on AML blasts directly suppresses memory T-cell function. *Leukemia*. **26**(9): 2148-51

Coles SJ, Hills RK, Wang EC, Burnett AK, Man S, Darley RL, Tonks A. (2012) Increased CD200 expression in acute myeloid leukemia is linked with an increased frequency of FoxP3+ regulatory T cells. *Leukemia*. **26**(9): 2146-8

Coles SJ, Wang EC, Man S, Hills RK, Burnett AK, Tonks A, Darley RL. (2011) CD200 expression suppresses natural killer cell function and directly inhibits patient anti-tumor response in acute myeloid leukemia. *Leukemia*. **25**(5): 792-9

Collin M and Bigley V. (2018) Human dendritic cell subsets: an update. *Immunology*. **154**(1): 3-20

Colmont CS, Benketah A, Reed SH, Hawk NV, Telford WG, Ohyama M, Udey MC, Yee CL, Vogel JC, Patel GK. (2013) CD200-expressing human basal cell carcinoma cells initiate tumor growth. *Proceedings of the National Academy of Sciences of the United States of America*. **110**(4): 1434-9

Cooper MA, Fehniger TA, Caligiuri MA. (2001) The biology of human natural killer-cell subsets. *Trends in Immunology*. **22**(11): 633-40

Corthay A. (2009) How do Regulatory T Cells Work? *Scandinavian Journal of Immunology*. **70**(4): 326-36

Creighton C, Morgan M, Gunaratne P et al. (2013) Comprehensive molecular characterization of clear cell renal cell carcinoma. *Nature*. **499**: 43-9

Damiani D, Tiribelli M, Raspadori D, Sirianni S, Meneghel A, Cavalllin M, Michelutti A, Toffoletti E, Geromin A, Simeone E, Bocchia M, Fanin R. (2015) Clinical impact of CD200 expression in patients with acute myeloid leukemia and correlation with other molecular prognostic factors. *Oncotarget*. **6**(30): 30212-21

Dias S, Silva H Jr, Cumano A, Vieira P. (2005) Interleukin-7 is necessary to maintain the B cell potential in common lymphoid progenitors. *The Journal of Experimental Medicine*. **201**(6): 971-9

di Bari MG, Lutsiak ME, Takai S, Mostböck S, Farsaci B, Semnani RT, Wakefield LM, Schlom J, Sabzevari H. (2009) TGF-beta modulates the functionality of tumor-infiltrating CD8+ T cells through effects on TCR signaling and Spred1 expression. *Cancer Immunology, Immunotherapy*. **58**(11): 1809-18

Diegmann J, Junker K, Loncarevic IF, Michel S, Schimmel B, von Eggeling F. (2006) Immune escape for renal cell carcinoma: CD70 mediates apoptosis in lymphocytes. *Neoplasia*. **8**(11): 933-8

Donskov F and von der Maase H. (2006) Impact of immune parameters on long-term survival in metastatic renal cell carcinoma. *Journal of Clinical Oncology*. **24**(13): 1997-2005

Dorfman DM and Shahsafaei A. (2010) CD200 (OX-2 membrane glycoprotein) expression in b cell-derived neoplasms. *American Journal of Clinical Pathology*. **134**(5): 726-33

Drake CG, Jaffee E, Pardoll DM. (2006) Mechanisms of immune evasion by tumors. *Advances in Immunology.* **90**: 51-81

Dudley EC, Girardi M, Owen MJ, Hayday AC. (1995) Alpha beta and gamma delta T cells can share a late common precursor. *Current Biology*. **5**(6): 659-69

Dunn GP, Bruce AT, Ikeda H, Old LJ, Schreiber RD. (2002) Cancer immunoediting: from immunosurveillance to tumor escape. *Nature Immunology*. **3**(11): 991-8

Dunn GP, Old LJ, Schreiber RD. (2004) The three Es of cancer immunoediting. *Annual Reviews of Immunology*. **22**: 329-60

Ebdon C, Batty P, Smith G. (2013) Haematopoiesis and red blood cells. *Surgery*. **31**(5): 200-5

Ehrlich P. (1909) Ueber den jetzigen Stand der Karzinomforschung. *Nederlands Tijdschrift voor Geneeskunde*. **5**: 273-90

Erin N, Podnos A, Tanriover G, Duymuş Ö, Cote E, Khatri I, Gorczynski RM. (2015) Bidirectional effect of CD200 on breast cancer development and metastasis, with ultimate outcome determined by tumor aggressiveness and a cancer-induced inflammatory response. *Oncogene*. **34**(29): 3860-70

Ewen CL, Kane KP, Bleackley RC. (2012) A quarter century of granzymes. *Cell Death and Differentiation.* **19**(1): 28-35

Falschlehner C, Schaefer U, Walczak H. (2009) Following TRAIL's path in the immune system. *Immunology*. **127**(2): 145-54

Farber DL, Yudanin NA, Restifo NP. (2014) Human memory T cells: generation, compartmentalization and homeostasis. *Nature Reviews. Immunology*. **14**(1): 24-35

Fauriat C, Long EO, Ljunggren HG, Bryceson YT. (2010) Regulation of human NK-cell cytokine and chemokine production by target cell recognition. *Blood*. **115**(11): 2167-76

Feldmann J, Callebaut I, Raposo G, Certain S, Bacq D, Dumont C, Lambert N, Ouachée-Chardin M, Chedeville G, Tamary H, Minard-Colin V, Vilmer E, Blanche S, Le Deist F, Fischer A, de Saint Basile G. (2003) Munc13-4 is essential for cytolytic granules fusion and is mutated in a form of familial hemophagocytic lymphohistiocytosis (FHL3). *Cell*. **115**(4): 461-73

Fontana S, Parolini S, Vermi W, Booth S, Gallo F, Donini M, Benassi M, Gentili F, Ferrari D, Notarangelo LD, Cavadini P, Marcenaro E, Dusi S, Cassatella M, Facchetti F, Griffiths GM, Moretta A, Notarangelo LD, Badolato R. (2006) Innate immunity defects in Hermansky-Pudlak type 2 syndrome. *Blood*. **107**(12): 4857-64

Fosså S. (2000) Interferon in metastatic renal cell carcinoma. *Seminars in Oncology*. **27**(2): 187-93

Freud AG, Mundy-Bosse BL, Yu J, Caligiuri MA. (2017) The Broad Spectrum of Human Natural Killer Cell Diversity. *Immunity*. **47**(5): 820-33

Freud AG, Yu J, Caligiuri MA. (2014) Human natural killer cell development in secondary lymphoid tissues. *Seminars in Immunology*. **26**(2): 132-7

Gameiro J, Nagib P, Verinaud L. (2010) The thymus microenvironment in regulating thymocyte differentiation. *Cell Adhesion and Migration*. **4**(3): 382-90

Gatta L, Calviello G, Di Nicuolo F, Pace L, Ubaldi V, Doria G, Pioli C. (2002) Cytotoxic T lymphocyte-associated antigen-4 inhibits integrin-mediated stimulation. *Immunology.* **107**(2): 209-16

Geissler K, Fornara P, Lautenschläger C, Holzhausen HJ, Seliger B, Riemann D. (2015) Immune signature of tumor infiltrating immune cells in renal cancer. *Oncoimmunology.* **4**(1): e985082

Gerlinger M, Horswell S, Larkin J, Rowan AJ, Salm MP, Varela I, Fisher R, McGranahan N, Matthews N, Santos CR, Martinez P, Phillimore B, Begum S, Rabinowitz A, Spencer-Dene B, Gulati S, Bates PA, Stamp G, Pickering L, Gore M, Nicol DL, Hazell S, Futreal PA, Stewart A, Swanton C. (2014) Genomic architecture and evolution of clear cell renal cell carcinomas defined by multiregion sequencing. *Nature Genetics*. **46**(3): 225-33

Germain RN. (2002) T-cell development and the CD4–CD8 lineage decision. *Nature Reviews. Immunology*. **2**(5): 309-22

Ghahremanloo A, Soltani A, Modaresi SMS, Hashemy SI. (2019) Recent advances in the clinical development of immune checkpoint blockade therapy. Cellular Oncology. **42**(5): 609-26

Ghatalia P, Gordetsky J, Kuo F, Dulaimi E, Cai KQ, Devarajan K, Bae S, Naik G, Chan TA, Uzzo R, Hakimi AA, Sonpavde G, Plimack E. (2019) Prognostic impact of immune gene expression signature and tumor infiltrating immune cells in localized clear cell renal cell carcinoma. *Journal of Immunotherapy of Cancer*. **7**(1): 139

Gill D, Hahn AW, Sonpavde G, Agarwal N. (2016) Immunotherapy of advanced renal cell carcinoma: Current and future therapies. *Human Vaccines and Immunotherapeutics*. **12**(12): 2997-3004

Gismondi A, Cifaldi L, Mazza C, Giliani S, Parolini S, Morrone S, Jacobelli J, Bandiera E, Notarangelo L, Santoni A. (2004) Impaired natural and CD16-mediated NK cell cytotoxicity in patients with WAS and XLT: ability of IL-2 to correct NK cell functional defect. *Blood*. **104**(2): 436-43

Gnarra JR, Tory K, Weng Y, Schmidt L, Wei MH, Li H, Latif F, Liu S, Chen F, Duh FM. (1994) Mutations of the VHL tumour suppressor gene in renal carcinoma. *Nature Genetics*. **7**(1): 85-90

Gorczynski R. (2012) CD200:CD200R-Mediated Regulation of Immunity. *International Scholarly Research Notices Immunology.*

Gorczynski R, Chen Z, Kai Y, Lee L, Wong S, Marsden PA. (2004) CD200 is a ligand for all members of the CD200R family of immunoregulatory molecules. *Journal of Immunology*. **172**(12): 7744-9

Gorczynski RM, Chen Z, Diao J, Khatri I, Wong K, Yu K, Behnke J. (2010) Breast cancer cell CD200 expression regulates immune response to EMT6 tumor cells in mice. *Breast Cancer Research and Treatment*. **123**(2): 405-15

Gorczynski RM, Chen Z, Hu J, Kai Y, Lei J. (2001) Evidence of a role for CD200 in regulation of immune rejection of leukaemic tumour cells in C57BL/6 mice. *Clinical and Experimental Biology*. **126**(2): 220-9

Gorczynski RM, Chen Z, Yu K, Hu J. (2001) CD200 immunoadhesin suppresses collagen-induced arthritis in mice. *Clinical Immunology*. **101**(3): 328-34

Gorris MAJ, Halilovic A, Rabold K, van Duffelen A, Wickramasinghe IN, Verweij D, Wortel IMN, Textor JC, de Vries IJM, Figdor CG. (2018) Eight-Color Multiplex Immunohistochemistry for Simultaneous Detection of Multiple Immune Checkpoint Molecules within the Tumor Microenvironment. *Journal of Immunology*. **200**(1): 347-54

Griffiths RW, Elkord E, Gilham DE, Ramani V, Clarke N, Stern PL, Hawkins RE. (2007) Frequency of regulatory T cells in renal cell carcinoma patients and investigation of correlation with survival. *Cancer Immunology, Immunotherapy*. **56**(11): 1743-53

Gu D, Ao X, Yang Y, Chen Z, Xu X. (2018) Soluble immune checkpoints in cancer: production, function and biological significance. *Journal for Immunotherapy of Cancer*. **6**(1): 132

Guicciardi ME and Gores GJ (2009). Life and death by death receptors. *FASEB journal*. **23**(6): 1625-37

Halfteck GG, Elboim M, Gur C, Achdout H, Ghadially H, Mandelboim O. (2009) Enhanced in vivo growth of lymphoma tumors in the absence of the NK-activating receptor NKp46/NCR1. *Journal of Immunology*. **182**(4): 2221-30

Hammers H, Plimack ER, Infante JR, Ernstoff M, Rini BI, McDermott DF, Razak A, Pal SK, Voss M, Sharma P, Kollmannsberger CK, Heng D, Shen Y, Kurland J, Spratlin J, Gagnier P, Amin A. (2014) Phase I study of nivolumab in combination with ipilimumab in metastatic renal cell carcinoma (mRCC). *Journal of Clinical Oncology*. **32**(Suppl. 15): 4504

Hanahan D and Weinberg RA. (2000) The hallmarks of cancer. *Cell.* **100**(1): 57-70

Hanahan D and Weinberg RA. (2011) Hallmarks of cancer: the next generation. *Cell.* **144**(5): 646-74

Hatherley D, Cherwinski HM, Moshref M, Barclay AN. (2005) Recombinant CD200 protein does not bind activating proteins closely related to CD200 receptor. *Journal of Immunology*. **175**(4): 2469-74

Hehlgans T and Pfeffer K. (2005) The intriguing biology of the tumour necrosis factor/tumour necrosis factor receptor superfamily: players, rules and the games. *Immunology*. **115**(1): 1-20

Heufler C, Koch F, Stanzl U, Topar G, Wysocka M, Trinchieri G, Enk A, Steinman RM, Romani N, Schuler G. (1996) Interleukin-12 is produced by dendritic cells and mediates T helper 1 development as well as interferon-gamma production by T helper 1 cells. *European Journal of Immunology*. **26**(3): 659-68

Hodi FS, O'Day SJ, McDermott DF, Weber RW, Sosman JA, Haanen JB, Gonzalez R, Robert C, Schadendorf D, Hassel JC, Akerley W, van den Eertwegh AJ, Lutzky J, Lorigan P, Vaubel JM, Linette GP, Hogg D, Ottensmeier CH, Lebbé C, Peschel C, Quirt I, Clark JI, Wolchok JD, Weber JS, Tian J, Yellin MJ, Nichol GM, Hoos A, Urba WJ. (2010) Improved survival with ipilimumab in patients with metastatic melanoma. *The new England Journal of Medicine*. **363**(8): 711-23

Hoek RM, Ruuls SR, Murphy CA, Wright GJ, Goddard R, Zurawski SM, Blom B, Homola ME, Streit WJ, Brown MH, Barclay AN, Sedgwick JD. (2000) Down-regulation of the macrophage lineage through interaction with OX2 (CD200). *Science*. **290**(5497): 1768-71

Karamitros D, Stoilova B, Aboukhalil Z, Hamey F, Reinisch A, Samitsch M, Quek L, Otto G, Repapi E, Doondeea J, Usukhbayar B, Calvo J, Taylor S, Goardon N, Six E, Pflumio F, Porcher C, Majeti R, Göttgens B, Vyas P. (2018) Single-cell analysis reveals the continuum of human lympho-myeloid progenitor cells. *Nature Immunology*. **19**(1): 85-97

Kolbeck PC, Kaveggia FF, Johansson SL, Grune MT, Taylor RJ. (1992) The relationships among tumor-infiltrating lymphocytes, histopathologic findings, and long-term clinical follow-up in renal cell carcinoma. *Modern Pathology*. **5**(4): 420-5

Hong CW. (2017) Current Understanding in Neutrophil Differentiation and Heterogeneity. *Immune Network*. **17**(5): 298–306

Hohlbaum AM, Moe S, Marshak-Rothstein A. (2000) Opposing effects of transmembrane and soluble Fas ligand expression on inflammation and tumor cell survival. *The Journal of Experimental Medicine*. **191**(7): 1209-20

Hsieh JJ, Purdue MP, Signoretti S, Swanton C, Albiges L, Schmidinger M, Heng DY, Larkin J, Ficarra V. (2017) Renal cell carcinoma. *Nature Reviews. Disease Primers*. **3**: 17009

Hunt JD, van der Hel OL, McMillan GP, Boffetta P, Brennan P. (2005) Renal cell carcinoma in relation to cigarette smoking: meta-analysis of 24 studies. International Journal of Cancer. 114(1): 101-8

Isakov N (1997) Immunoreceptor tyrosine-based activation motif (ITAM), a unique module linking antigen and Fc receptors to their signaling cascades. *Journal of Leukocyte Biology*. **61**(1): 6-16

Jacobs R, Hintzen G, Kemper A, Beul K, Kempf S, Behrens G, Sykora KW, Schmidt RE. (2001) CD56bright cells differ in their KIR repertoire and cytotoxic features from CD56dim NK cells. *European Journal of Immunology*. **31**(10): 3121-7

Jahn R and Scheller RH. (2006) SNAREs--engines for membrane fusion. *Nature reviews. Molecular Cell Biology*. **7**(9): 631-43

Kaiko GE, Horvat JC, Beagley KW, Hansbro PM. (2008) Immunological decision-making: how does the immune system decide to mount a helper T-cell response? *Immunology*. **123**(3): 326-38

Kamei DT, Lao BJ, Ricci MS, Deshpande R, Xu H, Tidor B, Lauffenburger DA. (2005) Quantitative methods for developing Fc mutants with extended half-lives. *Biotechnology and Bioengineering*. **92**(6): 748-60

Kapur P, Peña-Llopis S, Christie A, Zhrebker L, Pavía-Jiménez A, Rathmell WK, Xie XJ, Brugarolas J. (2013) Effects on survival of BAP1 and PBRM1 mutations in sporadic clear-cell renal-cell carcinoma: a retrospective analysis with independent validation. *The Lancet. Oncology*. **14**(2): 159-67

Kawasaki BT and Farrar WL. (2008) Cancer stem cells, CD200 and immunoevasion. *Trends in Immunology.* **29**(10): 464-8

Kawashima A, Kanazawa T, Kidani Y, Yoshida T, Hirata M, Nishida K, Nojima S, Yamamoto Y, Kato T, Hatano K, Ujike T, Nagahara A, Fujita K, Morimoto-Okazawa A, Iwahori K, Uemura M, Imamura R, Ohkura N, Morii E, Sakaguchi S, Wada H, Nonomura N. (2020) Tumour grade significantly correlates with total dysfunction of tumour tissue-infiltrating lymphocytes in renal cell carcinoma. *Scientific Reports*. **10**(1): 6220

Kibel A, Iliopoulos O, DeCaprio JA, Kaelin WG Jr. (1995) Binding of the von Hippel-Lindau tumor suppressor protein to Elongin B and C. *Science*. **269**(5229): 1444-6

Kim CH, Rott L, Kunkel EJ, Genovese MC, Andrew DP, Wu L, Butcher EC. (2001) Rules of chemokine receptor association with T cell polarization in vivo. *The Journal of Clinical Investigation*. **108**(9): 1331-9

Kim E and Zschiedrich S. (2018) Renal Cell Carcinoma in von Hippel–Lindau Disease—From Tumor Genetics to Novel Therapeutic Strategies. *Frontiers in Pediatrics*. **6**: 16

Kim KH, You D, Jeong IG, Kwon TW, Cho YM, Hong JH, Ahn H, Kim CS. (2012) Type II papillary histology predicts poor outcome in patients with renal cell carcinoma and vena cava thrombus. *BJU International*. **110**(11 Pt B): E673-8

Kondo M. (2010) Lymphoid and myeloid lineage commitment in multipotent hematopoietic progenitors. *Immunological Reviews*. **238**(1): 37-46

Kopcow HD, Allan DS, Chen X, Rybalov B, Andzelm MM, Ge B, Strominger JL. (2005) Human decidual NK cells form immature activating synapses and are not cytotoxic. *Proceedings of the National Academy of Sciences of the USA.* **102**(43): 15563-8

Kretz-Rommel A, Qin F, Dakappagari N, Ravey EP, McWhirter J, Oltean D, Frederickson S, Maruyama T, Wild MA, Nolan MJ, Wu D, Springhorn J, Bowdish KS. (2007) *Journal of Immunology*. **178**(9): 5595-605

Krzewski K, Chen X, Orange JS, Strominger JL. (2006) Formation of a WIP-, WASp-, actin-, and myosin IIA-containing multiprotein complex in activated NK cells and its alteration by KIR inhibitory signaling. *The Journal of Cell Biology*. **173**(1): 121-32

Krzewski K1 and Coligan JE. (2012) Human NK cell lytic granules and regulation of their exocytosis. *Frontiers in Immunology*. **3**: 335

Lanier LL. (2008) Up on the tightrope: natural killer cell activation and inhibition. *Nature Immunology*. **9**(5): 495-502

Larsen SK, Gao Y, Basse PH. (2014) NK cells in the tumor microenvironment. *Critical Reviews in Oncogenesis*. **19**(1-2): 91-105

Li L, Tian Y, Shi C, Zhang H, Zhou Z. (2016) Over-Expression of CD200 Predicts Poor Prognosis in Cutaneous Squamous Cell Carcinoma. *Medical Science Monitor*. **22**: 1079-84.

Lin A and Loré K. (2017) Granulocytes: New Members of the Antigen-Presenting Cell Family. *Frontiers in Immunology*. **8**: 1781

Linehan WM, Pinto PA, Srinivasan R, Merino M, Choyke P, Choyke L, Coleman J, Toro J, Glenn G, Vocke C, Zbar B, Schmidt LS, Bottaro D, Neckers L. (2007) Identification of the genes for kidney cancer: opportunity for disease-specific targeted therapeutics. *Clinical Cancer Research*. **13**(2 Pt 2): 671s-79s

Linehan WM, Spellman PT, Ricketts CJ et al. (2016) Comprehensive molecular characterization of papillary renal cell carcinoma. *New England Journal of Medicine*. **374**(2): 135-45

Linsley PS, Bradshaw J, Greene J, Peach R, Bennett KL, Mittler RS. (1996) Intracellular trafficking of CTLA-4 and focal localization towards sites of TCR engagement. *Immunity*. **4**(6): 535-43

Liotta F, Gacci M, Frosali F, Querci V, Vittori G, Lapini A, Santarlasci V, Serni S, Cosmi L, Maggi L, Angeli R, Mazzinghi B, Romagnani P, Maggi E, Carini M, Romagnani S, Annunziato F. (2011) Frequency of regulatory T cells in peripheral blood and in

tumour-infiltrating lymphocytes correlates with poor prognosis in renal cell carcinoma. *BJU International.* **107**(9): 1500-6

Lipson EJ and Drake CG. (2011) Ipilimumab: An Anti-CTLA-4 Antibody for Metastatic Melanoma. *Clinical Cancer Research*. **17**(22): 6958-62

Liu JY, Li F, Wang LP, Chen XF, Wang D, Cao L, Ping Y, Zhao S, Li B, Thorne SH, Zhang B, Kalinski P, Zhang Y. (2015) CTL- vs Treg lymphocyte-attracting chemokines, CCL4 and CCL20, are strong reciprocal predictive markers for survival of patients with oesophageal squamous cell carcinoma. *British Journal of Cancer*. **113**(5): 747-55

Lorenzo-Herrero S, Sordo-Bahamonde C, Gonzalez S, López-Soto A. (2019) CD107a Degranulation Assay to Evaluate Immune Cell Antitumor Activity. *Methods in Molecular Biology*. **1884**: 119-30

Love JE, Thompson K, Kilgore MR, Westerhoff M, Murphy CE, Papanicolau-Sengos A, McCormick KA, Shankaran V, Vandeven N, Miller F, Blom A, Nghiem PT, Kussick SJ. (2017) CD200 Expression in Neuroendocrine Neoplasms. *American Journal of Clinical Pathology*. **148**(3): 236-42

Low G, Huang G, Fu W, Moloo Z, Girgis S. (2016) Review of renal cell carcinoma and its common subtypes in radiology. *World Journal of Radiology*. **8**(5): 484-500

Lynch DH, Ramsdell F, Alderson MR. (1995) Fas and FasL in the homeostatic regulation of immune responses. *Immunology Today*. **16**(12): 569-74

Macleod LC, Hotaling JM, Wright JL, Davenport MT, Gore JL, Harper J, White E. (2013) Risk factors for renal cell carcinoma in the VITAL study. *The Journal of Urology*. **190**(5): 1657-61

Maghazachi AA. (2010) Role of chemokines in the biology of natural killer cells. *Current Topics in Microbiology and Immunology*. **341**: 37-58

Mahadevan D, Lanasa MC, Farber C, Pandey M, Whelden M, Faas SJ, Ulery T, Kukreja A, Li L, Bedrosian CL, Zhang X, Heffner LT. (2019) Phase I study of samalizumab in chronic lymphocytic leukemia and multiple myeloma: blockade of the immune checkpoint CD200. *Journal for Immunotherapy of Cancer*. **7**(1): 227

Marcenaro S, Gallo F, Martini S, Santoro A, Griffiths GM, Arico M, Moretta L, Pende D. (2006) Analysis of natural killer-cell function in familial hemophagocytic lymphohistiocytosis (FHL): defective CD107a surface expression heralds Munc13-4

defect and discriminates between genetic subtypes of the disease. *Blood*. **108**(7): 2316-23

Marcus A, Gowen BG, Thompson TW, Iannello A, Ardolino M, Deng W, Wang L, Shifrin N, Raulet DH. (2014) Recognition of tumors by the innate immune system and natural killer cells. *Advances in Immunology*. **22**: 91-128

McWhirter JR, Kretz-Rommel A, Saven A, Maruyama T, Potter KN, Mockridge CI, Ravey EP, Qin F, Bowdish KS. (2006) Antibodies selected from combinatorial libraries block a tumor antigen that plays a key role in immunomodulation. *Proceedings of the National Academy of Sciences of the United States of America*. **103**(4): 1041-6

Ménager MM, Ménasché G, Romao M, Knapnougel P, Ho CH, Garfa M, Raposo G, Feldmann J, Fischer A, de Saint Basile G. (2007) Secretory cytotoxic granule maturation and exocytosis require the effector protein hMunc13-4. *Nature Immunology*. **8**(3): 257-67

Menko FH and Maher ER. (2016) Diagnosis and Management of Hereditary Renal Cell Cancer. *Recent Results in Cancer Research*. **205**: 85-104

Mercer F and Unutmaz D. (2009) The biology of FoxP3: a key player in immune suppression during infections, autoimmune diseases and cancer. *Advances in Experimental Medicine and Biology*. **665**: 47-59

Mier JW, Vachino G, van der Meer JW, Numerof RP, Adams S, Cannon JG, Bernheim HA, Atkins MB, Parkinson DR, Dinarello CA. (1988) Induction of circulating tumor necrosis factor (TNF α) as the mechanism for the febrile response to interleukin-2 (IL-2) in cancer patients. *Journal of Clinical Immunology*. **8**(6): 426-36

Mimura K, Teh JL, Okayama H, Shiraishi K, Kua LF, Koh V, Smoot DT, Ashktorab H, Oike T, Suzuki Y, Fazreen Z, Asuncion BR, Shabbir A, Yong WP, So J, Soong R, Kono K. (2018) PD-L1 expression is mainly regulated by interferon gamma associated with JAK-STAT pathway in gastric cancer. *Cancer Science*. **109**(1): 43-53

Minas K and Liversidge J. (2006) Is the CD200/CD200 receptor interaction more than just a myeloid cell inhibitory signal? *Critical Reviews in Immunology*. **26**(3): 213-30

Min B and Paul WE. (2008) Basophils and type 2 immunity. *Current Opinion in Hematology*. **15**(1): 59-63

Moore N and Lyle S. (2011) Quiescent, slow-cycling stem cell populations in cancer: a review of the evidence and discussion of significance. *Journal of Oncology*. **pii**: 396076

Mora A, Bosch R, Cuellar C, Vicente EP, Blanco L, Martino R, Ubeda JM, Sierra J, Moreno C, Nomdedeu J. (2019) CD200 is a useful marker in the diagnosis of chronic lymphocytic leukemia. *Cytometry*. **96**(2): 143-8

Moreaux J, Hose D, Reme T, Jourdan E, Hundemer M, Legouffe E, Moine P, Bourin P, Moos M, Corre J, Möhler T, De Vos J, Rossi JF, Goldschmidt H, Klein B. (2006) CD200 is a new prognostic factor in multiple myeloma. *Blood*. **108**(13): 4194-7

Moreaux J, Veyrune JL, Reme T, De Vos J, Klein B. (2008) CD200: a putative therapeutic target in cancer. *Biochemical and Biophysical Research Communications*. **366**(1): 117-22

Moretta A, Biassoni R, Bottino C, Mingari MC, Moretta L. (2000) Natural cytotoxicity receptors that trigger human NK-cell-mediated cytolysis. *Immunology Today*. **21**(5): 228-34

Mosser DM and Edwards JP. (2008) Exploring the full spectrum of macrophage activation. *Nature Reviews Immunology*. **8**(12): 958-69.

Motzer RJ, Escudier B, McDermott DF, George S, Hammers HJ, Srinivas S, Tykodi SS, Sosman JA, Procopio G, Plimack ER, Castellano D, Choueiri TK, Gurney H, Donskov F, Bono P, Wagstaff J, Gauler TC, Ueda T, Tomita Y, Schutz FA, Kollmannsberger C, Larkin J, Ravaud A, Simon JS, Xu LA, Waxman IM, Sharma P. (2015) Nivolumab versus Everolimus in Advanced Renal-Cell Carcinoma. *The New England Journal of Medicine*. **373**(19): 1803-13

Motzer RJ, Rini BI, McDermott DF, Redman BG, Kuzel TM, Harrison MR, Vaishampayan UN, Drabkin HA, George S, Logan TF, Margolin KA, Plimack ER, Lambert AM, Waxman IM, Hammers HJ. (2015) Nivolumab for Metastatic Renal Cell Carcinoma: Results of a Randomized Phase II Trial. *Journal of Clinical Oncology*. **33**(13): 1430-7

Motzer RJ, Rini BI, McDermott DF, Arén Frontera O, Hammers HJ, Carducci MA, Salman P, Escudier B, Beuselinck B, Amin A, Porta C, George S, Neiman V, Bracarda S, Tykodi SS, Barthélémy P, Leibowitz-Amit R, Plimack ER, Oosting SF, Redman B, Melichar B, Powles T, Nathan P, Oudard S, Pook D, Choueiri TK, Donskov F, Grimm MO, Gurney H, Heng DYC, Kollmannsberger CK, Harrison MR, Tomita Y, Duran I, Grünwald V, McHenry MB, Mekan S, Tannir NM. (2019) Nivolumab plus ipilimumab versus sunitinib in first-line treatment for advanced renal cell carcinoma: extended

follow-up of efficacy and safety results from a randomised, controlled, phase 3 trial. *The Lancet. Oncology*. **20**(10): 1370-85

Motzer RJ, Tannir NM, McDermott DF, Arén Frontera O, Melichar B, Choueiri TK, Plimack ER, Barthélémy P, Porta C, George S, Powles T, Donskov F, Neiman V, Kollmannsberger CK, Salman P, Gurney H, Hawkins R, Ravaud A, Grimm MO, Bracarda S, Barrios CH, Tomita Y, Castellano D, Rini BI, Chen AC, Mekan S, McHenry MB, Wind-Rotolo M, Doan J, Sharma P, Hammers HJ, Escudier B. (2018) Nivolumab plus Ipilimumab versus Sunitinib in Advanced Renal-Cell Carcinoma. *The New England Journal of Medicine.* **378**(14): 1277-90.

Muglia VF and Prando A. (2015) Renal cell carcinoma: histological classification and correlation with imaging findings. *Radiologia Brasileria*. **48**(3): 166-74

Nabi S, Kessler ER, Bernard B, Flaig TW, Lam ET. (2018) Renal cell carcinoma: a review of biology and pathophysiology. *F1000Research*. **7**: 307

Nadal E, Garin M, Kaeda J, Apperley J, Lechler R, Dazzi F. (2007) Increased frequencies of CD4(+)CD25(high) T(regs) correlate with disease relapse after allogeneic stem cell transplantation for chronic myeloid leukemia. *Leukemia*. **21**(3): 472-9

Negrier S, Escudier B, Lasset C, Douillard JY, Savary J, Chevreau C, Ravaud A, Mercatello A, Peny J, Mousseau M, Philip T, Tursz T. (1998) Recombinant human interleukin-2, recombinant human interferon alfa-2a, or both in metastatic renal-cell carcinoma. *The New England Journal of Medicine*. **338**(18): 1272-8
Numerof RP, Aronson FR, Mier JW. (1988) IL-2 stimulates the production of IL-1 α and IL-1 β by human peripheral blood mononuclear cells. *Journal of Immunology*. **141**(12): 4250-7

Nutman TB. (2015) Looking beyond the induction of Th2 responses to explain immunomodulation by helminths. *Parasite Immunology*. **37**(6): 304-13

Odorizzi PM and Wherry EJ. (2012) Inhibitory receptors on lymphocytes: insights from infections. *Journal of Immunology*. **188**(7): 2957-65

Oldham KA, Parsonage G, Bhatt RI, Wallace DM, Deshmukh N, Chaudhri S, Adams DH, Lee SP. (2012) T lymphocyte recruitment into renal cell carcinoma tissue: a role for chemokine receptors CXCR3, CXCR6, CCR5, and CCR6. *European Urology*. **61**(2): 385-94

Orange JS, Harris KE, Andzelm MM, Valter MM, Geha RS, Strominger JL. (2003) The mature activating natural killer cell immunologic synapse is formed in distinct stages. *Proceedings of the National Academy of Sciences of the USA*. **100**(24): 14151-6

Orange JS, Ramesh N, Remold-O'Donnell E, Sasahara Y, Koopman L, Byrne M, Bonilla FA, Rosen FS, Geha RS, Strominger JL. (2002) Wiskott-Aldrich syndrome protein is required for NK cell cytotoxicity and colocalizes with actin to NK cell-activating immunologic synapses. *Proceedings of the National Academy of Sciences of the USA.* **99**(17): 11351-6

Orange JS. (2007) The lytic NK cell immunological synapse and sequential steps in its formation. *Advances in Experimental Medicine and Biology*. **601**: 225-33

Palumbo GA, Parrinello N, Fargione G, Cardillo K, Chiarenza A, Berretta S, Conticello C, Villari L, Di Raimondo F. (2009) CD200 expression may help in differential diagnosis between mantle cell lymphoma and B-cell chronic lymphocytic leukemia. *Leukemia Research*. **33**(9): 1212-6

Pardoll DM. (2012) The blockade of immune checkpoints in cancer immunotherapy. *Nature Reviews. Cancer.* **12**(4): 252-64

Paul S and Lal G. (2017) The Molecular Mechanism of Natural Killer Cells Function and Its Importance in Cancer Immunotherapy. *Frontiers in Immunology*. **8**: 1124

Paul S, Kulkarni N, Shilpi, Lal G. (2016) Intratumoral natural killer cells show reduced effector and cytolytic properties and control the differentiation of effector Th1 cells. *Oncoimmunology*. **5**(12): e1235106

Peña-Llopis S, Christie A, Xie XJ, Brugarolas J. (2013) Cooperation and antagonism among cancer genes: the renal cancer paradigm. *Cancer Research*. **73**(14): 4173-9

Peña-Llopis S, Vega-Rubín-de-Celis S, Liao A, Leng N, Pavía-Jiménez A, Wang S, Yamasaki T, Zhrebker L, Sivanand S, Spence P, Kinch L, Hambuch T, Jain S, Lotan Y, Margulis V, Sagalowsky AI, Summerour PB, Kabbani W, Wong SW, Grishin N, Laurent M, Xie XJ, Haudenschild CD, Ross MT, Bentley DR, Kapur P, Brugarolas J. (2012) BAP1 loss defines a new class of renal cell carcinoma. *Nature Genetics*. **44**(7): 751-9.

Penn I. (1988) Tumors of the immunocompromised patient. *Annual Review of Medicine*. **39**: 63-73

Perez OD, Mitchell D, Jager GC, Nolan GP. (2004) LFA-1 signaling through p44/42 is coupled to perforin degranulation in CD56+CD8+ natural killer cells. *Blood*. **104**(4): 1083-93

Petermann KB, Rozenberg GI, Zedek D, Groben P, McKinnon K, Buehler C, Kim WY, Shields JM, Penland S, Bear JE, Thomas NE, Serody JS, Sharpless NE. (2007) CD200 is induced by ERK and is a potential therapeutic target in melanoma. *The Journal of Clinical Investigation*. **117**(12): 3922-9

Podnos A, Clark DA, Erin N, Yu K, Gorczynski RM. (2012) Further evidence for a role of tumor CD200 expression in breast cancer metastasis: decreased metastasis in CD200R1KO mice or using CD200-silenced EMT6. *Breast Cancer Research and Treatment*. **136**(1): 117-27

Poggi A, Massaro AM, Negrini S, Contini P, Zocchi MR. (2005) Tumor-induced apoptosis of human IL-2-activated NK cells: role of natural cytotoxicity receptors. *Journal of Immunology*. **174**(5): 2653-60

Poli A, Michel T, Thérésine M, Andrès E, Hentges F, Zimmer J. (2009) CD56bright natural killer (NK) cells: an important NK cell subset. *Immunology.* **126**(4): 458-65

Pópulo H, Lopes JM, Soares P. (2012) The mTOR signalling pathway in human cancer. *International Journal of Molecular Sciences*. **13**(2): 1886-918

Prasad SR, Humphrey PA, Catena JR, Narra VR, Srigley JR, Cortez AD, Dalrymple NC, Chintapalli KN. (2006) Common and uncommon histologic subtypes of renal cell carcinoma: imaging spectrum with pathologic correlation. *Radiographics*. **26**(6): 1795-806

Prinz PU, Mendler AN, Brech D, Masouris I, Oberneder R, Noessner E. (2014) NK-cell dysfunction in human renal carcinoma reveals diacylglycerol kinase as key regulator and target for therapeutic intervention. *International Journal of Cancer*. **135**(8): 1832-41

Pu J, Guardia CM, Keren-Kaplan T, Bonifacino JS. (2016) Mechanisms and functions of lysosome positioning. *Journal of Cell Science*. **29**(23): 4329-39

Rabinovich GA, Gabrilovich D, Sotomayor EM. (2007) Immunosuppressive strategies that are mediated by tumor cells. *Annual Review of Immunology*. **25**: 267-96

Remark R, Alifano M, Cremer I, Lupo A, Dieu-Nosjean MC, Riquet M, Crozet L, Ouakrim H, Goc J, Cazes A, Fléjou JF, Gibault L, Verkarre V, Régnard JF, Pagès ON, Oudard S, Mlecnik B, Sautès-Fridman C, Fridman WH, Damotte D. (2013) Characteristics and clinical impacts of the immune environments in colorectal and renal cell carcinoma lung metastases: influence of tumor origin. *Clinical Cancer Research*. **19**(15): 4079-91

Riazalhosseini Y and Lathrop M. (2016) Precision medicine from the renal cancer genome. Nature Reviews. *Nephrology*. **12**(11): 655-66

Rijkers ES, de Ruiter T, Buitenhuis M, Veninga H, Hoek RM, Meyaard L. (2007) Ligation of CD200R by CD200 is not required for normal murine myelopoiesis. *European Journal of Haematology*. **79**(5): 410-6

Robb VA, Karbowniczek M, Klein-Szanto AJ, Henske EP. (2007) Activation of the mTOR signaling pathway in renal clear cell carcinoma. *The Journal of Urology*. **177**(1): 346-52

Roda JM, Parihar R, Magro C, Nuovo GJ, Tridandapani S, Carson WE 3rd. (2006) Natural killer cells produce T cell-recruiting chemokines in response to antibody-coated tumor cells. *Cancer Research*. **66**(1): 517-26

Rodríguez JA. (2017) HLA-mediated tumor escape mechanisms that may impair immunotherapy clinical outcomes via T-cell activation (Review). *Oncology Letters*. **14**(4): 4415-27

Romano M, Fanelli G, Albany CJ, Giganti G, Lombardi G. (2019) Past, Present, and Future of Regulatory T Cell Therapy in Transplantation and Autoimmunity. *Frontiers in Immunology*. **10**: 43

Romero JM, Aptsiauri N, Vazquez F, Cozar JM, Canton J, Cabrera T, Tallada M, Garrido F, Ruiz-Cabello F. (2006) Analysis of the expression of HLA class I, proinflammatory cytokines and chemokines in primary tumors from patients with localized and metastatic renal cell carcinoma. *Tissue Antigens*. **68**(4): 303-10

Rosales C. (2018) Neutrophil: A Cell with Many Roles in Inflammation or Several Cell Types? *Frontiers in Physiology*. **9**: 113

Rosenberg SA, Yang JC, Topalian SL, Schwartzentruber DJ, Weber JS, Parkinson DR, Seipp CA, Einhorn JH, White DE. (1994) Treatment of 283 consecutive patients with metastatic melanoma or renal cell cancer using high-dose bolus interleukin 2. *JAMA*. **271**(12): 907-13

Rosenblum MD, Olasz EB, Yancey KB, Woodliff JE, Lazarova Z, Gerber KA, Truitt RL. (2004) Expression of CD200 on epithelial cells of the murine hair follicle: a role in tissue-specific immune tolerance? *The Journal of Investigative Dermatology*. **123**(5): 880-7

Rosenblum MD, Yancey KB, Olasz EB, Truitt RL. (2006) CD200, a "no danger" signal for hair follicles. *Journal of Dermatological Science*. **41**(3): 165-74

Rosmaraki EE, Douagi I, Roth C, Colucci F, Cumano A, Di Santo JP. (2001) Identification of committed NK cell progenitors in adult murine bone marrow. *European Journal of Immunology*. **31**(6): 1900-09

Rossi M and Young JW. (2005) Human Dendritic Cells: Potent Antigen-Presenting Cells at the Crossroads of Innate and Adaptive Immunity. *The Journal of Immunology*. **175**(3): 1373-81

Rotte A. (2019) Combination of CTLA-4 and PD-1 blockers for treatment of cancer. *Journal of Experimental and Clinical Cancer Research*. **38**(1): 255

Sakaguchi S, Sakaguchi N, Asano M, Itoh M, Toda M. (1995) Immunologic self-tolerance maintained by activated T cells expressing IL-2 receptor alpha-chains (CD25). Breakdown of a single mechanism of self-tolerance causes various autoimmune diseases. *Journal of Immunology*. **155**(3): 1151-64

Salcedo TW, Azzoni L, Wolf SF, Perussia B. (1993) Modulation of perforin and granzyme messenger RNA expression in human natural killer cells. *Journal of Immunology*. **151**(5): 2511-20

Sánchez MJ, Spits H, Lanier LL, Phillips JH. (1993) Human natural killer cell committed thymocytes and their relation to the T cell lineage. *The Journal of Experimental Medicine*. **178**(6): 1857-66

Seita J and Weissman IL. (2010) Hematopoietic stem cell: self-renewal versus differentiation. *Wiley Interdisciplinary Reviews: Systems Biology and Medicine*. **2**(6): 640-53

Sato Y, Yoshizato T, Shiraishi Y, Maekawa S, Okuno Y, Kamura T, Shimamura T, Sato-Otsubo A, Nagae G, Suzuki H, Nagata Y, Yoshida K, Kon A, Suzuki Y, Chiba K, Tanaka H, Niida A, Fujimoto A, Tsunoda T, Morikawa T, Maeda D, Kume H, Sugano S, Fukayama

M, Aburatani H, Sanada M, Miyano S, Homma Y, Ogawa S. (2013) Integrated molecular analysis of clear-cell renal cell carcinoma. *Nature Genetics*. **45**(8): 860-7.

Schwartz RN, Stover L, Dutcher JP. (2002) Managing toxicities of high-dose interleukin-2. *Oncology (Williston Park)*. **16**(11 Suppl 13): 11-20

Shang B, Liu Y, Jiang SJ, Liu Y. (2015) Prognostic value of tumor-infiltrating FoxP3+ regulatory T cells in cancers: a systematic review and meta-analysis. *Scientific Reports*. **5**: 15179

Sharpe AH and Pauken KE. (2018) The diverse functions of the PD1 inhibitory pathway. Nature reviews. *Immunology*. **18**(3): 153-67

Shi F, Shi M, Zeng Z, Qi RZ, Liu ZW, Zhang JY, Yang YP, Tien P, Wang FS. (2011) PD-1 and PD-L1 upregulation promotes CD8(+) T-cell apoptosis and postoperative recurrence in hepatocellular carcinoma patients. *International Journal of Cancer*. **128**(4): 887-96

Shu X, Lin J, Wood CG, Tannir NM, Wu X. (2013) Energy balance, polymorphisms in the mTOR pathway, and renal cell carcinoma risk. *Journal of the National Cancer Institute.* **105**(6): 424-32

Siddiqui SA, Frigola X, Bonne-Annee S, Mercader M, Kuntz SM, Krambeck AE, Sengupta S, Dong H, Cheville JC, Lohse CM, Krco CJ, Webster WS, Leibovich BC, Blute ML, Knutson KL, Kwon ED. (2007) umor-infiltrating Foxp3-CD4+CD25+ T cells predict poor survival in renal cell carcinoma. *Clinical Cancer Research*. **13**(7): 2075-81

Siva A, Xin H, Qin F, Oltean D, Bowdish KS, Kretz-Rommel A. (2008) Immune modulation by melanoma and ovarian tumor cells through expression of the immunosuppressive molecule CD200. *Cancer Immunology, Immunotherapy*. **57**(7): 987-96

Smith MJ, Hardy WR, Murphy JM, Jones N, Pawson T. (2006) Screening for PTB domain binding partners and ligand specificity using proteome-derived NPXY peptide arrays. *Molecular and Cellular Biology*. **26**(22): 8461-74

Smith-Garvin JE, Koretzky GA, Jordan MS. (2009) T cell activation. *Annual Review of Immunology*. **27**: 591-619

Smyth MJ, Swann J, Kelly JM, Cretney E, Yokoyama WM, Diefenbach A, Sayers TJ, Hayakawa Y. (2004) NKG2D recognition and perforin effector function mediate

effective cytokine immunotherapy of cancer. *The Journal of Experimental Medicine*. **200**(10): 1325-35

Snelgrove RJ, Goulding J, Didierlaurent AM, Lyonga D, Vekaria S, Edwards L, Gwyer E, Sedgwick JD, Barclay AN, Hussell T. (2008) A critical function for CD200 in lung immune homeostasis and the severity of influenza infection. *Nature Immunology*. **9**(9): 1074-83

Sternberg-Simon M, Brodin P, Pickman Y, Onfelt B, Kärre K, Malmberg KJ, Höglund P, Mehr R. (2013) Natural killer cell inhibitory receptor expression in humans and mice: a closer look. *Frontiers in Immunology*. **4**: 65

Stinchcombe JC and Griffiths GM. (2007) Secretory mechanisms in cell-mediated cytotoxicity. *Annual reviews of cell and developmental biology*. **23**: 495-517.

Stinchcombe JC, Barral DC, Mules EH, Booth S, Hume AN, Machesky LM, Seabra MC, Griffiths GM. (2001) Rab27a is required for regulated secretion in cytotoxic T lymphocytes. *The journal of cell biology*. **152**(4): 825-34

Stojanovic A, Correia MP, Cerwenka A. (2018) The NKG2D/NKG2DL Axis in the Crosstalk Between Lymphoid and Myeloid Cells in Health and Disease. *Frontiers in Immunology*. **9**: 827

Stone KD, Prussin C, Metcalfe DD. (2010) IgE, mast cells, basophils, and eosinophils. *The journal of allergy and clinical immunology*. **125**(2 Suppl 2): S73-80

Swami U, Nussenzveig RH, Haaland B, Agarwal N. (2019) Revisiting AJCC TNM staging for renal cell carcinoma: quest for improvement. *Annals of Translational Medicine*. **7**(Suppl 1): S18

Takahashi T, Tagami T, Yamazaki S, Uede T, Shimizu J, Sakaguchi N, Mak TW, Sakaguchi S. (2000) Immunologic self-tolerance maintained by CD25(+)CD4(+) regulatory T cells constitutively expressing cytotoxic T lymphocyte-associated antigen 4. *The journal of experimental medicine.* **192**(2): 303-10

Tanaka M, Suda T, Takahashi T, Nagata S. (1995) Expression of the functional soluble form of human fas ligand in activated lymphocytes. *The EMBO Journal*. **14**(6): 1129-35

Tang BL. (2015) A unique SNARE machinery for exocytosis of cytotoxic granules and platelets granules. *Molecular membrane biology*. **32**(4):120-6

Terrén I, Orrantia A, Mikelez-Alonso I, Vitallé J, Zenarruzabeitia O, Borrego F. (2020) NK Cell-Based Immunotherapy in Renal Cell Carcinoma. *Cancers*. **12**(2): pii:E316

Theis RP, Dolwick Grieb SM, Burr D, Siddiqui T, Asal NR. (2008) Smoking, environmental tobacco smoke, and risk of renal cell cancer: a population-based case-control study. *BMC Cancer.* **8**: 387

Theoharides TC, Alysandratos KD, Angelidou A, Delivanis DA, Sismanopoulos N, Zhang B, Asadi S, Vasiadi M, Weng Z, Miniati A, Kalogeromitros D. (2012) Mast cells and inflammation. *Biochimica et Biophysica Acta*. **1822**(1): 21-33.

Thomas DA and Massagué J. (2005) TGF-beta directly targets cytotoxic T cell functions during tumor evasion of immune surveillance. *Cancer cell*. **8**(5): 369-80

Tiribelli M, Raspadori D, Geromin A, Cavallin M, Sirianni S, Simeone E, Bocchia M, Fanin R, Damiani D. (2017) High CD200 expression is associated with poor prognosis in cytogenetically normal acute myeloid leukemia, even in FlT3-ITD-/NPM1+ patients. *Leukemia Research*. **58**: 31-38

Tonks A, Hills R, White P, Rosie B, Mills KI, Burnett AK, Darley RL. (2007) CD200 as a prognostic factor in acute myeloid leukaemia. *Leukemia.* **21**(3): 566-8

Topham NJ and Hewitt EW. (2009) Natural killer cell cytotoxicity: how do they pull the trigger? *Immunology*. **128**(1): 7-15

Topalian SL, Drake CG, Pardoll DM. (2015) Immune checkpoint blockade: a common denominator approach to cancer therapy. *Cancer Cell*. **27**(4): 450-61

Tsivian M, Moreira DM, Caso JR, Mouraviev V, Polascik TJ. (2011) Cigarette smoking is associated with advanced renal cell carcinoma. *Journal of Clinical Oncology*. **29**(15): 2027-31

Twito T, Chen Z, Khatri I, Wong K, Spaner D, Gorczynski R. (2013) Ectodomain shedding of CD200 from the B-CLL cell surface is regulated by ADAM28 expression. *Leukemia Research*. **37**(7): 816-21

Uzzo RG, Rayman P, Kolenko V, Clark PE, Bloom T, Ward AM, Molto L, Tannenbaum C, Worford LJ, Bukowski R, Tubbs R, Hsi ED, Bander NH, Novick AC, Finke JH. (1999) Mechanisms of apoptosis in T cells from patients with renal cell carcinoma. *Clinical Cancer Research*. **5**(5): 1219-29

Valente T, Serratosa J, Perpiñá U, Saura J, Solà C. (2017) Alterations in CD200-CD200R1 System during EAE Already Manifest at Presymptomatic Stages. *Frontiers in Cellular Neuroscience*. **11**: 129

Varela I, Tarpey P, Raine K, Huang D, Ong CK, Stephens P, Davies H, Jones D, Lin ML, Teague J, Bignell G, Butler A, Cho J, Dalgliesh GL, Galappaththige D, Greenman C, Hardy C, Jia M, Latimer C, Lau KW, Marshall J, McLaren S, Menzies A, Mudie L, Stebbings L, Largaespada DA, Wessels LF, Richard S, Kahnoski RJ, Anema J, Tuveson DA, Perez-Mancera PA, Mustonen V, Fischer A, Adams DJ, Rust A, Chan-on W, Subimerb C, Dykema K, Furge K, Campbell PJ, Teh BT, Stratton MR, Futreal PA. (2011) Exome sequencing identifies frequent mutation of the SWI/SNF complex gene PBRM1 in renal carcinoma. *Nature*. **469**(7331): 539-42

Varshney N, Kebede AA, Owusu-Dapaah H, Lather J, Kaushik M, Bhullar JS. (2017) A Review of Von Hippel-Lindau Syndrome. *Journal of Kidney Cancer and VHL*. **4**(3): 20-9

Vera-Badillo FE, Conde E, Duran I. (2012) Chromophobe renal cell carcinoma: A review of an uncommon entity. *International Journal of Urology*. **19**(10): 894-900

Vesely MD, Kershaw MH, Schreiber RD, Smyth MJ. (2011) Natural innate and adaptive immunity to cancer. *Annual reviews of immunology*. **29**: 235-71

Vieites JM, de la Torre R, Ortega MA, Montero T, Peco JM, Sánchez-Pozo A, Gil A, Suárez A. (2003) Characterization of human cd200 glycoprotein receptor gene located on chromosome 3q12-13. *Gene*. **311**: 99-104

Vilgelm AE and Richmond A. (2019) Chemokines Modulate Immune Surveillance in Tumorigenesis, Metastasis, and Response to Immunotherapy. *Frontiers in immunology*. **10**: 333

Vivier E, Ugolini S, Blaise D, Chabannon C, Brossay L. (2012) Targeting natural killer cells and natural killer T cells in cancer. *Nature reviews. Immunology*. **12**(4): 239-52

Vogelzang NJ, Priest ER, Borden L. (1992) Spontaneous regression of histologically proved pulmonary metastases from renal cell carcinoma: a case with 5-year followup. *The Journal of Urology*. **148**(4): 1247-8

Volpe A, Novara G, Antonelli A et al. (2012) Chromophobe renal cell carcinoma (RCC): oncological outcomes and prognostic factors in a large multicentre series. *BJU International*. **110**(1): 76-83

Voskoboinik I, Dunstone MA, Baran K, Whisstock JC, Trapani JA. (2010) Perforin: structure, function, and role in human immunopathology. *Immunological reviews*. **235**(1): 35-54

Vyas YM, Mehta KM, Morgan M, Maniar H, Butros L, Jung S, Burkhardt JK, Dupont B. (2001) Spatial organization of signal transduction molecules in the NK cell immune synapses during MHC class I-regulated noncytolytic and cytolytic interactions. *Journal of immunology*. **167**(8): 4358-67

Walczak H. (2013) Death receptor-ligand systems in cancer, cell death, and inflammation. *Cold Spring Harbor Perspectives in Biology*. **5**(5): a008698

Walker DG, Dalsing-Hernandez JE, Campbell NA, Lue LF. (2009) Decreased expression of CD200 and CD200 receptor in Alzheimer's disease: a potential mechanism leading to chronic inflammation. *Experimental Neurology*. **215**(1): 5-19

Wallach D, Varfolomeev EE, Malinin NL, Goltsev YV, Kovalenko AV, Boldin MP. (1999) Tumor necrosis factor receptor and Fas signaling mechanisms. *Annual review of immunology*. **17**: 331-67

Wang S and El-Deiry WS. (2003) TRAIL and apoptosis induction by TNF-family death receptors. *Oncogene*. **22**(53):8628-33

Wei SC, Duffy CR2, Allison JP. (2018) Fundamental Mechanisms of Immune Checkpoint Blockade Therapy. *Cancer discovery*. **8**(9): 1069-86

Whiteside TL. (1999) Signaling defects in T lymphocytes of patients with malignancy. *Cancer immunology, immunotherapy*. **48**(7): 346-52

Whiteside TL. (2004) Down-regulation of ζ chain expression in T cells: a biomarker of prognosis in cancer? *Cancer Immunology, Immunotherapy*. **53**(10):865-78.

Whiteside TL. (2006) Immune suppression in cancer: effects on immune cells, mechanisms and future therapeutic intervention. *Seminars in cancer biology*. **16**(1): 3-15

Whiteside TL. (2012) What are regulatory T cells (Treg) regulating in cancer and why? *Seminars in Cancer Biology*. **22**(4): 327-34

Wong KK, Khatri I, Shaha S, Spaner DE, Gorczynski RM. (2010) The role of CD200 in immunity to B cell lymphoma. *Journal of Leukocyte Biology*. **88**(2): 361-72

Wong KK, Shaha S, Spaner D, Gorczynski RM. (2009) Potential role for serum soluble CD200 in human Chronic Lymphocytic Leukemia. *The Journal of Immunology*. **182**(1): 88

Wong KK, Zhu F, Khatri I, Huo Q, Spaner DE, Gorczynski RM. (2016) Characterization of CD200 Ectodomain Shedding. *PLoS One*. **11**(4): e0152073

Workman CJ, Szymczak-Workman AL, Collison LW, Pillai MR, Vignali DA. (2009) The development and function of regulatory T cells. *Cellular and Molecular Life Sciences.* **66**(16): 2603-22

Wright GJ, Cherwinski H, Foster-Cuevas M, Brooke G, Puklavec MJ, Bigler M, Song Y, Jenmalm M, Gorman D, McClanahan T, Liu MR, Brown MH, Sedgwick JD, Phillips JH, Barclay AN. (2003) Characterization of the CD200 receptor family in mice and humans and their interactions with CD200. *Journal of Immunology*. **171**(6): 3034-46

Wright GJ, Puklavec MJ, Willis AC, Hoek RM, Sedgwick JD, Brown MH, Barclay AN. (2000) Lymphoid/neuronal cell surface OX2 glycoprotein recognizes a novel receptor on macrophages implicated in the control of their function. *Immunity.* **13**(2): 233-42

Xiong Y, Wang Z, Zhou Q, Zeng H, Zhang H, Liu Z, Huang Q, Wang J, Chang Y, Xia Y, Wang Y, Liu L, Zhu Y, Xu L, Dai B, Bai Q, Guo J, Xu J. Identification and validation of dichotomous immune subtypes based on intratumoral immune cells infiltration in clear cell renal cell carcinoma patients. *Journal for Immunotherapy of Cancer*. **8**(1): e000447.

Xu G and Shi Y. (2007) Apoptosis signaling pathways and lymphocyte homeostasis. *Cell Research*. **17**(9): 759-71

Xu Y, Cheng Q, Yang B, Yu S, Xu F, Lu L, Liang X. (2015) Increased sCD200 Levels in Vitreous of Patients with Proliferative Diabetic Retinopathy and Its Correlation With VEGF and Proinflammatory Cytokines. *Investigative Ophthalmology & Visual Science*. **56**(11): 6565-72

Xu Y, Zhou S, Lam YW, Pang SW. (2017) Dynamics of Natural Killer Cells Cytotoxicity in Microwell Arrays with Connecting Channels. *Frontiers in Immunology*. **8**: 998

Yam-Puc JC, Zhang L, Zhang Y, Toellner KM. (2018) Role of B-cell receptors for B-cell development and antigen-induced differentiation. *F1000Research*. **7**: 429

Yang JC, Hughes M, Kammula U, Royal R, Sherry RM, Topalian SL, Suri KB, Levy C, Allen T, Mavroukakis S, Lowy I, White DE, Rosenberg SA. (2007) Ipilimumab (anti-CTLA4 antibody) causes regression of metastatic renal cell cancer associated with enteritis and hypophysitis. *Journal of Immunotherapy*. **30**(8): 825-30

Zhang J, Gao JX, Salojin K, Shao Q, Grattan M, Meagher C, Laird DW, Delovitch TL. (2000) Regulation of fas ligand expression during activation-induced cell death in T cells by p38 mitogen-activated protein kinase and c-Jun NH2-terminal kinase. *The Journal of Experimental Medicine*. **191**(6): 1017-30

Zhang N and Bevan MJ. (2011) CD8(+) T cells: foot soldiers of the immune system. *Immunity*. **35**(2): 161-8

Zhang Q and Vignali DA. (2016) Co-stimulatory and Co-inhibitory Pathways in Autoimmunity. *Immunity*. **44**(5): 1034-51

Zhang S and Phillips JH. (2006) Identification of tyrosine residues crucial for CD200R-mediated inhibition of mast cell activation. *Journal of Leukocyte Biology*. **79**(2): 363-8

Zhang SS, Huang ZW, Li LX, Fu JJ, Xiao B. (2016) Identification of CD200+ colorectal cancer stem cells and their gene expression profile. *Oncology Reports*. **36**(4): 2252-60

Zhu J. (2010) Transcriptional regulation of Th2 cell differentiation. *Immunology and Cell Biology*. **88**(3): 244-9

Zhu J. (2015) T helper 2 (Th2) cell differentiation, type 2 innate lymphoid cell (ILC2) development and regulation of interleukin-4 (IL-4) and IL-13 production. *Cytokine*. **75**(1): 14-24

Zhu J and Paul WE. (2008) CD4 T cells: fates, functions, and faults. *Blood*. **112**(5): 1557-69

Zhu J, Petit PF, Van den Eynde BJ. (2019) Apoptosis of tumor-infiltrating T lymphocytes: a new immune checkpoint mechanism. *Cancer Immunology, Immunotherapy*. **68**(5): 835-47

Zhu J, Yamane H, Paul WE. (2010) Differentiation of effector CD4 T cell populations. *Annual Reviews of Immunology*. **28**: 445-89

Zhu Y, Huang B, Shi J. (2016) Fas ligand and lytic granule differentially control cytotoxic dynamics of natural killer cell against cancer target. *Oncotarget.* **7**(30): 47163-72.

Zhu Y and Zhang X. (2019) Investigating the significance of tumor-infiltrating immune cells for the prognosis of lung squamous cell carcinoma. *PeerJ*. **7**: e7918